THE SEISMIC EVALUATION AND RETROFITTING OF BRIDGES

by

Joe Maffei

Supervised by Professor R. Park

A thesis
submitted in partial fulfilment
of the requirements for the degree
of
Doctor of Philosophy

Department of Civil Engineering
University of Canterbury
Christchurch, New Zealand

March 1996

Abstract

Past earthquakes have clearly shown the seismic vulnerability of existing bridges. Despite recent progress by the structural engineering profession in addressing bridge seismic risks, there are still several areas where improvements in bridge evaluation and retrofit practices are needed. The first part of this report reviews the common seismic deficiencies of bridges, procedures and criteria for seismically evaluating bridges, and the engineering techniques which have been used for retrofitting bridge seismic deficiencies. Information on seismic deficiencies, retrofit techniques, and related research has been organized by the author in a concise tabular form. The review indicates several areas where effective retrofit techniques have been established, and other areas where improved procedures or further research are needed. Seismic upgrade measures proposed for Wellington's Thorndon bridge, including an innovative retrofit of superstructure linkages, illustrate the benefits of a capacity-design approach to seismic evaluation and retrofitting.

The second part of this report describes the laboratory testing and inelastic computer analysis of a 1936-designed bridge which is typical of many of the older, reinforced-concrete, multi-span bridges in New Zealand. The structure has plain-round (undeformed) reinforcing bars and questionable anchorage details, shear strength, and column-transverse reinforcing. Despite the suspected seismic deficiencies, the testing and analysis of the bridge show that its seismic performance will be good. The results indicate that (a) seismic retrofitting is not warranted, (b) code criteria applicable to the design of new structures, with deformed reinforcing, can be overly conservative when used for the assessment of existing structures, and (c) plain-round reinforcing bars under cyclic seismic forces suffer extensive bond deterioration resulting in pinched hysteretic response which, for earthquake inputs with extreme pulses, can lead to greater seismic damage.

The third part of the report reviews procedures which have been used to prioritize bridges for seismic upgrading. A new method of managing and prioritizing bridge-upgrade work, developed by the author for New Zealand's Tasman district, offers several improvements over previously used procedures. The new method is based on cost-benefit and earthquake loss-estimation principles. The method outlines four levels of seismic evaluation and includes a seismic-vulnerability rating system, a flowchart assessment method, and formulas for estimating bridge value and benefit/cost ratios for seismic upgrading. The recommended methods have been implemented on a stock of 445 bridges using a minimum of data, and have also been applied to the in-depth evaluation of retrofit options for the Thorndon bridge.

Acknowledgments

I am very grateful to the organizations which helped fund this research. These include the United States Fulbright Scholarship Foundation, the New Zealand National Society for Earthquake Engineering, the Tasman District Council, and Transit New Zealand.

I am indebted to Professor Bob Park for his wise and decisive supervision, and his support and friendship.

I am grateful to Beca, Carter, Hollings and Ferner consulting engineers in Auckland for the opportunity to work on the retrofit-concepts phase of the Thorndon bridge project. This work provided the very pertinent material for Chapters 4 and 14. The structural engineering team for the project included project director Ian Billings, project manager Alan Powell, Clive Richardson, and consultant Nigel Priestley. The seismicity studies were carried out principally by Rob Jury, while the studies of ground improvement against liquefaction (Section 4.5) were carried out by John Marsh. The economic analysis of the retrofit options, (Section 14.6) was carried out by Ian Bone.

Much appreciation is also due to Rod Gibson and Jeff Robinson of the Tasman District Council for their initiative in proposing and approving the bridge seismic-risk and upgrade-management study which formed the basis for Chapters 12 and 13. Rod Gibson's input on bridge construction costs and transportation disruption costs (Section 12.7) is also appreciated.

I offer my thanks to Professor Nigel Priestley, Howard Chapman, Dr. Athol Carr, Bret Lizundia, Don Kennedy, Dr. Jose Restrepo, and others for their helpful input to this report. In particular I offer my gratitude to Ray Zelinski of Caltrans for his extensive comments on Chapters 2 and 3, and to Ian Billings for his thorough review and constructive comments. A very special thanks goes to Professor Emeritus Tom Paulay, for his thorough comments on several aspects of this report and for the lively and enlightening discussions we have had on so many different topics.

Gratitude is also due to Norrie Hickey, Dominic McCarthy, and Mark Griffin who were the laboratory technicians for the testing of the column/foundation-beam specimen, to Val Grey who skilfully prepared many of the figures, to Catherine Price who typed the report, and to Billie-Jo at Adept Secretarial Services who did the final typing corrections and arrangement of the report. For proofreading, profound and immeasurable gratitude is due to the poorly remunerated Dagny Baltakmens (who inserted the words profound, immeasurable, and poorly remunerated into this sentence).

Finally, I offer my thanks to the Department of Civil Engineering and the colleagues and friends who helped make my time in New Zealand a wonderful experience.

TABLE OF CONTENTS

CHAPTER 1
INTRODUCTION

Background

As emphasized recently in Kobe, Japan and Northridge, California, damage to bridges can be one of the most catastrophic results of strong earthquakes. Past earthquakes have clearly shown that bridges can be seismically vulnerable; and the inadequacy of many types of existing bridge structures to resist earthquake shaking has been well established.

Over the last few years there has been substantial progress in addressing the seismic risk posed by existing bridges. Since the 1989 Loma Prieta earthquake, an intensive program of seismic retrofitting for Californias highway bridges has been undertaken. Other US states, and other countries, have also begun or intensified seismic evaluation and retrofit programs for their bridges. Along with the implementation of seismic retrofit measures, numerous research programs have been carried out. The research has resulted in greatly improved procedures for evaluating bridges and designing retrofit measures.

Despite the recent progress, there is still room for improvement. Because of the complexities of bridge seismic performance and seismic risk, there are still many gaps in our knowledge of, and ability to provide, effective seismic-retrofit solutions. The problem is compounded by the wide variety of structure types and characteristics, seismicity levels, soil conditions, and available resources for seismic upgrading, which are found in different locations or within a single jurisdiction. In some areas further research is needed; in other cases sufficient research has been carried out, but engineers in practice may not be fully aware of the research results or their implications. For the management and prioritization of bridge seismic upgrading, a better overlap of understanding among the disciplines of structural engineering, risk analysis, and seismology may be needed.

Objectives

The aim of this report is to fill in some of the gaps in knowledge and knowledge-transfer in the structural engineering profession regarding the seismic evaluation and retrofitting of bridges. The emphasis of this report is on the practical aspects of the problem. It is intended to provide useful information to structural-engineering designers as well as researchers. The report includes:

(i) a comprehensive review of seismic evaluation and retrofit technology, focused on practical and specific examples,

(ii) a detailed study of a prevalent New Zealand bridge type—a concrete structure with plain-round reinforcing bars, and

(iii) an improved method for the management and prioritization of bridge seismic upgrading.

In New Zealand, the upgrading of seismically deficient bridges is lagging behind the progress in other earthquake-prone areas such as California and Japan. Fortunately, the research results and implementation experience from overseas can be put to use in New Zealand. It is hoped that the information contained in this report will help in the task of implementing an effective bridge seismic retrofit program here in New Zealand and elsewhere.

Evolution

The scope of this study has changed somewhat since its inception. The work began in July 1992 with the experimental study of the column-foundation region of a 1936-designed bridge. The study included a literature review on bridge seismic retrofitting.

Originally the issue of bridge-upgrade prioritization was a small part of the work. However, two circumstances led to a deeper exploration of this topic, which now constitutes the final third of the report. First, the literature review of procedures for bridge-upgrade prioritization revealed both the critical importance of the topic and the tremendous room for improvement over previous methods. Second, the opportunity came up to conduct a bridge seismic-risk and upgrade-management study for the Tasman District, a local authority in New Zealand.

Another unique opportunity to report on bridge retrofit issues in more detail and from a real-world perspective was presented by Beca, Carter, Hollings and Ferner consulting engineers. The author worked for BCHF on the design of retrofit concepts for the Thorndon bridge in Wellington, New Zealand. The Thorndon project provided several pertinent examples of state-of-the-art seismic evaluation and retrofit principles, which are presented in Chapters 4 and 14.

Organization

This report is divided into three parts. The conclusions of the report are presented within each of the three parts—in Chapters 5, 10, and 15.

Part I of the report covers bridge seismic evaluation and retrofitting in general. Within Part I, Chapter 2 reviews bridge seismic deficiencies, and procedures and criteria for seismic evaluation; Chapter 3 reviews seismic-retrofit techniques. The five-page Table 2.1 summarizes much of the information from Chapters 2 and 3. Chapter 4 provides some examples in more detail of recommended seismic evaluation and retrofit practices, taken from the Thorndon bridge project.

Part II of the report covers the experimental and analytical studies of a 1936-designed concrete bridge with plain-round reinforcement. Chapter 6 reviews previous studies of the bridge, which include an initial seismic assessment and tests of the column/crossbeam region of the structure. Chapters 7 and

8 discuss the laboratory testing of a second critical portion of the structure, the column/foundation-beam region. Chapter 9 presents inelastic, dynamic time-history analyses of the bridge which complement the experimental studies.

Part III of the report covers the topic of prioritizing bridges for seismic upgrading and managing bridge-seismic retrofitting. Chapter 11 is a comprehensive review of previously proposed procedures for bridge-upgrade prioritization. Chapter 12 describes a new method of bridge-upgrade management and prioritization which was developed by the author. Chapter 13 presents results from the implementation of the new method on a group of 445 bridges in the Tasman district. Chapter 14 describes the implementation of the recommended methods to evaluate retrofit options for the Thorndon bridge.

Part I

SEISMIC EVALUATION
AND RETROFIT TECHNOLOGY

CHAPTER 2
SEISMIC EVALUATION OF BRIDGES

This Chapter reviews several aspects of the problem of evaluating a bridge's ability to withstand earthquake effects. Section 2.1 reviews the possible seismic deficiencies of bridges, which show the clear seismic vulnerability of many common features of existing bridges. Section 2.2 discusses the procedures and criteria which have been proposed for the seismic evaluation of bridges, including recommendations for improved procedures.

2.1 Observed Seismic Deficiencies in Bridges

Past earthquakes have revealed the structural deficiencies of bridges throughout the world. Since reviews of earthquake damage to bridges have already been written [Priestley et al 1992a], only a summary is given here. Although many existing bridges were designed considering earthquake effects, the inadequate seismic design criteria used before the early 1970s makes these bridges vulnerable to collapse. Typically, seismic design forces and expected deflections were too low, members critical in earthquakes were not designed for ductility and thus could suffer brittle failures, and the concept of capacity design (i.e., precluding the failure of brittle elements by providing them with strength exceeding that of a ductile yield mechanism) was not used.

In California, the February 1971 San Fernando earthquake brought about a number of improvements in seismic design practice which were implemented over the next decade. Consequently, the California Department of Transportation (Caltrans) considers that its seismic design code was not fully developed until 1980 [Zelinski pers. comm. 1994], and has carried out an extensive program of evaluation and retrofitting for structures built before 1980.

Several observed deficiencies in bridge structures are discussed below. The deficiencies are presented in the sequence that a structural designer might consider them, roughly following the seismic load path from the roadway superstructure, through the beams, connections, columns, and foundations and abutments, to the supporting soil.

Figure 2.1 illustrates the structural locations of potential seismic deficiencies discussed. Table 2.1 summarizes the information on seismic deficiencies discussed in this chapter. The left-hand side of the table outlines the common bridge seismic deficiencies and the structural engineering research associated with them. The right-hand side of the table indicates the possible retrofit solutions, discussed in Chapter 3, for each of the seismic deficiencies. The various deficiencies are considered below.

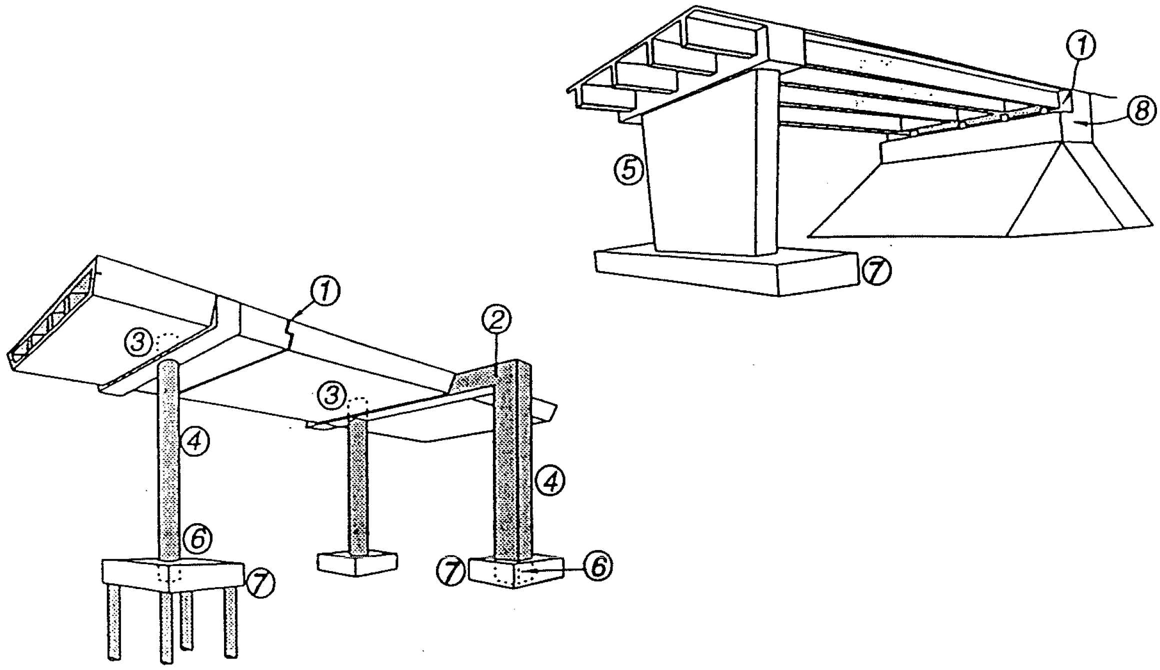

1. *Movement joints: seats, restrainers, and bearing supports*

2. *Outrigger beams and joints*

3. *Cap beam joints and bar anchorage*

4. *Columns*
   - *(a) Concrete confinement*
   - *(b) Restraint of longitudinal bar buckling*
   - *(c) Shear strength*
   - *(d) Lap splices*

5. *Pier Walls*

6. *Column to foundation joints and bar anchorage*

7. *Footings and pile foundations*

8. *Abutments*

NOT ILLUSTRATED:
Pounding
Soil liquefaction
Surface fault displacement
Slope failure/landslide
Tsunami

Figure 2.1 Potential regions of seismic deficiencies for typical reinforced concrete bridge structures.

Unseating of Bridge Spans

The unseating of bridge spans has been a common type of seismic failure in bridges. The bridge girders move off their supports at unrestrained movement joints because actual seismic displacements exceed the displacements provided for in the design of the girder seats. Even where restrainer mechanisms have been provided, they may have inadequate strength to keep the spans from unseating. Bridges with support lines skewed to the axis of the bridge have a greater tendency to unseat than right angle bridges; skew bridges undergo increased lateral displacements in earthquakes caused by the plan rotation of the bridge superstructure [Priestley et al 1992a]. Research on the earthquake response of bridge structures with movement joints has been carried out by Maragakis et al [1993], Singh and Fenves [1993], and Priestley [pers. comm. 1993].

Beams and Beam-Column Joints

This category includes seismic deficiencies which have been identified in outrigger and non-outrigger cap beams and beam-column joints, and in two-level bridge structures.

Outrigger Beams

Outrigger piers are commonly used in US freeway bridge structures at locations where underpassing roadways or other obstacles do not allow columns directly beneath the bridge deck. Seismic deficiencies of outrigger beams were revealed in the 1989 Loma Prieta, California earthquake. The principal deficiencies of these beams are: (1) inadequate shear capacity, particularly when seismic shears are additive to dead load shears, (2) the premature cut-off of top-beam reinforcement to resist negative moments, and (3) insufficient anchorage of longitudinal beam reinforcement into the column. Outrigger beams in San Francisco's China Basin viaduct and Oakland's Cypress structure had these deficiencies for transverse earthquake loading, and were damaged by the Loma Prieta earthquake. Outrigger beams are also potentially vulnerable to torsional failure caused by earthquake response in the longitudinal direction [Priestley et al 1992a]. Sometimes the superstructure flexural capacity to sustain longitudinal-direction column hinging or outrigger torsion is lacking. Also calculations often show that the shear-friction capacity of the outrigger-beam to superstructure connection is deficient [Zelinski pers. comm. 1994].

The ninety-degree joints connecting outrigger beams to columns (knee joints) are also prone to earthquake damage. The deficiency of these joints is not limited to pre-1970 designs: a 1984-built outrigger knee joint for the I-980 freeway structure in Oakland was damaged by the Loma Prieta earthquake. This knee joint lacked sufficient joint shear reinforcement horizontally, where 6.4 mm diameter (W5) wire reinforcement at a 100 mm (4-inch) spacing was used, and vertically, where the 57 mm (#18) column bars were not hooked and were stopped 300 mm (12 inches) below the top of the 2.4 m (8 ft) deep joint. In addition to the lack of adequate shear reinforcement, the detailing of the beam and column longitudinal bars with ninety-degree bends at the outside corner of the knee joint is problematic. Under cyclic opening and closing moments in the plane of the knee-joint, the cover concrete of the outside corner spalls off, allowing the ninety-degree bends of the longitudinal bars to open up so that they can no longer support the compression force of the diagonal strut which is the mechanism of joint shear resistance [Priestley et al 1992a]. Research on outrigger beams and knee joints has been carried out by Ingham et al [1993] and Thewalt and Stojadinovic [1993].

Two-Level Bridge Structures

A similar condition to the outrigger knee joints is found in the lower beam to column joint in the double-deck bridge structures found in San Francisco and Oakland, California, which were damaged by the Loma Prieta earthquake. These bridges include the I-880 Cypress structure which collapsed, the Embarcadero freeway which was damaged and was subsequently torn down, and the I-280 freeway which was damaged and is being retrofitted. In these T-shaped joints, seismic deficiencies include poor anchorage of beam flexural reinforcement into the joint and the lack of adequate shear reinforcement [Priestley et al 1992a]. Tests on surviving portions of the Cypress elevated highway structure [Bollo et al 1990] and on laboratory specimens [Moehle and Sawyer 1993] provide further information on these types of structures.

Beam-column Joints

The exterior beam-column joint of a (non-outrigger) multi-column bent is similar to the outrigger knee joint. Non-outrigger bents are more common than outrigger bents, but there has been less evidence of earthquake damage to joints in non-outrigger piers. The interaction of the elastically responding bridge deck girders perpendicular to the bent can provide beneficial lateral confinement to the beam-column joints. Such confinement is not present in outrigger joints. Nevertheless, in the 1971 San Fernando, California earthquake, shear failure occurred in the beam-column joints of several multi-column bents.

Inadequate anchorage of column longitudinal reinforcement into beam-column joints is a common seismic deficiency. Seible et al [1993] have carried out full-scale tests on joints with 57 mm diameter (#18) column longitudinal bars with relatively short anchorages. The actual anchorage capacity may be better than the codes imply, because the bond failure mechanism occurs in the bearing of the steel deformations on confined concrete rather than the splitting of the concrete assumed in design codes. Park et al [1993] have improved the anchorage of plain-round (undeformed) bars by welding anchorage plates to the ends of the straight bars. To avoid overly conservative assessments of apparently deficient joints, mechanisms of joint shear transfer and possible bond failure patterns should be carefully investigated [Priestley 1993a, Priestley et al 1992a]. The techniques for such an assessment are as yet not well established in the structural design profession.

Table 2.1 **Summary of bridge seismic deficiencies, recommended retrofit methods, and related research.**

Bridge Seismic Deficiencies	Observed Earthquake Damage	Research on Earthquake Performance	Recommended Retrofit Methods	Research on Retrofit Methods	Examples of Application of Retrofit Methods	Remarks on Design Criteria
1 Movement joints, seats, restrainers, bearings	Numerous earthquakes, particularly 1971 San Fernando	On Restrainers: University of California Los Angeles (18,19) Babaei and Hawkins [1991] Dynamic analysis of structures with movement joints: Maragakis et al [1993], Singh and Fenves [1993], Priestley [pers. comm. 1993]	High-strength bar restrainers, looped cable restrainers, straight-through cable restrainers	University of California Los Angeles (18,19)	Numerous applications in California and elsewhere	Analysis techniques and design criteria need further development. Babaei and Hawkins [1991] present typical details and cost estimates.
			Steel pipe seat extenders	Cypress Viaduct tests of Dec. 1989 [Zelinski 1994]	Numerous applications in California	
			Concrete or steel bracket abutment seat extenders and stopper devices, steel chain and steel plate restrainers	-	Applications in Japan and elsewhere	
			Base isolation and energy absorbing devices	Various research	Pioneered in New Zealand. Used on several bridge retrofit projects in New Zealand and the United States (68), Used in Italy, Japan and Canada [Skinner et al 1993]	Inelastic behaviour of isolators can be modelled elastically using equivalent stiffness and increased damping - Generic specifications, needed
			Elimination of movement joints by deck slab replacement	-	Used in Italy	Applicable only to shorter bridges
			Addition of high-strength slack restrainers to distribute movement to several joints	-	Proposed for Thorndon Bridge, New Zealand	Applicable to bridges with closely-spaced movement joints
2 Cap beams	1989 Loma Prieta	-	Strengthening by concrete or steel jacketing and pre-stressing, retrofit by adding a new link-beam below	Proof tests at UC Berkeley and UC San Diego [Zelinski 1994]	China Basin Viaduct, San Francisco (jacketing)	Designed to force plastic hinging into columns
			Cored internal prestressing, Fibre wrapping and prestressing	Univ. of British Columbia, with Klohn-Crippen Assoc.[Kennedy 1995]	Oak St, and Granville St Bridges, British Columbia	At Oak St designed to force hinging into columns. At Granville St designed for elastic earthquake forces

Table 2.1 Continued

Bridge Seismic Deficiencies	Observed Earthquake Damage	Research on Earthquake Performance	Recommended Retrofit Methods	Research on Retrofit Methods	Examples of Application of Retrofit Methods	Remarks on Design Criteria
3 Outrigger beam knee joints	1989 Loma Prieta	Ingham et al [1993], Thewalt and Stojadinovic [1993]	As for cap beams, plus removal of existing knee joint concrete and rebuilding of joint	Ingham et al [1993], Thewalt and Stojadinovic [1993]	I-980 Freeway, Oakland California	Designed to force hinging into columns or ductile - torsional hinging in capbeam. Reduces capbeam cracking in minor earthquakes.
4 Anchorage of column longitudinal bars in beam-column joints	1971 San Fernando	Seible et al [1993], Priestley [1993a]	Addition of new link beam, Prestressing of joint region, Clamped steel confining jacket.	-	Santa Monica Viaduct, Los Angeles (Link beam)	Design criteria and retrofit methods need development.
			Added anchorage end plates on straight bars	Park et al [1993]	-	-
5 Column flexural confinement and bar buckling restraint	1971 San Fernando	University of California (UC) San Diego (16), UC Berkeley (22), UC Irvine (23), Washington State University Pullman (29), University of Canterbury (numerous)	Elliptical (or circular) steel jacketing	UC San Diego (15)(26) [Yuk Hon Chai et al 1991], Japan Public Works Research Institute (29)	Numerous applications in California, Used for circular columns in Japan. Proposed for Thorndon Bridge, New Zealand. Used in British Columbia.	Detailed design criteria are provided by Caltrans [1992]. Can be full or partial height. Fibreglass method needs material certifications and durability assurances.
			Active fibreglass jacketing	UC San Diego (27) British Columbia [Kennedy 1995]	Trial applications in California for circular columns. Used in British Columbia for square columns.	
			Reinforced concrete jacketing	Rodriguez and Park (61)	Applications in Japan and British Columbia	-
			Removal and replacement of cover concrete with added transverse reinforcing steel	University of Canterbury [Dekker and Park 1992]	-	-
			External steel hoops with turnbuckles	University of Washington, Seattle (1)	-	For circular columns only. Typically more costly than other methods
			Prestress wire jacketing	UC San Diego	-	
			Carbon fibre jacketing	Japan Highway Public Corporation (32)	-	-

Table 2.1 Continued

Bridge Seismic Deficiencies	Observed Earthquake Damage	Research on Earthquake Performance	Recommended Retrofit Methods	Research on Retrofit Methods	Examples of Application of Retrofit Methods	Remarks on Design Criteria
6 Column lap splices	1971 San Fernando 1982 Urakawa-oki 1989 Loma Prieta	UC San Diego (15) Yuk Hon Chai et al [1991]	Partial confinement elliptical (or circular) steel jacketing (with polyethylene cusion)	UC San Diego [Yuk Hon Chai et al 1991] (only circular column tested)	Numerous applications in California on rectangular and circular columns	Intended to improve ductility capacity, while keeping moment capacity limited by allowing some lap-splice slippage [Caltrans 1990].
			Elliptical (or circular) steel jacketing (Full confinement), Active and passive fibreglass/epoxy jacketing (Full confinement), Reinforced concrete jacketing, Added transverse reinforcing, External steel hoops, Prestress wire jacketing, Carbon fibre jacketing	See item 5	See item 5	See item 5
			New foundation topping	See item 9	See item 9	Effective for thick toppings which cover lap-splice region
7 Column Shear Strength	1971 San Fernando, 1987 Whittier, 1989 Loma Prieta	UC San Diego (28), University of Canterbury (numerous) University of British Columbia with Klohn-Crippen Associates [Kennedy 1995].	Elliptical (or circular) steel jacketing (Full confinement), Passive fibreglass jacketing (Partial confinement), Reinforced concrete jacketing, Added transverse reinforcing, External steel hoops, Prestress wire jacketing, Carbon fibre jacketing	See item 5 Univ. of British Columbia with Klohn-Crippen Assoc.	See item 5	See item 5, Jackets are typically full height, except for some flared columns
8 Pier Walls	1995 Hyogo-ken Nanbu (Kobe) earthquake	Haroun et al [1993] (33)	Steel Jacketing with through bolts	UC Irvine (33) [Haroun et al 1993] Tests in weak direction	Used in California, with full confinement and partial confinement jackets	Design criteria need development. Caltrans does not retrofit if axial load is low and ductility demand $\leq$ 4.0

Table 2.1 Continued

Bridge Seismic Deficiencies	Observed Earthquake Damage	Research on Earthquake Performance	Recommended Retrofit Methods	Research on Retrofit Methods	Examples of Application of Retrofit Methods	Remarks on Design Criteria
9 Column to Foundation Joints	1971 San Fernando	Yan Xiao et al [1993], Yuk Hon Chai et al [1991]	New foundation topping	Yan Xiao et al [1993]	Used in California. Proposed for Thorndon Bridge, New Zealand	Effectiveness is limited. Design criteria need development. Caltrans recommends connecting topping with perimeter ties to bottom reinforcing mat.
			Prestressing through foundation	-	Proposed for Thorndon Bridge, New Zealand	Design criteria and research are needed.
10 Footings and Pile Caps	No failures noted	Yan Xiao et al [1993]	Foundation strengthening with new piles or soil anchors, foundation topping and prestressing (See item 9).	-	Applications in California, including China Basin Viaduct. Oak St. Bridge and Queensborough Bridge, British Columbia.	Further study of foundation rocking could reduce the need to retrofit.
11 Abutments	Failures due to poor soil conditions in 1990 Costa Rica, 1987 Edgecumbe New Zealand, and other earthquakes	UC Davis (20)	Anchor slab, Tension tie backs, Anchor piles	-	Applications in California and Japan	Analysis and design criteria need further development.
Retrofit Methods Addressing Multiple Deficiencies						
12 Two-level bridge structures	1989 Loma Prieta	Bollo et al [1990], Moehle and Sawyer [1993]	Substantial rebuild of structure with added longitudinal beams	Priestley et al [1992b] Moehle et al [1993]	I-280 Freeway, San Francisco, California	
13 Columns and cap beams in multi-column bents	See items 5, 6, 7	See items 5, 6, 7	Infill structural wall between columns	-	Used in Japan, US, and British Columbia. Proposed for Thorndon Bridge, New Zealand	Eliminates transverse moments in cap beams, but can increase loads to foundations.

Table 2.1 Continued

Bridge Seismic Deficiencies	Observed Earthquake Damage	Research on Earthquake Performance	Recommended Retrofit Methods	Research on Retrofit Methods	Examples of Application of Retrofit Methods	Remarks on Design Criteria
14 Column and beam deficiencies	See items 2, 5, 6, 7	See items 2, 5, 6, 7	External longitudinal post-tensioning, cored internal post-tensioning	-	Used in Japan, US, and British Columbia	Applicable to elements protected from failure by other ductile elements
15 Column or pier wall deficiencies	See items 5, 6, 7, 8	See items 5, 6, 7, 8	Added reinforced concrete outrigger frame	-	Used in California	Cap beam retrofit is difficult.
Site-Related Seismic Deficiencies						
16 Pounding of adjacent structures	1989 Loma Prieta	Kasai et al [1990], Assessment of Auckland Harbour Bridge, New Zealand [Kennedy 1995].	-	-	-	-
17 Soil Liquefaction	1990 Costa Rica and other earthquakes	Various research	Ground improvement methods such as vibro replacement (stone columns), jet grouting, driven displacement piling compaction grouting, and ground containment using bored piles, jet grouting, or concrete walls.	-	Vibro replacement (stone columns) and jet grouting proposed for Thorndon Bridge, New Zealand, and used in British Columbia.	-
18 Potential for landslides, surface fault rupture and tsunami	1993 Hokkaido-nansei-oki and other earthquakes	Various research		-	-	-

Note

References given in [ ] are listed at the end of this report.
Items not referenced or references with ( ) are taken from Priestley et al [1992a]; the number in ( ) corresponds to the reference listed in that report.

Columns and Pier Walls

Several deficiencies in bridge columns have been evident in past earthquakes. Columns can have inadequate flexural resistance because of: (1) understrength, (2) inadequate ductility capacity, or (3) insufficient lap splices or the premature termination of reinforcement. Because of the inadequate seismic criteria required by pre-1970 design codes, understrength of columns is common. This deficiency is somewhat mitigated, however, by the conservative design practice of assuming a linear axial load versus moment interaction, which was customery for bridges designed before the 1970s [Priestley et al 1992a].

Concrete Confinement and Bar Buckling

Few existing bridge columns have enough strength to permit them to respond elastically to major earthquakes. Thus most columns need to respond inelastically in a ductile manner. It is now well known that to ensure ductile performance, a close spacing of transverse tie reinforcing is usually required to confine the compressed concrete of the column core in plastic hinge regions. The transverse ties are also necessary to prevent the longitudinal bars from buckling. Bridge columns designed before the early 1970s typically lack this transverse reinforcement. Dramatic plastic hinge failures occurred in bridge columns with low levels of transverse reinforcing in the 1971 San Fernando earthquake, in the Struve Slough bridge during the 1989 Loma Prieta earthquake [Priestley et al 1992a], and in the 1994 Northridge earthquake.

Lap Splices and Cut-off of Reinforcement

The lap splices of bridge column reinforcement typically were designed based on gravity loads or unrealistically low service-level earthquake forces and often cannot transfer the yield-level forces that will occur in the reinforcing steel under severe earthquakes when the splices are located in plastic hinge regions. In the Loma Prieta earthquake, columns suffered damage at their bases attributed to lap-splice bond failure. Columns of the Shizumai bridge in Japan suffered brittle failure at midheight of the column during the magnitude 7.1 1982 Urahawa-ohi earthquake caused by the premature termination of a portion of the flexural reinforcing extending up from the foundation [Priestley et al 1992a].

Shear Strength

Inadequate column shear strength is another common deficiency in existing bridges. Current capacity-design practices (used in New Zealand since the late 1970's and in California since the early 1990's) dictate that the shear strength of a member should exceed its flexural strength, so that only a ductile flexural mechanism can occur. This was not the design practice for pre-1970 bridges. Because of flexural overstrengths and low design shears, it is not uncommon to find bridge columns with a shear strength less than one-third of the flexural strength. This was the case for the I-5/I-605 separator, a major freeway bridge structure which suffered dramatic column shear failures in the 1987 Whittier

California earthquake. Similar shear failures occurred in bridge columns during the 1971 San Fernando earthquake, the 1994 Northridge earthquake, and the 1995 Hyogo-ken-Nanbu (Kobe) Earthquake. In some cases, also evident in the San Fernando tremor, shear failure can occur subsequent to flexural plastic hinging. This is a consequence of the reduction in capacity of shear mechanisms assigned to concrete (the "V_C" term) in plastic hinge regions once flexural degradation begins. For most existing bridges it was not recognized that the concrete in the hinge regions will inevitably be damaged and that these regions should be designed more conservatively for shear than non-plastic hinge regions [SANZ 1982, Priestley et al 1992a].

Research on the seismic behaviour of existing bridge columns is extensive. Recent test programs related to retrofitting have been carried out at the San Diego, Berkeley, and Irvine campuses of the University of California, and at Washington State University, Pullman [Priestley et al 1992a].

Pier Walls

Pier walls for bridges are another area of potential seismic deficiency. Until the 1995 Kobe, Japan earthquake, there seems to have been no reported earthquake damage to the pier walls of bridges. But reinforced concrete structural walls in buildings, designed on a similar basis to many bridge pier walls, have been damaged in several earthquakes including the 1964 Alaska earthquake and the 1989 Loma Prieta earthquake. As with columns, the desired failure mode for pier walls is flexural rather than in shear. Park and Paulay [1975] and Paulay and Priestley [1992] describe the undesirable failure modes of reinforced concrete structural walls: diagonal tension or compression failure caused by shear, sliding shear along construction joints, failure of lap splices or anchorage, buckling of compression reinforcement, and, in the case of thin walls, wall instability. It is likely that most pier walls in existing bridges have insufficient shear strength compared to their flexural strength about the strong axis. However, the shear strength of the walls may exceed the foundation capacity so that foundation rocking or pile failure occurs, precluding damage to the wall itself. Research on the seismic behaviour of pier walls has been carried out at the University of California, Irvine [Haroun et al 1993, Priestley et al 1992a].

Pounding of Adjacent Structures

Structural pounding of bridges can cause damage during earthquakes. In the I-280 freeway in San Francisco, a separate connector roadway structure was built alongside the main freeway columns with 150 mm (6 inches) of clearance. This separation proved inadequate during the Loma Prieta earthquake and both structures suffered pounding damage. In many past earthquakes, building structures have provided evidence of the disastrous effects of pounding. In the 1985 Mexico City earthquake, pounding of adjacent buildings caused brittle column failures leading to severe damage or collapse of several multi-story reinforced concrete frame structures [Aguilar et al 1989]. Recent analytical research has shown that pounding impact forces can be up to ten times the magnitude of typical seismic forces [SEAONC 1991, Kasai et al 1990].

Foundations and Abutments

Bridge foundations are another area of potential seismic deficiency. Currently hundreds of bridges in California are having their footings and pile caps strengthened to resist earthquake forces. Common deficiencies include: (a) the lack of a top reinforcement mat for seismic flexure and uplift, (b) the lack of footing shear reinforcement, (c) the lack of joint shear reinforcement at the column-foundation joint, and (d) the bending of the main column reinforcement outward rather than inward at the base, aggravating joint shear problems [Priestley et al 1992a]. Figure 2.2 shows other possible failures in bridge foundations, as identified by the Applied Technology Council [ATC 1983].

Despite the perceived need for bridge foundation retrofit, earthquake damage to foundations has seldom been reported. Only a few of the failure modes depicted in Figure 2.2 have actually been observed in earthquakes. There are several possible reasons for this:

(1) Foundations are usually buried and thus not inspected following an earthquake,

(2) The premature failure of the structure above the foundation due to column shear, joint failure, lap splice failure, etc, may have prevented the full plastic column moment from being applied to the foundation, and

(3) Foundation rocking may have occurred, limiting the forces in footings or pile-caps.

A critical seismic deficiency for bridge foundations is the potential anchorage failure of column bars. This deficiency can be closely related to insufficient joint shear capacity and the lack of a top mat of footing reinforcement. Inadequate anchorage of column bars into footings allowed the complete pull-out of the column bars resulting in the collapse of a freeway structure in the San Fernando earthquake [Priestley et al 1992a].

Although not reported for bridges, pile shear failures have been observed for buildings. In the 1993 Hokkaido-nansei-oki earthquake, a school building of nearly new construction displaced laterally 40 cm because of pile shear failures. This failure may not have been observed except that the soil liquified and slumped away from the building exposing the piles [Tanaka pers. comm. 1993]. Yan Xiao et al [1993] have studied the seismic behaviour of bridge column footings and have done tests on the rocking response of footings.

For earthquakes acting in the longitudinal direction of a bridge, almost all of the seismic force may be transferred into the abutments. (This depends on the degree of contact between the end of the bridge, the abutment, and the approach fill.) Abutment failures have been evident in past earthquakes mainly caused by poorly compacted or liquifiable soil conditions. Damage caused by soil slumping and consequent abutment settlement or rotation occurred to the Rio Viscaye, Rio Banano, and Rio Bananito bridges during the 1990 Costa Rica earthquake [Priestley et al 1992a]. Large scale tests on the seismic resistance of bridge abutments have been conducted at the University of California Davis [Maroney and Chai 1994].

Geotechnical Hazards

Soil liquefaction is a seismic hazard that needs to be considered when evaluating an existing bridge. Typically liquefaction potential is highest for cohesionless soil layers which are below or near to the

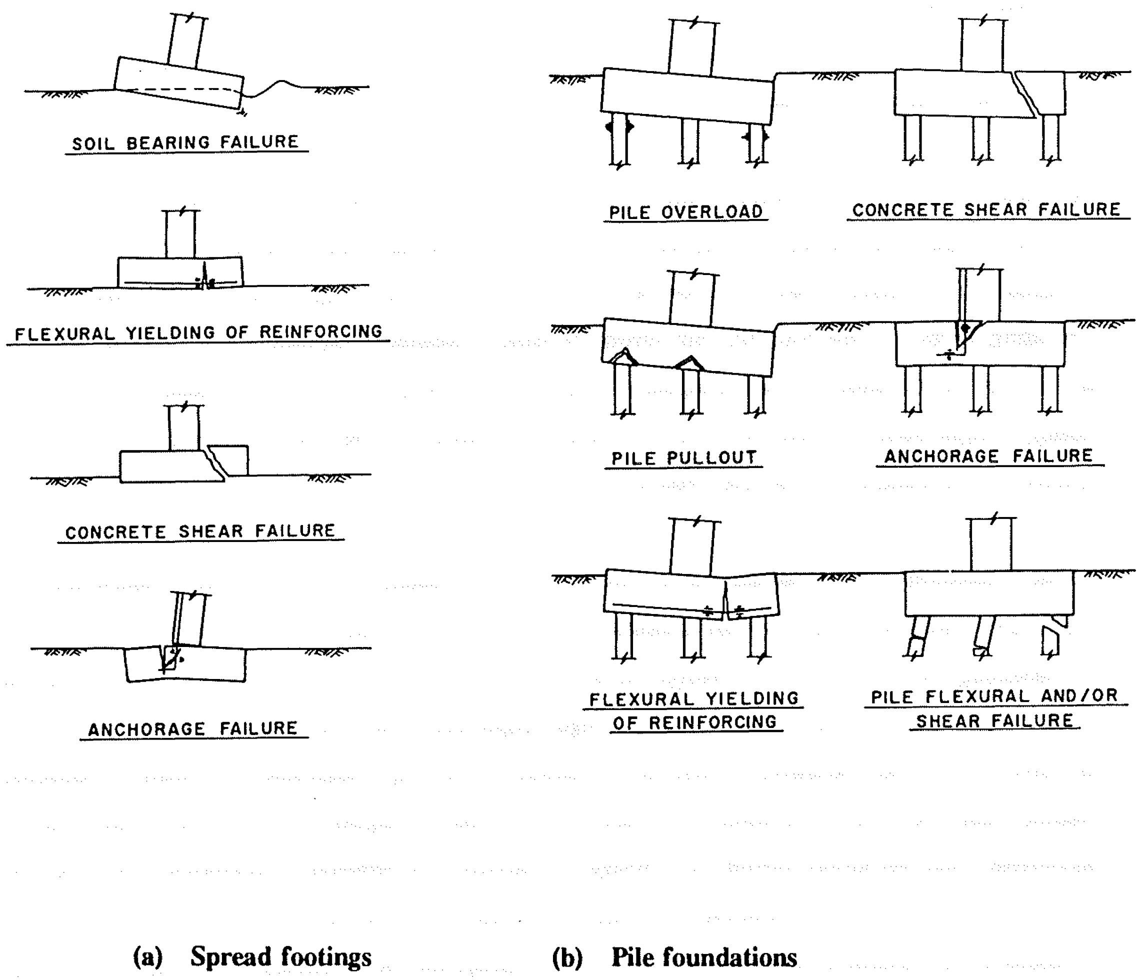

Figure 2.2 Possible failure modes for bridge foundations [ATC 1983].

groundwater table. Soil liquefaction beneath footing or pile foundations can lead to the displacement of bridge supports. Unrestrained simply supported spans have frequently collapsed from liquefaction-induced displacements. Examples of such failures are found in the 1964 Alaska earthquake, the 1985 Chile earthquake, and the 1990 Costa Rica earthquake.

In addition to liquefaction, other soil-related seismic hazards exist. Bridges on sloping sites can be damaged by earthquake-induced landslides or slope failures. Bridges located near or over faults can be damaged by the structural displacements induced by surface fault rupture. The potential for tsunami should also be considered when investigating the seismic hazards to a bridge.

2.2 Procedures and Criteria for the Seismic Evaluation of Bridges

To identify the seismic hazards of existing bridges and to assess the severity of these hazards in a consistent manner, seismic evaluation procedures and criteria are needed. A systematic procedure for seismic evaluation is useful because (a) a step-by-step or checklist approach, following the seismic-force path of the structure, will ensure that no seismic deficiencies are overlooked, and (b) a more uniform basis for assessment assumptions can result. Evaluation criteria are required to define what is acceptable seismic performance for a given bridge.

The evaluation criteria for existing bridges should be different from the design criteria for new bridges. For new bridge construction, conservative design and detailing requirements generally cost little compared to the seismic safety they provide. However, few older bridges can meet the requirements of building codes for new bridges, and retrofit to these standards is expensive. Some older bridges may be able to withstand severe earthquakes despite not meeting all code requirements. Criteria for existing bridges must be based on a more in-depth understanding of the available strength and ductility capacity of "substandard" structural details.

Seismic evaluations can be carried out at different levels of detail. For a first-pass identification of potentially vulnerable bridges, a brief assessment is usually appropriate. As shown in Chapters 11 and 12, discussing the prioritization of bridge retrofitting, this assessment may be based on only a handful of risk factors such as year of construction, bridge height and skew, soil type, and seismic zone. At the other end of the spectrum, a detailed evaluation—involving assessment of as-built conditions, dynamic analyses, and calculation of plastic mechanisms, strengths, and ductility capacities—is appropriate once the actual retrofit of a bridge is planned. In between, evaluations involving (for example) only quick hand calculations of seismic demands and capacities may be required. This type of middle-level evaluation procedure is likely to be appropriate for secondary screenings of a bridge stock to identify the highest priority retrofits. With the limited availability of funds for bridge retrofitting, procedures for seismic evaluations of low to medium detail are important.

Priestley et al [1992a] have briefly reviewed the seismic evaluation methods used in Italy, Japan, New Zealand, and the United States. Further information on these methods is contained in the proceedings of the *International Workshop on the Seismic Retrofitting of Bridges* held in Bormio, Italy [Calvi and Priestley, 1991]. The most established seismic assessment methods have been two procedures from the United States: The Applied Technology Council *ATC 6-2* approach [ATC 1983] and the current procedure of the California Department of Transportation [Caltrans 1992], which are described below.

ATC 6-2 Evaluation

The *ATC 6-2* [1983] publication was a pioneering effort towards a consistent seismic assessment approach for bridge structures. Figure 2.3 shows a flow chart of the ATC procedure for evaluating existing bridges. The method requires the designer to follow the seismic load path for the bridge structure, and for evaluating existing bridges each element—eg, cap beam, column, or footing—to calculate the seismic force demand from analysis, and the element capacity. The demand on an element is considered to be the member forces resulting from a linear-elastic response spectrum (LERS) dynamic analysis for irregular bridges, or equivalent static lateral loads for regular bridges. The ATC procedure requires the demand to equal the sum of 100% of the response in one direction plus 30% of the response in the perpendicular direction, and vice versa.

ATC 6-2 recommends that bridges with movement joints be modelled with two separate analyses. In one analysis, a spring element is used to model the movement joint restrainer stiffness; in the second analysis the two sides of the joint are connected with a pin restraint. Column and foundation forces are taken as the worst of the two cases.

Element Capacities

The capacity of a member is determined based on conventional principles for calculating shear or flexural/axial strength, and is then multiplied by a ductility "indicator" (ie, ductility capacity) to give an equivalent capacity. Requirements for confinement and reinforcement anchorage and splices are similar to the New Zealand concrete code requirements [SANZ 1982]. For "substandard" details in existing bridges, the ductility indicator is reduced from that assigned to code-complying details.

For columns, ductility indicators are separately calculated for longitudinal bar anchorage, lap splices, column shear, and confinement. For confinement, the column ductility capacity depends on the amount of confining-steel area, the spacing of confining ties, and whether the ties are well anchored to the column core. The assigned column ductility capacity μ ranges from 2 to 6. For columns which fail in shear prior to flexural hinging, the ductility capacity is taken as 1. For columns which can begin to yield in flexure, the ductility indicator for shear ranges from 2 to 5.

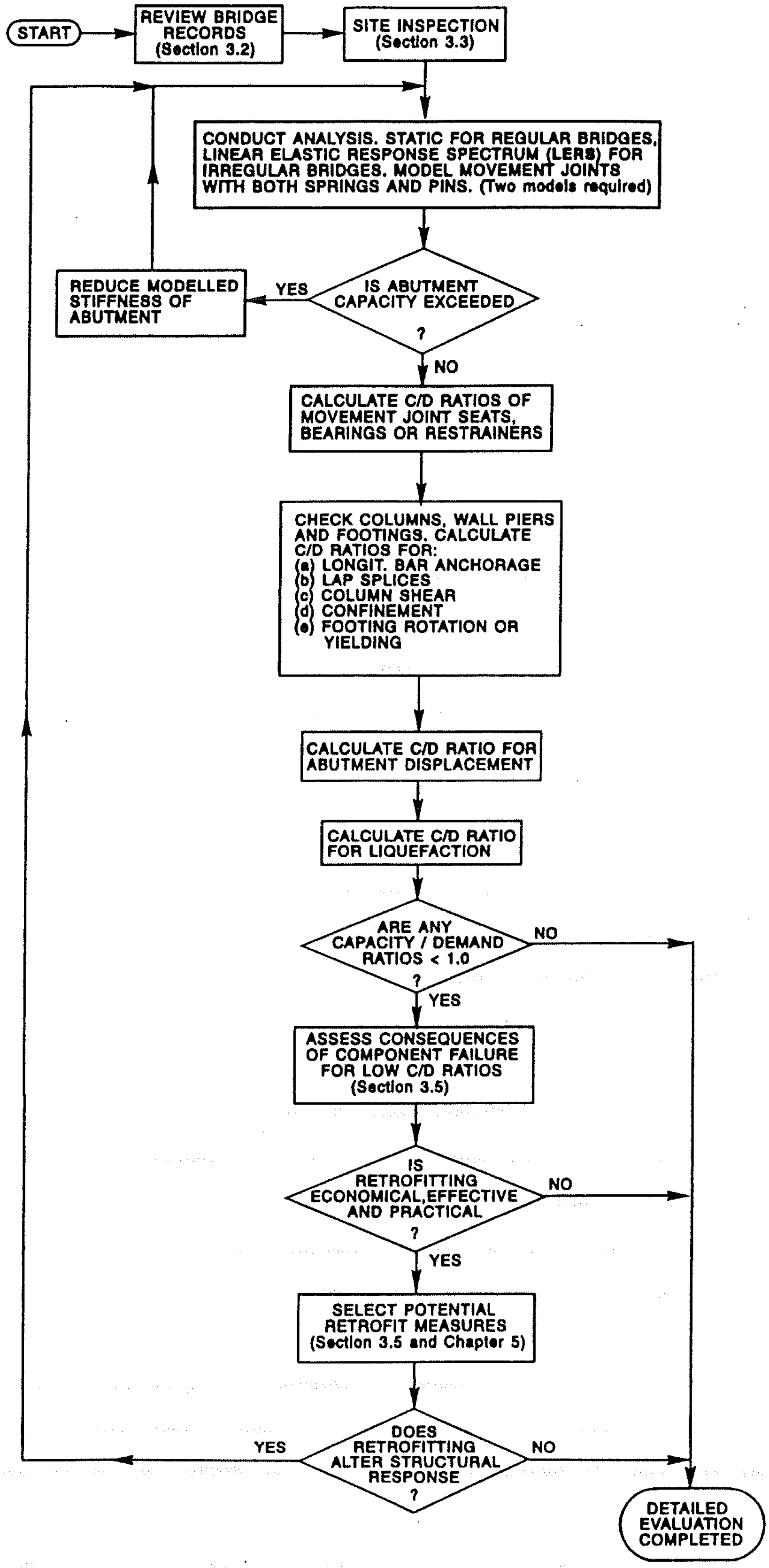

Figure 2.3 *ATC 6-2* **Seismic evaluation and retrofit procedure** [ATC 1983].

The ductility capacity calculation for column lap-splices considers the transverse reinforcement clamping the splices, and the splice length. The calculation for the capacity of bars anchored into foundations considers bar-anchorage length, transverse clamping-steel area, the presence of bar end hooks and their orientation inwards or outwards, and whether the foundation has a top mat of steel reinforcement.

For footings, ductility indicators, μ, are as shown in Table 2.2. The ductility indicators correspond to the failure modes shown in Figure 2.2.

At movement joints, support length demand is taken as the larger of (a) that resulting from the elastic analysis, or (b) the length N calculated by the following formula:

$$N_{[mm]} = 305 + 2.5L_{[metres]} + 10H_{[metres]},$$

where L is the length of the adjoining bridge segments, and H is the average height of supporting columns or wall piers adjacent to the movement joint. This empirical formula is used because elastic analyses may underestimate movement demands. If movement joint restrainers are used, the support length demand can be computed by considering only the elastic analysis method but a minimum restrainer force of 0.20 times the deadload reaction must be used because "a linear analysis of a bridge often results in relatively low bearing or restrainer forces" [ATC 1983].

Seismic demand for abutment displacements is taken as the computed abutment deflection in both the longitudinal and transverse directions. Displacement capacity of the abutments is taken as 76 mm (3 in) in the transverse direction and 152 mm (6 in) in the longitudinal direction. This seemingly arbitrary criterion is applied regardless of the abutment type or its construction details. The criterion is based on engineering judgement, experience from past earthquakes, and the consideration that large abutment displacements can prevent vehicles from using the bridge. For liquefaction, the capacity to demand (C/D) ratio is taken as the effective peak ground acceleration at which damaging liquefaction is expected to occur, divided by the design acceleration coefficient.

Capacity/Demand Ratios

When all of the demands and equivalent capacities are determined, the engineer computes a capacity to demand (C/D) ratio for each item checked. Structural elements with C/D ratios less than one are susceptible to failure. The smaller the C/D ratio, the more vulnerable the element is. An advantage of this approach is that it allows the engineer, by scanning the C/D ratios, to quickly identify the vulnerable elements of the structure. This process can quickly indicate those elements which are likely to require retrofitting.

The general approach of *ATC 6-2* has been applied to buildings in the subsequent publications *ATC 14* and the *NEHRP Handbook for the Seismic Evaluation of Buildings* [BSSC 1991] (formerly *ATC 22*). As the ATC evaluation approach has evolved, the procedure has become more thorough and more user-friendly. The *NEHRP Handbook*, now widely used in the United States by structural engineers evaluating buildings, provides checklists designed to identify seismic deficiencies in 15 common building structure types (plus a none-of-the-above category). The text of the handbook provides background information for assessing the seismic behaviour of particular types of structure elements. The handbook could be considered a "middle-level" evaluation procedure as previously described.

Table 2.2 Footing ductility indicators from *ATC 6-2* [1983, page 36].

Type of Footing	Factor Limiting the Capacity	Ductility Capscity μ
Spread Footing	Soil Bearing Failure	4
	Reinforcing Steel Yielding in the Footing	4
	Concrete Shear or Tension in the Footing	1
Pile Footing	Pile Overload, Compression	2
	Pile Overload, Tension	3
	Reinforcing Yielding in the Footing	4
	Pile Pullout at Footing	2
	Concrete Shear or Tension in the Footing	1
	Flexural Failure of Piles	4
	Shear Failure of Piles	1

<u>*Drawbacks to the ATC 6-2 Method*</u>

Priestley et al [1992a] identify the following four drawbacks with *ATC 6-2*:

(a) Some requirements such as reinforcement-anchorage provisions are overly conservative due to the assumption that full compliance with the current code is necessary for ideal performance,

(b) The method may be unconservative because demands are based on the elastic distribution of forces whereas the local ductility demand may be much higher than global ductility,

(c) Some critical areas of bridge structures such as beam to column connections and column to footing connections are not covered, and

(d) The calculation of demand, based on an elastic distribution of forces, ignores the capacity-design principle that the demand on non-yielding elements depends on the capacity of the yielding elements.

The first three of these faults can be corrected with little change to the basic *ATC 6-2* procedure. The last point requires a more fundamental (but beneficial) change in the seismic evaluation procedure. To properly understand the expected seismic performance of a structure, the engineer should determine the critical inelastic mechanism for the structure. Once the mechanism is identified, the associated strength and ductility capacities of the yielding elements should be calculated. The demand on the other

elements of the structure is then based on this mechanism strength. Elements whose capacity exceeds the demand based on the mechanism strength are protected from failure and need not be ductile. This is the basic procedure of the New Zealand-born concept called capacity design [SANZ 1982]. The concept is used explicitly by engineers in New Zealand and several other countries, but it is not consistently used in the United States. One advantage of an explicit capacity design procedure is that the engineer develops a feel for the actual seismic behaviour of the structure. A capacity design procedure proposed by Priestley [1992a] for the seismic evaluation of bridges is outlined later in this section.

Caltrans Evaluation Procedure

The seismic evaluation procedure which was used by Caltrans [1992] is a revised and simplified version of the *ATC 6-2* provisions, although in some areas much more specific procedures are provided. The Caltrans approach is outlined in Figure 2.4, which has been simplified (by the author of this report) from a procedural flow chart in *Memo to Designers 20-4* [Caltrans 1992] which describes the current Caltrans seismic evaluation procedure. The memo notes that "the designer must be cautioned to follow all load path demands and assure that no portion of the resisting structural frame is deficient. Seismic evaluation must not be limited to column or pier ductility capacities." However, unlike *ATC 6-2* or the *NEHRP Handbook*, the Caltrans procedure is not strictly organised around a load-path approach.

Bridge Analysis

Memo 20-4 alludes to the advantages and drawbacks of a collapse-mechanism type of analysis:

> "Structural evaluation at ultimate conditions (ie, failure analysis) is an extreme challenge to an engineer. Cookbook or prefabricated processes do not lend themselves well to such a situation. Yielding of a single element in a particular mode may not cause collapse.

> A potential failure mechanism must be achieved before collapse can take place. The distribution, or redistribution, of additional load in a structural system after incremental yielding will be different for each structure. Therefore, each structure must be thoroughly evaluated."

However, as Figure 2.4 indicates, the Caltrans method relies upon computer LERS analyses, rather than hand-calculations or collapse-mechanism calculations, for its first-stage evaluations. Recently the Caltrans evaluation procedure has been revised as shown in Figure 2.5 [Zelinski 1994].

Similar to the *ATC 6-2* recommendations, the Caltrans elastic analysis procedure requires that the stiffnesses assumed of abutments and movement joints be iteratively determined. *Bridge Design Aids* Chapter 14 [Caltrans 1990] provides guidance on dynamic analysis modelling assumptions. For longitudinal earthquake response, abutments provide horizontal restraint to a bridge principally in compression but not in tension. To account for this, Caltrans recommends allocating in the analysis model one half of the compressive stiffness to each abutment. This gives the correct total longitudinal stiffness to the bridge, and the correct output for abutment displacement, but the resulting compressive reactions to the abutments must be doubled.

Caltrans *Memo to Designers 5-1/5-2* [Caltrans 1990] discusses the expected seismic behaviour of various types of abutments. Caltrans policy is "to accept abutment damage caused by earthquake action provided the damage does not result in collapse of the bridge". Design loads and typical abutment details are provided in *Bridge Design Aids*, Chapter 1 [Caltrans 1990]. *Interim Memo to Designers 20-4* [Caltrans 1992] notes that "field inspections after the 1971 San Fernando earthquake suggest that abutments which moved up to 60 mm (0.2 ft) in the longitudinal direction into backfill soil appeared to survive with little need for repair." *Attachment A* to *Memo 20-4* gives the bridge retrofit designer additional guidelines for linear elastic computer modelling, using the STRUDL computer program. Curved bridges are modelled with several computer runs in an attempt to represent the different tension and compression stiffnesses of the abutments. Long bridges are modelled in units of up to five spans. The number of vibration modes included in the analysis is typically taken as three times the number of spans. As with *ATC 6-2*, orthogonal direction effects are accounted for by combining 100% of the response in one direction with 30% of the response in the perpendicular direction, and vice-versa. Live loads are not combined with seismic forces, except for outriggers and C-bents (ie, single-column bents with large gravity-load eccentricities) where the effects of live loads and vertical accelerations can be significant. Special response spectrum curves are used in cases of deep and very soft soil such as the bay mud prevalent in the San Francisco area.

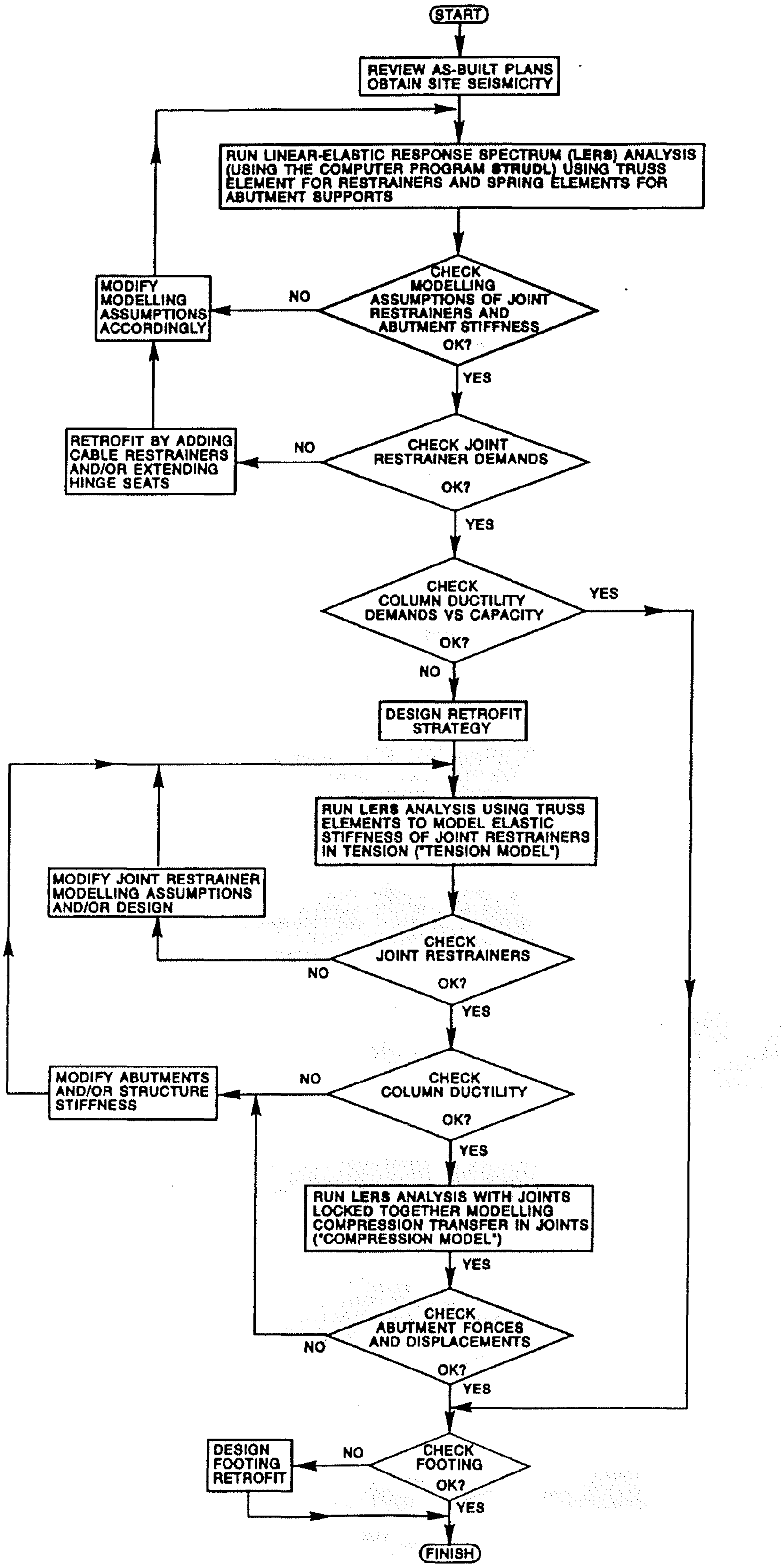

Figure 2.4 Caltrans seismic evaluation and retrofit procedure. Adapted from Caltrans Memo 20-4 [1992] (subsequently revised, see Figure 2.5).

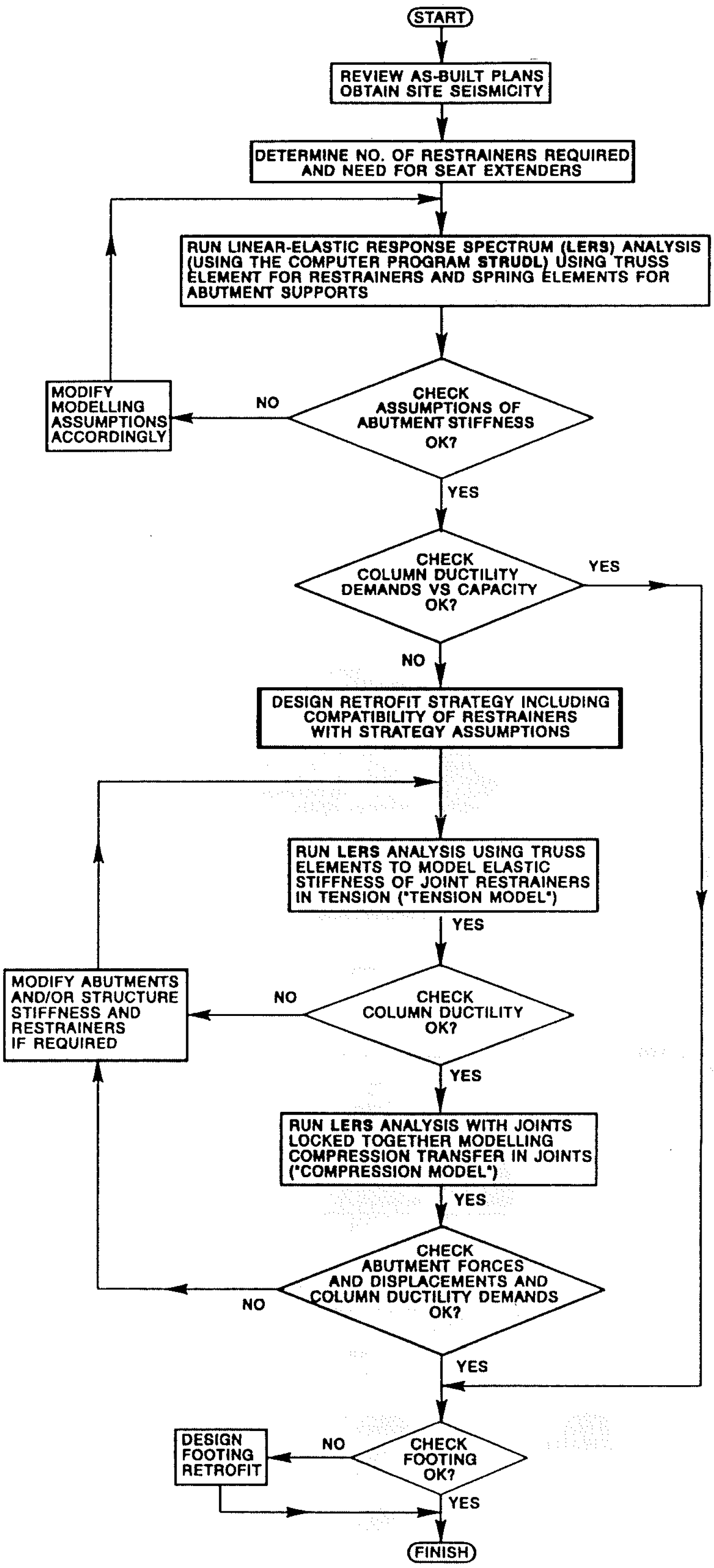

Figure 2.5 Revised Seismic Evaluation and Substructure Retrofit Procedure [Zelinski 1994].

Caltrans recommends that foundation springs be included in the computer model when such soft soil is present. Bridges less than 91m (300 ft) long, with no movement joints and with little or no skew are allowed higher damping values, 10 to 15% , compared to the 5% otherwise used [Caltrans 1992]. An equivalent static analysis is used to design restrainers at movement joints. In the Caltrans approach, "results obtained from [linear-elastic computer] analyses for the design of restrainer units have been proven to be inappropriate because of the demand to resist extremely large elastic column forces which are not actually attained" [Caltrans 1992]. The equivalent static method, described in Chapter 14 of *Bridge Design Aids* [Caltrans 1990] recommends that the longitudinal stiffness of bridge segments be calculated assuming that a majority of columns develop plastic hinges before the restrainer capacity is reached. In the example analysis given by Caltrans the longitudinal stiffness is calculated assuming that plastic hinges with zero stiffness (ie, pinned conditions) form in 75% of the column ends, resulting in a stiffness which is one-eighth of the elastic value. The restrainer forces are calculated based on this reduced longitudinal stiffness. Clearly, this approach involves gross approximations and assumptions. However, a study using non-linear models of movement joints indicates that the equivalent static approach may provide conservative results for the design of restrainers. [Priestley pers. comm. 1993]. More recent Caltrans policy is to model column end conditions according to expected behaviour or retrofit type. Well-confined column ends are assumed to develop a plastic hinge at full yield forces, while those retrofitted with partial-confinement jackets (allowing lap-splice slip) are assumed to develop into a pin condition [Zelinski 1994]. Caltrans *Memo to Designers 20-3* [Caltrans 1990] gives a useful discussion of design issues and practical considerations for the use of movement joint restrainers, considering typical bridge types and configurations.

Column and Pier-Wall Capacities

The Caltrans assessment of column capacities has been much more simplistic than the *ATC 6-2* procedure. Rather than calculating separate capacities for anchorage, lap splices, confinement, and shear, Caltrans uses a single ductility capacity depending on the column and bent type. These ductility capacities are shown in Table 2.3. In some cases the columns are modelled with a moment-released pin condition at one or both ends, thus reducing or eliminating the calculated contribution of the column to the required lateral strength of the structure. The pin condition is assumed at the bottom of a column if it has inadequate lap splice capacity at the base (ie, the lap length or amount of transverse "clamping" steel is deficient such that lap splices will slip before the column reaches its capacity). A pin condition at the base is also assumed if the column footing fails before the column capacity can be reached. At the top of the column, a pin condition is assumed if bar development into the superstructure is judged deficient, or if the superstructure fails before column capacity is reached [Zelinski 1994].

Pier walls are assumed to have weak-axis ductility capacities of up to 4.0. In many cases, however, the pier walls are assumed pinned at the base because the foundation fails before the wall's weak-axis moment capacity can be developed.

Table 2.3 Column ductility capacities assigned by Caltrans for assessment purposes [Caltrans 1992].

Column Type	Single Column Bent	Multi-Column Bent
Round Columns	1.5-2.0	2.0-3.0
Rectangular Columns	1.0	1.5-2.0
Round Column Pile Shafts (In-ground hinge only)	2.0-3.0	3.0-4.0

Note For multi-column bent bridges with larger amounts of redundancy, such as several sets of three (or more) column bents, the maximum of the allowable ductility range may be used on columns.

For single-column bent bridges, the maximum of the allowable ductility range should not predominate (more than 33% of the fixed column ends) the range of ductility demands for the total bridge. [Caltrans 1992].

This procedure for assigning ductility capacities has been questioned [Chapman pers. comm. 1994] because it is made without evaluating the likely failure mode of the column. The procedure also ignores the strength and flexibility of the foundation, which can affect the failure of the columns and the displacement capacity of the structure.

Attachment A to *Memo 20-4* [Caltrans 1992] provides background discussion on using the equal energy assumption to relate inelastic force reductions to ductility capacities. The assumption is thought to be applicable for shorter period structures. Despite this commentary, the Caltrans procedure seems to be based only on the equal displacement principle: ductility capacities are used directly as force reduction factors. This approach may be unconservative for shorter period structures. Zelinski [1994] notes, however, that "for short bridges and short-period structures, general retrofit practice includes a rotational displacement capacity check".

Caltrans computes column moment capacities based on probable material strengths. If the actual steel yield strength is not known, a strength of 1.1 times the specified yield is used. Column shear strength is compared to the demand corresponding to full flexural plastic hinging. *Attachment B* to *Memo 20-4* describes how column shear strength is assumed to vary with ductility. In potential plastic-hinge regions the shear stress carried by the concrete, v_c, is assumed to degrade linearly from 0.58 $\sqrt{f'_c}$ MPa (3.5 $\sqrt{f'_c}$ psi) prior to ductility 2, to zero at ductility 4. For columns with "moderate" levels of confinement, v_c is assumed to degrade from 0.58 $\sqrt{f'_c}$ MPa at ductility 2, to 0.20 $\sqrt{f'_c}$ MPa (1.2 $\sqrt{f'_c}$ psi) at ductility 4.

If the shear strength is less than the shear force corresponding to a flexural response at overstrength, then shear retrofit is required. Note that flexural overstrength is taken to be 1.5 times nominal flexural strength. If lap splices occur in a potential plastic hinge region, retrofit is required. As is discussed in Chapter 3, lap splice regions can be retrofitted with either a full-confinement or partial-confinement column jacket depending on retrofit design assumptions. As a final evaluation step, foundations are checked. Compared to new designs, more liberal soil and pile capacities are sometimes allowed for retrofit design.

Until recently little guidance has been given for the evaluation of pier walls about their strong axes. Current Caltrans policy assigns a ductility capacity of 2.0 to pier walls in the strong direction. It is felt that the massive size and ample horizontal reinforcing found in most pier walls will allow them to respond elastically to major earthquakes. In the strong direction of the walls, the foundation piles or pile connections are usually determined to fail (or "fuse") long before the wall would reach its shear or flexural capacity. Thus the designer would assume that either foundation sliding or rocking (whichever is more likely) will govern the earthquake response.

The Caltrans approach has been continually evolving in recent years. Some bridges are evaluated using a capacity design approach and an incremental plastic-mechanism (push-over) analysis. Until recently, these were usually borderline cases where a more detailed analysis can show that retrofit is not required. Initially, more than ninety percent of bridge retrofits were based on an elastic structural analysis only. Since 1993 however, the capacity-design and push-over analysis approach has been used on almost all major bridge evaluations. Caltrans engineers had felt that the elastic approach was easier to put into a step-by-step procedure, that the results were conservative, and that some added protection of serviceability in smaller earthquakes was provided as a side benefit [Zelinski pers. comm. 1993, 1994]. Note, however, that the Caltrans criteria are intended "to prevent collapse. ... Where structure serviceability is defined as a design requirement, a more conservative design approach than that outlined in this *Memo 20-4* must be followed."

Improved Evaluation Approaches

Researchers have shown that elastic analysis methods for bridges can be inadequate. Priestley et al [1992a] have developed an improved evaluation approach.

Inadequacies of Elastic Analyses

Priestley et al [1992a] provide a good discussion of the inadequacies of elastic dynamic analyses, noting that there "is a tendency to think, as a result of advances in computational models and the widespread availability in design offices of computers with considerable power, that our ability to predict the seismic demand on a bridge in terms of required moments, shears, displacements, etc, is at a much higher level of precision than our ability to predict capacities. This is a delusion, ...". The following inadequacies of elastic analysis are identified:

1 The basic parameters of elastic analysis and modal combination—mode shapes, periods and effective damping—are all altered by inelastic action,

2 Predictions of site seismicity and elastic response spectra involve "uncertainty" factors in the order of 2,

3 Modelling of movement joints involves significant and compounded approximations. Initial gaps, frictional resistance, three dimensional effects, and the effects of bridge curvature are usually neglected,

4 Abutments and foundations are poorly modelled especially in the usual case when the compression and tension stiffnesses of an abutment are different,

5 The effect of non-coherent (out-of-phase) seismic input is ignored. In softer soils seismic wavelengths may only be 150 to 450 m (500 to 1500 ft) causing out-of-phase effects in medium to long bridges, and

6 Pre-yield member stiffnesses are often poorly modelled.

Approach Recommended by Priestley et al

Instead of an elastic analysis and a check of capacity to demand ratios, Priestley et al [1992a] propose an approach more representative of actual structural seismic behaviour. The approach is more general than the Caltrans method and has not been developed into a "procedure". However, Figure 2.6 shows a flowchart (prepared by the author of the present report) which outlines the basic steps of the method. As shown in the figure, the method requires (1) explicit consideration of the serviceability, damage-control, and survival limit states, and (2) a diagnosis of the critical plastic mechanism for the structure. Rather than using an elastic dynamic analysis, the approach recommends a frame by frame incremental plastic mechanism, or "push-over", analysis which will identify critical structural elements and define

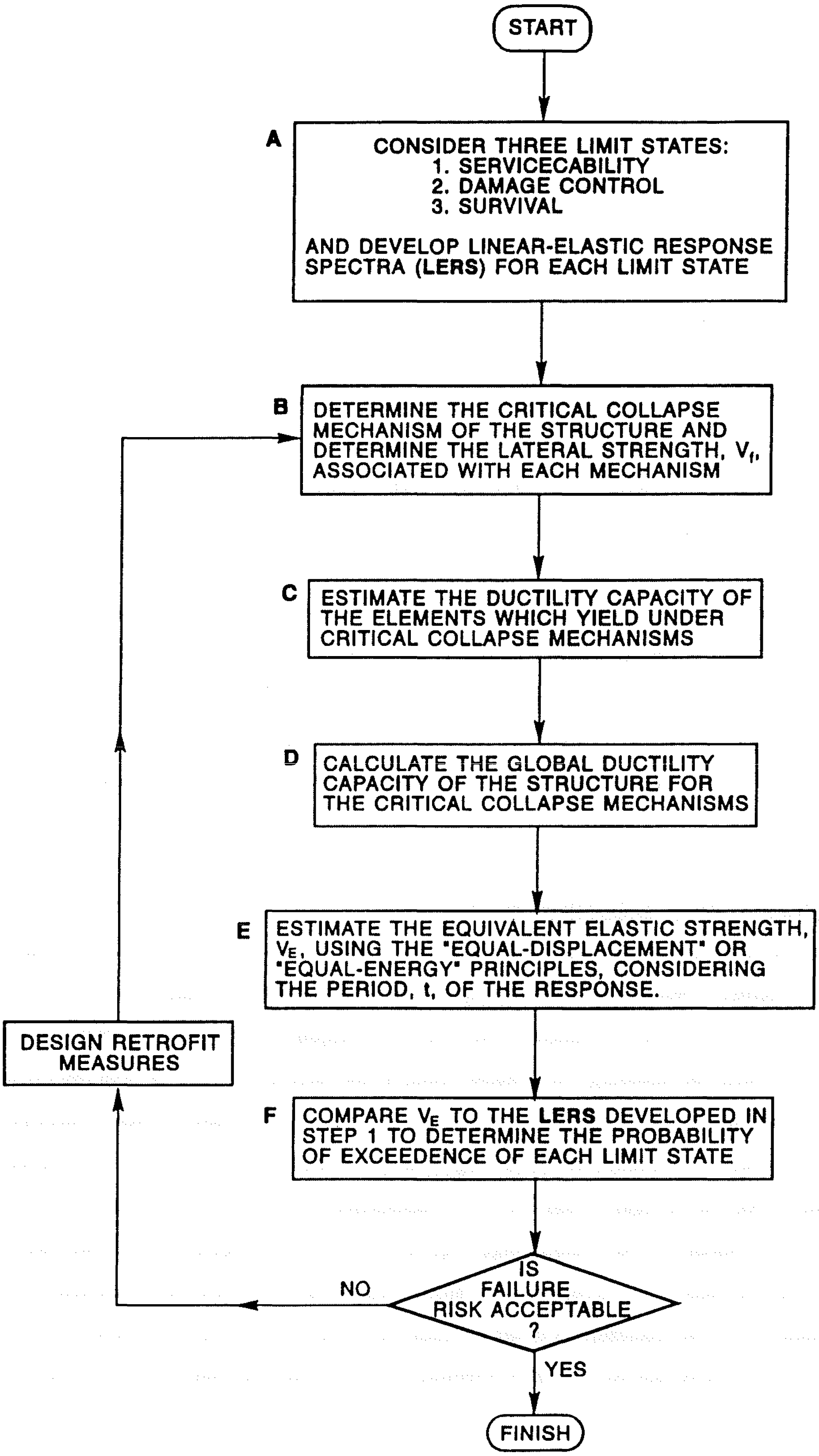

Figure 2.6 Seismic evaluation and retrofit approach proposed by Priestley et al. Adapted from Priestley et al [1992a].

a force-versus-deformation curve for each frame in the transverse direction. Such analyses have been used by bridge designers in New Zealand for many years [Chapman pers. comm. 1993] but their use in California is new, and until recently, for most bridge evaluations plastic analyses were not conducted. For longitudinal response the same push-over analysis is recommended, with the consideration that the moment transfer between a column and its superstructure may be limited by the torsion capacity of the cap beams. Note that although the above calculations can be done by hand, a computer program for plastic analysis would simplify the designer's job. The capability to write this type of program is straightforward, but no such software has been in wide use.

Along the same line of thinking, Moehle and Aschheim [1993] note that for the evaluation of bridge structures "linear analysis methods fail to capture essential response characteristics of structures for which inelastic response is expected." In agreement with Priestley et al, they recommend the use of non-linear "push-over" analyses for evaluating bridges. Elastic response spectrum analyses are still recommended for use in tandem with the "push-over" analysis, because they "are easily done and provide a useful benchmark for the estimation of inelastic displacement response". It is recommended that the relationship of strength and ductility capacity to equivalent elastic response to be based on the equal displacement principle for longer period structures, with linear interpolation to the zero period case for shorter period structures. This is the same as recommended by Priestley et al, except that some refinements are suggested in the determination of the period beyond which the equal displacement principle applies.

Evaluation of Member Strengths and Ductility Capacities

In the Priestley et al evaluation approach, strengths and ductility capacities are to be calculated as realistically as possible. Several guidelines are provided, and areas where further research is needed are indicated. The guidelines recommend that flexural strengths be based on probable material strengths. An approach for assessing the flexural strength and ductility of sections with inadequately anchored or spliced longitudinal bars is presented. More test results are needed to further quantify this approach for the range of anchorage or splice lengths and amount of transverse steel encountered in existing bridges. Flexural strength versus ductility relationships are suggested for columns with poor confinement or lap splices in the plastic hinge region, as shown in Figure 2.7. Note that such relationships could be used in an incremental collapse mechanism or "push-over" computer analysis program. Equations for the prediction of shear strength are given which have been shown to be more accurate than current code equations. Further refinements to the proposed equations have subsequently been made [Priestley et al 1994].

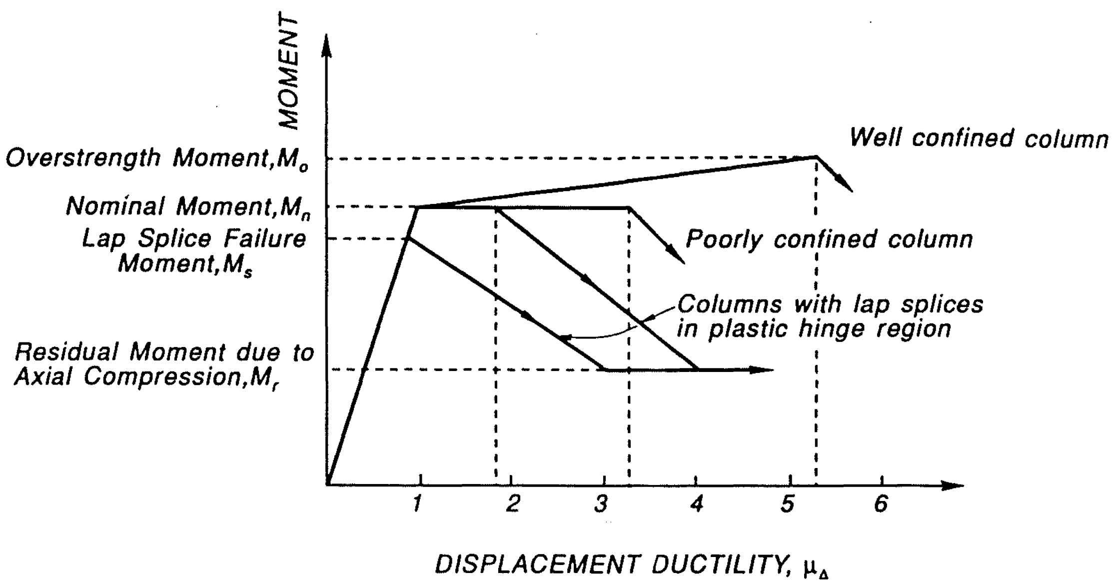

Figure 2.7 Flexural strength versus ductility capacity relationships [Priestley et al 1992a].

The *Design Guidelines* report by Priestley et al [1992a] also gives guidance on the design of beam to column knee joints, beam to column T-joints, and column to footing joints. Research is currently underway which should provide more information on the evaluation of these connecting joints. General guidance on the evaluation of footings is provided, and it is postulated that the rocking response of foundations is permissible and perhaps desirable. An iterative method for predicting the rocking response of structures, based on a displacement response spectrum analysis, is presented. In the plastic mechanism type of analysis, foundation rocking can be considered in the same way as plastic hinging —with an assumed strength versus ductility relationship. More research is needed on the seismic performance of footings, including the behaviour of footings which yield in flexure.

Determination of local ductility demands also depends on assumptions of elastic displacements. Priestley et al recommend that some attempt be made to assess which members will be essentially uncracked and which will be cracked when computing elastic displacements. Foundation flexibility effects should also be considered. As discussed in the next subsection, there is some question as to what stiffness assumptions are appropriate for elastic systems.

After individual section strengths, stiffnesses, and ductility capacities are determined, a global ductility capacity should be calculated. The global ductility depends on the local section ductilities, the geometry of the structure, and the correct identification of the inelastic deformation mechanism. Priestley et al provide some examples of how to calculate global ductility. In a computer "push-over" analysis program, the global ductility could be automatically calculated.

Once the plastic mechanism strength and associated global ductility capacity are known they can be compared with the elastic response spectrum demand of the appropriate limit state earthquake. Maximum ductility capacities would be used for comparison against the survival limit state, while lower ductilities—corresponding to less allowable damage—would be used for comparison against the damage-control or serviceability limit states.

In the Priestley et al approach, the structure capacity V_f is increased by a factor to give equivalent elastic capacity V_E. The factor V_E/V_f is equal to the global displacement ductility capacity for longer period structures (the equal displacement assumption). For shorter period structures, V_E/V_f is less than the global ductility capacity, and is calculated according to an interpolation formula. The resulting value of equivalent elastic capacity, V_E, is compared with the elastic response spectrum demand to give an "annual probability of exceedance."—that is to say the likelihood of the capacity being exceeded, based on the return period of the specified limit-state earthquake.

Inelastic Response Assumptions

One problem with the ductility-based approach to design is that stiffnesses of the elastic structure must be appropriately determined. Moehle and Aschheim [1993] discuss the problem and its effect on ductility-based design assumptions. Figure 2.8(a) shows the moment versus displacement response of a vertical cantilever column. For this structure, elastic stiffness could be considered as the initial stiffness, slope A, based on gross-section properties, or alternatively a reduced stiffness, slope B, calculated from cracked-section properties.

Two problems are evident:

1. If slope A is used in the evaluation procedure as the basis for computing ductility demands, much higher demands would be predicted than if slope B were chosen.

2. As shown in Figure 2.8(b), if slope A is considered as the elastic stiffness, a shorter elastic period will be assumed, and from the displacement response spectrum, smaller displacements will be predicted than if slope B were considered. But for a given moment-displacement relationship and earthquake input only one inelastic displacement will result. Under the equal

displacement assumption, which elastic displacement is it *equal* to? It cannot be equal to both values. Thus the validity of the equal displacement assumption depends on what elastic stiffness assumptions are made.

Preliminary research results [Moehle and Aschheim 1993] indicate that if Caltrans response spectra are used as earthquake input, the equal displacement assumption is more accurate when gross section stiffness (slope A) is assumed. If effective section stiffness (slope B) is assumed, displacement predictions using the assumption are conservative. Note, however, that it has been suggested [Priestley pers. comm. 1993] that the Caltrans ARS spectra are in themselves conservative in the longer period range. Although analytical studies have been done, it seems that more research is needed to validate the equal displacement assumption and to give guidance on selecting elastic stiffnesses for analysis. The research should compare inelastic analysis results with appropriate and corresponding elastic spectra.

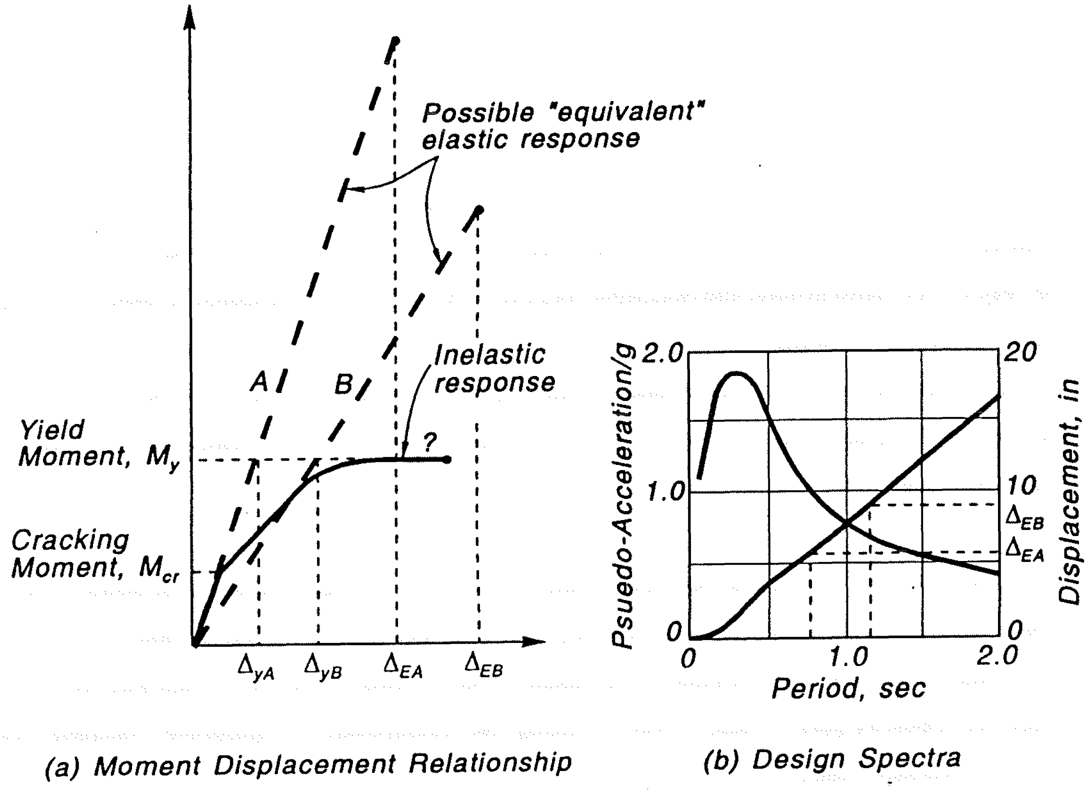

Figure 2.8 **Effect of assumed elastic stiffness on the validity of the equal displacement principle. Adapted from Moehle and Aschheim [1993].**

The idea of using a displacement approach to design rather than a force approach is promising, and could correct some of the problems with current analysis approaches [Priestley 1993b, Moehle 1992]. A displacement-based design procedure would require, however, a fundamental change in design codes and engineering practice.

Analysis of Movement-Joint Effects

One evaluation area which still presents problems is the assessment of movement joint and restrainer displacements and forces. Priestley et al [1992] discuss four different procedures which all seem unsatisfactory.

The first two, previously discussed here, are the empirical *ATC 6-2* approach based on span length and bridge height, and the Caltrans equivalent static procedure.

The third procedure, also used by Caltrans, is an elastic dynamic analysis with restrainers modelled as elastic springs. This approach cannot account for the nonlinear behaviour of the movement joint as restrainers slacken or stiffen, or as the joint closes and the compression stiffness suddenly and dramatically increases. Also, the inelastic behaviour of the adjacent bridge segments is not accounted for.

A fourth procedure—the relative ground motion approach—is based on assuming relative ground motions at the foundations as a result of non-coherent seismic input. The worst case input results from the largest anticipated ground displacements coupled with the shortest anticipated seismic wavelengths. This approach is appealing for its simplicity, but it ignores the fact that structure displacements may be larger than peak ground displacements, depending on the dynamic properties of the structure. Also, the approach implies that if ground motion is coherent there is no movement or force demand at movement joints, which is not true.

The fifth procedure to evaluate movement joints is by using inelastic dynamic time-history analyses. This more complicated procedure is potentially the most rational and accurate method for determining the critical forces and displacements at movement joints. Efforts at this type of analysis are currently underway [Priestley pers. comm. 1993], including the development of appropriate hysteresis models for the movement joints.

CHAPTER 3
SEISMIC RETROFIT TECHNIQUES

Various seismic retrofit techniques have been proposed, tested, and/or used for bridges in California, Japan, and elsewhere. Table 2.1 (in Chapter 2) outlines, for several common bridge seismic deficiencies, recommended seismic retrofit techniques. A number of effective seismic retrofit techniques for movement-joints, columns, and other potential seismic deficiencies are discussed in this chapter. Structural engineering research plays an important role in validating proposed retrofit techniques. In some cases further research is needed.

Table 2.1 and this chapter are organized to consider the deficiencies of a bridge along a seismic-force path from the superstructure through to the foundations and abutments. It should be noted however, that in seismic retrofit design the bridge must be considered as a whole, as well as element by element. The retrofitting of one bridge element can affect the seismic response, and the need to retrofit other portions of the bridge.

As in the previous chapter, the primary aim of this chapter is to summarize that information which would be most useful to the bridge retrofit designer. Thus, emphasis is placed on design criteria, actual applications of retrofit designs, and on those techniques which seem to be the most effective structurally. For further details of retrofit *research*, the reader is referred to the *Design Guidelines* report by Priestley et al [1992a], and to the proceedings of the Caltrans *Second Annual Seismic Research Workshop* [1993].

3.1 Movement Joints, Seats, Restrainers, Bearings, and Base Isolation

Seismically deficient movement joints can be retrofitted by adding restrainer (ie, linkage) rods or cables, seat extensions, or base isolation devices.

Restrainers or Linkages

The most common way of retrofitting deficient movement joints is by adding restrainers. The restrainer ties the two ends of the movement joint together using (typically) steel cables or high-strength rods.

Research on three types of restrainers used by Caltrans has been carried out at the University of California, Los Angeles as described in 1989 publications by Selna, Malvar and Zelinski [Priestley et al 1992]. The restrainer types tested include high strength bars, looped cable restrainers attached to box girder diaphragms, and straight-through cable restrainers attached to the box girder deck flanges. Cable restrainers can also be attached to box girder webs.

Figure 3.1 shows a retrofit plan of a movement joint using added cable restrainers and pipe seat extenders. Figure 3.2 shows the details of the cable restrainers. The restrainers are attached with brackets to the box girder webs at one side of the joint, and looped around the strengthened end diaphragm of the box girder at the other side of the joint. Restrainer cables for precast girders are often wrapped around the supporting cross beam as shown in Figure 3.3 [Zelinski 1993]. In addition to steel bars and cables, the Japanese have used steel chains and hinged steel plates to restrain movement joints. Design of restrainers should specify the initial tension or slackness of the restrainers considering the expected temperature movement of the joint and the temperature of the time of the restrainer installation. In New Zealand, bar-restrainers and linkage bolts for bridges usually have thick rubber pads under the plate washers at each end of the bar. The rubber pads allow temperature movements to occur, and they reduce impact forces on the restrainer bar.

As discussed in Section 2.3, the design of movement joint restrainers by Caltrans is based on an equivalent static analysis which involves gross approximations and assumptions. Although the method may be satisfactory for the time being, more accurate design methods should be developed.

Seat Extensions

Movement joint restrainers are intended to limit the movement of spans so that the spans do not fall off their supporting seats. Another solution to the problem, often used in conjunction with restrainers, is to extend the seat length. For box-girder bridges, Caltrans commonly uses steel pipe seat extenders. The pipes are placed through core-drilled holes in the end diaphragms of the spans on either side of the movement joint as shown in Figure 3.2. Typically the steel pipes are 220 mm outside diameter with a 22 mm wall thickness (8 inch nominal diameter, double-extra strong).

Other types of seat extensions, which have been used in Japan, include added concrete corbels or added steel brackets anchored to the lip of the existing concrete seat. "Stopper" devices have also been used. These stoppers consist of steel or reinforced concrete brackets which restrain the movement of the end diaphragms of the spans. The seat extension and stopper devices discussed above can be used at abutment movement joints but may not be applicable at intermediate movement joints.

Base Isolation

Vulnerable types of support bearings such as steel rocker bearings can be replaced by base-isolation devices. For the Sierra Point overbridge on Route US101 near San Francisco, California, the existing spherical steel bearings were replaced with elastomeric bearings containing lead plugs. In addition, movement joints were restrained using 22 mm (7/8 in) diameter high-strength steel rods.

As well as addressing the problem of vulnerable movement joint details, the retrofit reduced the seismic forces in the bridge columns, because of the increased damping and the shift in fundamental period provided by the base isolators. For the Sierra Point bridge, the reduced lateral forces due to the isolation of the superstructure made column retrofitting unnecessary [Priestley et al 1992a].

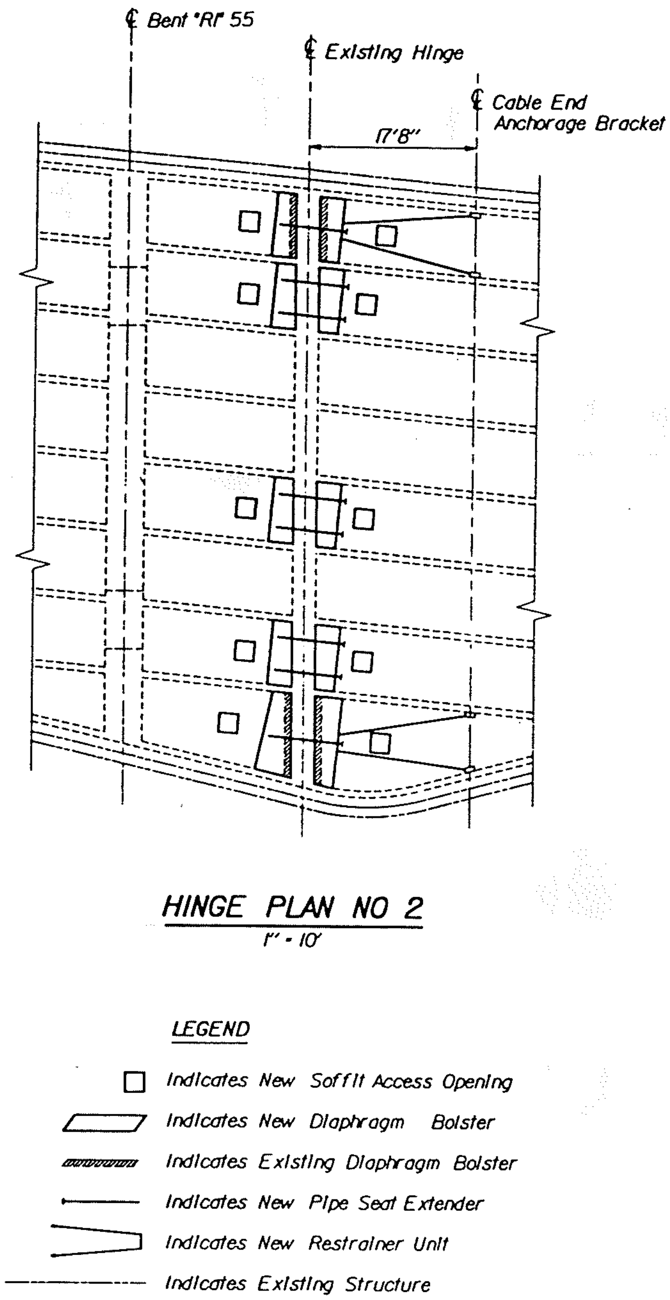

Figure 3.1 **Retrofit plan for the movement joints of a concrete box girder bridge using cable restrainers and steel pipe seat extenders** [Zelinski pers. comm. 1993].

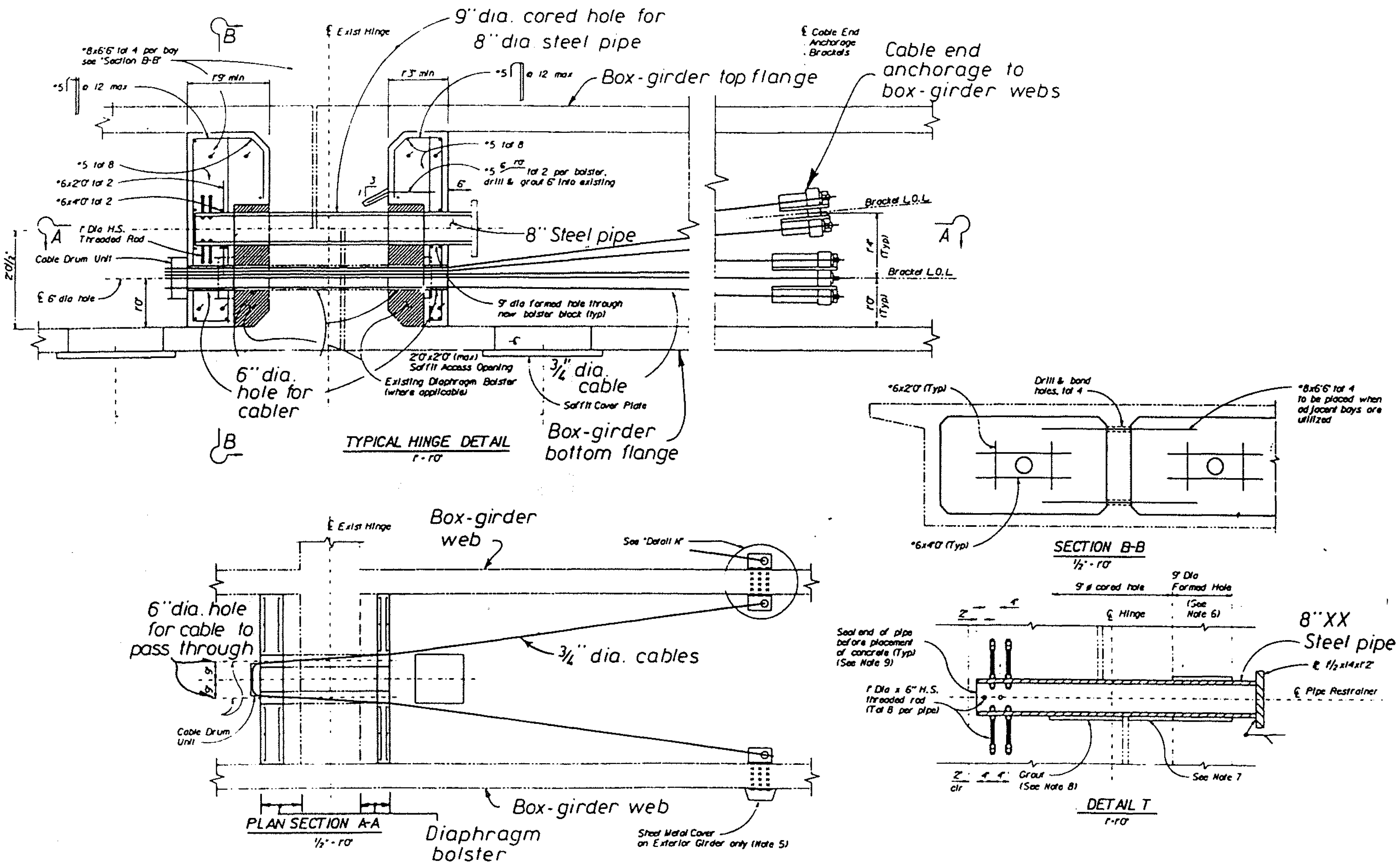

Figure 3.2 **Details of cable restrainers and steel pipe seat extender** [Zelinski pers. comm. 1993].

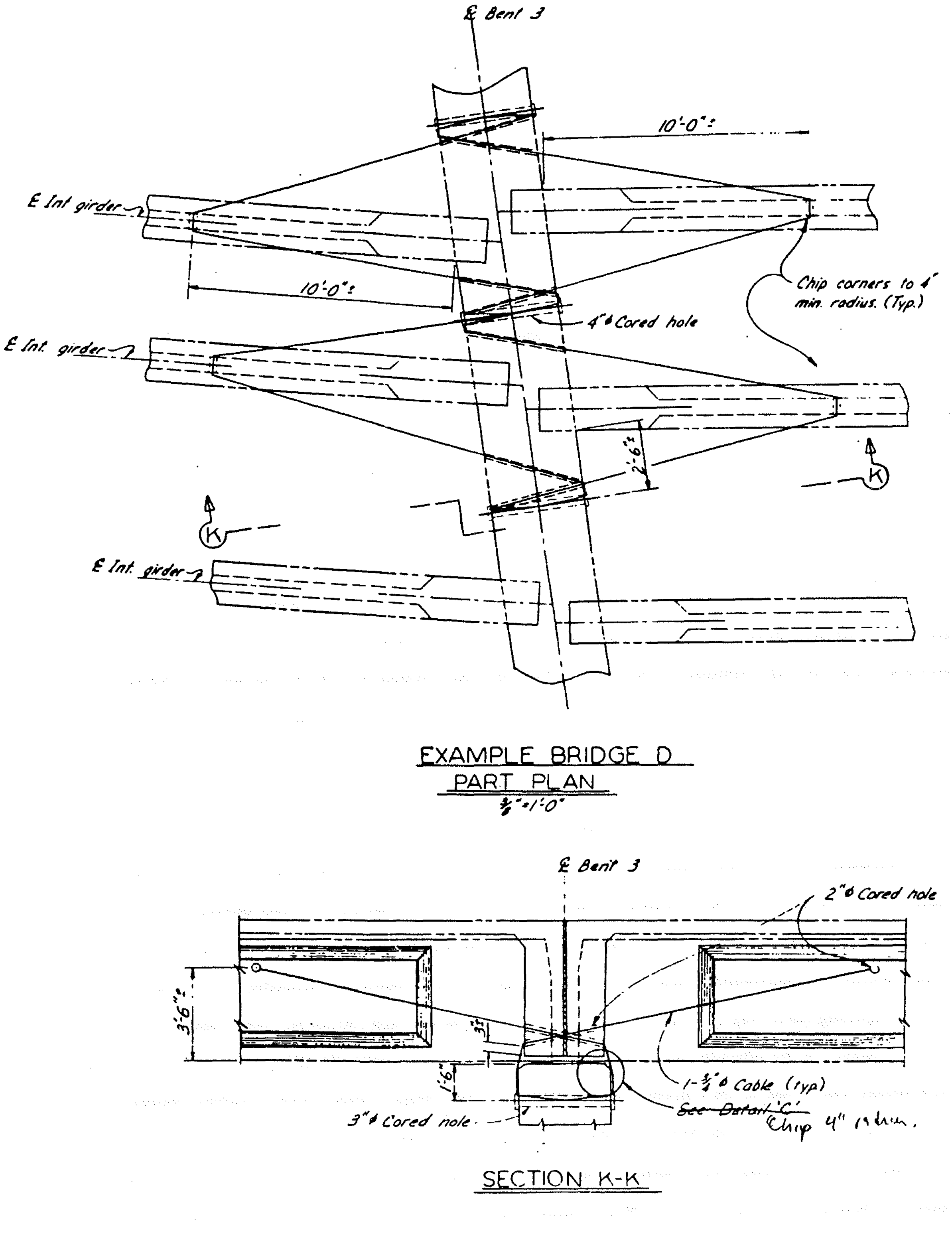

Figure 3.3 Cable restrainers for a bridge with precast girders [Zelinski pers. comm. 1993].

Skinner, Robinson, and McVerry [1993] cover the principles of seismic isolation and give a comprehensive list of projects where isolation has been implemented. Base Isolation and Energy Dissipation devices have been used for bridge retrofits in New Zealand, the United States, Japan, Italy and Canada. In Italy, large elasto-plastic absorbers are used at abutments to provide longitudinal restraint and damping. For relatively short bridges, the Italians have retrofitted movement joints by eliminating them; the bridge deck slab in the vicinity of the movement joint is replaced with a new slab made continuous over the joint.

Babaei and Hawkins [1991] review seismic retrofit techniques for bridge superstructures. Their report discusses the seismic performance of movement-joint retrofit measures, and provides design information and cost estimates for retrofitting with restrainers, seat extenders, and base isolators.

3.2 Beams, Beam-Column Joints, and Anchorage of Longitudinal Reinforcement

If the beams of bents are identified as seismically deficient, they are typically difficult to retrofit because of interferences with the superstructure girders. Usually it is easier to add strength to the beam by prestressing and concrete jacketing than it is to add ductility capacity by improving confinement, anchorage, or shear capacity. Thus the best approach to retrofitting the beams of bents can be to strengthen the beam to force plastic hinging into the columns. The columns must then be checked for ductility capacity, and retrofitted if necessary. If clearances allow, beam deficiencies can also be remedied by adding a new beam between the columns, below the existing beam. This "link" beam can preclude failure in the original beam or beam-to-column joints as well as increasing the transverse strength and stiffness of the bent. Column shear demands will be increased however, so shear retrofit of columns may be necessary. Also, this retrofit does not mitigate moment demands in the bridge's longitudinal direction.

An outrigger beam knee joint for the I-980 freeway in Oakland, which was damaged in the Loma Prieta earthquake, has been repaired and retrofitted by Caltrans. The joint was retrofitted by completely removing all of the concrete in the joint region (by jackhammer) while leaving the existing reinforcement in place. New interlocking spiral joint reinforcement, at a close spacing, was added around the column longitudinal bars. An exterior cage of reinforcement consisting of 10 mm bars at a 115 mm spacing each way (#3 @ 4½ inches), tied together through the joint, was added. Concrete was then placed, to the slightly increased dimensions of the new joint [Priestley et al 1992a]. This retrofit detail was tested at the University of California, San Diego, under cyclic in-plane loading and showed greatly improved response compared to the original detail [Ingham et al 1993]. Other types of retrofits for knee joints and external T-joints have been studied at the University of California, Berkeley [Thewalt and Stojadinovic 1993, Moehle and Sawyer 1993].

The beam-column joints of non-outrigger multi-column bents are often deficient because of an inadequate anchorage length of the longitudinal column bars into the joint. Retrofit of such a deficiency is difficult. The addition of a new "link" beam below the existing bent beam, as discussed above, may be an effective solution in some cases. Prestressing of the joint region longitudinally along the beam and transversely through the beam, may be an effective retrofit method, but testing of the detail has been limited [Priestley 1993].

3.3 Elliptical and Circular Steel Column Jacketing

The typical deficiencies of bridge columns—inadequate lap splice length, shear strength, anti-bar-buckling reinforcing, and concrete confinement—can all be mitigated by adding an external jacket to the column. Although several jacketing techniques have been studied, not all are fully effective or widely applicable.

The success of a column-jacketing retrofit upgrade depends on the stiffness of the jacket to resist the column's tendency, caused by concrete cracking and spalling, to expand laterally. If this lateral dilation is effectively restrained by a column jacket then four potential seismic deficiencies can be corrected:

(1) Existing longitudinal bar lap splices become more effective because a transverse clamping force across the splice is created,

(2) Column shear strength is increased because the jacket acts in the same way as hoop reinforcing, allowing a truss mechanism for shear resistance to develop—also, diagonal shear cracks are restrained from opening by the jacket, preventing the degradation of aggregate-interlock shear resistance,

(3) Bar-buckling is restrained because the concrete cover does not spall, and

(4) The lateral confining pressure on the concrete increases its ultimate strain.

Most jacketing methods are applicable mainly to circular columns. Rectangular columns are more difficult to retrofit, because providing adequate jacket stiffness to confine the long flat sides of the column is problematic. For columns with high plan aspect ratios, through-bolts may be necessary to hold the long sides of the column jacket together.

Elliptical or circular steel jacketing is the most common column retrofit method, and has been shown to be fully effective in increasing the inelastic displacement capacity and strength of seismically deficient columns.

Retrofit Details

Circular columns are retrofitted using a circular steel jacket. In the typical Caltrans details, the jacket is fabricated in two semi-circular halves from steel plate of 10 mm to 25 mm (⅜ inch to 1 inch) thickness. The two sections are placed around the column and field-welded together using complete penetration groove welds continuous along the length of the column.

The space between the jacket and the existing column, specified to be 38 mm (1½ inches) minimum, is then injected with grout. For full height jackets a 50 to 100 mm (2 to 4 inch) gap is provided between the top of the steel jacket and the beam or superstructure, and between the bottom of the steel jacket and the foundation surface. The gap at each end of the jacket is necessary to prevent an inadvertent increase in moment capacity caused by the jacket bearing against the foundation or superstructure [Caltrans 1992].

Rectangular columns are retrofitted using elliptical steel jackets, constructed in a similar manner to the circular jackets. Details of the jacketing of a single-column bent with a rectangular column are shown in Figure 3.4.

Elliptical or circular steel jackets are provided over the full height of the column if the retrofit is for inadequate shear capacity. Jackets may also be provided full-height for aesthetic reasons. If the retrofit is for inadequate concrete confinement, the jacket may be partial height, covering only the potential plastic hinge region. For partial height jackets, Caltrans specifies a minimum jacket length of 1.5 times the largest dimension of the original column. (For example, a 1.2 m x 1.8 m rectangular column could be retrofitted with an elliptical steel jacket 2.7 m tall covering the plastic hinge region.) If lap splices are deficient, partial height jackets can also be used. Caltrans specifies the same minimum length for such jackets. In older California bridges, lap splices were commonly placed at the base of columns to facilitate construction, and since these locations are typically potential plastic hinge regions, the jacketing retrofit for lap splices can be the same as that for inadequate confinement.

"Partial-Confinement" Jacketing

For many bridge retrofit designs it is desirable to improve the inelastic displacement capacity of columns without increasing column moment capacity. If a column has deficient lap splices, a "partial confinement" retrofit may achieve this goal. The partial confinement retrofit used by Caltrans (called a "Class P" retrofit) has a 13 mm (½ inch) thickness of compressible plastic (polyethylene) placed around the column prior to the installation and grouting of the elliptical or circular steel jacket. The presence of this compressible layer allows cracking and dilation of the concrete at the column base, and consequently allows some slip of the column bar lap splices.

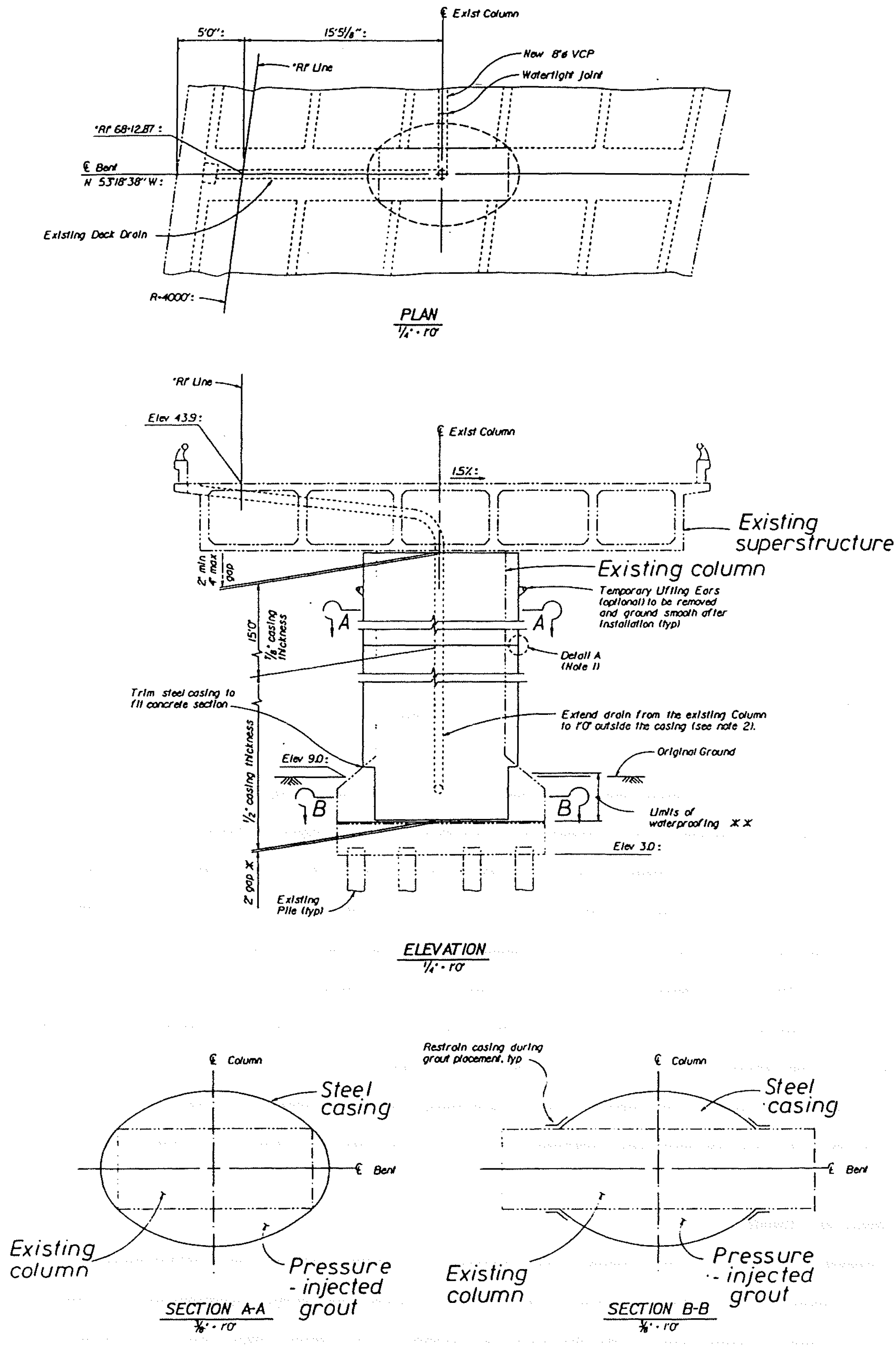

Figure 3.4 **Elliptical steel jacketing retrofit of a single-column pier having a rectangular column section [Zelinski 1993].**

However, the jacket prevents major spalling and deterioration of the concrete and buckling of the column bars. Therefore, the column can maintain its vertical-load-carrying capacity even when subjected to large inelastic displacement demands.

In Caltrans bridge retrofits, a partial confinement steel jacket may be placed at the bottom plastic hinge region of a column with inadequate lap splices. The retrofit allows enough column rotation for the structure to meet its expected ductility demands, but, by allowing lap-splice slip, the retrofit limits the level of force which is delivered to the foundation. Thus the need to retrofit the foundation is avoided. With this approach, of course, adequate lateral capacity must still be provided somewhere in the structure. For many structures the Caltrans approach is to "fully retrofit one bent per frame". That is, if a bridge structure between adjacent movement joints (ie, a frame) is supported on three bents, the columns and foundations of one bent are fully strengthened for the design lateral forces. The base regions of the columns in the other two bents are retrofitted to maintain their vertical-load-carrying capacities at the expected inelastic displacements, but are assumed for design to have zero moment capacity at the base [Caltrans 1992].

Although a pin connection may be used to model the base of a column with a partial-confinement jacket, the foundation capacities and column-shear strength should be based on the peak moment-capacity of the column base (eg, that at $\mu = 1.5$ in Figure 3.6[c]).

Figure 3.5 shows the column and foundation retrofit and strengthening design of a two-column bent with rectangular columns. The columns are retrofitted with full-height elliptical steel jackets. For the top 4.6 m (15 ft) of the columns, a partial confinement retrofit, with a 13 mm thick polyethylene layer, is used. This unusual detail is intended to allow greater strains in the continuous longitudinal bars in this region and thus limit the moment demand transferred into the beam, which is not retrofitted [Zelinski 1994]. The bottom to mid-height portion of the columns receive a full-confinement retrofit, plus the moment capacity at the bottom of the column is increased with the addition of 25 reinforcing bars, 36 mm diameter (#11), placed around the rectangular column inside the elliptical steel jacket. Note that in conjunction with this column strengthening, the foundations are extensively retrofitted; new piles and pile caps are used and temporary support of the superstructure is required. (Figure 2.27).

Research Results

Research on elliptical and circular steel jacketing of bridge columns has convincingly shown the effectiveness of such jackets. Figure 3.6(a) shows the lateral load versus displacement hysteresis loops for a circular column with 20-bar-diameter lap splices in the plastic hinge zone; the strength of the column degrades rapidly after the first cycle to displacement ductility, $\mu = 1.5$ and the hysteresis loops are pinched showing poor energy absorption capacity. An identical column with a grouted circular steel jacket over the lap splice region responds as shown in Figure 3.6(b).

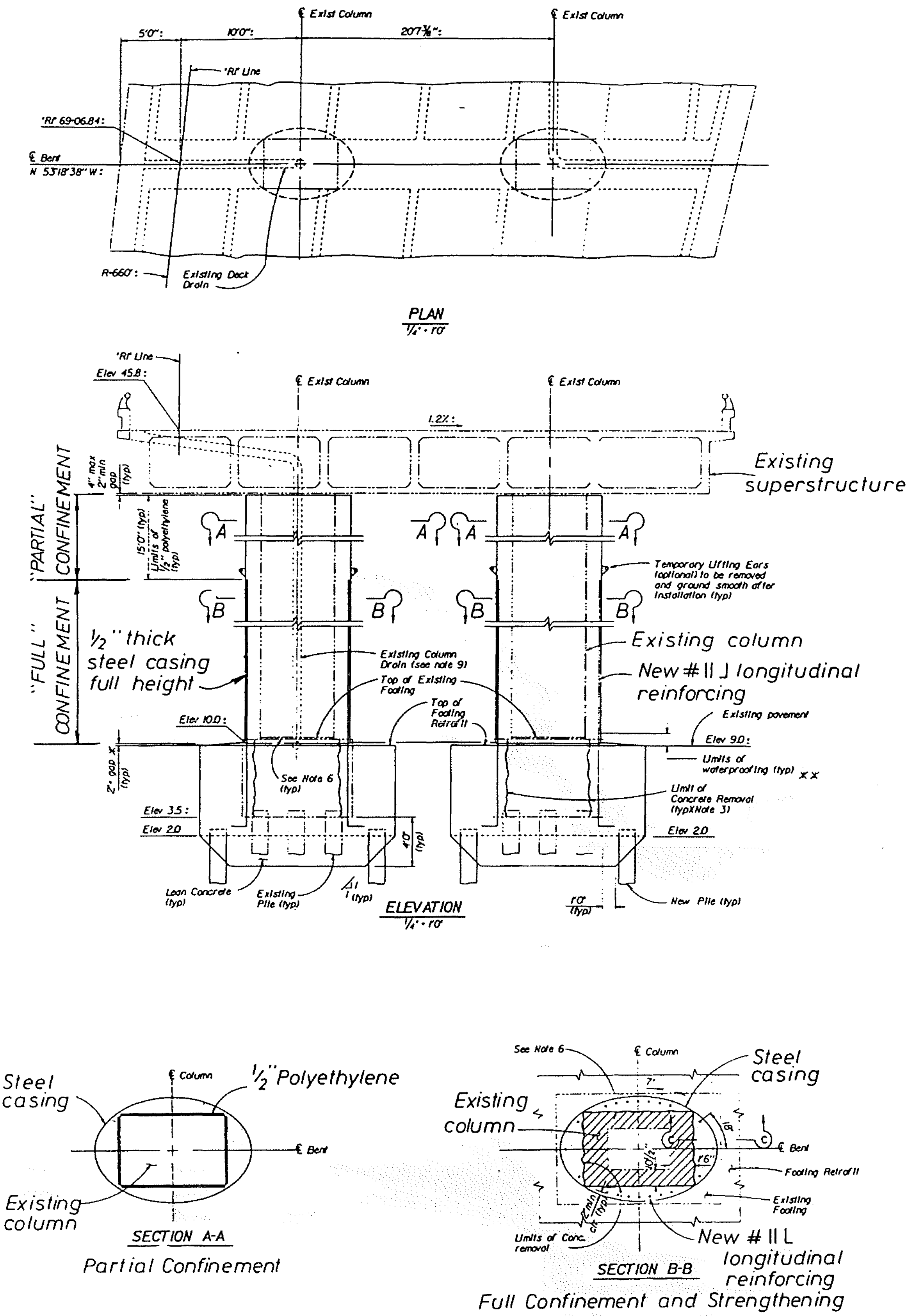

Figure 3.5 **Elliptical steel jacketing column retrofit and strengthening and foundation strengthening, for a two-column pier having rectangular columns** [Zelinski 1993].

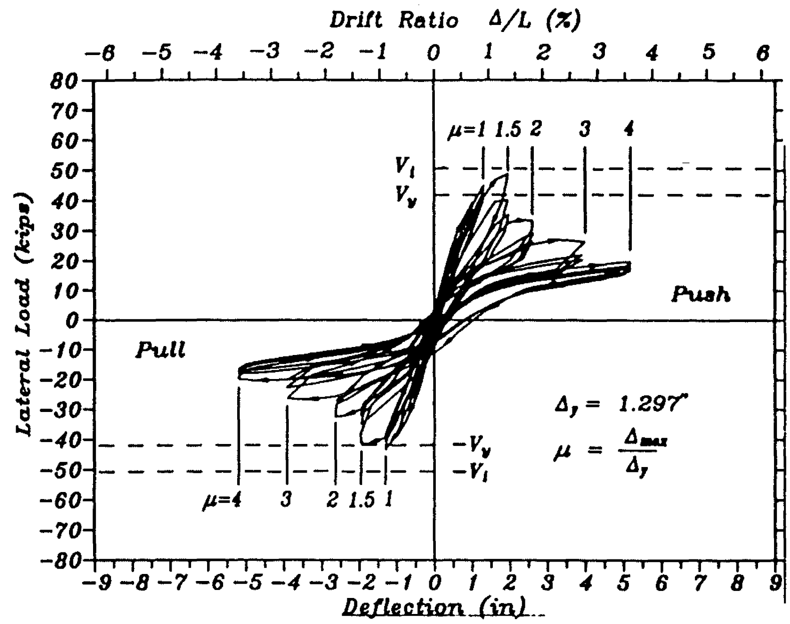

As-built circular column

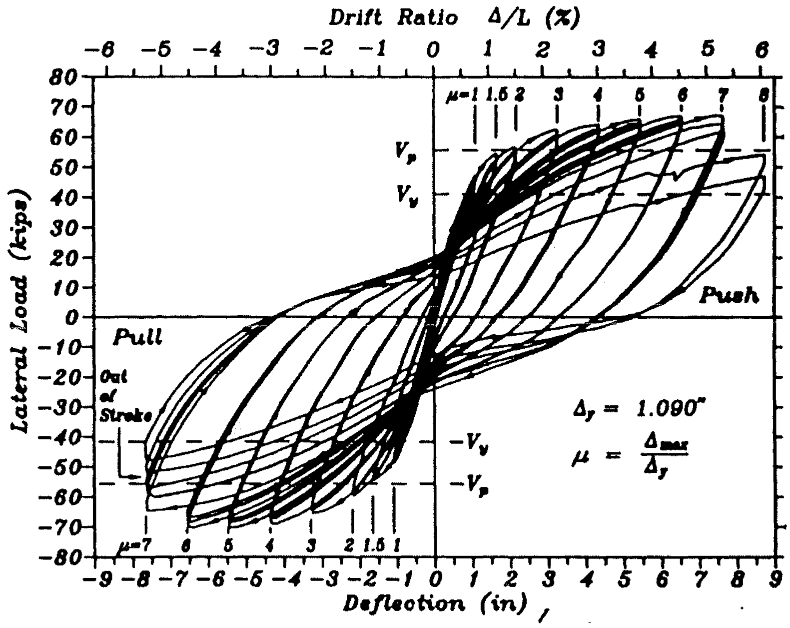

Full confinement circular steel jacket retrofit

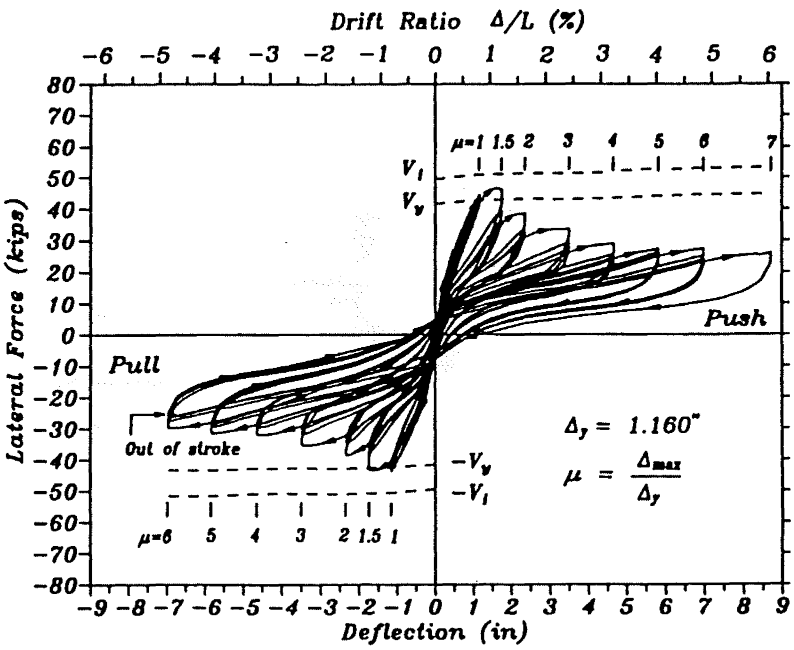

Partial confinement circular steel jacket retrofit

Figure 3.6 Steel jacket retrofit test results for circular columns with 20-bar-diameter lap splices [Yuk Han Chai et al 1991, Priestley et al 1992a].

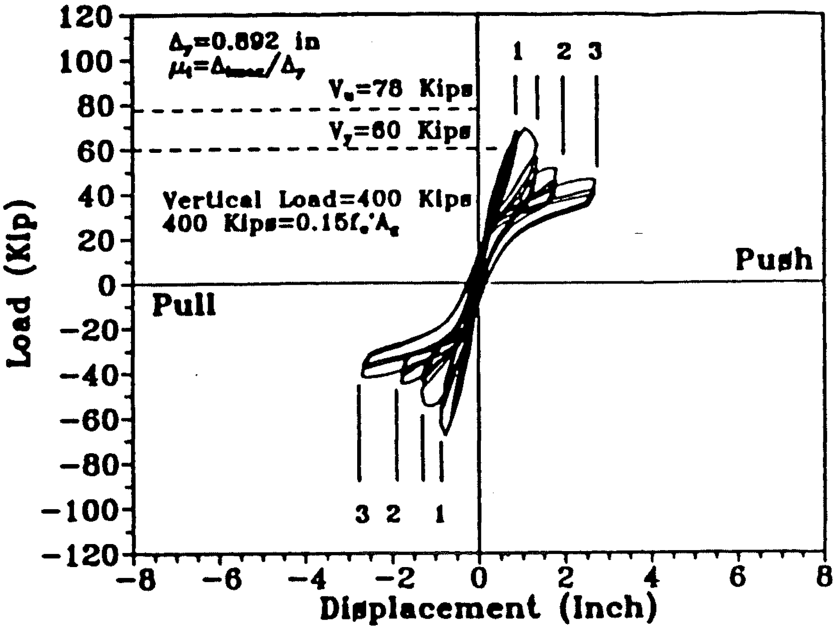

(a) As-built rectangular column

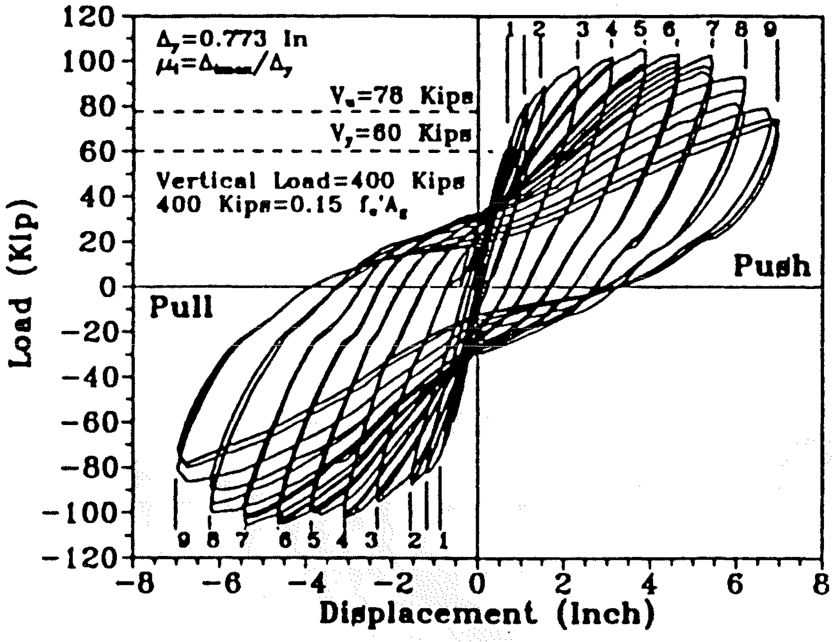

(b) Elliptical steel jacket retrofit

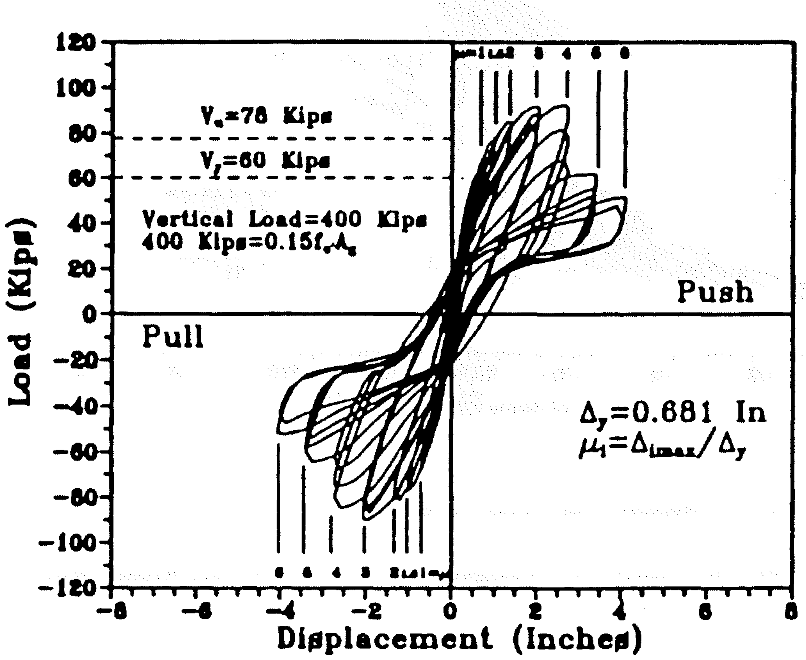

(c) Stiffened-steel-plate rectangular jacket retrofit

Figure 3.7 Steel jacket retrofit test results for rectangular columns with 20-bar-diameter lap splices [Priestley et al 1992a].

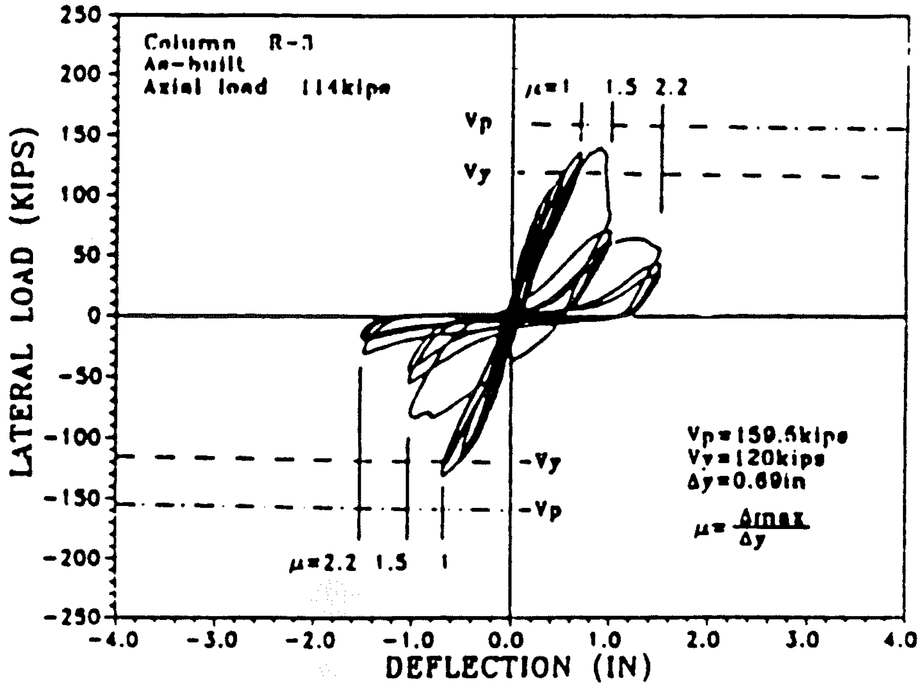

(a) As-built rectangular column

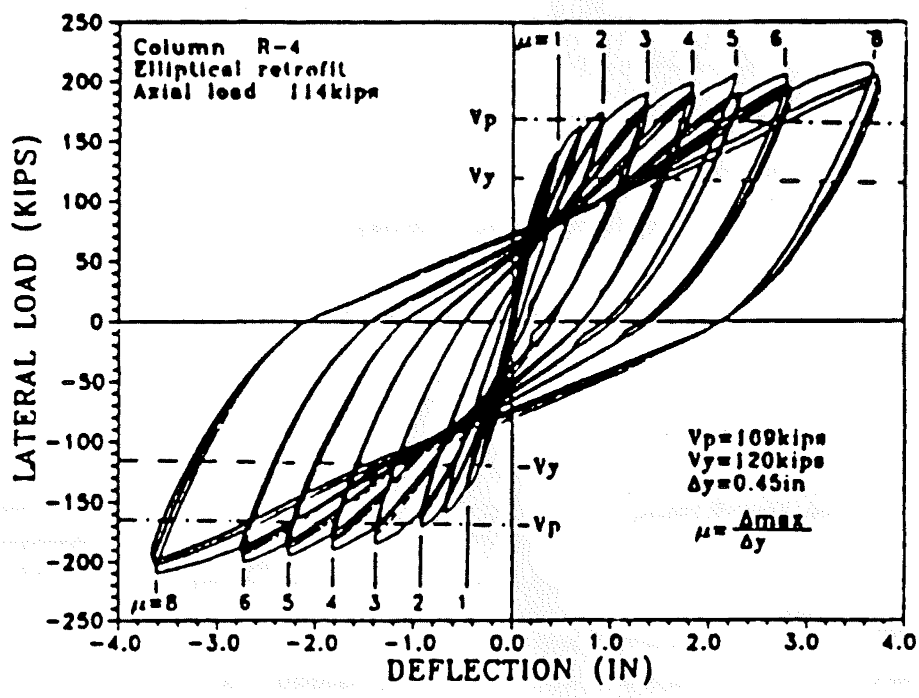

(b) Elliptical steel jacket retrofit

Figure 3.8 Steel jacket retrofit test results for rectangular columns with insufficient shear capacity [Priestley et al 1992a].

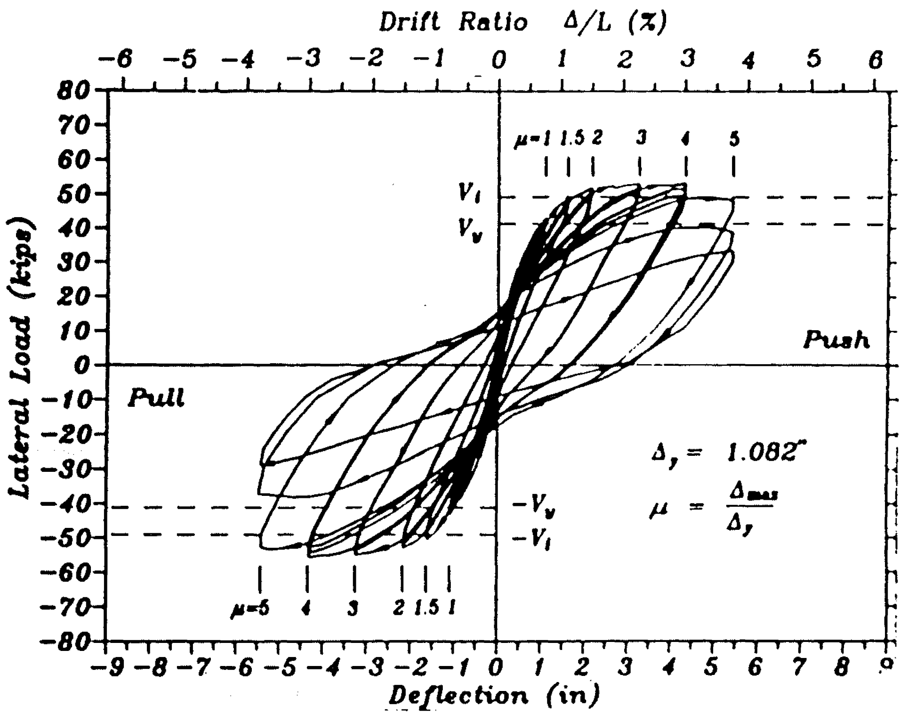

(a) As-built circular column

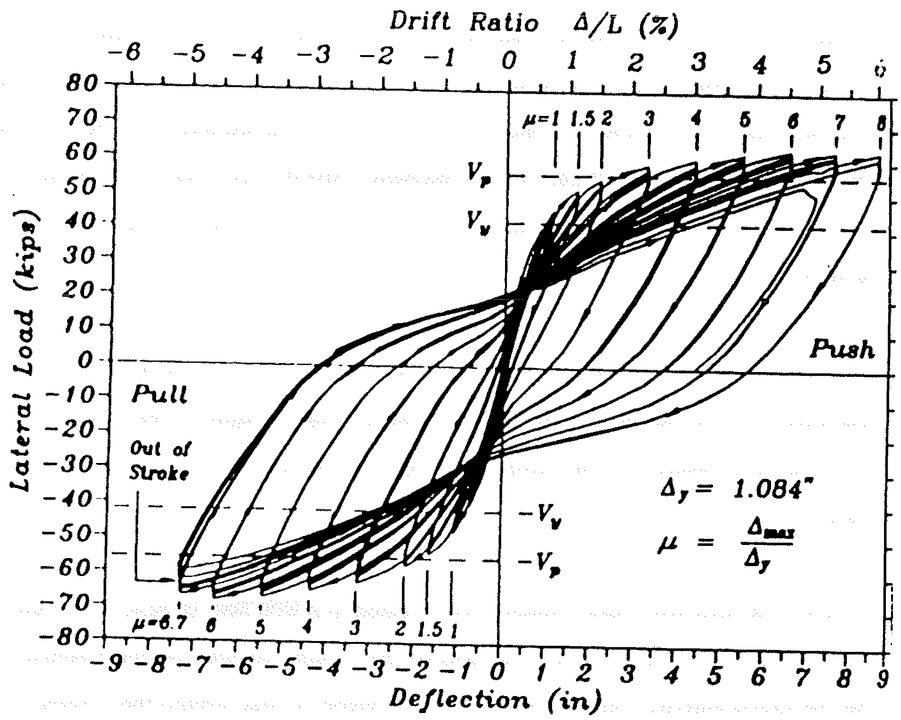

(b) Circular steel jacket retrofit

Figure 3.9 Steel jacket retrofit test results for circular column with continuous longitudinal bars, but with insufficient ties for flexural confinement and bar-buckling restraint [Yuk Hon Chai et al 1991].

The hysteretic load versus displacement response is stable up to $\mu = 7$ with good energy dissipation capacity and no strength degradation until $\mu = 8$ when column longitudinal reinforcement is fractured.

Performance of Partial-Confinement Jackets

Figure 3.6(c) shows the hysteresis loops for a third column which was retrofitted using a "partial confinement" steel jacket. As with the original column, bond failure occurred at the lap splice at $\mu = 1.5$. However, strength degradation was less rapid and it was possible to displace the column to $\mu = 7$ without losing the vertical load carrying capacity [Yuk Hon Chai et al 1991, Priestley et al 1992a]. Thus it appears that the concept of a partial confinement retrofit is valid. It may be prudent, however, to conduct further research on partial confinement retrofit designs for the following reasons:

1 Partial confinement jacketing of *rectangular* columns is now common in California, but the detail has not been tested on rectangular columns.

2 The hysteresis loops for the partial confinement retrofit, Figure 3.6(c), show a reasonable ductility capacity, but also show strength degradation and pinching. This degradation and pinching may or may not be a problem for the bridge structure, depending on the overall retrofit design, the actual hysteretic response characteristics, and on the earthquake demand. Inelastic, dynamic time-history analyses of structures with partial-confinement jacketed columns could help verify the adequacy of such retrofits and to evaluate the overall retrofit strategies which use partial confinement jacketing. Consideration of the residual moment capacity of a column with a partial-confinement retrofit may lead to more accurate seismic evaluations and more efficient retrofit designs than the currently-used assumption of a pin-condition.

3 A thinner or less compressible layer of polyethylene could be explored to see if strength degradation can be reduced, while not increasing peak strength. This could further improve the seismic performance of the retrofitted bridge, while not increasing peak shear or foundation demands.

4 Columns with deficient shear capacity are sometimes retrofitted using a full height steel jacket which provides full confinement over most of the column height, and only partial confinement at the lap splice region, where a layer of polyethylene is used around the column. Figure 2.20 is an example of this type of jacketing detail. Such retrofit methods for shear-deficient columns have not been laboratory tested for either circular or rectangular columns. It may be that the partial confinement detail is not as effective in improving shear capacity as a jacket providing full confinement over the full height of the column.

Rectangular Columns with Lap Splices

Figure 3.7(a) shows the lateral load versus displacement hysteresis loops for a rectangular column with inadequate lap splices. Similar to the circular column, bond failure occurred in the lap splices at $\mu = 1$, after which the strength degraded rapidly. The hysteresis loops were pinched and the ideal moment capacity was not reached. Figure 3.7(b) shows the response of an identical column retrofitted using an elliptical steel jacket. The hysteresis loops are stable up to $\mu = 7$, when lap-splice failure eventually occurred. The energy dissipation, (equal to the area inside the hysteresis loops) is good up until the end of the test at $\mu = 9$.

Note that not all jacketing methods are so successful. Figure 3.7(c) shows the lateral load versus displacement response of a column retrofitted with a stiffened steel-plate rectangular jacket. As evidenced by the limited ductility capacity and poor energy dissipation, this retrofit method is only marginally effective [Priestley et al 1992a]. Consequently, this method was not used for permanent retrofit work in California.

Retrofit of Shear Strength, Confinement, and Bar-Buckling Deficiencies

Figure 3.8 shows the effectiveness of elliptical steel jacketing for rectangular columns with deficient shear strength. The hysteresis loops in Figure 3.8(a) are for a column that suffered a brittle shear failure at displacement ductility, μ, of 1.5. An identical column which was retrofitted with an elliptical steel jacket showed excellent seismic performance with hysteresis loops stable up to $\mu = 8$ (Figure 3.8(b)). Similar results have been obtained for circular columns deficient in shear strength [Priestley et al 1992a].

The improvement in seismic response provided by jacketing is less dramatic for columns whose only deficiency is insufficient transverse reinforcement for confinement and bar buckling restraint. Figure 3.9 shows the original and retrofit hysteresis loops for circular columns without lap splices. The original column showed good hysteretic response up to $\mu = 5$ when the longitudinal bars in the compression zone of the plastic hinge buckled. (Note that with higher axial loads the original column performance would not be as good.) The column retrofitted with a circular jacket, Figure 3.9(b), showed improved behaviour with good hysteretic response up to $\mu = 8$.

Research on steel jacketing has also been carried out in Japan with emphasis on retrofitting regions where reinforcing is prematurely terminated. For the Japanese jacketing designs, epoxy is sometimes used between the jacket and column instead of cementitious grout [Priestley et al 1992a].

Dimensions of Steel Jackets

Caltrans [1992] has developed tables of recommended steel jacket dimensions and thicknesses for various column sizes. The tables are based on providing a specified amount of confining pressure at a specified radial dilation strain. This design approach was developed at the University of California, San Diego [Priestley et al 1992a]. For columns with lap splices, the critical radial dilation strain is taken as 0.001. For concrete confinement where no lap splices are present a larger radial dilation strain, 0.004, is permissible. The contribution of the steel jacket to shear strength is considered in the same manner as for hoop or spiral reinforcing, based on a truss analogy with diagonal compression struts between inclined cracks in the concrete section. Specific design equations for elliptical and circular steel jackets are given by Priestley et al [1992a, 1994].

For a given rectangular column, different elliptical jacket dimensions can be used as shown in Figure 3.10. More oblong-shaped elliptical jackets, Figure 3.10(a), will provide better shear strength and confinement for strong axis behaviour, while more circular-shaped jackets, Figure 3.10(b), will provide better shear strength and confinement for weak axis behaviour. Caltrans [1992] design criteria define the overall dimensions of the jacket so that the aspect ratio A/B of the ellipse is equal to the aspect ratio h/b of the column. The jacket shape and dimensions end up being different from those of a true ellipse, however, because the elliptical shape is approximated as four circular segments. A true ellipse has a continuously variable radius; in practice the steel jackets are typically fabricated with just two different radii, r_1 for the long sides of the column and r_2 for the short sides of the column, as shown in Figure 3.10. The points of tangency of the two radii are usually taken at the corners of the rectangular column.

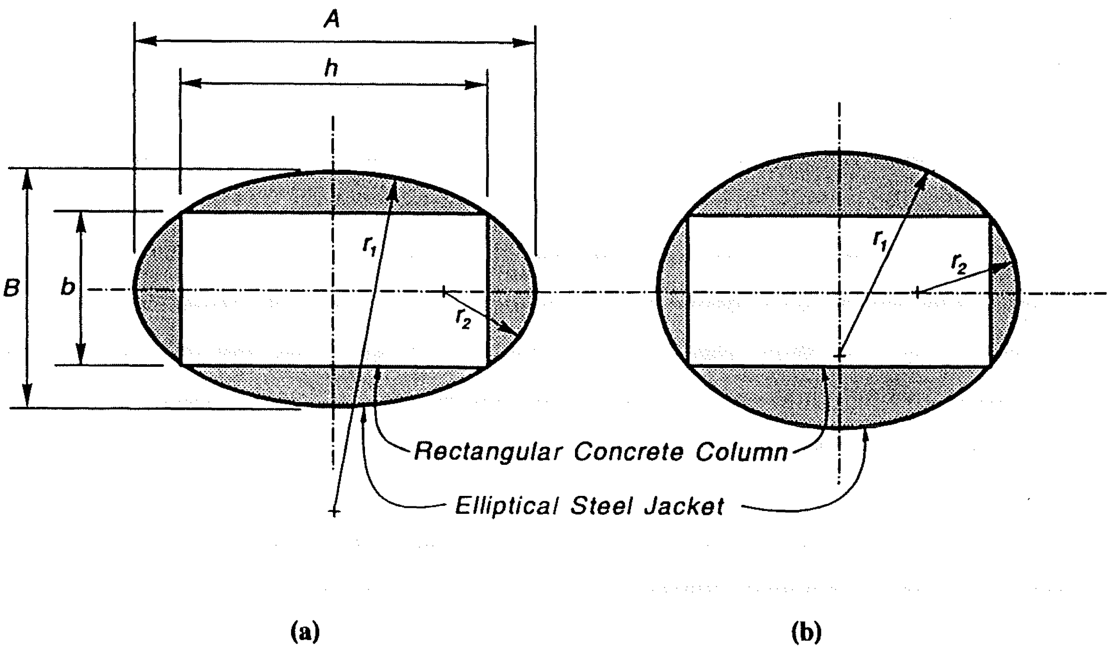

Figure 3.10 Geometry of elliptical column jacketing.

3.4 Other Column Jacketing Methods

Besides elliptical steel jacketing, other materials and methods can be used to add confining jackets to bridge columns. Most of these other methods are applicable mainly to circular columns. Although some methods may be applied to rectangular columns, the designer must ensure that the jacket provides sufficient confining stiffness and strength on all sides of the column where it is needed. In general, jackets of rectangular geometry, even if they are stiffened, are not as effective as elliptical jackets or jackets with through bolts. It is important that unproven techniques for column jacketing be laboratory tested. Several retrofit methods designed on engineering judgement have been shown by laboratory tests not to be effective.

Fibreglass/Epoxy Column Jackets

Fibreglass/epoxy jackets may be preferable for circular columns near salt-water environments, where steel would be likely to corrode. In some cases the final column diameters for fibreglass/epoxy jackets are 50 mm to 100 mm (2 to 4 inches) less than for steel jackets, so the fibreglass/epoxy retrofit may also be preferred in situations of tight clearances. Approval of fibreglass/epoxy jackets by Caltrans has been delayed, however, by questions of durability [Zelinski 1994].

Research on fibreglass/epoxy retrofitting has been carried out at the University of California, San Diego [Priestley et al 1992a]. Their tests have shown that columns with inadequate lap-splice lengths, jacketed with fibreglass and epoxy and pressure grouted to 1700 kPa (250 psi), show excellent seismic response, similar to that of steel jacketed columns.

Caltrans specifies three levels of confinement with fibreglass/epoxy jacketing: active confinement at 1700 kPa (250 psi), active confinement at 690 kPa (100 psi), and passive confinement. The active confinement is accomplished by installing an elastomeric bladder around the column before wrapping with fibreglass and epoxy. After wrapping, cement grout is pumped into the bladder up to the specified pressure. For passive confinement, the fibreglass/epoxy is wrapped directly around the column without grout. For both active and passive jacketing, multiple layers of the fibreglass/epoxy are used to achieve the desired total thickness.

Active confinement is used only at potential plastic hinge regions in columns. The lower confining pressure, 690 MPa, is used where the required displacement ductility capacities are less than 4.5 or where there are no lap splices. For lap splice regions, and for higher ductility demands, a confinement pressure of 1700 MPa is used. The passive fibreglass/epoxy jacketing is used outside of the plastic hinge regions where column shear strength is inadequate. For columns where shear strength is the only seismic deficiency, a full-height passive jacket is used [Caltrans, 1992]. The passive jacket can also be used for plastic hinge zones without lap splices. The thicker jacket required for active confinement may not be cost competitive with steel jackets [Zelinski pers. comm. 1994].

Passive fibreglass/epoxy jacketing is also used at lap splice locations where a "partial confinement" retrofit is desired. As discussed in the section on steel jacketing, the intent of partial confinement is to allow some lap splice slip (thus limiting force demands in the foundations) but to prevent serious degradation of the plastic hinge region and the consequent loss of the column's vertical load carry capacity.

Caltrans had developed a standard specification for the fibreglass/epoxy jacketing materials—glass and polyaramid fibres and high-elongation epoxy—and has tabulated required thicknesses of the jacketing. For a 1.8 m (6 ft) diameter column, for example, the total fibreglass/epoxy jacket thickness was specified as 6.1 mm (0.24 inches) for passive confinement, 13.8 mm (0.54 inches) for low pressure active confinement and 17.5 mm (0.69 inches) for the higher pressure active confinement [Caltrans 1992]. However, after two trial installations, use of the fibreglass/epoxy jacketing is on hold until issues of durability are resolved [Zelinski pers. comm. 1994]. Priestley at al [1992a] present the basis for some of the design criteria used by Caltrans.

Other Methods

Active confinement of circular columns can also be provided using prestressed wires wrapped around the column. The effectiveness of such jacketing has been demonstrated in tests of the University of California, San Diego, and general design criteria have been developed. However, cost-effective installation methods have not yet been developed [Zelinski 1994]. Carbon fibre wrapping can also be used to jacket both circular and rectangular columns. Tests conducted in Japan indicate that the jacketing improves the ductility and strength of columns which have prematurely terminated reinforcement and are prone to shear failure [Priestley et al 1992a].

Column confinement can also be added to bridge columns by removing the cover concrete, adding additional reinforcing steel ties, and then placing new cover concrete. This retrofit method was investigated by Dekker and Park [1992] on a full scale specimen representative of a 1936-designed New Zealand bridge. The test is discussed in Chapter 6 of this report. Reinforced concrete jackets with substantial transverse reinforcing can be used to retrofit bridge columns, although the approach is generally more expensive than using a steel or fibreglass/epoxy jacket.

3.5 Pier Walls

Bridge pier walls have been retrofitted in California using jacketing methods which are similar to those used for columns. In fact, for bridge structures the distinction between a pier wall and a column is not always clear; rectangular "columns" may have plan aspect ratios of 3 or more. As mentioned in the previous section, for such columns the jacket may need through-bolts to provide the necessary confinement to the long sides of the column. The situation is the same with pier walls.

Steel jackets for pier walls have been designed by Caltrans with flat steel plates along the long sides of the wall, joined around the ends of the wall with flat or circular steel-plate segments. The long sides of the jacket are tied together with through-bolts. Typically these are 32 mm (1¼ inch) diameter high-strength bolts, in holes drilled through the existing wall on a grid spacing of 1.2 to 2.4 meters (4 to 8 ft) in each direction. Cementitious grout is injected between the steel jacket and the concrete column.

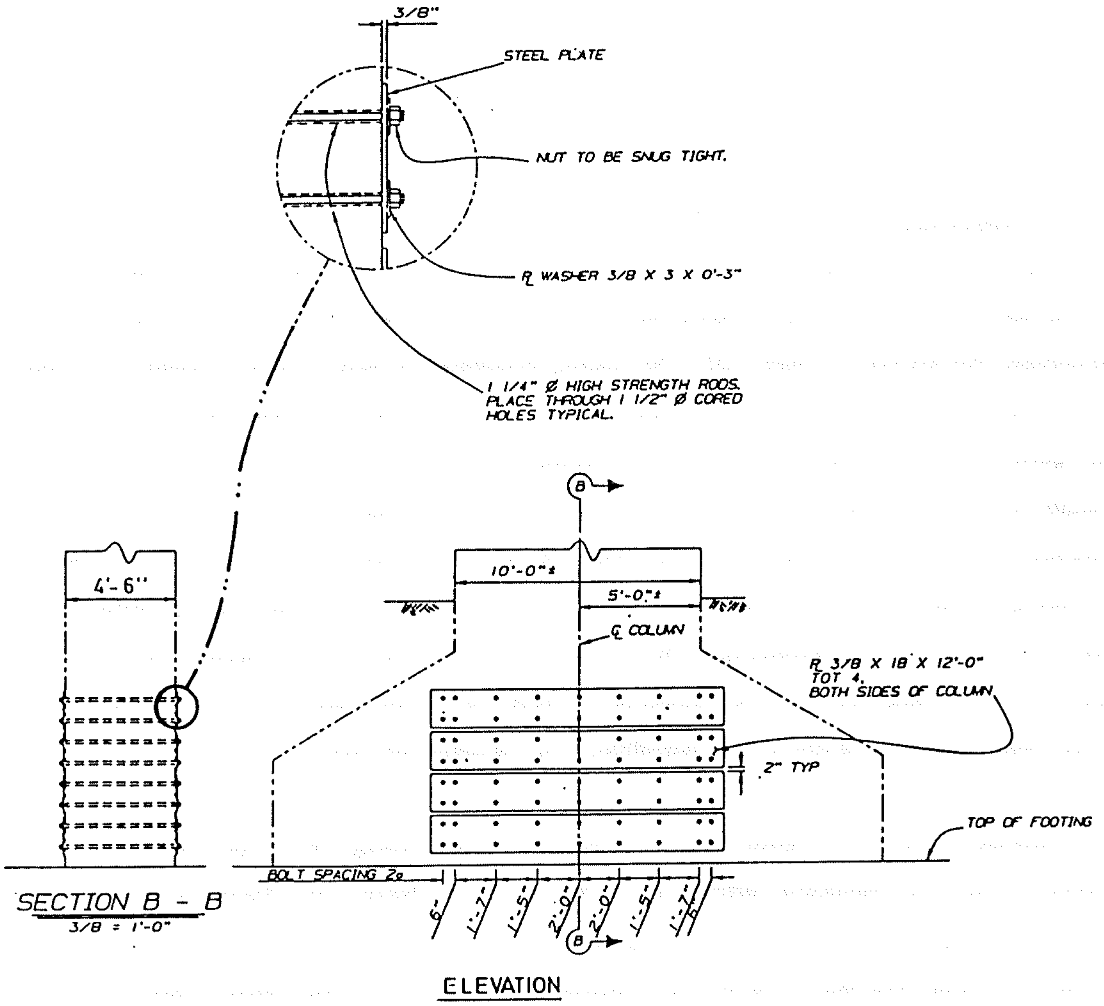

Figure 3.11 Column or pier wall retrofit using confinement plates at the lap splices [Zelinski pers. comm. 1993].

As with steel column jackets, the pier wall retrofit can be full or partial height, and full or partial confinement. Full height jackets are used if the strong-direction shear strength of the wall is deficient. The partial confinement detail at lap splices uses a 13 mm (½ inch) layer of compressible polyethylene wrapped around the wall before jacketing.

For wide columns with flared bases, which are similar to pier walls, Caltrans has used through-bolted plates in an attempt to confine lap splices. This detail is shown in Figure 3.11.

Research on retrofit methods for pier walls has been carried out at the University of California, Irvine [Haroun et al 1993]. Half-scale wall specimens were retrofitted with steel jackets, or plates, of various heights and with various arrangements of through-bolts. The wall specimens were then tested in the weak direction. The specimens had either 16-bar-diameter-long or 28-bar-diameter-long lap splices in the vertical reinforcing at the base of the wall. Specific design recommendations based on the research have yet to be developed. Continued testing may be necessary to (a) assess the effectiveness of the through bolts in providing weak direction confinement, (b) develop retrofit methods for strong direction shear strength deficiencies, and (c) investigate the performance of partial confinement retrofits.

3.6 Foundations

For bridge retrofits in California, footings are often substantially strengthened using added piles and an expanded pile cap. Figure 3.12 shows the details of the strengthening of the pile foundation for the two-column bent retrofit of Figure 2.20. The existing foundation for each column consisted of six steel H-piles and a 2.7 m x 1.8 m (9 ft x 6 ft) plan pile cap. The strengthened foundation contains twenty-four added steel pipe piles with a pile cap expanded to 4.9 m x 5.5 m (16 ft x 18 ft). For this strengthening, the superstructure is temporarily supported on shoring, while the existing pile cap is undermined so that new bottom mat reinforcing can be placed underneath it. A new top mat of reinforcing is added above the existing pile cap to provide the negative flexural capacity needed when piles are in tension due to overturning. The top mat of reinforcement can also improve the anchorage capacity of the column bars into the foundation, because the reinforcement restrains flexural-tension cracks from opening at the top of the foundation, near the anchored bars.

Such methods as shown in Figure 3.12 are effective in strengthening the bridge foundation. The problem is that such foundation retrofits are expensive—several times more expensive than column-jacket retrofitting. Paradoxically, while a large portion of retrofit costs are spent on foundations, few foundation failures have been noted in past earthquakes. However, this observation is likely to change as more of the once fragile columns are strengthened. Tests at the University of California San Diego

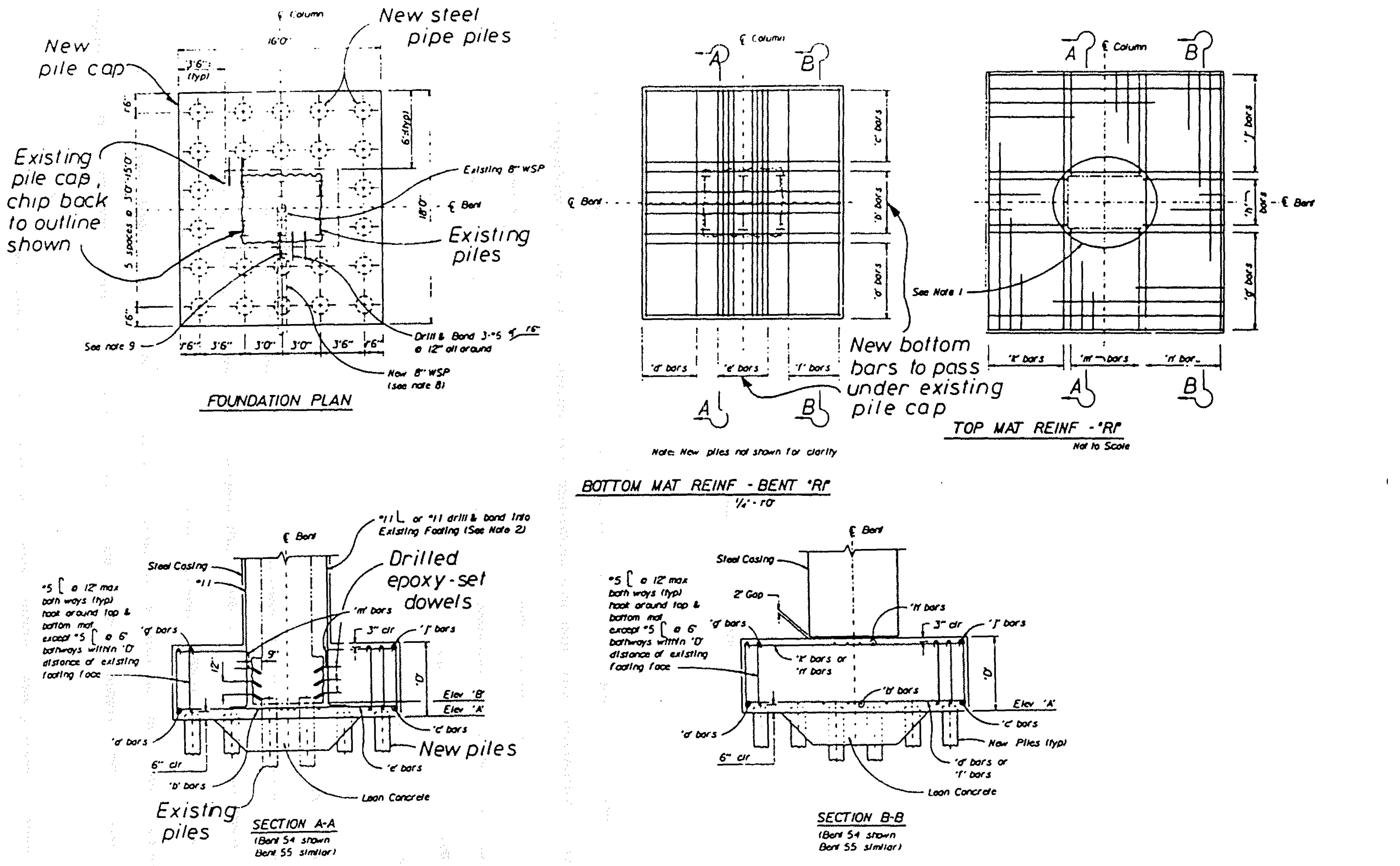

Figure 3.12 Details of foundation strengthening using new pipe piles and a new pile cap [Zelinski 1993].

have highlighted the lack of toughness in foundations once columns are retrofitted [Zelinski pers. comm. 1994].

A less expensive foundation strengthening scheme, using soil tension anchors, is also used by Caltrans. This retrofit, shown in Figure 3.13 is most efficient when the compressive capacity of the soil is not being fully utilized. Otherwise the full tension cannot be applied to the soil anchors without overloading the soil. If the anchors are not tensioned the rotational stiffness of the foundation is greatly reduced. As shown in Figure 3.13 the soil anchors are often placed between the existing piles, and a reinforcing concrete topping is added to the existing footing or pile cap.

More important than strengthening foundations to increase their capacity in the soil may be the retrofit of foundation joint shear and anchorage deficiencies. Yan Xiao et al [1993] tested a footing retrofit with an added reinforced concrete topping which had two layers of reinforcing and was attached to the existing footing with drilled dowels. The as-built specimen had failed in shear at the column-footing joint at a load of less than 60 percent of the column capacity. The retrofit footing of a second test specimen allowed the column to reach its flexural strength, and the ultimate displacement of the column was 1.5 times greater than for the as-built specimen. The final failure was caused by a degradation of the footing overlay at a ductility of 4. Thus the retrofit appears to be effective to *limited* ductility levels.

Adding external prestressing to existing footings and pile caps may be an effective retrofit technique for column to foundation joint shear and anchorage deficiencies. However, the development of feasible design details and experimental research is needed to validate this retrofit concept. Research is also needed on establishing requirements for tying the top reinforcing mat of a foundation down to the bottom reinforcing mat [Zelinski 1994]. Priestley et al [1992a] provide some general design criteria for bridge foundation retrofits.

3.7 Abutments

Caltrans has occasionally used a seismic anchor slab to strengthen and stiffen the abutments of existing bridges. As shown in Figure 3.14, the waffle-shaped slab connects the existing abutment to new piles or drilled piers. The goal of this type of retrofit is to "attract larger seismic forces to the abutments and [thereby] reduce the amount of column, footing, or other retrofit which may be required in adjacent bents. The seismic anchor slab is more effective on shorter bridges with no hinges. However, it has been proposed for use on larger structures with expansion hinges" [Caltrans 1992]. In New Zealand, below-grade friction slabs have been used to restrain abutments.

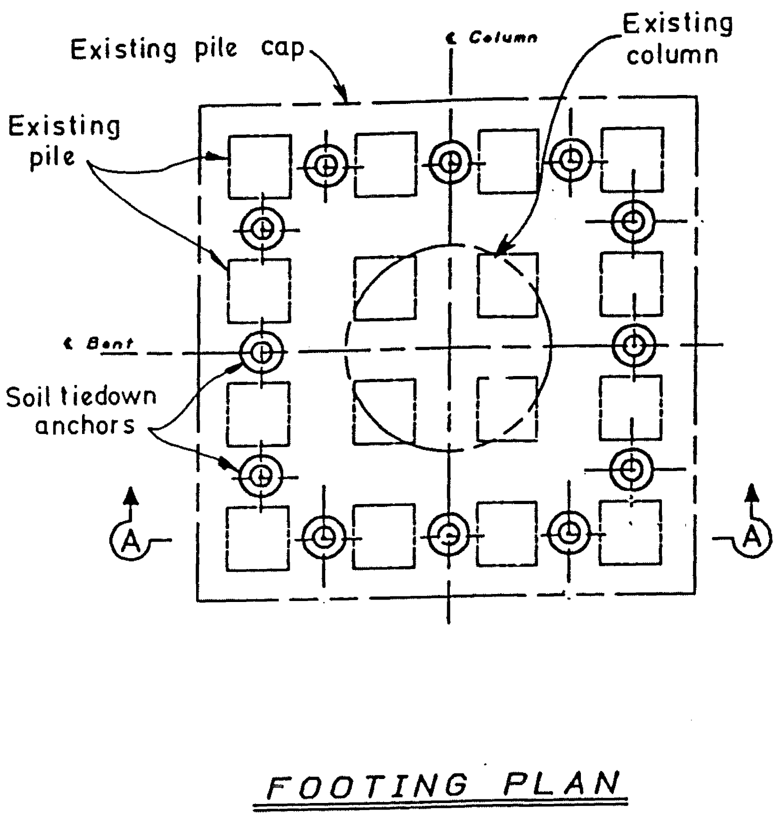

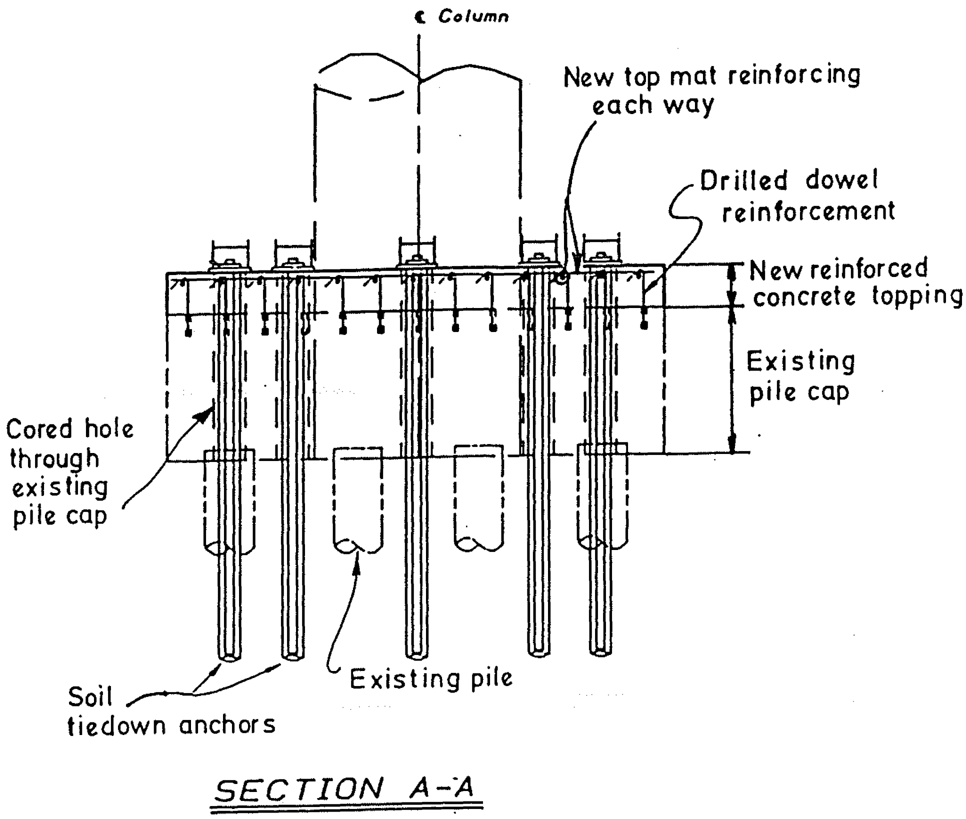

Figure 3.13 Foundation strengthening using soil tension anchors [Caltrans 1992].

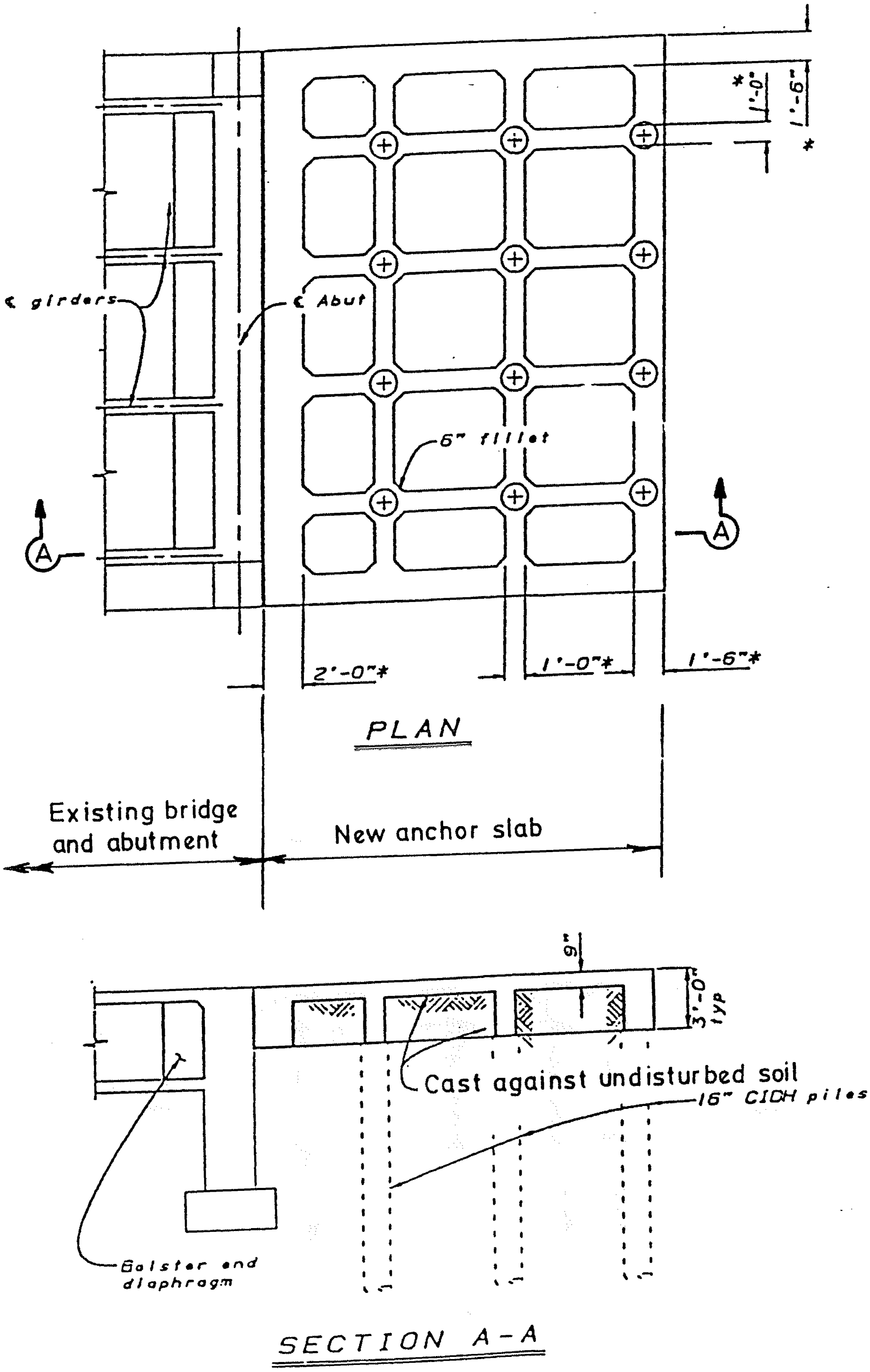

Figure 3.14 Abutment retrofit using new anchor slab and piles [Caltrans 1992].

If the abutments of a straight bridge are being retrofitted primarily for longitudinal direction earthquakes, then soil tieback anchors can be used instead of an anchor slab. For transverse direction earthquakes, large anchor piles can be installed and monolithically tied to the existing abutments. Figure 3.15 shows the schematic seismic retrofit of a curved bridge using tension tie backs for north-south direction earthquake, and cast-in-drilled-hole anchor piles for restraint in the east-west direction [Caltrans 1992]. Similar retrofits using anchor piles were used on the Kunou viaduct for the Tomei expressway in Japan [Priestley 1992a].

3.8 Other Retrofit Techniques

Multi-column bents can sometimes be strengthened with the addition of an infill structural wall (or "shear" wall) between two of the columns. This method was used for the retrofit of two-column bents on the Nishiokazu viaduct on the Tomei expressway in Japan [Priestley 1992a]. The designer of such a retrofit must consider the effects of the retrofit on increasing the seismic forces in the bent's foundations.

For the Asada ramp of the Metropolitan expressway in Kawasaki Japan, columns and cantilever beams were strengthened using added external post-tensioning [Priestley 1992a]. Again, for such a retrofit the designer must be careful to determine whether the potential seismic failure has been redirected into other elements, and to assess the strength and ductility capacity of the new mechanism.

In San Bernadino County California, on the Colton I-10/I-215 interchange, seismically deficient pier wall bents were strengthened with the addition of a new reinforced concrete outrigger frame as shown in Figure 3.16. The outrigger frame is used in conjunction with a partial confinement steel jacket at the base of the pier walls. For this design, the designer must take care to consider the high shear forces and flexural rotations which can develop in the short cap-beam spans between the existing pier walls and the new columns [Priestley 1992a, Zelinski 1994].

For the retrofit of San Francisco's double deck viaducts, an extensive strengthening design which included replacing columns and adding new longitudinal edge beams has been employed. This retrofit concept, using independent edge beams, was proof tested with a large scale model at the University of California, San Diego. A similar retrofit scheme using integral edge beams was tested at the University of California, Berkeley. Both retrofit schemes were shown to offer excellent seismic performance [Priestley 1992a].

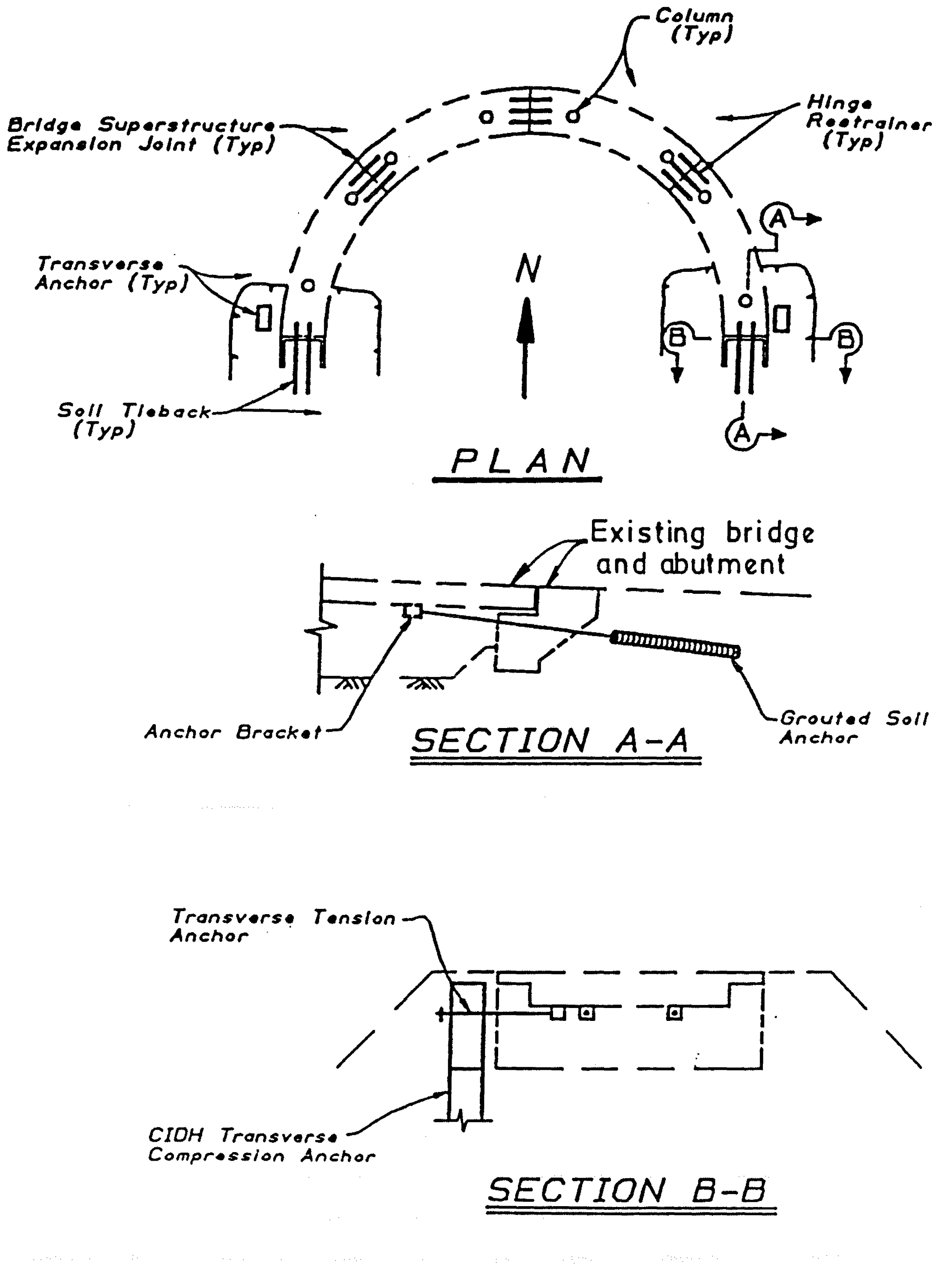

Figure 3.15 Retrofit of a curved bridge using movement joint restrainers, abutment tension tiebacks, and concrete piles for the transverse anchoring of the abutment [Caltrans 1992].

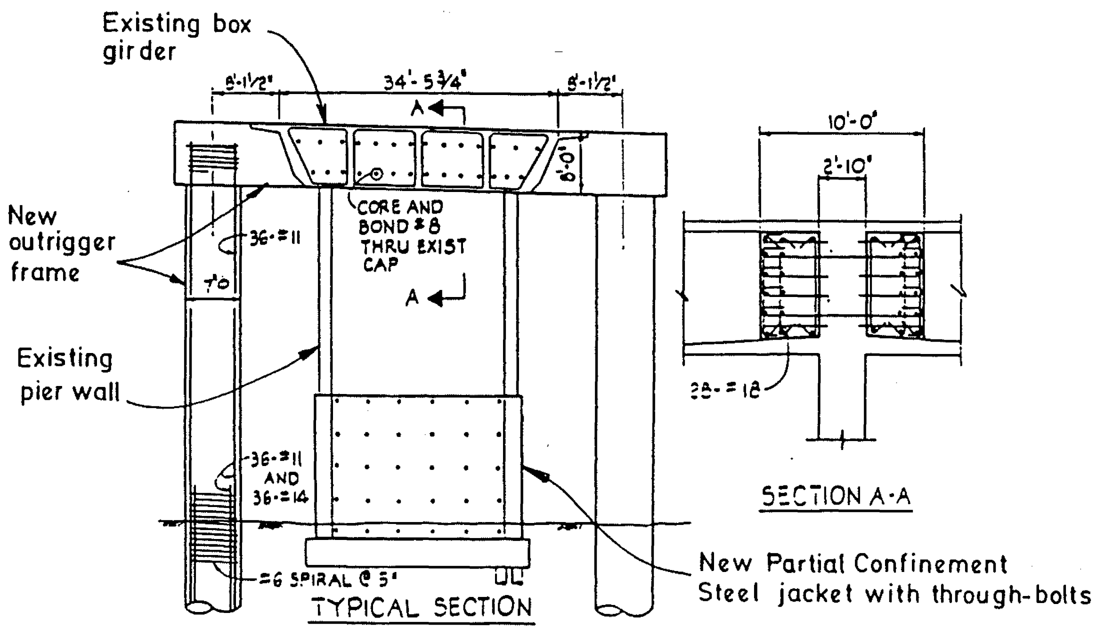

Figure 3.16 **Retrofit of a pier wall bent using a new outrigger frame and a partial confinement steel jacket by Caltrans in 1988** [Priestley et al 1992a].

CHAPTER 4
EVALUATION AND PROPOSED RETROFIT MEASURES FOR THE THORNDON BRIDGE

The seismic evaluation and retrofit designs for the Thorndon bridge in Wellington illustrate the practical application of some of the evaluation and retrofit methods discussed in Chapters 2 and 3. The project made use of the most recent research results available, and followed a capacity-design approach. Although the capacity design approach has been used in New Zealand for over 15 years, it is only in the last few years that it has been used for bridge retrofit work in California and elsewhere. The example of the Thorndon bridge shows how the capacity-design method can avoid the problems, discussed in Chapter 2, of the great uncertainty in modelling complex structures and predicting earthquake demands.

Three main examples from the Thorndon bridge project are presented here: the retrofit of superstructure linkages in Section 4.2, of single-column piers in Section 4.3, and of multi-column piers in Section 4.4. Some additional proposed retrofit measures for the bridge, including a comprehensive investigation of possible ground-improvement methods, are reviewed in Section 4.5. The superstructure linkage retrofit is a unique application of the capacity-design principle.

The design of retrofit concepts for the bridge was carried out by BCHF consulting engineers from June to October of 1994, with the present author as part of the engineering team (see acknowledgements). The material in this chapter emphasizes work conceived and developed by the present author, such as the superstructure linkage retrofit, but also reviews work principally done by others at BCHF.

4.1 Background

The Thorndon bridge and its expected seismic performance have been described by Chapman and Kircaldie [1992] and BCHF consulting engineers [BCHF 1994a, Billings and Powell 1994]. Retrofit concepts have also been proposed by BCHF [1994b]. Information from these papers and reports is summarized below.

Description of the Bridge and Site

The Thorndon bridge carries the Wellington Urban Motorway over railway and harbour facilities for a length of 1.34 km (0.85 miles). Ramps at the halfway point provide access to and from a major local street, Aotea Quay. The bridge comprises two parallel structures, each with three lanes, carrying traffic volumes of 71,000 vehicles per day on the section north of the ramps, and 53,000 vpd on the section south of the ramps. In 1992 the replacement value of the bridge was estimated to be NZ$50 million [Chapman and Kirkcaldie 1992].

Structural Features

Planning for the bridge began in the mid 1950s, design took place between 1963 and 1967, and construction was finally completed in October 1969. Design was undertaken in three stages, with each stage tending to reflect the current developments in seismic design, which were undergoing major evolution in New Zealand during this time.

Figures 4.1 through 4.4 show some typical portions of the structure (also showing retrofit measures which are discussed later). The bridge superstructure consists of precast, prestressed I-girders, simply supported with spans ranging from 20 to 42 metres (66 to 136 ft). At the northern end (the first construction stage), these are supported on 9 multi-column piers founded on groups of 600 mm diameter steel-encased concrete piles. For the remainder of the bridge the I-girders are typically supported on single-column piers with cast-in-place box girder umbrellas.

North of the ramps (the second stage of construction), these single-column piers are founded on groups of 600 mm diameter steel-encased concrete piles. South of the ramps (the third construction stage), 1.5 metre diameter cast-in-place drilled piers are typically used at the foundations [Chapman and Kircaldie 1992].

The original structure was designed for a lateral seismic acceleration of 0.3g and typically the seismic detailing improved with each stage of construction. The structure was not designed using the "capacity design" concept and consequently the inelastic mechanisms are not well defined [Billings and Powell 1994].

Site Conditions

The bridge is sited on the shore of the Wellington Harbour on reclamations which were constructed in stages between 1882 and 1970 and which contain potentially liquefiable hydraulic fills. The reclamations were placed over sediments which are also susceptible to liquefaction. The fill typically consists of silts and sands varying in depth from 4.5 metres to a maximum of 17 metres. Considerable variability is exhibited by the fill, reflecting several stages of deposition. For a short length along the bridge, the fill is retained by a mass concrete seawall, up to 17 metres high, which runs adjacent to the seaward side of the bridge.

The active Wellington fault trace runs adjacent to the bridge over much of its length and passes beneath the bridge approximately midway between the ramps and the south abutment. An earthquake on this fault could result in permanent ground movements of up to 5 metres horizontally and 1 metre vertically. Permanent ground displacements of up to 1 metre can also occur in a "fault-disturbed" area which covers the southern half of the bridge. Movement on the fault has been estimated to recur on average every 480 to 780 years, with the last rupture estimated to have occurred between 300 and 450 years ago. Seismologists estimate that there is an 11% probability of the Wellington fault rupturing over the next 50 years [Chapman and Kirkcaldie 1992, BCHF 1994b].

The bridge spans over numerous railway tracks, two major city streets, and a number of utilities and services. There are several buildings and parking areas located near to and underneath the bridge, including a busy passenger ferry terminal.

Assessed Seismic Performance

A detailed seismic assessment of the Thorndon bridge [BCHF 1994a] revealed several potential seismic deficiencies. The study indicated that the bridge:

was vulnerable to major damage and collapse at relatively low levels of seismic ground shaking. Vulnerable items included collapse of the off-ramp due to liquefaction of an underlying sand layer, collapse of spans due to either insufficient seating length or due to failure of the bridge pilecaps, and collapse of spans onto the ferry terminal due to failure of the seawall and retained ground in this area. In an earthquake caused by the Wellington fault, which runs under the bridge, collapse of the main bridge and the off-ramp where they cross the fault can be expected [BCHF 1994b].

Some of the specific seismic deficiencies are discussed in Sections 4.2 through 4.5.

Approach to Seismic Retrofitting

The weak link in many of the piers of the bridge is yielding of the pilecap reinforcement. Accordingly, most of the proposed retrofit work strengthens the pile caps. In the assessment of the unretrofitted bridge, column performance was typically not identified as critical. However, after retrofitting the pilecaps, the force and displacement demands on the columns are increased and in many cases necessitate column retrofitting.

The retrofit measures proposed to address the column and pilecap deficiencies are based on the extensive programs of bridge retrofit research and implementation carried out in California and elsewhere, and particularly rely on the recommendations of Priestley et al [1992a, 1994] and Yan Xiao et al [1994].

The retrofit measures proposed for the columns and foundations do not include adding any new piles. For most piers the capacity of the existing piles is adequate to resist the overstrength of the column or pilecap mechanism above. For some piers compression or uplift demand on the piles exceeds nominal capacity; foundation rocking could occur in these cases. The research results of Yan Xiao et al [1994] show that such rocking is not detrimental to seismic response; in fact limited rocking of foundations can be beneficial in dissipating earthquake energy and isolating the structure above. Shear or flexural failures in the piles do not occur, except for the ductile flexural mechanisms for the multi-column piers (described in Section 4.4) and for ground-block sliding movements due to liquefaction (described in Section 4.5). Accordingly no retrofit is needed for any of the existing bridge piles.

An explicit capacity design approach was used for both the seismic assessment of the unretrofitted bridge and the design of proposed retrofit measures. The essential first step in this approach is the identification of the governing mechanism for the inelastic lateral displacement of the structure. In many cases the proposed retrofit measures change the governing mechanism. Retrofitting is designed to eliminate undesirable mechanisms such as pilecap yielding, cap-beam flexure-shear failures, column-shear failures, or beam-column joint failures, and instead support the development of more ductile mechanisms such as the flexural hinging of steel-jacketed columns or existing steel-encased concrete piles, or in some cases foundation rocking. These effects of retrofitting are described in Sections 4.3 and 4.4. The retrofitting of the superstructure linkage bolts, described in Section 4.2, is a unique application of the capacity-design principle, where linkage capacities are designed to exceed the overstrength linkage force demands which can come from the adjacent movement joints.

4.2 Evaluation and Retrofit of Superstructure Linkages

Because of the use of precast simply-supported girders, the Thorndon bridge has numerous superstructure movement joints—typically two joints at each pier. Such movement joints are commonly a source of seismic vulnerability in bridges. A unique retrofit scheme of providing a few high-strength slack linkage bolts at each movement joint has been proposed for the Thorndon bridge.

Seismic Assessment

By the standards of the day, the Thorndon bridge was constructed with good seismic detailing at the superstructure movement joints. Seating lengths at the ends of the superstructure girders vary from approximately 450 mm (18 inches) for construction stages 1 and 2, to 760 mm (30 inches) for construction stage 3. In California, bridges of the same era can have seating lengths of only 150 to 200 mm (6 to 8 inches). On the Thorndon bridge, substantial linkage bolts are provided to tie adjacent spans together. Thick rubber pads are used under the ends of the linkage bolts to reduce earthquake impact forces. For construction stages 2 and 3, the linkage bolts are 8 to 12 metres long (25 to 40 ft), extending across the umbrellas, and a welded end detail is used rather than threaded bolt ends. This allows the entire length of the bolt to yield, giving excellent elongation capacity. At the multi-column piers of stage 1 however, much shorter linkage bolts, with threaded ends, were used. Little elongation capacity could be expected in these bolts because failure would occur at the threads.

Despite the reasonable seating lengths and restrainer capacities for the Thorndon bridge, span unseating could still occur due to permanent ground deformations. The ground deformations can result from liquefaction, or from movements of up to 1 metre in the Wellington fault-disturbed area. (The main 5-metre offset of the Wellington fault is addressed separately.)

Stage 3 Portion of the Bridge

In the stage 3 area of the bridge, ground movements from fault-disturbance are anticipated, but the linkage bolts typically have a greater capacity than that corresponding to the failure of the pilecaps. Thus, for this region of the bridge, the linkage bolts will not yield and there would be no span unseating from movement-joint deficiencies. However, as discussed in Section 4.4, the failure of the pilecaps in this portion of the bridge could lead to excessive settlement of the supporting piers and possibly to span collapses. This situation is shown in Figure 4.1(a).

To address the seismic deficiency of the pilecaps, retrofitting would be implemented to strengthen the substructure as will be discussed in Section 4.4. Once the substructure is strengthened, the columns and foundations would have enough capacity to cause the yielding of the linkage bolts under induced ground movements. This yielding could tend to concentrate at a single movement joint. (Typically this would be at whichever movement joint the vertical hold down bolts first failed.) With only one movement joint to take up the major portion of induced ground movements, span unseating could occur. This situation is shown in Figure 4.1(b).

Stage 2 Portion of the Bridge

In the stage 2 area of the bridge, permanent ground movements due directly to disturbance from the Wellington fault are not expected. However, this area of the bridge site is susceptible to liquefaction which could result in permanent sliding movements of the blocks of ground on which the bridge is founded. The failure of the mass concrete seawall is also possible, which would increase ground-block sliding movements.

In the stage 2 area of the bridge, the existing linkage bolts are of a smaller diameter than those used in the stage 3 area. These linkage bolts can typically yield under longitudinal ground displacements before the columns or pilecaps reach their capacities. The yielding could tend to concentrate at one movement joint resulting in span unseating as shown in Figure 4.1(b). In the stage 2 area this type of failure is possible even if the pilecaps are not strengthened.

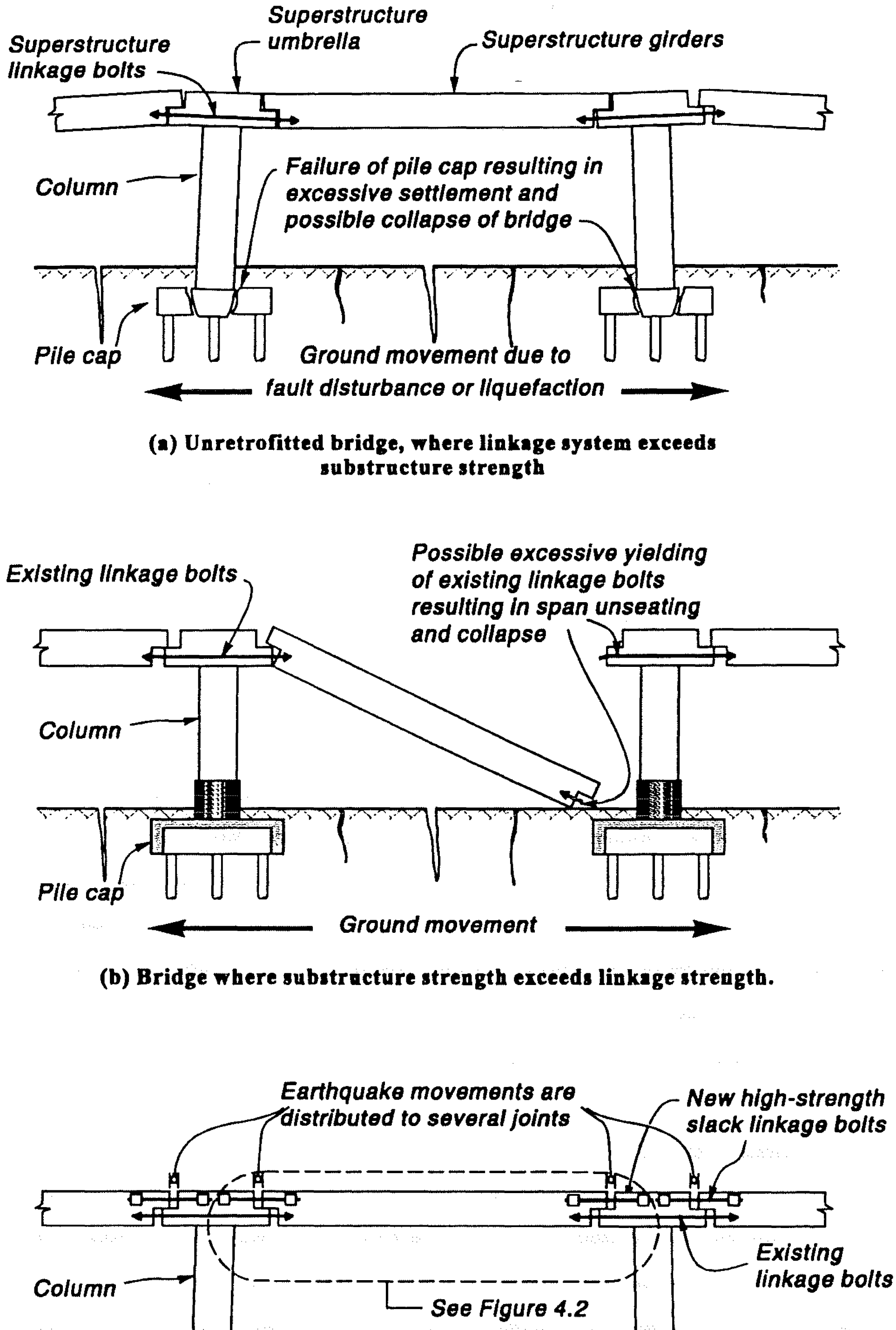

(a) Unretrofitted bridge, where linkage system exceeds substructure strength

(b) Bridge where substructure strength exceeds linkage strength.

(c) Superstructure retrofit using high-strength slack linkage bolts

Figure 4.1 **Bridge performance under earthquake-induced permanent ground movements, before and after retrofitting superstructure linkages with high-strength slack linkage bolts.**

Proposed Retrofit Measures

A scheme of linkage-bolt retrofitting has been devised to prevent unseating collapses due to permanent ground movements. The retrofit requires replacing typically 3 or 4 of the existing linkage bolts at each superstructure umbrella with high strength Dywidag or Macalloy bolts. The retrofit is shown schematically in Figure 4.1(c) and Figure 4.2. Figure 4.4 shows the location of the existing and replacement linkage bolts on a cross-section of the bridge.

The new Dywidag or Macalloy bolts are installed with slackness at each end of the umbrella. The slack bolts are anchored within the umbrella to allow equal displacement at each end of the umbrella. If the fault-disturbance tends to pull the bridge apart, the existing linkage-bolts will yield, but the high-strength slack bolts will engage before unseating occurs. Thus ground displacement demands can be distributed to several adjacent movement joints without any span collapses.

Typically, the initial linkage-bolt yield strength after retrofitting is less than the column lateral strength. Thus for longitudinal-direction displacements the linkage-bolt yielding can preclude serious damage to the substructure, assuming that the weak pilecaps in the area have been retrofitted.

The slack bolts are designed so that the ultimate strength of linkages at a movement joint before unseating exceeds the overstrength of the linkage bolts in the adjacent joints, including the hold-down bolt overstrength. This is illustrated in Figure 4.2, which shows that the design strength of the initially slack bolts plus the yield strength of the snug bolts at the left movement joint ($T_{n,SLACK}$ + $T_{y,SNUG}$) should exceed the hold-down bolt overstrength plus the snug bolt overstrength at the right movement joint (1.6 $V_{n,HOLD\text{-}DOWN}$ + 1.3 $T_{y,SNUG}$). The overstrength factors of 1.6 and 1.3 are chosen by judgement. For the hold-down bolts a higher overstrength factor of 1.6 was chosen because strain hardening, bolt kinking, and shear-friction type mechanisms could increase strengths. For the existing snug linkage bolts, strain hardening will be limited because of the long bolt lengths. Laboratory testing has been recommended to verify the bolt strengths, overstrengths, and displacement capacities [BCHF 1994b].

The linkage bolt retrofitting is complicated by variations, among different bridge piers, in the number and size of the existing linkage bolts. A general aim of the retrofit is to protect against abrupt changes in the linkage capacity along the length of the bridge. The snug and slack linkage capacity is designed to exceed the snug linkage plus hold-down overstrength at the adjacent joints, considering at least two movement joints on either side. This is illustrated in Figure 4.3.

At the umbrellas, replacement linkage bolts are anchored where possible in umbrella box girder cells which have existing access manholes. Otherwise replacement linkage bolts are grouted into the existing steel pipe ducts, or new access manholes are cut. High strength linkage bolts are not placed in the

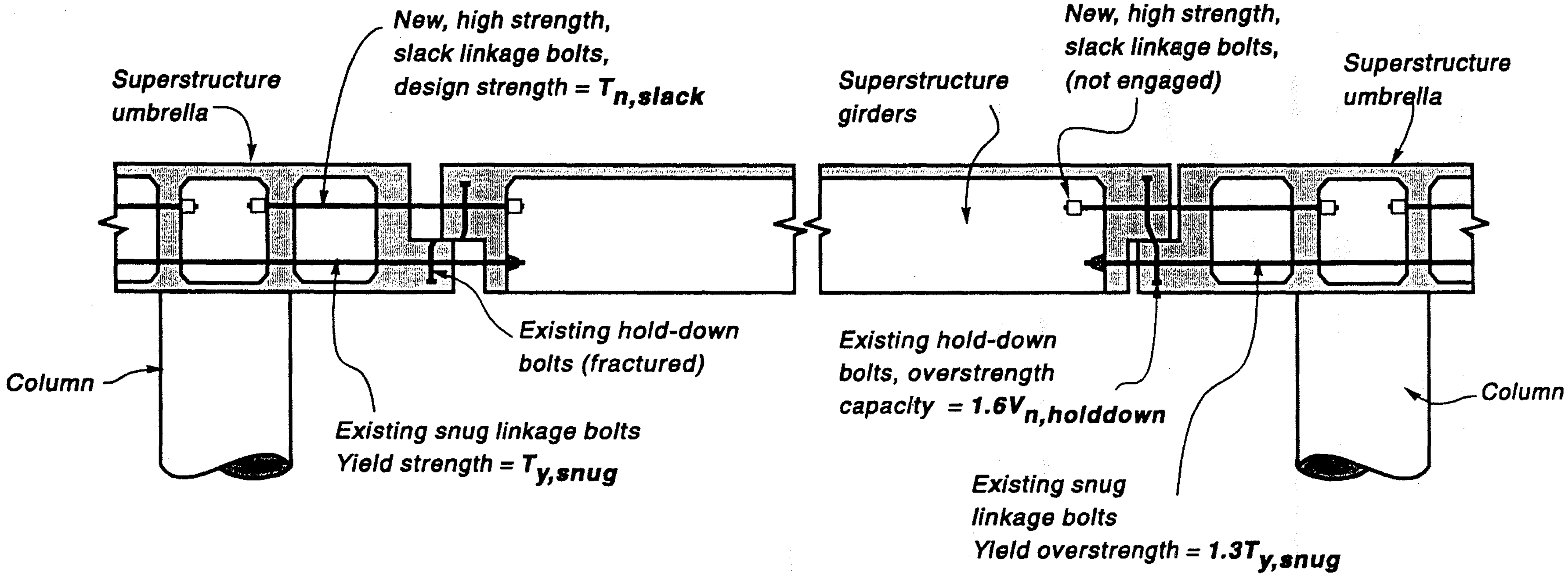

To prevent unseating, want:

$$\left(T_{n,slack} + T_{y,snug}\right)_{\substack{\text{Movement}\\ \text{Joint } i}} \geq \left(1.6V_{n,hold\text{-}down} + 1.3T_{y,snug}\right)_{\substack{\text{Movement}\\ \text{Joint } i\pm1,\ i\pm2}}$$

Figure 4.2 **Retrofitting of superstructure linkages using high-strength bolts installed with slackness.**

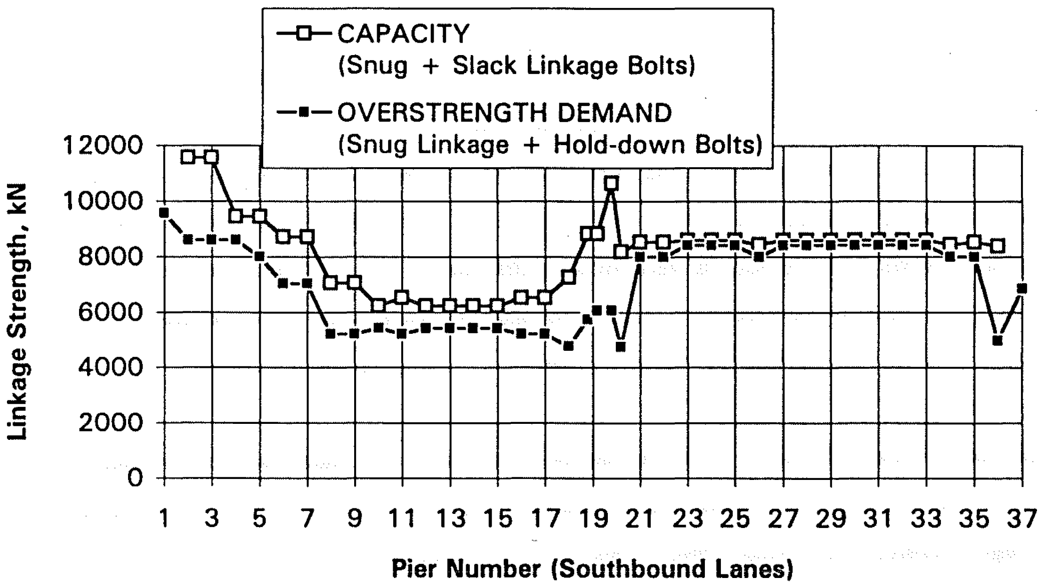

Figure 4.3 Strength of superstructure linkages along the bridge length after retrofitting

bottom locations of the umbrellas because girder end-diaphragms are weaker in these locations. To provide the maximum plan rotation capacity at the movement joints, the new slack linkage bolts are located near the center of the superstructure width at the umbrellas [BCHF 1994b].

4.3 Evaluation and Retrofit of Single-Column Piers

The majority of the piers on the Thorndon bridge are supported on single columns. Seismic evaluations indicate deficiencies in the performance of these piers, which can be addressed by foundation strengthening and column jacketing retrofit measures.

Seismic Assessment

Structural calculations reveal that the pilecaps typically represent the weak link in the seismic resistance of the single-column piers. The assessment of pilecap strength considered likely crack patterns, yield-line mechanisms, and strut and tie modelling.

The reinforcing of the existing pilecaps was apparently designed primarily for gravity loads, because the amount of reinforcing in the top mat of the pilecaps is typically very small compared to that in the bottom mat. Consequently a ratcheting type of permanent displacement can occur when the pilecap is subjected to cyclic flexural yielding due to earthquake actions. The ratcheting results from the following sequence of effects: (a) for earthquake actions in one direction, flexural cracks open from the bottom of the pilecap and the bottom reinforcing steel yields and elongates; (b) upon reversal of the earthquake actions, the top reinforcing steel yields in tension and the bottom reinforcing steel is subjected to a matching compression force. However, this compression force is not enough to reverse the permanent tensile strain present in the bottom reinforcement, or to close the cracks at the bottom of the pilecap; (c) therefore on successive cycles, the inelastic tensile strain in the bottom reinforcement accumulates, and the pilecap hinge develops a cumulative rotation in one direction.

According to Dr Richard Fenwick of the University of Auckland, the strain-ductility demands on such "one-way" plastic hinges, for a given plastic rotation, can be three times those for a conventional plastic hinge [Billings and Powell 1994]. This type of pilecap failure is schematically illustrated in Figures 4.1(a) and 4.5(b).

For the single-column piers of the unretrofitted bridge, failure of the columns is typically precluded by yielding of the pilecaps. After pilecap retrofitting is implemented, however, column yielding becomes a likely inelastic mechanism for many of the single-column piers. The original designers of the Thorndon bridge made an effort to increase the amount of transverse reinforcement at the column ends above what was typically used in construction of that era. However, the amount of transverse reinforcement is still typically inadequate to provide the desired column ductility capacities, as judged by current evaluation methods. For the seismic assessment, column strengths and ductility capacities were calculated using a moment-curvature analysis based on the Mander stress-strain model for confined concrete [Billings and Powell 1994]. Column shear capacities were assessed according to the recommendations of Priestley et al [1994].

Proposed Retrofit Measures

The proposed retrofit measures for a typical single-column pier of the Thorndon bridge are shown in Figure 4.4. The figure shows that the pilecap is strengthened using a new reinforced-concrete overlay, and post-tensioned reinforcement which is cored through the existing pilecap. The overlay is tied to the existing pilecap with drilled, grouted dowels, so that the overlay and pilecap will behave compositely. The overlay covers the sides of the existing pilecap with end-blocks which protect the post-tensioning anchors. The dowels across the overlay-pilecap interface are calculated to act in shear friction, and the end-blocks of the overlay, which contain stirrups as vertical reinforcement, are assumed to contribute to the shear capacity at the interface.

Drilled dowels are also provided to lap with the reinforcement of the existing piles, to develop the potential pile tension force through the full depth of the pilecap plus overlay. Considering a strut-and-tie model of the forces in the retrofitted pilecap, the additional dowels at the existing piles allow a steeper compression-strut mechanism to develop on the uplift side of the pilecap. These additional drilled dowels at the existing piles are also assumed to contribute to the horizontal shear-friction capacity at the overlay-pilecap interface.

Among the numerous single-column piers of the Thorndon bridge there is considerable variation in the layout, geometry and reinforcing details of the existing pilecaps, as well as variation in column capacities and construction constraints. Consequently, the proposed retrofit designs for different pilecaps also vary. For some pilecaps the reinforced-concrete overlay is not needed and the added post-tensioning alone strengthens the pilecap sufficiently to force plastic hinging into the columns. For other pilecaps, the post-tensioning is not needed, and an overlay alone is proposed. Typically the pilecap retrofitting is designed for strength only, to force plastic hinging into the columns. In some cases, however, inelastic behaviour of the pilecaps, either retrofitted with an overlay only or unretrofitted, may be acceptable. Laboratory testing has been recommended to assess the ductility capacity of the inelastic pilecap response.

Where column plastic hinging is possible, new steel jackets are provided over the potential plastic-hinge zone of the column as shown in Figure 4.4. The jackets improve the confinement of the concrete and restrain the column bars against buckling. Fibreglass/epoxy jackets have also been considered for use on the Thorndon bridge [BCHF 1994b]. Compared to the pilecap retrofit measures, the design criteria for the column jacketing are well established, as described in Section 3.3 of this report.

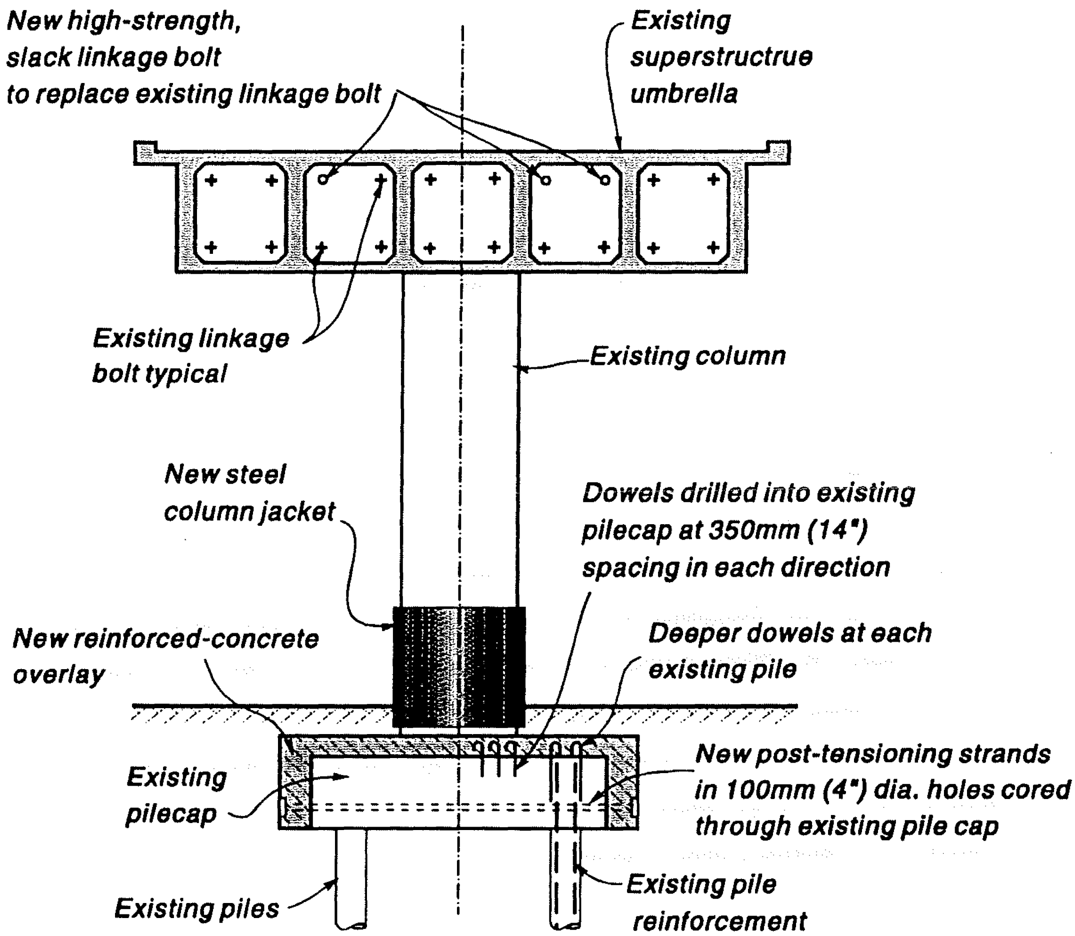

Figure 4.4 **Proposed retrofit measures for a typical single-column pier.**

4.4 Evaluation and Retrofit of Multi-Column Piers

The first construction stage for the Thorndon bridge used four to five columns per pier. The columns of each pier are connected by a continuous pilecap below, and a continuous cap-beam above which supports the superstructure girders. A number of deficiencies are evident in these multi-column piers which are addressed with retrofit measures such as infill concrete walls, pilecap overlays, and column jackets.

Seismic Assessment

Figure 4.5 shows the expected earthquake failure mechanisms for the typical multi-column piers of the Thorndon bridge.

Transverse Direction

Under transverse-direction earthquake effects, a strong-column-weak-beam mechanism develops as shown in Figure 4.5(a). The yielding zones of this mechanism, in the capbeam and pilecap, have not been detailed for ductile performance and the inelastic rotation capacity of these elements is assessed as being deficient. Flexure/shear failures could develop in the pilecap and capbeam possibly leading to collapse. In addition, the beam-column joints of the cap-beam may be vulnerable to failure, particularly if the overstrength of the cap-beam is developed, or if the cap-beam alone were to be retrofitted.

Longitudinal Direction

In the longitudinal direction, the multi-column bents are vulnerable to pilecap failures, as shown in Figure 4.5(b). This potential pilecap failure is similar to that described in Section 4.4 for the single column piers. The inelastic rotation capacity at the pilecap yielding areas is diminished due to the bottom of the pilecap being much more heavily reinforced that the top of the pilecap.

The heights of the multi-column piers vary along the length of the bridge. For the shorter columns, a column shear failure could preclude a pilecap failure as shown in Figure 4.5(c). As described in Section 2.2, there is virtually no inelastic displacement capacity in such a failure mode, and several catastrophic bridge collapses have occurred in earthquakes due to the shear failure of short columns.

Proposed Retrofit Measures

The proposed retrofit measures for the multi-column piers of the Thorndon bridge are shown in Figure 4.6.

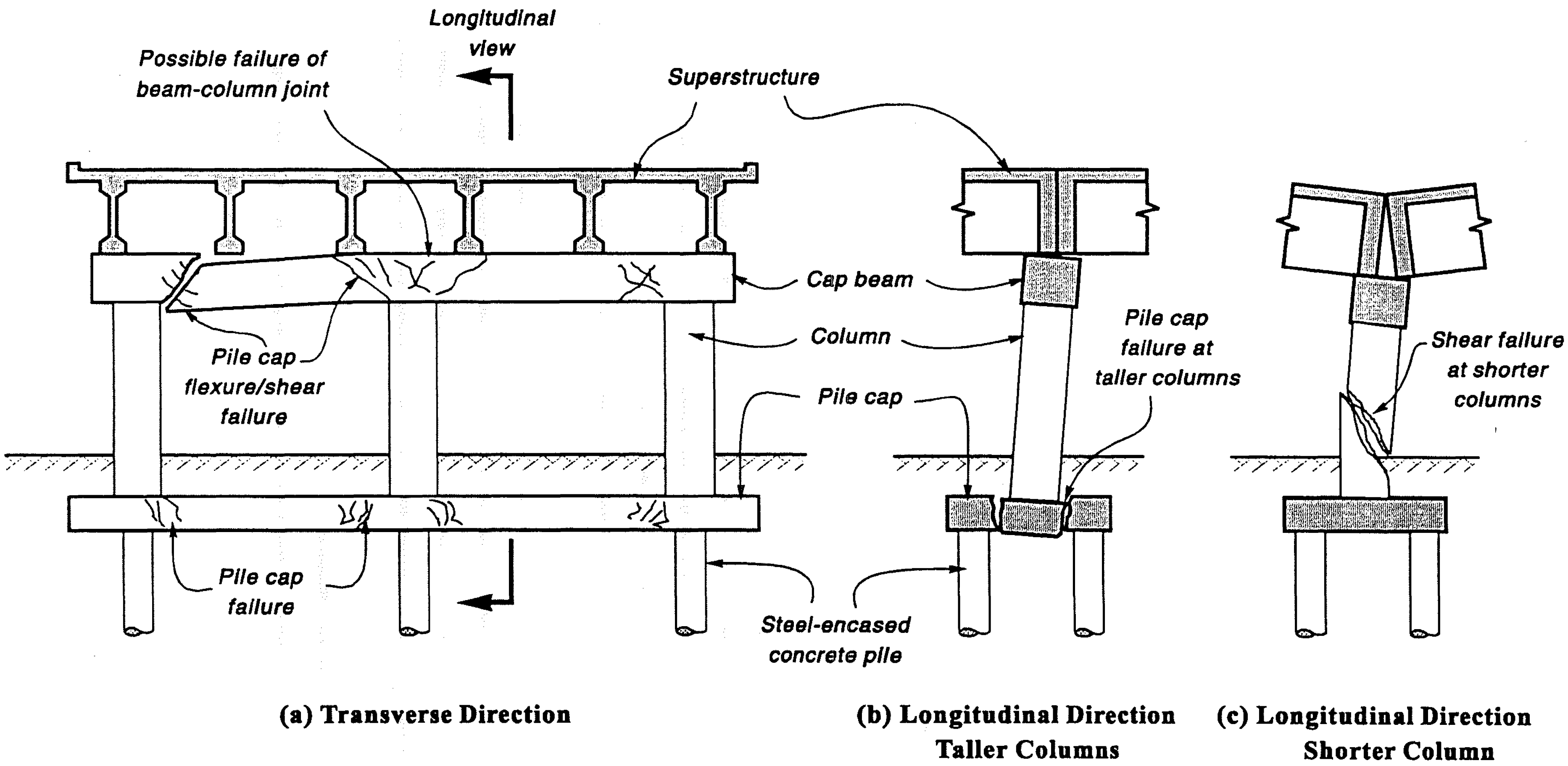

Figure 4.5 Expected earthquake failure mechanisms for typical multi-column piers of the Thorndon bridge, before retrofitting.

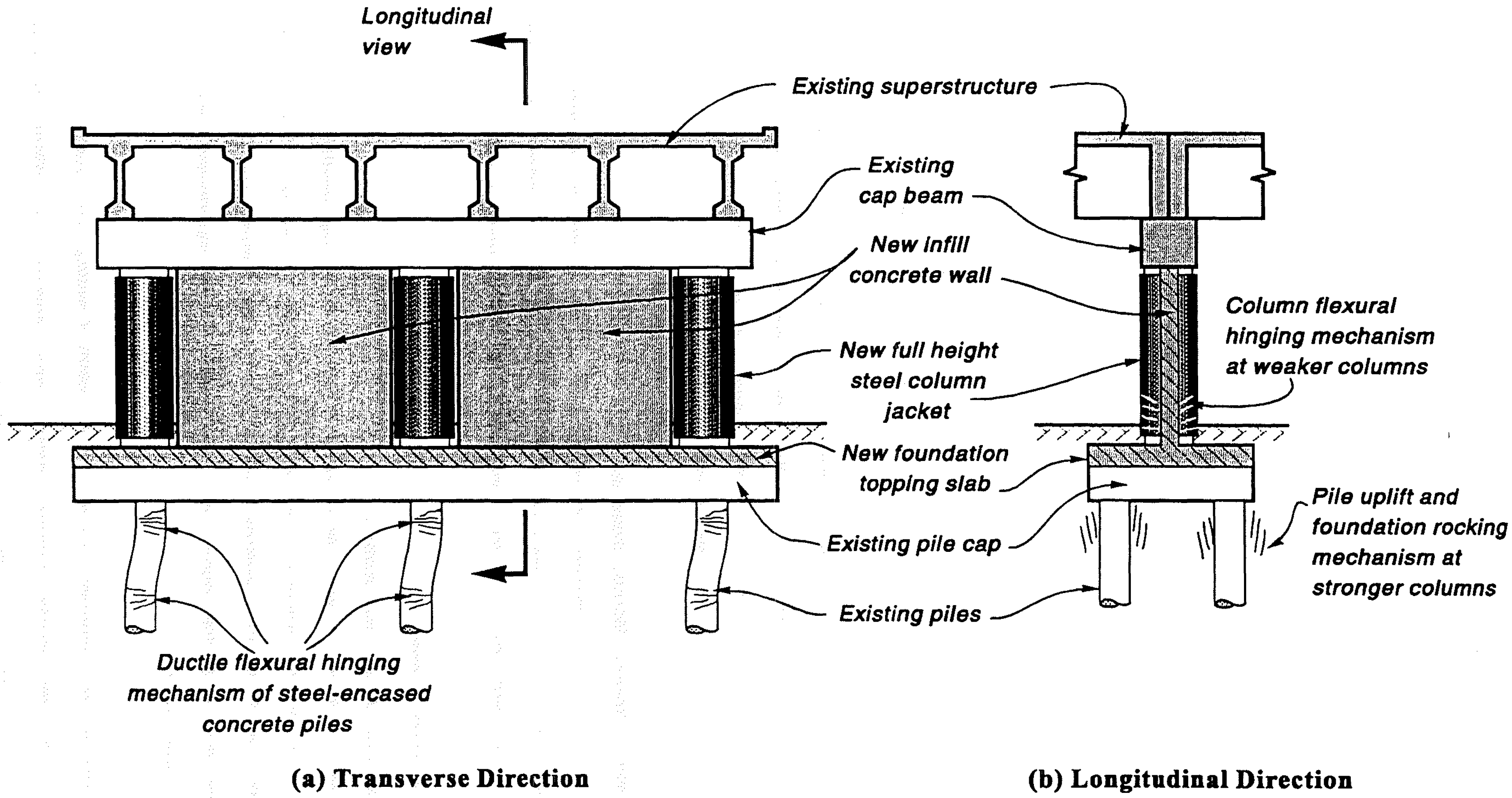

Figure 4.6 Retrofit measures for multi-column piers of the Thorndon bridge, and earthquake response mechanisms.

Transverse Direction

For transverse direction earthquake effects, reinforced concrete walls are infilled between the columns of the pier.

The infill walls are dowelled into the cap-beam above and the pilecap below. The addition of the walls causes an entirely new inelastic mechanism to govern the seismic response of the pier: a ductile flexural hinging of the existing piles as shown in Figure 4.6(a). The existing piles were constructed with steel sleeves (or jackets) which confine the reinforced-concrete pile core, providing excellent inelastic rotation capacity. The infill walls are designed for the overstrength of the pile-hinging mechanism and effectively prevent failures in the cap-beam, pilecap, or beam-column joints.

Longitudinal Direction

For longitudinal-direction earthquake effects, full-height steel jackets are added to the columns, and a reinforced concrete overlay is added to the existing pilecap. The steel jackets prevent shear failures from occurring in the columns. The overlay is used to strengthen the pilecap and force an inelastic mechanism elsewhere in the pier. For the more lightly reinforced columns, flexural hinging of the jacketed columns is expected to govern the seismic response. For the more heavily reinforced columns a pile uplift and foundation rocking mechanism may govern seismic response. These possible mechanisms are shown in Figure 4.6(b). The pilecap strengthening is designed for the lesser of the overstrength of these two possible mechanisms. Because of the uncertainty in pile uplift values, a high overstrength factor is used for the foundation rocking mechanism.

4.5 Other Proposed Retrofit Measures

Sections 4.2, 4.3, and 4.4 described the evaluation and typical retrofit of superstructure linkages, single-column piers, and multi-column piers for the Thorndon bridge. Additional retrofit measures are proposed for the bridge [BCHF 1994b], some of which are briefly described in this section.

Structural Retrofit Measures

Seat Extensions at Ramps and Abutments

Two of the most vulnerable areas of the Thorndon bridge are the seating conditions of the two ramps where they meet the main structure. No linkage bolts have been provided at these locations. The recommended retrofit measure to address this deficiency is to add reinforced-concrete seat extensions dowelled into the existing ramp support seats. The details of the existing structure make such a retrofit relatively straight forward.

The seat extension was considered preferable to the option of adding new linkage bolts at the ramp connections. The ramp juncture locations represent major geometric and stiffness discontinuities in the bridge structure where large relative movements are prone to occur. If the retrofit attempted to restrain these movements with linkage bolts, it is doubtful that the failure of the linkage bolts could be protected against. There would be practically no upper limit to the force demands on linkage bolts in such a location. Instead of trying to restrain relative movements at the ramp junctures, the seat-extension retrofit allows considerable movements to take place without span collapse. Reinforced-concrete seat extensions are also used at the bridge abutments, where it would be expensive and disruptive to replace the existing linkage bolts [BCHF 1994b].

Wellington Fault Offset

A seismic retrofit solution has been proposed to prevent collapse of the main bridge structure where it crosses the Wellington fault. The rupture of this strike-slip fault is predicted to cause a relative offset displacement of up to 5 metres (16 ft) horizontally. The main bridge axis crosses the fault trace at an angle of 25 to 30 degrees. The strike-slip offset of the fault would principally cause pulling-apart displacements of adjacent bridge piers with some relative transverse movement between the piers.

The proposed retrofit consists of frames built up of steel beams, dowelled and bolted to the undersides of the superstructure umbrellas on either side of the fault. Several of the linkage bolts at these umbrellas are replaced with slack linkage bolts. The steel frames act as 2.5 metre-long seat extensions to allow the relative pulling-apart and transverse movement of the piers on either side of the fault. The frames are designed with a shear-key stopper which, along with the slack linkage bolts, ensures that pull-apart fault offsets are distributed to each end of the span and that transverse offsets are accommodated by the plan rotation of the suspended span. The goal of the retrofit is only to prevent collapse and reduce the likelihood of casualties; the bridge spans above the fault would need to be replaced after the Wellington fault earthquake to correct roadway geometrics [BCHF 1994b].

Ground Improvement to Prevent Liquefaction

A major part of the Thorndon bridge site is susceptible to soil liquefaction. Several methods of improving ground conditions to reduce the likelihood of liquefaction were investigated by BCHF consulting engineers [BCHF 1994b]. Their findings and recommendations are summarized below.

Seismic Assessment

Underneath the northern half of the Thorndon bridge is a layer of beach sediments which is susceptible to liquefaction. Liquefaction of this soil layer would result in permanent slope displacements occurring as the overlying reclamation fill material would move in a large-scale sliding block type of ground failure. The ground acceleration at which the beach sediments liquefy is assessed to be 0.16g in a magnitude M=7.4 earthquake. The slope displacements are predicted to occur in arcs forming scallops, eventually joining up to form a complete block movement. Where the original sea bed profile is steep, this block movement may extend as far back as the original high water mark.

At a ground acceleration of approximately 0.2g, permanent slope displacements are assessed to be small, with magnitudes less than 25 mm. At higher levels of shaking the magnitude of the displacements increases, with values up to 1,500 mm predicted for ground accelerations of around 0.74g. The foundations of the overbridge are assessed to maintain gravity support at this higher shaking level, but the piles would suffer significant and irreparable damage.

Underneath the off-ramp of the Thorndon bridge is a layer of sandy hydraulic fill which is assessed to liquefy at a peak ground acceleration of around 0.19g in a magnitude $M = 7.4$ earthquake, or at a ground acceleration of around 0.25g in a magnitude $M = 6.0$ earthquake.

When the sandy fill deposit liquefies, the seawall retaining the fill is expected to fail by either overturning or sliding. This failure would permit a seaward movement of the body of liquefied material and the gravel rockfill above. It is possible that the seawall may move as much as 10 to 20 meters. Ground movements were assessed to decrease with distance back from the seawall, but would remain large (in the order of meters) as far back as the off-ramp pier foundations. These ground movements would apply very large lateral loads to the off-ramp piles and pilecaps, almost equal to the soil passive pressure, and the off-ramp would most likely collapse [BCHF 1994b].

Preferred Retrofit Measures: Stone Columns and Jet Grouting

To reduce the magnitude of the permanent slope displacements which could occur underneath the main bridge, it is necessary to improve the strength of the liquefiable materials, which are located some 10 metres below existing ground level. This improvement would not need to eliminate the permanent slope displacements, but would aim to reduce the magnitude of the displacements to a level at which the bridge foundations could maintain structural integrity.

The preferred method of ground improvement to the Thorndon bridge site to mitigate liquefaction effects involves a combination of *stone columns (vibro-replacement)* and *jet grouting* techniques. The stone columns would be implemented at discrete points along 10 m wide strips on both sides of the overbridge where there are no headroom restrictions. The stone columns would extend beneath the interface beach layer, to depths of approximately 15 m.

With the stone column technique a vibrating cell or "vibroflot" is lowered through the sandy deposit, partially being driven and partially aided by the vibrating action and water jets liquefying the deposit locally. When at the desired depth, aggregate is fed down a central column and compacted in place from the bottom up. As the vibroflot is withdrawn a dense stone column is formed in place. Both the vibrating action of the vibroflot and the compaction of the stone column densify the surrounding sandy material to a level designed to prevent liquefaction. For the liquefiable area underlying the off-ramp, preliminary designs suggest installing stone columns at approximately 2.0 m centres on a triangular grid along 10 to 20 meter wide strips of ground both on the seaward and landward side of the off-ramp.

Beneath the overbridge where headroom is restricted, jet grouting methods would be used to improve the strength of the weak fill and beach materials. With the jet grouting technique, injection tubes are installed through the fill and beach materials to the desired depth, and then a system of high pressure water, air, and grout jets are employed to mix the material in place with the grout. The injection tubes are rotated and withdrawn to form columns of "soilcrete" of up to 1.5 m diameter. A portion of the insitu material is removed through the centre of the injection tube. The diameter of the injection tube is small in comparison to the diameter of the soilcrete column formed. The soilcrete columns would be constructed over approximately 50% of the ground area beneath the overbridge, over a depth of approximately 5 m centred at mid-depth of the liquefiable soil layer. The soilcrete columns are constructed so that adjacent columns are in contact with each other, forming the system of celled walls [BCHF 1994b].

<u>*Alternative Ground-Improvement Methods*</u>

In addition to the stone column (vibro-replacement) and jet grouting systems recommended above, additional ground improvement techniques were investigated. Compared to the preferred methods, these alternative techniques were generally found to be more costly for application on the Thorndon bridge.

Two of the alternative ground improvement techniques, *displacement piling* and *compaction grouting*, are similar to the stone column method in that their effectiveness lies in densifying ground material to prevent liquefaction and loss of strength. Like the stone column technique the methods involve treatment of the ground at discrete points on a (typically triangular) grid. The spacing of the grid is designed so that the area in between the treatment points is densified. The two alternative ground densification methods are described below [BCHF 1994b]:

> *Displacement Piling*
>
> Solid piles are driven through the sandy deposit to the desired depth, displacing and compacting the loose soils around the piles. This action reduces the void spaces in the loose deposit, and therefore increases the insitu density. Several options are possible for the type of displacement pile, with timber piles, steel tube piles, and precast concrete piles available.
>
> *Compaction Grouting*
>
> Grout pipes are installed to the desired depth, and then a stiff low-slump grout mortar is injected under high pressure. This grout displaces and compresses the surrounding material, increasing its density as described above for the displacement piling. Ground heave needs to be carefully controlled so that the grout compacts the soil instead of displacing it vertically.

Two additional ground improvement methods were investigated which, similar to the jet grouting technique, rely on ground containment rather than ground densification.

The objective common to these techniques is to form a system of structural cells which contain the liquefied soil and prevent large scale lateral ground spreading. The cells can be arranged on a square grid, with the spacing of the grid designed so that the walls are capable of withstanding the lateral forces from the liquefied mass, and so that they provide sufficient shear resistance to earthquake shaking. The two methods are described below [BCHF 1994b]:

Contiguous Concrete Piles

Bored reinforced concrete piles are constructed in the sandy fill to the desired depth. It is likely that the bored holes will have to be cased before placement of the concrete, unless continuous flight auger equipment is used which pumps the concrete from the base of the auger as the auger is withdrawn. The piles are constructed so as to be touching, forming the system of celled walls.

Diaphragm Walls

Diaphragm walls are constructed with heavy hydraulic grabs to the desired depth, with a bentonite slurry mixture keeping the excavations open before the concrete is pumped in place. The system of interlocking strong walls can be constructed to a similar design as with the concrete bored piles or soilcrete columns.

CHAPTER 5
CONCLUSIONS AND RECOMMENDATIONS

Conclusions

The review of seismic evaluation and retrofit methods and examples, presented in Chapters 2, 3, and 4, leads to several conclusions:

A Past earthquakes have clearly demonstrated the seismic vulnerabilities of existing bridges—particularly for bridges designed before the early 1970s. The most serious seismic problems include the unseating of bridge spans, and the non-ductile failure of columns, beam-column joints, and column-foundation joints. Although these deficiencies are typically more severe for California bridges, New Zealand bridges also have these seismic deficiencies.

B Improvement of bridge structural analysis methods is needed. Elastic analyses give an inadequate picture of the true seismic response. Incremental plastic mechanism or "push-over" analyses are recommended. These plastic-analysis methods have been more commonly used in New Zealand than they have in California or elsewhere. Methods of modelling movement joints need to be improved.

C Analysis assumptions such as initial stiffness which are used to correlate elastic analyses with expected inelastic behaviour (eg, the equal displacement assumption) seem to need verification. Displacement-based design procedures are a promising alternative to the ductility-factor approach now used.

D Step-by-step seismic evaluation procedures are useful to bridge engineers. The development of a bridge evaluation handbook, similar in format to the *NEHRP Handbook* for buildings [BSSC 1991], and improved and updated from the *ATC 6-2* document, would be valuable.

E Several seismic retrofit techniques are now well established in California and elsewhere. Grouted elliptical and circular steel jacketing of columns is an effective retrofit solution for columns with inadequate lap splices, shear capacity, bar-buckling restraint, or concrete confinement. Effective details for restrainers and seat extenders at bridge movement joints have been developed and are widely used in California. However, methods for analytically modelling the movement joints and restrainers need improvement.

F Experimental testing of new retrofit designs is important. Some retrofit measures, designed based on engineering judgement, were subsequently shown by testing to be ineffective. Additional research may be needed in the following areas:

- Partial-confinement jacketing of columns with lap-splices is now common in California, but further experimental and analytical research should be done to validate this retrofit concept for rectangular columns and shear-deficient columns, and to improve hysteretic response.

- The evaluation of movement-joint behaviour in bridge superstructures is problematic. Experimental studies of the force-displacement capacities of typical movement-joint details, and studies of earthquake demands on movement joints would be useful.

- Seismically deficient beam-column joints and column-foundation joints are difficult to effectively retrofit. Additional development and experimental testing of potential retrofit methods, such as added external prestressing, are needed.

- Strengthening foundations and abutments to resist greater seismic forces has been common in California. These seismic strengthening measures are expensive, and paradoxically, little earthquake damage has been observed in bridge foundations. Further study of bridge abutment and foundation behaviour is warranted, including studies of foundation rocking response.

G A novel scheme of retrofitting the superstructure linkages at the numerous movement joints of the Thorndon bridge has been developed. The retrofit uses high-strength, slack linkage bolts and a capacity-design philosophy to ensure that earthquake displacement demands can be distributed to several movement joints, rather than being concentrated at one location and possibly causing span unseating. The retrofit design eliminates the need for complex modelling of the structure or precise estimation of earthquake demands at movement joints, procedures which would be of questionable accuracy.

H The proposed column and foundation retrofit measures for the Thorndon bridge illustrate the application of recent bridge seismic retrofit research and the capacity-design approach to seismic evaluation and retrofitting. The design of the retrofit measures emphasizes the development of desirable inelastic seismic response mechanisms, with less emphasis on computer modelling of the structure. This approach will make the structure less sensitive to the large uncertainties inherent in predicting earthquake force and displacement demands.

Part II

STUDIES OF A 1936-DESIGNED NEW ZEALAND BRIDGE

CHAPTER 6
BACKGROUND AND REVIEW OF COLUMN/CROSSBEAM TESTS

This chapter describes the structural features of the subject bridge on reviews previous seismic investigations and laboratory testing. The previous studies include an initial seismic assessment by Works Consultancy [Chapman 1991], testing of the column/crossbeam portion of the bridge by Rodriguez and Park [Park et al 1993], and testing of two retrofit measures for the column/crossbeam specimen by Dekker and Park [1992].

Although this chapter only covers work done by others, the discussions of the work presented here are influenced somewhat by the subsequent findings of the present author. The testing of the column/foundation-beam specimen and the inelastic analysis of the bridge offer some new insights into the results of the previous studies.

6.1 Description of the Bridge Structure

The subject bridge is typical of many of the long, multi-span bridges in New Zealand which were built to cross the country's wide shallow rivers and flood plains. The overall length of the bridge is 1100 m (3600 ft) consisting of ninety 12.2 m (40.0 ft) spans. The bridge has a reinforced concrete T-beam superstructure supported on four-column bents. The four columns are in turn supported on a foundation beam with five octagonal reinforced concrete piles. The piles extend 8.2 m (27 ft) below the bottom of the foundation beams. Figure 6.1 shows a partial elevation of the bridge, and Figure 6.2 shows a typical bridge cross-section.

Figure 6.3 shows the reinforcing details of the four-column bents. Plain-round (undeformed) reinforcing bars were used throughout the structure. Deformed reinforcing was not commonly used in New Zealand concrete construction until the middle 1960s.

Structural Integrity

At the time the bridge was designed, structural integrity was emphasized as an important seismic design consideration. A New Zealand Public Works Department design instruction from 1933 required that "wherever possible the structure should be made monolithic, and where this is not possible the structure shall be well tied together." This sound design philosophy was a result of the magnitude 7.8 Napier earthquake in 1931, New Zealand's most destructive earthquake to date [Chapman 1991].

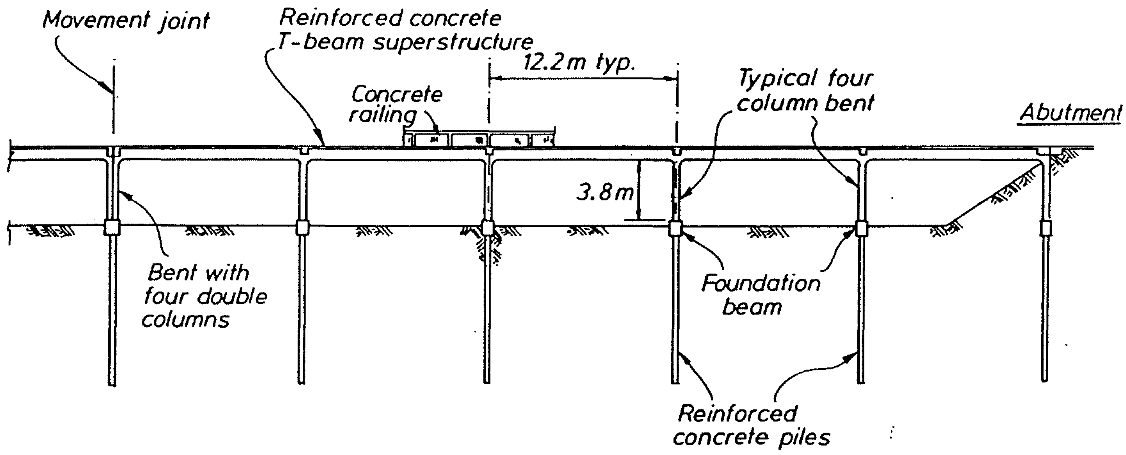

Figure 6.1 **Partial elevation of the prototype bridge.**

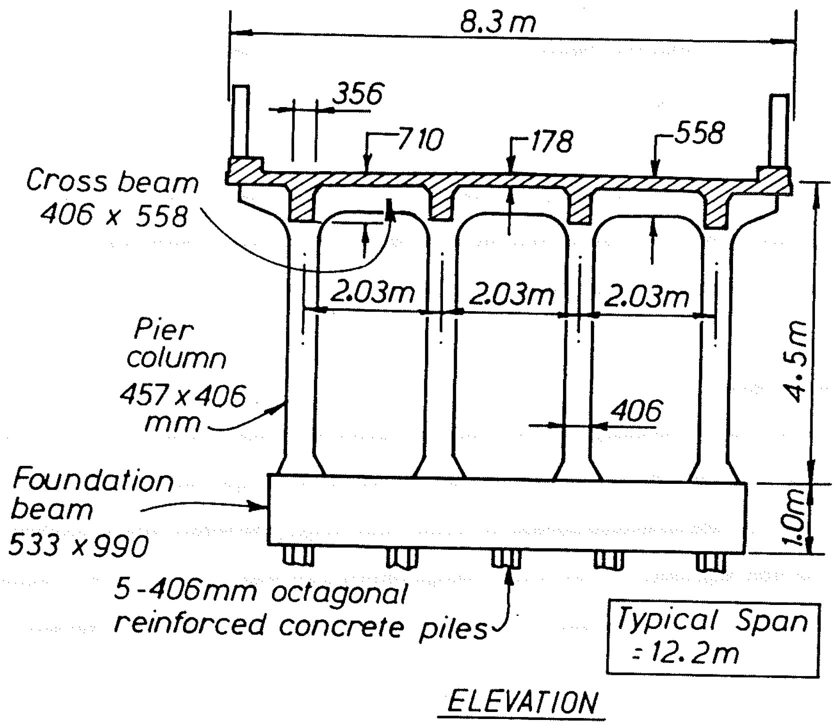

Figure 6.2 **Cross-section of the prototype bridge** [Chapman 1991].

Although long structures need movement joints, the design of the subject bridge incorporates the movement joints without sacrificing the monolithic integrity of the structure. The bridge contains 17 movement joints, one at every fifth span. At each movement joint, double columns are used so that separate columns support the spans on each side of the joint as shown in Figure 6.1. The double columns share a common pile foundation. Additional control joints are placed between every span, down the center of the transverse crossbeam (bent-beam) as shown in Figure 6.3, Section D-D. The girder top reinforcing is not continuous through this joint, so that despite the continuous appearance of the bridge, each span of the superstructure is in fact simply supported.

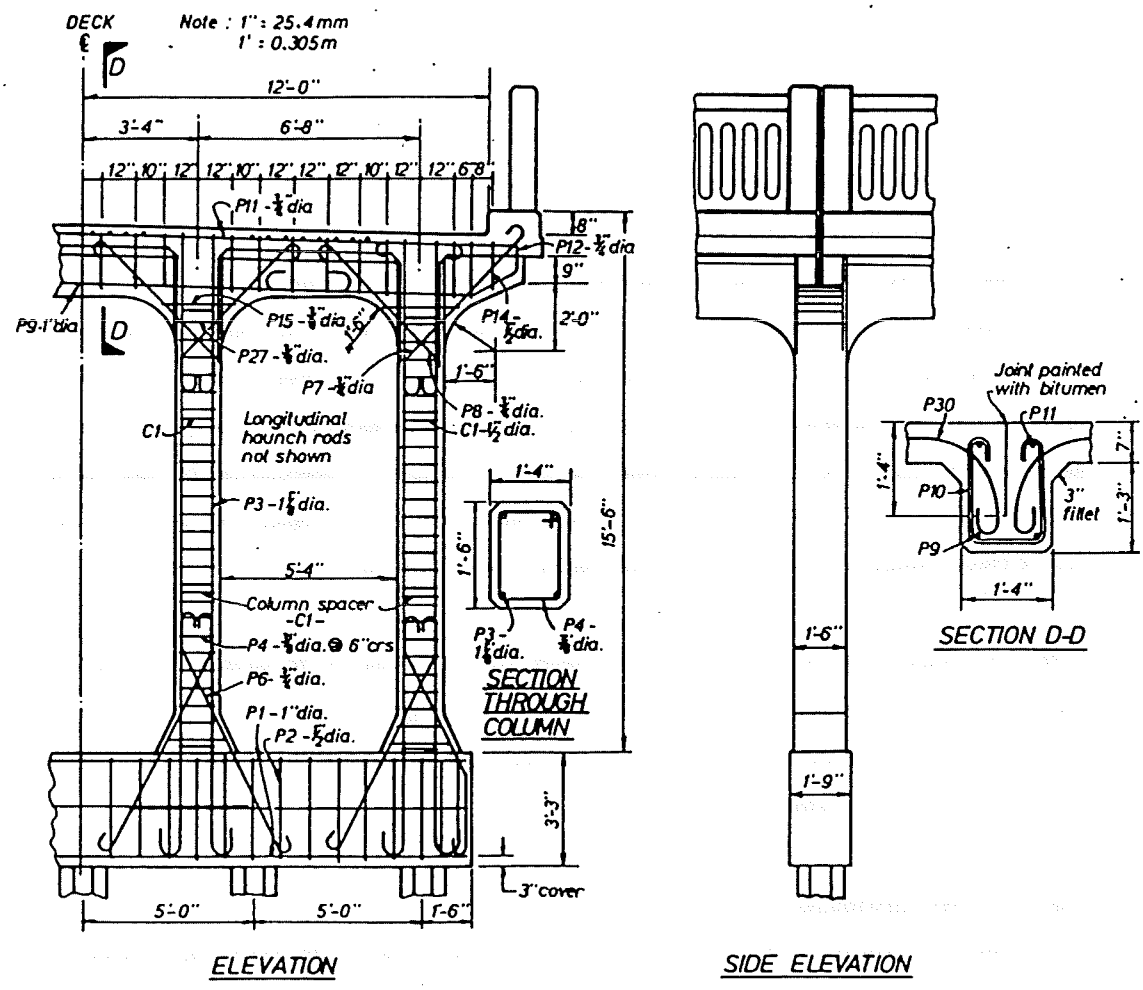

Figure 6.3 Reinforcement details of bridge column investigated [Park et al 1993].

Column Details

As shown in Figure 6.3, the columns of the typical bent are each 457 mm wide by 406 mm deep (18 by 16 inches). The longitudinal reinforcement in each column consists of four 28.6 mm (1⅛ inch) diameter bars. Transverse reinforcement steel consists of 9.5 mm (⅜-inch) diameter rectangular hoops at a 152 mm (6-inch) spacing. Four 19.0 mm (¾-inch) diameter diagonal bars are used at the flared bottom end of the column, at a slope of 2 vertical to 1 horizontal. The top end of each column is flared both longitudinally and transversely, and eight 19.0 mm (¾-inch) diagonal bars—two pairs of bars in each direction—are used at a slope of 1 to 1. The column longitudinal bars have 180- degree end hooks at the bottom and a straight anchorage length at the top. The diagonal bars and transverse hoops all have 180-degree hooks at both ends [NZPW 1936].

6.2 Initial Seismic Assessment

As a pilot study on the seismic assessment of bridges, Works Consultancy Services conducted seismic evaluations of five structures selected to be representative of common New Zealand bridge types [Chapman 1991]. One of these five bridges was the subject structure. The pilot study indicated that the bridge columns were likely to be the weakest link in the seismic resistance of the structure. The crossbeam and foundation beam which the columns frame into each have greater moment capacity than the column section itself. Thus a weak-column strong-beam plastic mechanism is expected to develop under lateral seismic forces in the plane of the bent (ie, forces transverse with respect to the bridge axis). Although this is an undesirable mechanism in multi-storey buildings, it is an acceptable mechanism for single-level structures such as bridges. In fact, the weak-column strong-beam plastic mechanism may be preferable for bridges because damage to columns is easier to inspect and repair than damage to bent-beams or foundation beams. The critical areas of the subject structure, then, are the potential plastic-hinge regions at the top and bottom of each column.

For the subject bridge, the pile foundations are typically well contained by the surface soil, thus the foundation was judged not to be a critical link in the seismic capacity of the bridge. This may not be the case for other New Zealand bridges of similar construction which have foundation piles in river beds subject to erosion and scour.

Transverse-direction Earthquake

The brief seismic assessment of the bridge from the pilot study came to the following conclusions [Chapman 1991]. For transverse seismic forces:

[1] "assuming the probable, rather than the specified minimum yield strength of the reinforcing steel, the pier columns would yield at a seismic loading of 0.3 g, provided that the piles do not yield first and that the column reinforcement anchorages do not fail (see below).

[2] with the above structure yield strength, an available structure displacement ductility of four is necessary to meet current design requirements for the most important bridges in the most active seismic areas.

[3] the pier-columns are unlikely to tolerate cyclic displacements much exceeding yield because:

[a] the rectangular hoops are widely spaced so that the column core concrete is poorly confined and the main reinforcement would be poorly restrained against buckling,

[b] the capacity of the upper part of the column to resist shear forces necessary to develop a plastic mechanism is marginal, and,

[c] the top anchorage length of the plain round column bars into the cross beam is approximately 50% of the current design code requirements, suggesting that bar anchorage failure would be likely.

[4] the piles are strong enough to resist the shear forces from the column hinging, but would themselves hinge first in flexure if they are standing as columns with a free height of more than approximately 1.5 to 2 metres (such as in a river bed)."

The subsequent experimental and analytical studies of the bridge at the University of Canterbury have provided additional information on the above conclusions. The details of the further studies are presented later in this report, but a preview of the results directly relating to the above pilot-study conclusions is as follows:

- *For conclusion 3(c):* Bar-anchorage failure does indeed control the moment capacity at the top of the column. Test results [Dekker and Park 1992] indicate that the moment capacity is diminished by 24% compared with an anchorage-retrofit specimen.

- *For conclusion 1:* the test results and calculations by the present author indicate a lateral strength of 0.45 times the seismic weight. The calculations consider (a) the contribution of the diagonal bars and axial load to flexural strength, (b) the shorter clear span between column plastic hinges related to the end flares and diagonal bars, (c) the 24% strength reduction at the top bar anchorages, and (d) probable material strengths and seismic weights.

- *For conclusion 3(b):* Calculations based on the New Zealand concrete code [SANZ 1982] indicate inadequate shear strength at the plastic hinges (90 kN capacity to 102 kN demand) if the diagonal bars are ignored. However, the diagonal bars increase the shear capacity significantly. Also, the code assumption that the concrete mechanism carries no shear ($V_c = 0$) is a conservative one.

- *For conclusion 3(a):* The transverse ties meet current code requirements for bar-buckling restraint, and bar buckling did not occur in the tests even at very high ductility. The confinement of concrete was also shown by the tests to be adequate. The conservative confinement requirements of the former New Zealand concrete code [SANZ 1982] have recently been relaxed for columns with low axial load levels [SANZ 1995].

Longitudinal-direction Earthquake

For seismic forces in longitudinal direction, the pilot study [Chapman 1991] concluded that:

> "the bridge is likely to be supported by the abutment approach fills and by interaction between sections of its length. Longitudinal behaviour is unlikely to be critical on firm ground as each span is monolithic with its supporting piers. On soft or sandy silts where soil liquefaction could occur pier/pile damage could result from individual longitudinal movements of the piles relative to the superstructure."

6.3 Tests of Original Column/Crossbeam Specimen

The initial assessment identified the critical areas of the subject bridge to be the top and bottom end regions of the columns. The amount of transverse column reinforcing was well below that required by the 1982 New Zealand concrete code [SANZ 1982], and the top bar-anchorage detail was suspect. Experimental testing of specimens representing the column-hinge regions of the bridge was carried out at the University of Canterbury to determine the severity of the presumed seismic deficiencies and the likely effectiveness of possible retrofit measures.

Test Specimen

A full-scale specimen representing the top half of the column and a portion of the crossbeam and deck slab was constructed following the original structural drawings for the bridge. The specimen was tested upside-down with the crossbeam bolted to the laboratory floor. Figure 6.4 shows the column/crossbeam test specimen and reinforcing details.

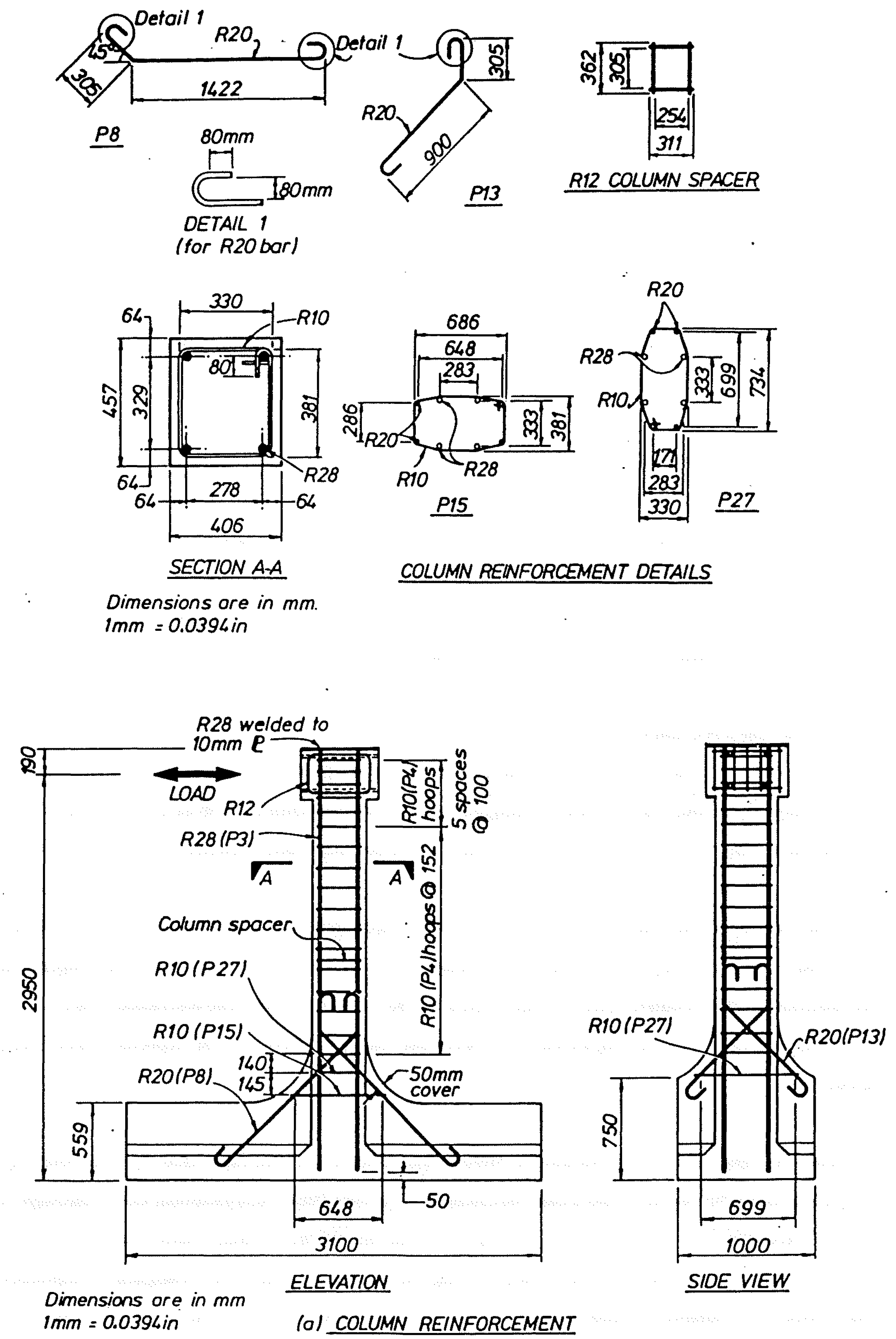

Figure 6.4 Details of column/crossbeam test specimen and reinforcing [Park et al 1993].

The rectangular column section is 457 mm by 406 mm (18.0 by 16.0 inches) and is reinforced by four plain (undeformed) longitudinal bars 28 mm in diameter. The concrete was placed with the formwork in the upright position (with the crossbeam on top) as it would have been in the construction of the actual bridge. The specimen was cast with one batch of concrete. Before testing, the specimen was inverted.

Materials

The compressive strength of the concrete for the specimen, obtained by testing 200 mm high x 100 mm diameter (7.9 x 3.9 inch) cylinders at 28 days, was f'_c = 19 MPa (2800 psi). The measured yield strengths of the plain-round steel reinforcement were f_y = 308 MPa (44,700 psi) for the R28 (1.10 inch diameter) longitudinal reinforcement and f_{yh} = 350 MPa (50,800 psi) for the R10 (0.39 inch diameter) hoops.

The longitudinal and transverse column reinforcement was from Grade 275 steel, as was the crossbeam and slab reinforcement. The prototype bridge would have been constructed using steel with a specified yield strength of 240 MPa (34,800 psi). However, Chapman [1991] reports that site sampling in New Zealand has shown that in structures built during the period 1930 to 1970, 95% of the samples of steel reinforcement possessed a yield strength which was at least 15 to 20% greater than the specified value. That is, the 5 percentile value was 276 to 288 MPa (40,000 to 41,800 psi).

Test Set-up and Procedure

Figure 6.5 shows the test set-up for the column/crossbeam specimen. A 100-tonne hydraulic jack was used to apply the cyclic, static lateral loading at the top of the specimen. The axial compressive load was applied to the column by steel rods on each side of the specimen, tensioned by hydraulic jacks.

The axial load ratio was maintained at P/f'_cA_g = 0.085 throughout the testing. Linear potentiometers were used for measuring the lateral displacements of the top of the unit and the longitudinal deformations in the potential plastic hinge region of the column. Electrical-resistance strain gauges were attached to the column longitudinal reinforcement and to the hoops in the expected plastic-hinge region.

As shown in Figure 6.6, the experimental yield displacement, Δ_y, was calculated by extrapolating a straight line from the origin of the measured lateral-load versus lateral-displacement curve through the point on the curve at 0.75 V_i, up to V_i, where V_i is the theoretical ultimate lateral capacity. V_i was calculated from the column flexural strength using the code approach of a rectangular compressive stress block, an ultimate concrete stain of 0.003, the measured values of the concrete compressive strength and steel yield strength, and assuming a strength reduction factor ϕ = 1.

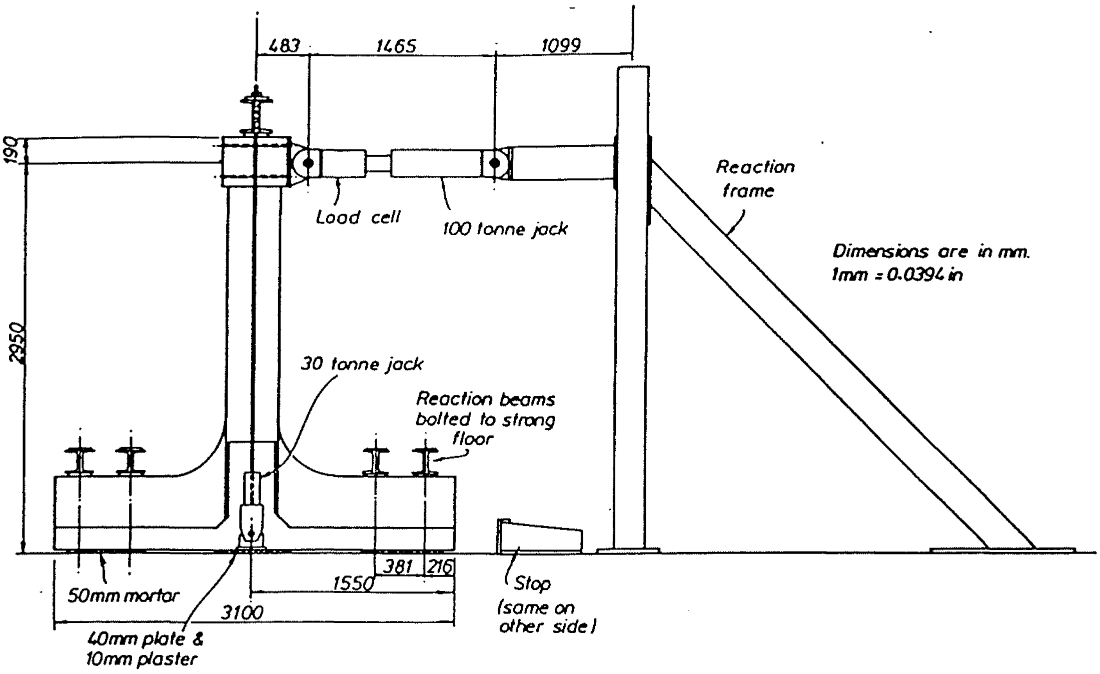

Figure 6.5 Test set-up for column/crossbeam specimen [Park et al 1993].

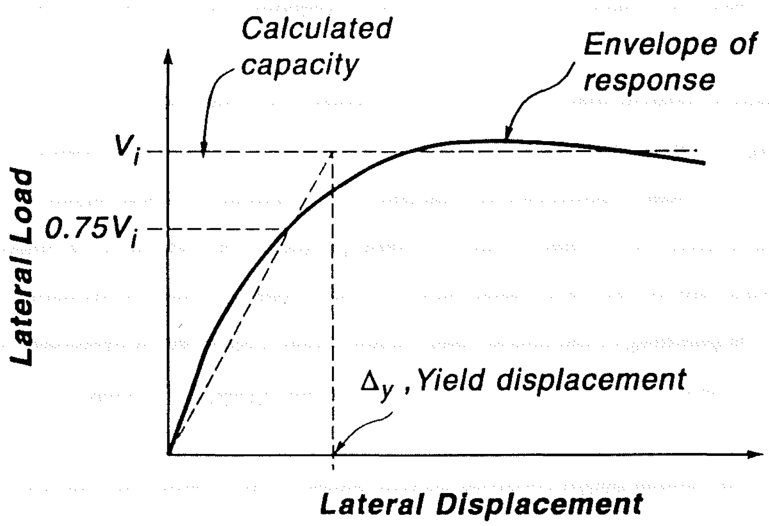

Figure 6.6 Definition of yield displacement.

Having defined Δ_y, the subsequent cycles of loading were displacement-controlled to increasing levels of displacement ductility ratio, $\mu = \Delta/\Delta_y$.

The specimens were tested with (typically) two cycles of lateral load at each ductility level up to a displacement ductility, μ, of 7. Figure 6.7(a) shows the measured lateral-load versus lateral-displacement hysteresis loops for the specimens. The dashed lines in the figure indicate the theoretical ultimate lateral load V_i including the reduction due to the P - Δ effect.

Test Results

The first flexural cracks in the unit commenced at about 50% of the theoretical ultimate lateral load. Starting from low levels of ductility, one main flexural crack developed at the critical section of the column. At $\mu = 6$ this crack opened to a width of about 10 mm. As the testing progressed, the measured lateral load versus lateral displacement hysteresis hoops became pinched and there was a significant loss of stiffness in the column.

The maximum measured lateral load was about 70% of the theoretical lateral capacity, V_i, calculated assuming adequate anchorage of longitudinal reinforcement. The flexural strength was calculated at the critical section of the column and included the contributions from both the longitudinal column bars and the inclined column bars at that section. The test confirmed the poor anchorage of the straight, undeformed longitudinal column bars. The poor anchorage led to reduced lateral capacity and to an increasingly flexible structure as the test progressed.

The test was terminated after the load cycle to a displacement ductility, $\mu = \pm 7$. At this level of lateral load there was some concrete crushing and the longitudinal and transverse reinforcement were exposed in one corner of the column. The critical section in the column, where the major crack formed, was about where the diagonal bars crossed the longitudinal bars in the column.

The strain measurements confirm that, as the test progressed, the anchorage of the longitudinal bars deteriorated, resulting in slip of the bars. The longitudinal concrete strain at the critical region of the column, measured by the linear potentiometers attached to the column, is much higher than the strain measured on the longitudinal bars in that region by strain gauges. The difference in measured strains indicates that significant slip of the plain round bars occurred from the onset of inelastic behaviour of the subassemblage. The pinching of the lateral-load versus lateral-displacement hysteresis loops shown in Figure 6.7(a) also reflects the bond deterioration of the plain-round reinforcing bars.

The strain gauges on the column hoops recorded strains below yield. Hence the concrete mechanisms of transferring shear were making a significant contribution to the shear strength of the column [Park et al 1993].

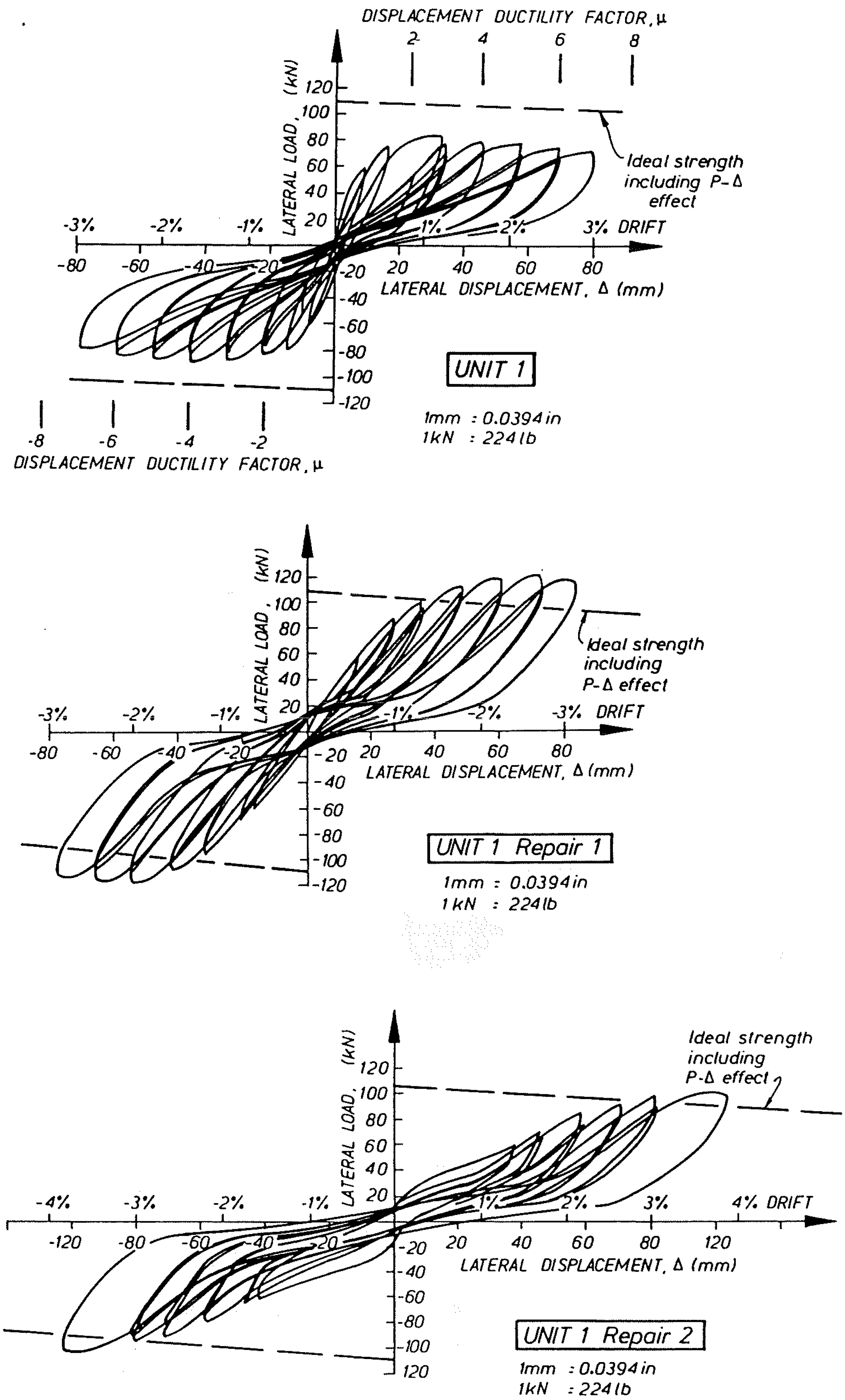

Figure 6.7 Lateral-load versus displacement hysteresis loops for column/crossbeam specimen: (a) As-built specimen, (b) Anchorage-retrofit specimen, and (c) Confinement retrofit specimen [Park et al 1993].

6.4 Tests of an Anchorage-Retrofit Specimen

The first repair and upgrade of the original specimen was designed to improve the anchorage of the column longitudinal bars. This was achieved by breaking into the deck-slab concrete, welding steel plates onto the exposed ends of the column longitudinal bars, and reinstating the removed concrete.

Anchorage Test Block

First a trial of the procedure was conducted by casting a concrete block with a 28 mm (1.10 in) diameter plain round Grade 275 bar in it, as shown in Figure 6.8. When the concrete had gained strength a hole was chipped in the end of the block to expose the end of the bar, so that a steel plate with a centrally drilled hole could be fitted over the bar and welded in place from above. The remaining cavity was then filled with a cement-based mortar. The 28-day compressive strength of the concrete was 24 MPa (3500 psi); the 28-day strength of the mortar was 30 MPa (4400 psi).

The protruding end of the bar at the other end of the block was loaded in tension in a testing machine, with the block held to provide the reactive load. The test revealed that the steel plate provided sufficient anchorage to allow the bar to develop its yield strength in tension. The anchorage block was then tested with the reinforcing bar in compression. At a force of 64 percent of the steel yield strength the specimen failed with a cracking around the concrete-mortar interface.

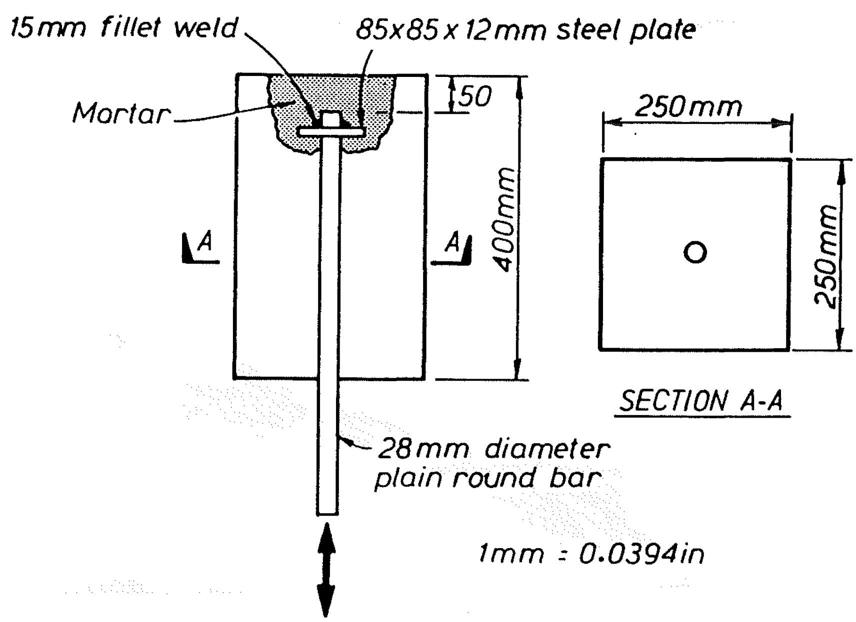

Figure 6.8 Test specimen for anchorage-retrofit detail using a steel end plate [Park et al 1993].

Retrofit Procedure

The procedure was then used to retrofit the anchorage of the longitudinal bars in the column/crossbeam specimen. After chipping out the deck concrete to expose the ends of the longitudinal bars, it was discovered that the deck reinforcement running in both directions directly adjacent to the column bars prevented the square steel plates from sliding over the column bars far enough for adequate welding. To get around this problem, the plates were trimmed to fit past the slab bars, and were welded to the slab bars as well as to the end of the longitudinal columns bars. In practice, construction adjustments of this type resulting from "on-site discoveries" are common in the seismic retrofitting of structures. The excavated concrete around the ends of the bars was replaced with cement mortar as for the test block, shown in Figure 6.8.

The repair of the specimen was completed by injecting epoxy resin into the flexural cracks of the specimen which had formed in the previous lateral load test.

Test Results

The anchorage-retrofitted specimen was then tested under the same set-up and loading as were previously used for the original specimen. For this test, it was again found that cracking tended to concentrate in one or two large cracks. Figure 6.7(b) shows the measured lateral-load versus lateral-displacement hysteresis loops. The test demonstrated that the addition of the end-plate anchorages permitted the column to reach its full theoretical flexural strength, although the lateral-load versus lateral-displacement hysteresis loops again showed a marked pinching and loss of stiffness at low lateral-load levels. It was evident that significant elongation of the column bars was occurring over their unbonded length, between the critical section for flexure in the column and the anchor plates at the bar ends. Hence the degradation of bond strength that had occurred along the column bars during the first test had not been restored by the epoxy-resin injection. Some crushing of column concrete was observed at the end of the test, particularly at the column corners in the plastic hinge region [Park et al 1993].

6.5 Tests of a Confinement-Retrofit Specimen

The second repair and retrofit of the column/crossbeam specimen involved chipping off the cover concrete of the column in the vicinity of the plastic hinge region and placing additional transverse hoops. The three new hoops, shown as A2, B2, and C2 in Figure 6.9, were each placed as two C shaped halves, lapped, and fillet welded in place. The removed cover concrete was then reinstated. The installation of the new hoops reduced the hoop spacing from 152 mm in the original specimen to 76 mm in the confinement-retrofit specimen.

The confinement-retrofit specimen was then tested under the same set-up and loading as were used previously. It was found that the lateral-load versus lateral-displacement behaviour of the sub-assemblage was again dominated by the earlier bond failure along the end regions of the longitudinal column bars (Figure 6.7(c)). The column deformations resulted mainly from the elongation of the unbonded lengths of longitudinal bar between the critical section in the column and the anchor plates. Hence large plastic hinge rotations were not required to occur in the column. The unit achieved its theoretical ultimate strength only at large lateral displacements, because of its very flexible behaviour [Park et al 1993]. The added transverse reinforcing is likely to have had *no effect* on the response.

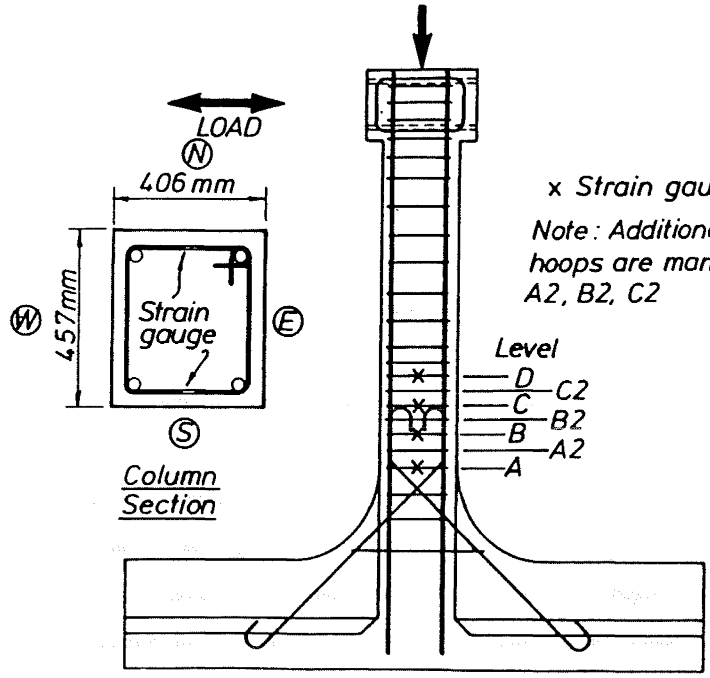

Figure 6.9 **Confinement-retrofit specimen with new hoops added at A2, B2 and C2** [Dekker and Park 1992].

CHAPTER 7

COLUMN TO FOUNDATION-BEAM TEST AND OBSERVATIONS

After the testing of the as-built and retrofitted column-top plastic-hinge detail, by Rodriguez, Dekker and Park, described in Chapter 6, the present author undertook the testing of the second critical area of the bridge, the column-bottom plastic-hinge region. This chapter describes the column to foundation-beam testing and observations. Originally it was planned to test a confinement-type retrofit of the column/foundation-beam specimen, but the seismic evaluation and initial testing results showed clearly that such a retrofit would have little effect on the seismic response of the structure.

7.1 Test Specimen and Materials

A full-scale specimen representing the bottom half of the column and a portion of the foundation beam was constructed following the original structural drawings of the bridge. Figure 7.1 shows the column to foundation-beam test specimen and reinforcing details.

Reinforcement Details

As with the previous test specimen the rectangular column section is 457 mm by 406 mm (18.0 by 16.0 inches). It is reinforced with four plain-round longitudinal bars 28 mm in diameter, approximating the 1⅛-inch (28.6 mm) bars of the actual bridge. The bars are anchored into the foundation beam with a 915 mm embedment length and 180-degree end hooks, as shown in Figures 7.1 (test specimen) and 6.3 (the actual bridge). Diagonal bars 20 mm in diameter approximate the ¾-inch (19.1 mm) diameter diagonal bars of the prototype, and 10 mm hoops are used to represent the ⅜-inch (9.53 mm) diameter hoops of the prototype. The diagonal bars and hoops both have 180 degree hooks at the ends of the bars. The hook diameters and extensions are representative of the standard used at the time of the bridge's design [NZBRC 1931] and check against the overall bar lengths given in the reinforcement schedule of the original drawings.

At the top of the specimen, the column longitudinal bars are welded to a 10 mm-thick steel plate. Similarly, at each end of the foundation beam the beam longitudinal bars are welded a 10 mm-thick end plate. The reinforcing cage for the column to foundation-beam specimen is shown in Figure 7.2(a). All of the reinforcing is undeformed.

Concrete Placement and Strengths

The specimen was held upright for the placement of the concrete. The concrete was placed in two batches as would have been done for the construction of the actual bridge. The first batch of concrete was used to place the foundation beam. The specified slump of the concrete was 100 mm, however the actual slump of the concrete when delivered to the laboratory was 180 mm. It was decided to

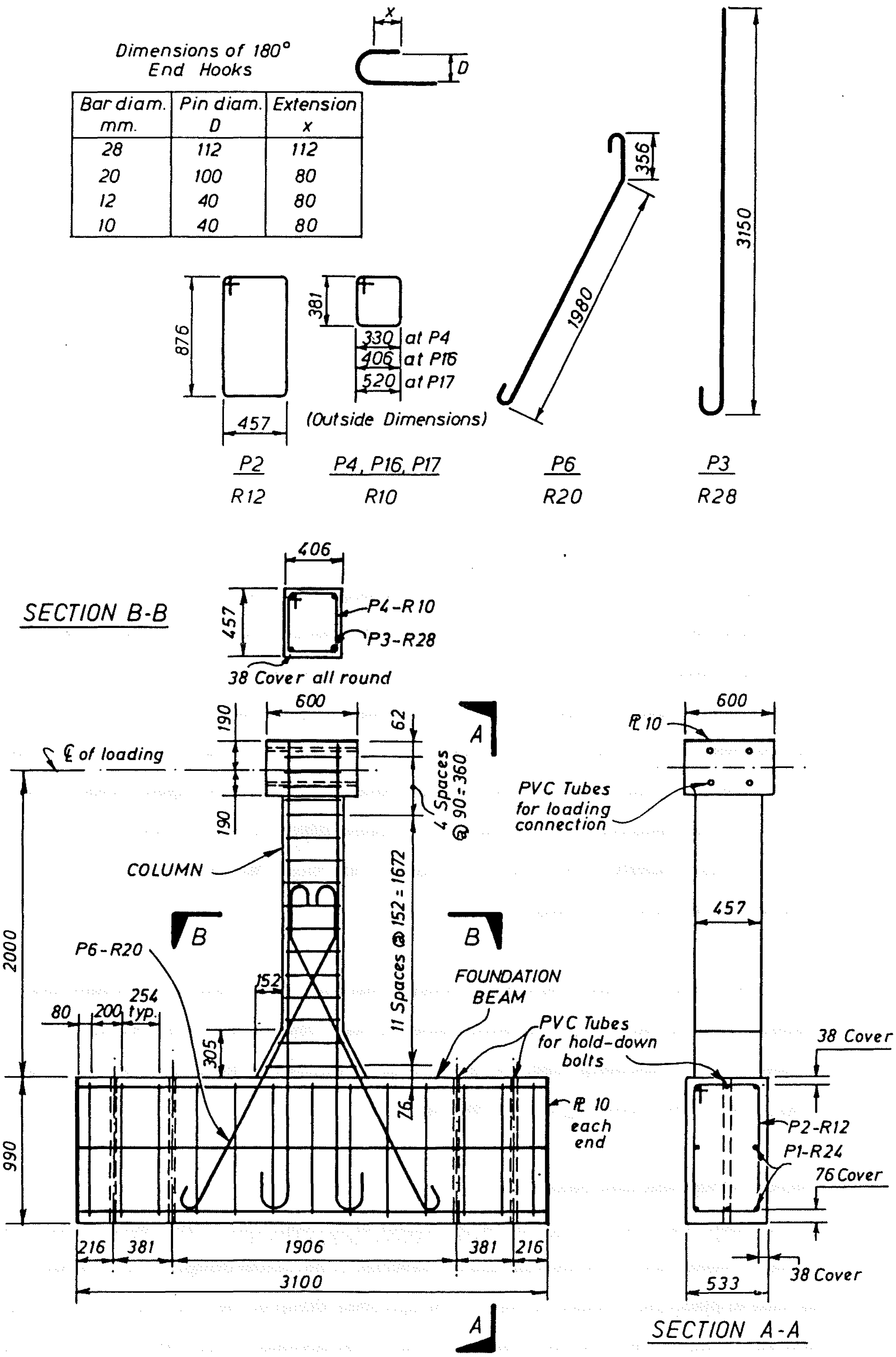

Figure 7.1 Column to foundation-beam test specimen and reinforcing details.

accept the concrete despite its non-conformance to the slump specification, because (a) the expected critical plastic hinge region did not extend into the foundation beam, (b) it was judged that the concrete would still come up to near its specified strength, and (c) material specifications and quality control in 1937 were probably not strict, particularly for foundation concrete, so that it could well be that some of the actual bridge foundations were cast with higher-slump concrete mixes.

Construction Joint

The column to foundation-beam specimen is designed to have a construction joint level with the top surface of the foundation beams, between the two pours of concrete. One day after the concrete placement it was intended to roughen the construction joint surface by wire-brushing away the still-pliant mortar paste and exposing a rough surface of course aggregate to an amplitude of 6 mm (¼-inch). This was not possible, however, because the high-slump mix allowed segregation of the concrete, and the top few centimetres of the foundation beam contained little course aggregate. To create a sound construction joint, the concrete at the column location was chipped down 70 mm (3 inches) below the top surface of the foundation beam, where a rough surface of projecting course aggregate could be exposed. The surface was air-blasted clean prior to the placement of the column concrete. The original structural drawings for the bridge give no details regarding construction joints. In practice the joints may have been prepared with a roughened surface or may have been formed with keys.

Concrete Strength

The column concrete was placed, from one batch in two lifts, eight days after the placement of the foundation concrete. The slump was 110 mm. Both batches of concrete were specified to have a 20 mm top-size aggregate and 19 MPa compressive strength at 28 days. Table 7.1 shows the results of the compressive strength tests, taken from 200 mm high by 100 mm diameter (7.9 by 3.9 inch) uncapped cylinders. The foundation concrete had a 28-day strength of 19.3 MPa (2800 psi) and a strength of 20.1 MPa (2920 psi) at the time of the column to foundation-beam test. The column concrete had a 28-day strength of 20.0 MPa (2900 psi) and a strength at test of 23.6 MPa (3430 psi). For the structural calculations, a strength of 23.6 MPa was typically used for the test specimen, and 20 MPa was assumed for the actual bridge.

Steel Strengths

Grade 275 (40,000 psi) reinforcing steel was used in the test specimen. Tension tests on sample lengths of the reinforcing steel showed that actual yield strengths are 15 to 23% greater than the 275 MPa specified minimum. Figure 7.3 shows the stress-strain behaviour of one of the test samples. All of the test samples showed a well-defined yield point and yield plateau as shown in Figure 7.3. It is interesting to note that the plain-round reinforcing exhibits an upper yield point approximately 10 MPa above the lower yield point and yield plateau. Deformed reinforcing typically does not show such a sharp yield transition or an upper yield point [Restrepo pers. comm. 1993]. This is because stress

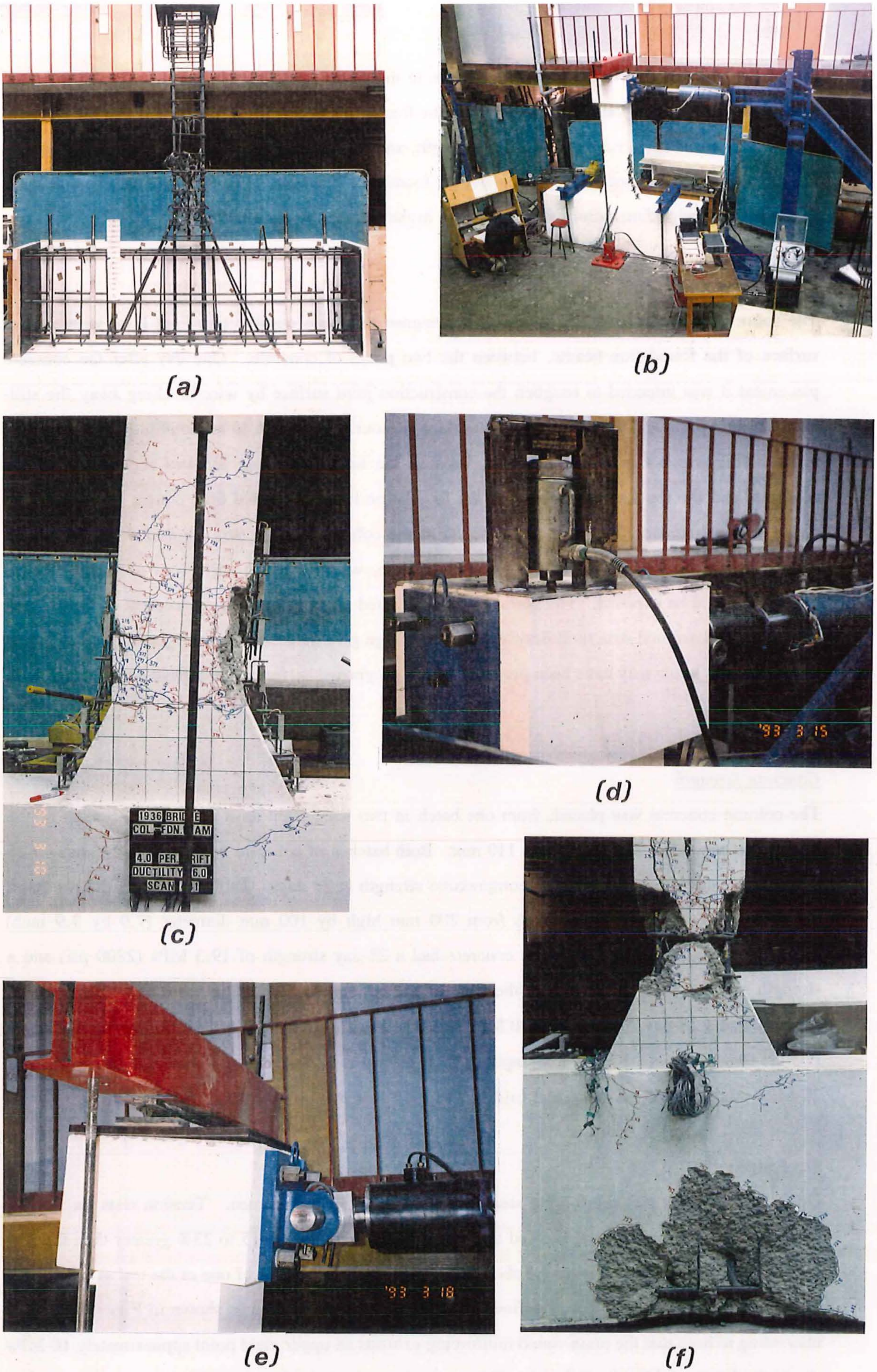

Figure 7.2 **Test of the column to foundation-beam specimen: (a) Reinforcing steel cage, (b) Test set-up, (c) Damage to the plastic hinge region at $\mu = 6$, (d) Top plate where three of the longitudinal bar end welds failed; testing the capacity of the fourth weld, (e) Displacement of the new top plate due to bond slip, (f) Anchorage splitting failure at the bottom ends of the longitudinal bars.**

concentrations at the deformations cause a slight premature yielding and a rounding of the stress-strain curve for deformed reinforcing.

Table 7.1 Concrete Strengths

Location/Date Placed	Slump (mm)	Age at Test (days)	Compressive Strength Results (MPa)	Average Strength (MPa)
Foundation 23 November 1992	180	1.2	1.8	1.8
		7	12.0, 12.6, 10.2	11.6
		29	17.8, 21.0, 19.0	19.3
		105 (at test)	19.9, 20.2, 20.1	20.1
Column 1 December 1992	110	7	13.0, 14.8, 14.0	14.3
		28	20.4, 19.9, 19.7	20.0
		97 (at test)	23.2, 23.3, 24.3	23.6

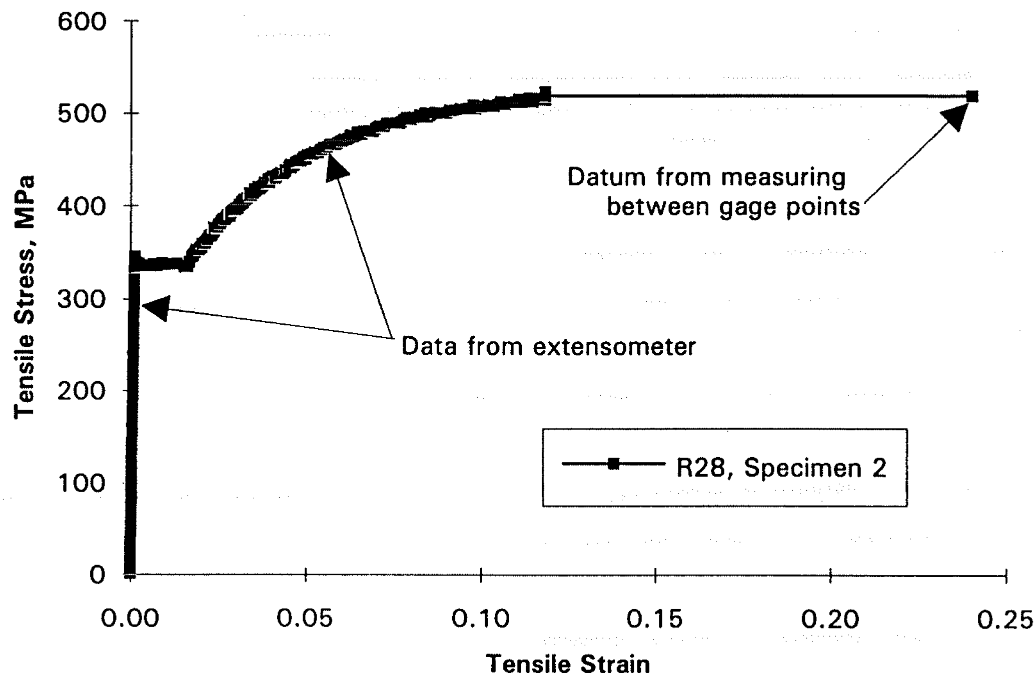

Figure 7.3 Typical stress versus strain behaviour of the reinforcing steel used in the column to foundation-beam specimen.

Table 7.2 shows the results of the reinforcing steel testing. In the structural calculations 337 MPa (48,900 psi), the average for the R28 specimens, is used as the steel yield strength for the test specimen. For the actual bridge, the specified yield strengths would have been 240 MPa (34,800 psi). However, accounting for typical overstrengths [Chapman 1991], a strength of 280 MPa (40,600 psi) is used for the prototype bridge in the structural calculations.

Table 7.2 Reinforcing Steel Strengths

Bar Size	Yield Strength Results (MPa)	Average Yield (MPa)	Ultimate Strength Results (MPa)	Average Ultimate (MPa)	Elongated lengths between 60 mm gauge points (mm)	Average Percent Elongation**
R28	431 331 349	337	519 519 519	519	73-76-85*-74-74 72-74-88*-76-76-74 74-90*-74-75-77-74	24
R24	314 330 312	319	485 487 480	485	74-74-86*-76-74 76-77-88*-74-72 72-76-87*-79-73	23
R20	334 341 339	338	495 495 495	495	70-72-84*-73-73-72 72-85*-74-74-72 71-73-85*-72-73-73	21
R12	319 312 319	317	432 434 437	434	68-68-79*-70-69 68-78*-71-67-68 66-69-71-78*-68	14
R10	335 341 333	336	463 472 463	466	68-81*-70-69 70-67-76*-67-69 78*-72-70-68-68	15

* Indicates gauge segment where necking and fracture occurred.

** Average percent elongation is the average for all those gauge segments except those where necking and fracture occurred.

Strength of Test Specimen versus Prototype

The strength of the test-specimen column differs from the strength of the prototype column. This is due to:

(a) the difference in steel yeild strengths as indicated above,

(b) the slight difference in reinforcing bar areas, eg, a 28.0 mm diameter bar is used to model the prototype's 1 1/8 inch (28.6 mm) diameter bar, and

(c) the slight difference in concrete strength.

These differences result in the moment strength of the test column being 16% greater than that of the prototype. The differences in moment strength as well as shear strength have been taken into account in the calculations and the results in this and the subsequent chapters.

7.2 Test Set-up and Instrumentation

As shown in Figure 7.4, the test set-up for the column to foundation-beam specimen was similar to that for the column to crossbeam specimen. Cyclic, static lateral loading was applied to the top of the specimen, the load point corresponding to the mid-column-height inflection point in the actual structure. The lateral load was applied by a hydraulic jack reacting against a steel frame, and was monitored by a full-bridge load cell on an 8-volt DC power supply. The lateral displacement of the column was recorded by two linear potentiometers, one at the level of the lateral load and one at a level 500 mm below.

Axial Load

An axial compressive load of 300 kN (67,000 lb) was applied to the column at its centerline, by a crosshead and roller assembly over the top of the specimen. The crosshead was pulled down by two steel rods, one on each side of the specimen, tensioned with hydraulic jacks. The tensioned rods were connected to a 40 mm steel plate which passed underneath the specimen and was bolted to the laboratory reaction strong floor. Hydraulic lines connected the two axial-load jacks in parallel to a single hand pump, so that the loads on the jacks were equal. The applied axial load of 300 kN was monitored by calibrating the pressure gauge on the hand pump.

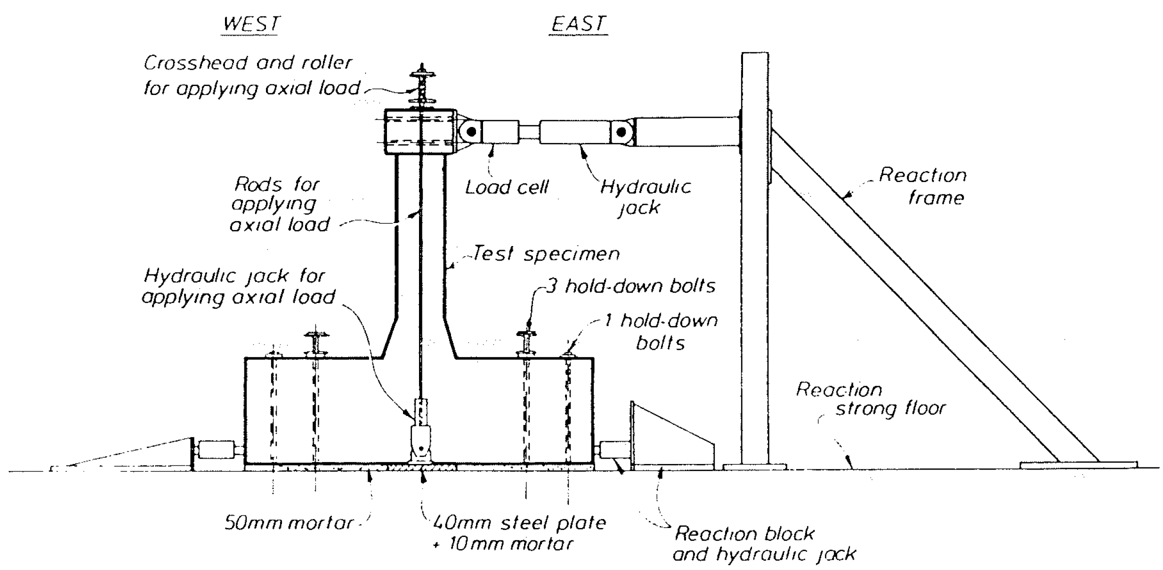

Figure 7.4 Test set-up for column/foundation-beam specimen.

Base Reaction

Hydraulic jacks were also placed between the base of the specimen and reaction blocks at each end to prevent the potential sliding of the specimen. The pressure gauge for each of these jacks was calibrated so that any change in the horizontal reaction force, indicating sliding at the base of the specimen, could be observed. Before testing, a compressive load of 200 kN was applied to each jack to lock the base of the specimen in place. A horizontal dial gauge was set up to record any sliding movement.

Four 38 mm (1½-inch) diameter bolts held each end of the foundation beam down to the reaction floor. This tie-down reaction was located at points on the foundation beam corresponding to the likely inflection points of the actual bridge foundation beam under lateral forces—ie at points half-way between adjacent bridge columns. For compressive base reactions, a 50 mm (2-inch) thick layer of cement mortar was placed underneath the entire specimen. A vertical dial gauge was installed to check if there was any uplift displacement of the specimen at the hold-down bolts during testing. The test specimen was painted white so that the development of cracks could be observed more clearly.

Instrumentation

The instrumentation of the column plastic hinge region is shown in Figure 7.5. Six linear potentiometers were attached to each side of the column to measure the longitudinal deformations of the concrete. Eighty electrical-resistance strain gauges were attached to the reinforcing steel in the column plastic hinge region. Strain gauges were placed on each of the four longitudinal bars at five levels, on each of the four diagonal bars at three levels, and on both legs of four of the transverse hoops. At each strain gauge location, two gauges were used on opposite sides of the bar, so that bar-bending strains could be accounted for.

The load-cell, linear potentiometers, and strain gauges were all connected to a data- acquisition unit. Half-bridge circuits were used for the potentiometers and quarter-bridge circuits were used for each of the strain gauges. Excitation for the potentiometers and strain gauges was 4 volts DC. The data acquisition unit was controlled by a micro-computer and the custom-designed *PC Lab* software. In addition to the digital data acquisition, an analog x-y plotter was used to record lateral-load versus lateral-displacement, and a strain indicator was used to check the load cell output. Figure 7.2(b) shows the test set-up just prior to testing.

Interior versus Exterior Column Effect

The test models one of the interior columns of the typical four-column bridge pier shown in Figures 6.2 and 6.3. The details at the base of the exterior column are somewhat different than those at the interior column as shown in Figure 6.3. The significance of the different detailing the exterior columns is discussed in Section 8.4.

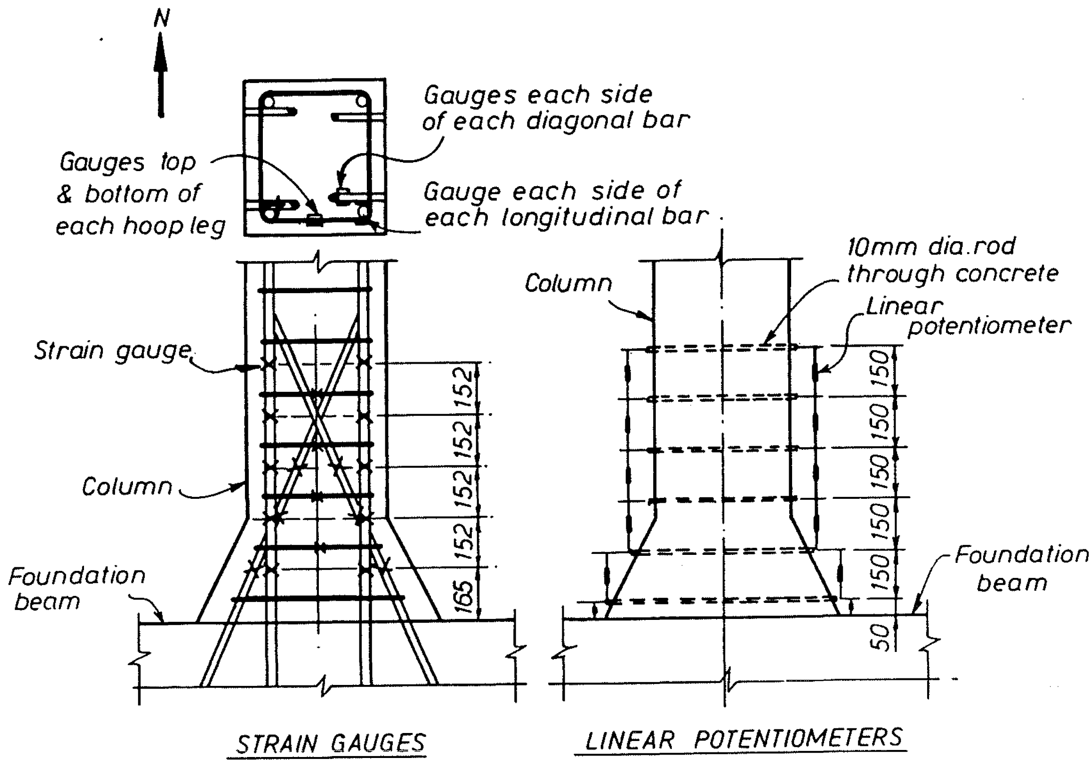

Figure 7.5 **Instrumentation of column plastic hinge region.**

7.3 Test Procedure and Observations

Figure 7.6 shows the loading sequence for the column to foundation-beam specimen. Lateral loading and displacements to the east (ie, tension in the load cell) were defined as positive. The first two cycles in each direction were load-controlled to 0.75 times the calculated ideal capacity of the specimen, V_i. Following the method illustrated in Figure 6.6, the experimental yield displacement, Δ_y, was calculated as 1.33 times the deflection recorded at 0.75 V_i. The yield displacement Δ_y for the specimen was 16.0 mm (0.67% structure drift). Because of an error in calibrating the load-cell, the first cycle was actually taken to a load of only 0.68 V_i. However, the calibration error was detected by comparing the strain indicator readings to those of the data acquisition system, the load cell was re-calibrated, and the readings from the first cycle were corrected.

After the first four cycles of load, remaining cycles were displacement controlled. The specimen was displaced two cycles in each direction to the yield displacement, 16.0 mm, then two cycles in each direction to $\mu = 2$ ($\Delta = 32.0$ mm), then to $\mu = 3$ ($\Delta = 48.0$ mm), and so on up to $\mu = 7$, with two cycles in each direction at each increment of ductility, μ. At each of the ductility levels $\mu = 8$, 9, and

10, one cycle of displacement in each direction was applied. Although it is not shown in Figure 7.6, three additional cycles in each direction to the maximum displacement stroke of the hydraulic jack (approximately $\mu = 12$) were applied before finishing the test. The cycles of testing to the larger ductilities were conducted because they could potentially provide further useful information about the structural behaviour. However, for the actual bridge such large ductility demands would not be expected.

Specimen Cracking

The first flexural cracking of the specimen in each direction was observed during the first cycles at a lateral load of approximately 30 kN, 23% of the flexural capacity of the section. Cracks in the specimen occurring under eastward displacement cycles were marked with a red pen; cracks occurring under westward displacement cycles were marked with a blue pen. The number of the data scan at the time of cracking was also marked on the specimen alongside each crack as shown in Figure 7.2(c). The first cracking of concrete due to compression occurred, on the eastern face of the column, at a ductility, μ of 2. Only minor cracking due to compression on the opposite, western face occurred during cycles to $\mu = -2$ in the opposite direction. It was not until $\mu = -3$ that a similar level of cracking due to compression occurred on the western column face. Likewise, spalling of the compression concrete occurred one ductility level sooner for the eastern column face than for the western column face. Spalling at the eastern face occurred at $\mu = 5$; spalling at the western face occurred at $\mu = 6$. Figure 7.2(c) shows the column plastic hinge region of the specimen at $\mu = 6$. Throughout testing, the flexural cracks which developed in the specimen were spaced relatively far apart, as would be expected in concrete members with plain-round reinforcing bars. The spacing between adjacent cracks over the height of the column was typically 150 to 300 mm (6 to 12 inches). For each direction of loading, the first crack in the specimen occurred just at the top of the flared column base, 300 mm (12 inches) above the foundation beam. The column diagonal bars cross the longitudinal bars at approximately this location. Up to ductility, $\mu = 5$, the horizontal crack in this location was the widest of the flexural cracks. Figure 7.7 shows that the width of this crack was 6.0 mm (0.24 inches) at $\mu = 3$ and 10.5 mm (0.41 inches) at $\mu = 5$.

This crack and the two horizontal cracks 200 mm and 350 mm above it were where most of the crack opening and closing took place. Beyond ductility level 5, the upper two of the three cracks began opening wider, indicating that the plastic-hinge region was lengthening. As shown in Figure 7.2(c) diagonal shear cracking occurred in the upper part of the column but did not occur in the region where the diagonal bars are present.

Axial Load and Horizontal Reactions

During the testing, the force in the axial load jacks fluctuated as the column was displaced laterally. The tendency is for the axial load to increase with lateral displacement and as testing progresses, because the axial loading system restrains the lengthening of the column. For the actual bridge under earthquake movement, column lengthening is not restrained and the axial load would not increase in

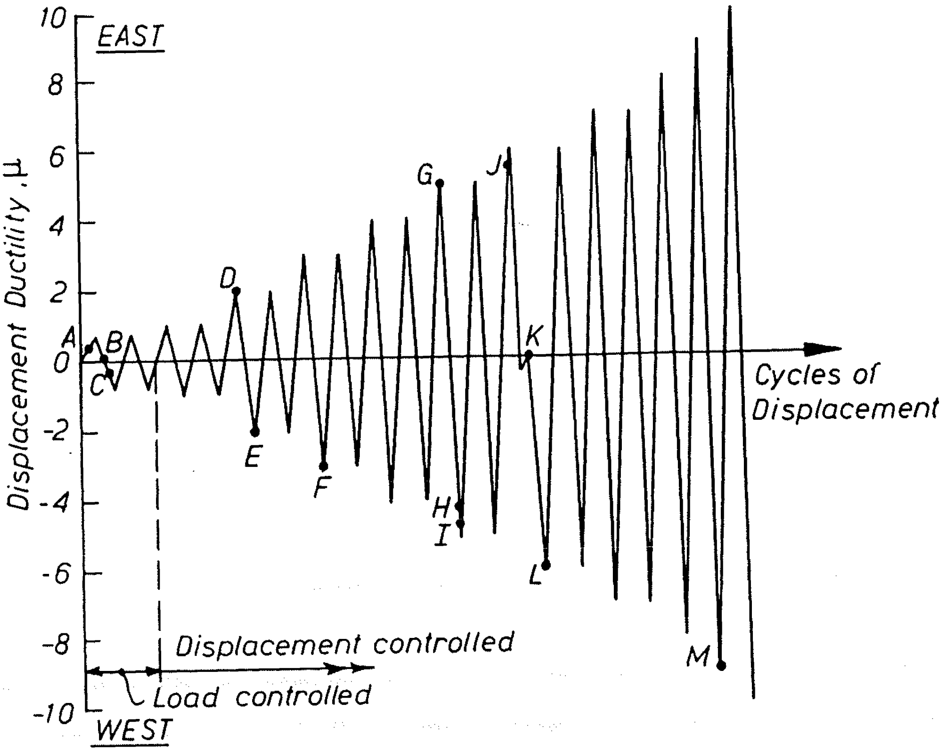

Test Observations:

A	Flexural-tension cracks on west face first observed at V = 35 kN.
B	Remove and recalibrate load cell.
C	Flexural-tension cracks on east face first observed at V = -26 kN.
D	Cracking due to compression crushing on east face (μ = +2.0).
E	Minor cracking due to compression crushing on west face.
F	More extensive cracking due to compression crushing on west face (μ = -3.0).
G	Spalling on east face (μ = +5.0).
H	Fracture of top-plate weld for first east longitudinal bar.
I	Fracture of top-plate weld for second east longitudinal bar.
J	Fracture of top-plate weld for one west longitudinal bar.
K	Test remaining top-plate weld and repair top plate.
L	Spalling on west face (μ = -6.0).
M	Anchorage splitting cracks occur at the base of the foundation beam.

Figure 7.6 Load sequence and test observations.

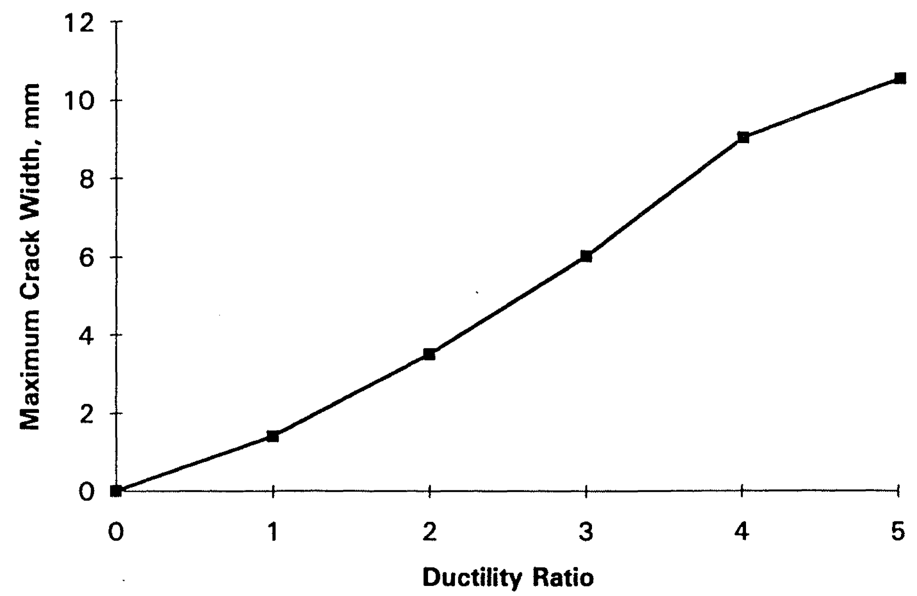

Figure 7.7 Maximum crack width measured during testing.

this way. Therefore, during testing, the pressure in the axial load jacks was periodically adjusted so that the applied axial load would remain roughly constant at 300 kN. Typically the axial load was adjusted two or three data scans before the peak lateral displacement was reached. At the peak lateral displacement of each cycle, recordings of axial load varied from 283 kN to 326 kN. Between the peak lateral displacements in each direction the axial load tended to drop slightly. The minimum recorded axial load was 254 kN.

Readings taken from the dial gauges and reaction rams at the base of the specimen indicate that there was no sliding of the specimen and that the foundation beam remained fixed at its hold-down locations throughout the test, as intended. Periodic readings of the excitation voltage to the load cell, displacement potentiometers, and strain gauges indicate that the voltage remained constant.

Lateral Force-displacement Hysteretic Behaviour

The lateral-load versus lateral-displacement hysteresis loops of the column to foundation beam test up to ductility 7 are shown in Figure 7.8. The decreasing slope of the loops during the first four cycles in each direction (μ = 0.75 and μ= 1.0) indicates some stiffness degradation of the specimen occurring prior to the yielding of the tension reinforcing steel. This yielding occurred at ductility μ = 2 in each direction, at which time the specimen reached its theoretical capacity, as shown by the hysteresis loops of Figure 7.8. Slight pinching of the hysteresis loops can be observed at μ = 1.0.

The pinching becomes pronounced by $\mu = 3$. As is discussed later, the stiffness degradation and pinching of hysteresis loops indicates bond-slip of the flexural reinforcing.

The theoretical lateral-force capacity of the specimen—calculated using (a) the (approximate) actual material strengths, $f_y = 337$ MPa and $f'_c = 22$ MPa, (b) the contributions of the diagonal bars, and (c) an ultimate concrete strain of 0.005—was 135 kN (30.3 kips). The maximum capacity measured during testing was 138 kN in the eastward direction and 144 kN in the westward direction. Both maximum capacities were reached at the first cycle to ductility, $\mu = 2$ in each direction.

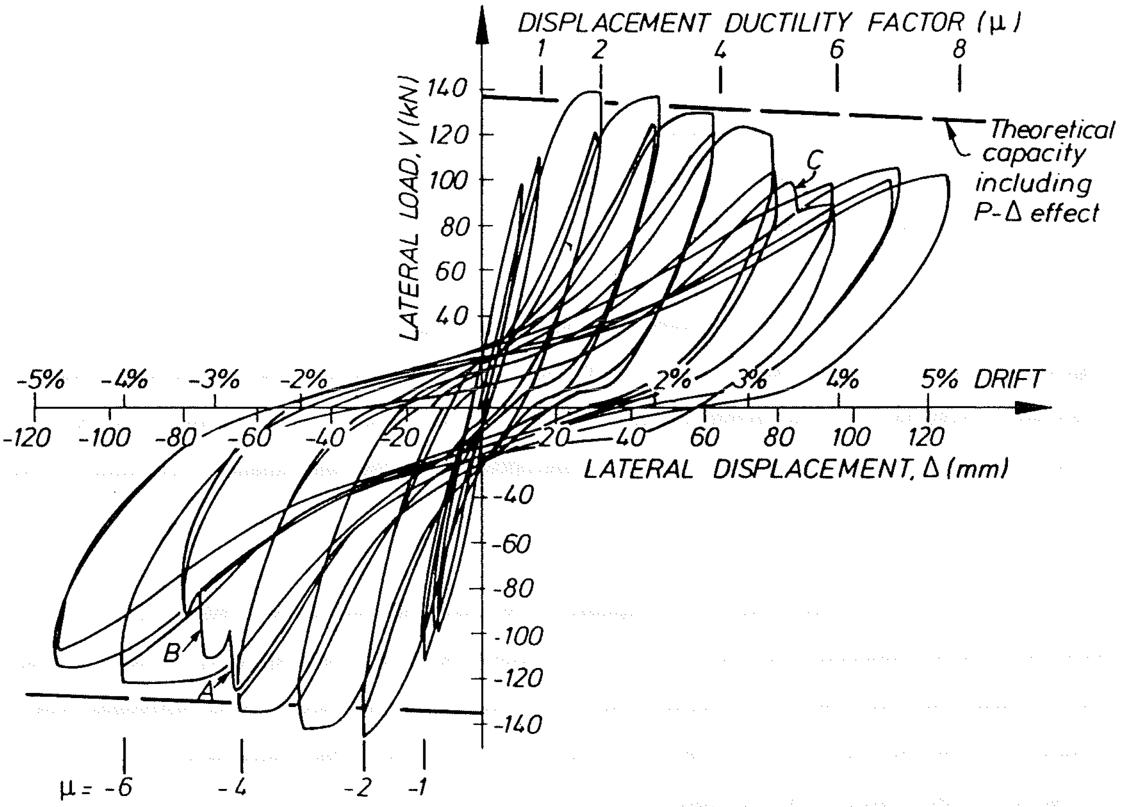

Figure 7.8 **Lateral-load-versus-displacement hysteresis loops, to $\mu = 7$, for the column/foundation-beam test.**

7.4 Failure and Subsequent Testing of the Longitudinal-Bar End Welds

On the first cycle of displacement to ductility, $\mu = -5$, nearing the peak displacement at a lateral load of 124 kN (27.9 kips), two loud bangs were heard indicating that something had broken. At each of these loud noises the lateral-load capacity suddenly dropped by approximately 20 kN (4.5 kips) as shown at points A and B in Figure 7.8.

Failure of Bar-End Welds

Upon inspecting the specimen it was discovered that the welds had fractured at the connection of the two longitudinal bars on the east side of the column to the steel plate at the top of the specimen. As shown in Figure 7.9(a), the longitudinal bars slipped approximately 5 mm with respect to the top-plate as a result of the weld fracture.

Testing was continued. On the next cycle in the other direction, to $\mu = +5$, capacity was diminished 13% compared with the previous cycle to $\mu = +5$ (103 kN compared with 119 kN previously). But the welds of the two tension bars on the west side of the column did not fracture as had the welds on the east bars. The slightly diminished capacity in this direction at $\mu = +5$ probably resulted from the loss of anchorage of the two compression bars, whose end welds had failed.

The second cycle to ductility $\mu = -5$ showed a 30% drop in capacity (87 kN compared with 125 kN just before the weld fracture). This loss of capacity clearly resulted from the loss of end anchorage at the top of the column, of the two tension bars. The slip of these bars with respect to the top plate was again approximately 5 mm.

On the first cycle to $\mu = +6$, at a displacement corresponding to $\mu = +5.3$, one of the westward longitudinal-bar end welds failed with a loud bang. At this failure, the lateral-load capacity immediately dropped 15 kN as shown at point C of Figure 3.17. Testing was continued and the peak displacement at $\mu = +6$ was reached without failure occurring in the last remaining longitudinal-bar end weld.

The failure of these end welds was not anticipated. The end welds are located 190 mm (7.5 inches) above the column inflection point and 1.9 m (6.2 ft) above the critical section of the column. It had been assumed that over this 1.9 m length, equal to 68 bar diameters, enough bond resistance would be present so that the tension force in the end welds would be small. This assumption was shown, by the fracture of the welds, to be incorrect.

Testing of Bar-End Weld

Because no instrumentation was in place to measure bar strains away from the plastic hinge region, the tension force present at the ends of the R28 bars, which caused the welds to fail, was not known. To gain this important piece of data, it was decided to test the capacity of the remaining intact weld. This was accomplished by setting up a hydraulic jack which pushed down on the end of the bar and reacted against the steel top-plate.

The testing of the weld is shown in Figures 7.2(d) and 7.9(b). As shown in the latter figure, the top end of the R28 bar was countersunk so that a concentric point load could be applied to it through a ball bearing. The reaction to this load was carried into the steel top-plate through a small cross-head frame

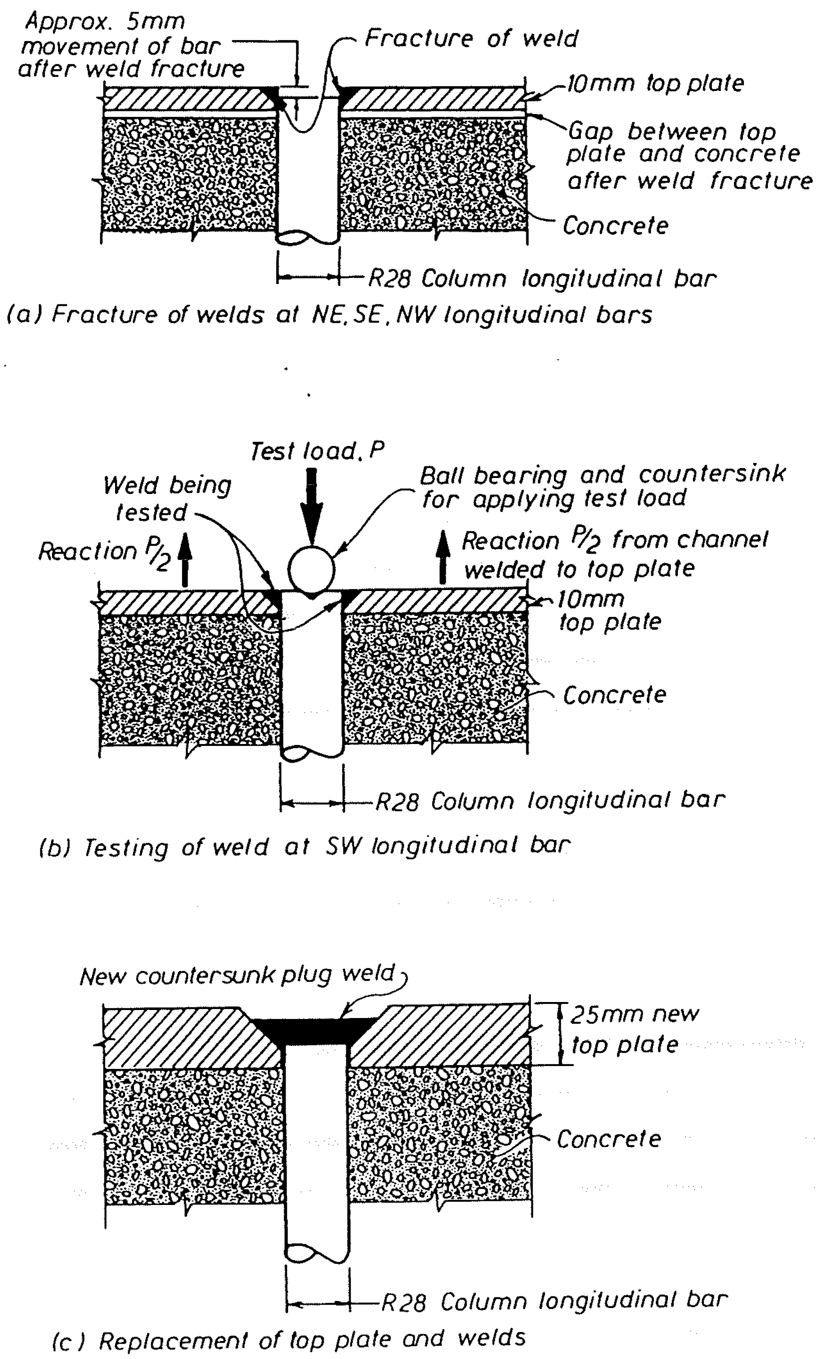

Figure 7.9 **Fracture, testing and repair of the longitudinal-bar end welds to the specimen top-plate.**

around the hydraulic jack as shown in Figure 7.2(d). The cross-head frame was made up of 150 mm-deep steel channel sections, and was welded to the top plate. The hydraulic jack and its pressure gauge were calibrated before the weld test.

Estimate of Tension Force at Weld Failure

The weld failed under a test load of 95 kN (22 kips). This equals 46% of the yield strength of the R28 bar. How representative this test result is of the capacity of the three other welds which failed previously, during the testing of the column to foundation-beam specimen, must be considered. On the one hand, the capacity of the fourth weld should be somewhat greater than the capacity of the first three welds, because it did not fail under the column testing to $\mu = 6$. On the other hand, a small amount of grinding on top of the top-plate at the weld was necessary to locate the bar before testing the weld. This grinding may have slightly reduced the capacity of the weld.

The capacity of the first three welds which failed can also be estimated based on the drop in lateral load at fracture during the column test. Assuming a moment arm between internal tension and compression forces that stays constant at 300 mm at the critical section, the lateral-load drop of 20 kN (for the first two bars) corresponds to a drop in bar tension of 110 kN at the critical section. The lateral-load drop of 15 kN for the third bar corresponds to a bar-tension drop of 85 kN. However, the drop in bar-tension at the critical section is not necessarily equal to the loss of capacity at the end weld, because the amount of bond-resistance along the 1.9 m length between the critical section and the end weld may have changed due to the sudden increase in bar-slip upon the fracturing of the end welds.

Considering the above factors and test data, it is estimated that the tension in the ends of the longitudinal bars, at a column displacement ductility of 5, was between 35 and 55% of the yield force (72 kN to 114 kN).

7.5 Continuation of Column-specimen Testing and Observations

After testing the weld, the top-plate of the specimen was removed and replaced with a new 25 mm thick top-plate. The new top-plate was attached to the four longitudinal bars using countersunk plug welds as shown in Figure 7.9(c). Testing of the column to foundation-beam specimen was then continued.

It was observed that slip of the bars at the top of the specimen was still occurring. Upon loading in each direction, the two longitudinal bars which were in compression pushed the new top-plate away from the specimen. At a ductility of 10, the slip at the compression bars caused a gap of as much as 10 mm between the top-plate and the concrete as shown in Figure 7.2(e).

Because the stiffness and strength degradation characteristics of the specimen seemed to result mainly from the poor bond characteristics of the plain-round reinforcing bars, it was judged that there would be little purpose in testing a confinement retrofit or jacketing of the column. Thus it was decided to test the original specimen to extreme ductility levels. Figure 7.10 shows the lateral-load versus lateral-displacement hysteresis loops through to the end of testing, approximately $\mu = 12$.

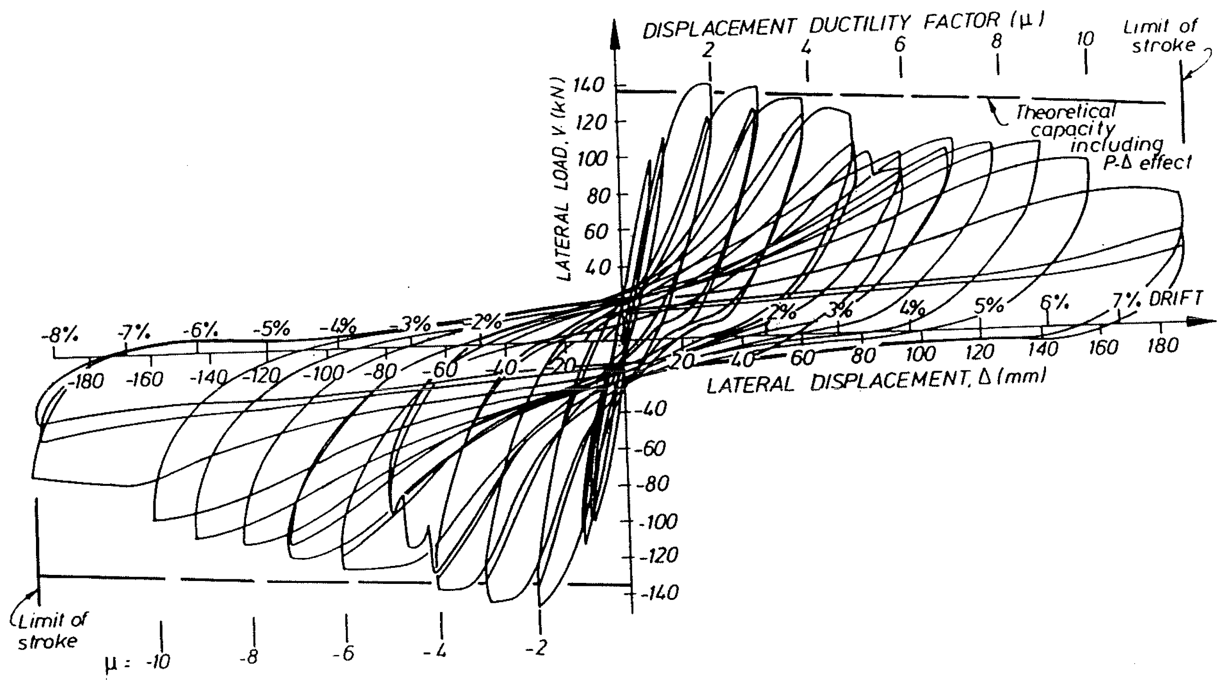

Figure 7.10 **Lateral-load-versus-displacement hysteresis loops, to $\mu \approx 12$, for the column/foundation-beam test.**

Splitting Failure at Bar Bottom Anchorage

At a displacement ductility factor, $\mu = 9$, splitting cracks were observed in the bar-anchorage region of the foundation beam. At $\mu = 10$ the foundation beam concrete was spalling as a result of the splitting failure at the bar anchorage. Figure 7.2(f) shows, at the conclusion of testing, the splitting failure at the bottom end-hooks of the column longitudinal bars. The splitting failure occurred at both sides of the foundation beam. After the conclusion of testing the specimen was laid on its side, and it was observed that the longitudinal splitting cracks had propagated to the bottom surface of the beam. Upon removing the loose concrete, it was observed that the end hooks of the longitudinal bars had slipped approximately 4 mm, and the concrete above and below the hooks was pulverized because of anchorage bearing stresses.

Figure 7.2(f) also shows the spalling of the column plastic-hinge zone at the conclusion of the test. Close inspection of the plastic hinge region showed a gap of approximately 1 mm between the longitudinal bars and the surrounding concrete. This gap probably caused by the dilation of the crushed concrete rather than to the diameter reduction of the reinforcing due to Poisson's effect. Measurement between the longitudinal-bar strain gauge locations, originally 152 mm apart, showed almost no residual elongation in the reinforcing. This confirms that because of the poor bond, the yielding of the steel was distributed over a substantial length of the longitudinal bar, and that there was no concentration of large steel strains in the plastic hinge region. The longitudinal bars did not buckle during the testing.

CHAPTER 8

EVALUATION OF EXPERIMENTAL RESULTS AND POSSIBLE RETROFIT SOLUTIONS

The analysis of the column/foundation-beam test results presented in this chapter is organised around three topics: (a) the effect of the plain-round reinforcing bars and the consequent bond slip and stiffness degradation, (b) the effect of the supplementary diagonal bars and the column shear capacity—these two topics are related because the diagonal bars contribute to shear capacity—and (c) the plastic hinge behaviour related to concrete confinement and bar-buckling restraint. The experimental results are compared with the seismic performance which would be predicted by a typical engineering assessment, using structural design codes or similar provisions. The results indicate better seismic performance for the subject structure than that implied by design codes, which are not strictly applicable to structures with plain-round reinforcing bars.

8.1 Effect of the Plain-Round Reinforcing Bars and Bond Slip

As mentioned in the previous chapter, the slope of the load-versus-displacement hysteresis curves for the column/foundation beam specimen decreased during the first four cycles in each direction (μ = 0.75 and μ = 1.0, Figure 7.8). This stiffness degradation, prior to yielding of the reinforcing steel, suggests that bond slip in the specimen began in the very early stages of testing. The steel and concrete strain measurements confirm that bond slip occurred in the specimen even in the first "elastic" cycles of testing.

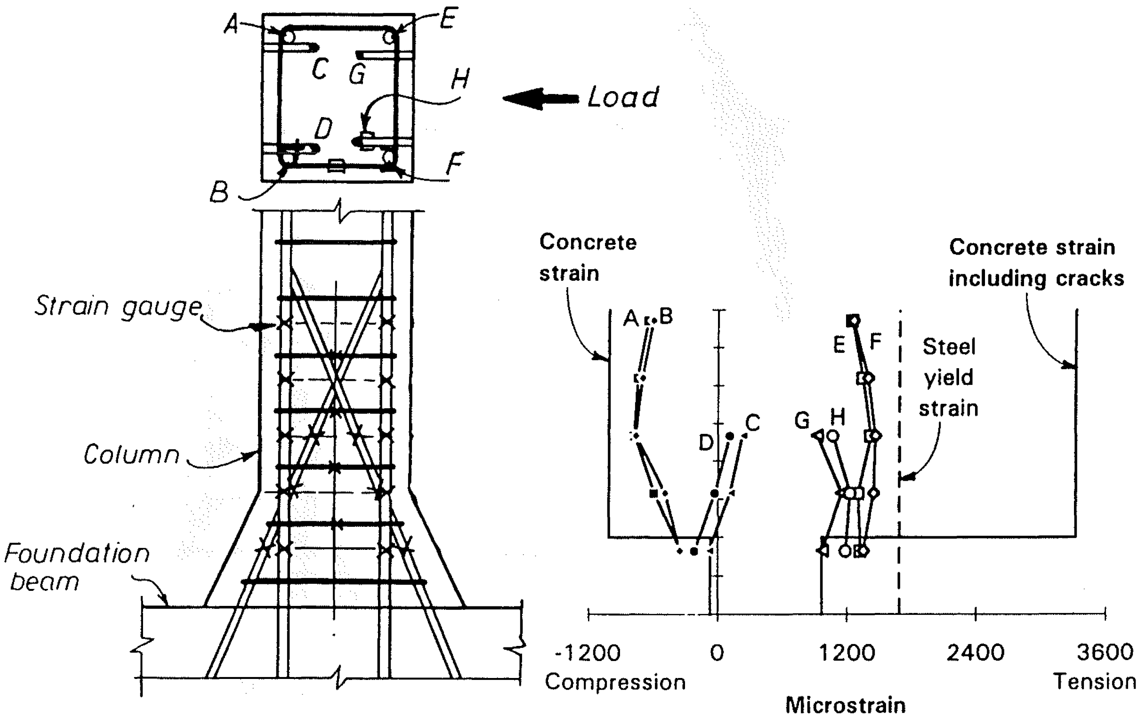

Figure 8.1 Concrete and steel strain profiles in the column plastic hinge region at $\mu = +1$.

Strain Results at $\mu = 1$

Figure 8.1 shows readings of steel and concrete strains in the column plastic-hinge region at the peak westward displacement of the first cycle to ductility factor 1. The steel strains are taken at five heights on each of the four longitudinal bars, and at three heights on each of the four diagonal bars as shown in the figure. The concrete strains include crack-opening displacements and are averaged over the first 200 mm above the foundation beam, where one flexural crack was present, and over the next 600 mm of the plastic hinge height, where the three main flexural cracks of the column were present. The concrete strain readings are measured by the linear potentiometers attached to the tension and compression faces of the column and translated to strains at the depths of the longitudinal bar centerlines. Thus the difference between concrete and steel strain readings in Figure 8.1 indicates the bond slip between the two materials, at the longitudinal bars.

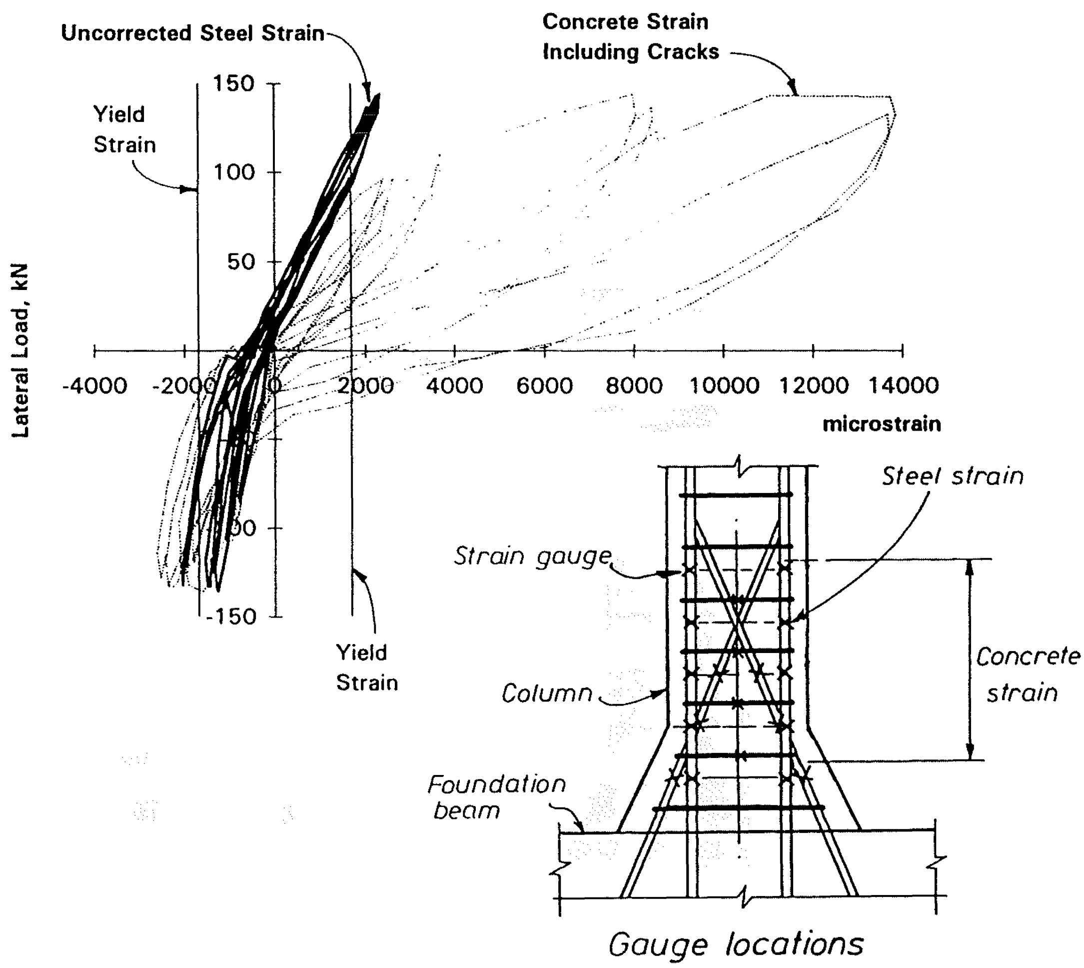

Figure 8.2 Lateral-load versus strain hysteresis loops up to and including $\mu = 3$.

At $\mu = 1$, the longitudinal tension reinforcement had reached a maximum strain equal to 87% of yield. The average concrete strain (including crack opening) over the same region is almost twice the steel yield strain and 2.2 times the maximum steel strain. Thus, bond slip at the tension reinforcement is evident.

There is also some bond slip at the compression reinforcement. At $\mu = 1$, the maximum strain in the compression longitudinal bars is 46% of yield strain. The average compression strain in the concrete at the same location is 60% of the steel yield strain, and 1.3 times the maximum steel strain.

Strain Results to $\mu = 3$

The amount of bond-slip between the reinforcing steel and the surrounding concrete increases with testing to higher ductility levels. Figure 8.2 shows lateral-load versus strain hysteresis loops for steel strain and average concrete strain in the plastic-hinge region of the column specimen. The steel strain is taken at a point on one of the longitudinal bars near the center of the plastic hinge region. The concrete strain includes crack displacements and is taken at the location of the longitudinal bars, on a 600 mm gauge length over the plastic-hinge region. Again, the difference between concrete and steel strains indicates the amount of bond-slip taking place.

Figure 8.2 indicates that at $\mu = 3$ the tensile strain in the longitudinal reinforcing steel is 1.4 times yield. The concrete tensile strain at the same location is 8.3 times the steel yield strain and 5.9 times the strain in the longitudinal steel. The large difference between concrete and steel strains shows that extensive bond-slip occurs, and confirms that bond-slip is the cause of the pinching of the lateral-load versus displacement hysteresis loops.

Figure 8.2 also shows that bond-slip increases with testing to increased ductility levels. Table 8.1 indicates that the longitudinal reinforcing reaches a strain of 1.4 times yield at ductility $\mu = 2$. Then at increasing column displacements to ductility 3, the steel strain does not increase beyond the previous maximum value of 1.4 times yield. Thus the column is accommodating increasing lateral displacements without increasing steel strain, but instead with an increasing zone of yielding, ie, an increasing length of the longitudinal reinforcement yields with each cycle to increasing displacement. Thus the zone of yielding of the reinforcement becomes much longer than the typical plastic-hinge lengths found in columns with well-bonded deformed reinforcing.

Figure 8.2 and Table 8.1 show that the ratio of concrete strain to steel strain in the plastic-hinge region steadily increases with increasing column displacement ductility. The ratio is 2.2 at ductility 1, 3.6 at ductility 2, and 5.9 at ductility 3. These results indicate that substantial bond-slip occurs even at low to moderate ductility levels.

Table 8.1 Comparison of Average Concrete Strain, Including Cracking, With Steel Strains at Longitudinal Bars

Displacement Ductility Factor	$\frac{\text{Steel Tensile Strain}}{\text{Yield Strain}}$	$\frac{\text{Concrete Strain}}{\text{Steel Yield Strain}}$	$\frac{\text{Concrete Strain}}{\text{Steel Strain}}$
1	0.87	2.0	2.2
2	1.4	5.0	3.6
3	1.4	8.3	5.9

Additional Evidence of Bond Slip

Unfortunately the strain gauges on the longitudinal bars debonded after $\mu = 3$, and no steel strain data were obtained for the testing to higher ductilities. However, other data confirm that the bond of the flexural reinforcing steadily deteriorated as testing continued. The severe deterioration of bond is evident in the following observations:

1. The pinching of the lateral-load versus lateral-displacement hysteresis loops, shown in Figure 7.8, begins at $\mu = 1$ and becomes more pronounced with cycles to increasing displacement. This directly reflects the progressive degradation of bond along the length of the longitudinal reinforcing. The lateral-load versus displacement hysteresis loops for the previous test, of the column/crossbeam specimen (Figure 6.7), show similar pinching and progressive stiffness degradation.

2. The failure of the longitudinal-bar end welds at the top of the column/foundation-beam specimen, occurring at $\mu = 5$, indicates that a tremendous amount of bond deterioration had taken place. As discussed in Section 7.4, the end-welds were located 1.9 m above the critical section of the column and failed under a tensile load of approximately 45 percent of the bar yield force. This means that over the 1.9 m length, equal to 68 bar-diameters, only 55% of the bar yield force could be taken out in bond resistance. If a uniform bond stress is assumed over the surface area of the bar for the 1.9 m length, a very low bond stress is calculated:

$$\text{Bond stress} = \frac{.55\ f_y\ A_s}{\pi\ d_b\ l}$$

$$= \frac{0.55\ (337\text{MPa})\ (616\text{mm}^2)}{\pi\ (28\ \text{mm})\ (1900\text{mm})}$$

$$= 0.69\ \text{MPa} = 0.14\sqrt{f_c'}\ \left(100\text{psi} = 1.7\ \sqrt{f_c'}\right)$$

3 The anchorage-splitting failure of the concrete at the column-bar end hooks in the foundation beam indicates very low bond resistance in the straight embedment length above the end hooks. The splitting failure, described in Section 7.5, initiated at the end hooks at a displacement ductility of 9, when the bond-resistance along the length of the longitudinal bar was well degraded. The longitudinal bars are embedded 1.2 metres below the critical column section into the column haunch and foundation beam where they are terminated with 180-degree hooks. For the anchorage splitting failure to occur, almost all of the tensile force in the longitudinal bars must have been transferred to the end hooks, meaning that there was almost no bond resistance along the 1.2 m of anchorage length above the hooks.

Effect on Structural Performance

Compared with deformed reinforcing, the plain-round reinforcing bars offer poor bond-resistance and undergo a more rapid deterioration of bond strength under cyclic earthquake actions. The New Zealand concrete code NZS 3101 [SANZ 1982] specifies that the embedment length of plain-round reinforcing should be twice that required of deformed reinforcing. This factor of two may be unconservative for plain-round reinforcing subjected to cyclic earthquake forces, particularly at higher ductility levels. The pending 1995 revision of NZS 3101 prohibits the use of plain-round bars for main longitudinal reinforcing. In other circumstances where plain-round bars may be used, straight bar anchorages or lap splices are prohibited. Bar anchorages must have hooks, and both bars of lap splices must have hooks [SANZ 1995, Bull 1995].

Structures with plain-round reinforcing suffer greater stiffness degradation under earthquake actions than structures with deformed reinforcing. This stiffness degradation, and a pronounced pinching of lateral-load versus displacement hysteresis loops, are due to the bond-slip at the reinforcing bars. Further insight into the behaviour of structures with plain-round reinforcing could be gained by mechanically modelling structures which undergo bond slip.

The pinched hysteresis loops indicate a reduced ability of the structure to dissipate earthquake energy, compared with a structure with deformed reinforcing steel. The stiffness degradation and pinched loop shape could compromise the earthquake performance of structures with plain-round reinforcing steel. However, the extent to which earthquake performance is affected is unknown and requires further study.

Lateral Capacity and Strength Degradation

There is relatively little strength degradation in the response of the column/foundation-beam specimen. The reduction of lateral capacity which is evident results from the spalling of the concrete in the plastic-hinge region and to the P-Δ effect. At a structure drift of 2.7 percent, the lateral capacity of the column/foundation-beam specimen had diminished by 8%. The 8% reduction is calculated by comparing, from the hysteresis loops of Figure 7.8, the lateral capacity of 130 kN at 2.7 percent drift with the 141 kN maximum capacity at 1.2 percent drift.

The column/crossbeam test specimen, with its straight bar anchorages, showed a more rapid degradation of strength. From the hysteresis hoops of Figure 6.7(a), the lateral strength at 2.7 percent structure drift (equal to 3.0 percent test-specimen drift) is 74 kN. The peak lateral strength is 88 kN, indicating a strength degradation of 16%. The column/crossbeam specimen suffers strength degradation due to the end-anchorage deterioration of the straight column bars. This causes a capacity reduction in addition to that caused by concrete spalling and the P-Δ effect.

Combined Capacity of Top and Bottom Hinge Regions

The lateral-load-versus-displacement characteristics of the two tests can be combined to estimate the earthquake response of the whole bridge structure. The column/foundation-beam test describes the behaviour of the bottom plastic-hinge region, while the column/crossbeam test describes the behaviour of the top plastic hinge region. These two sets of test results are adjusted from the steel-yield strengths of the test specimens (308 MPa for the column/crossbeam and 337 MPa for the column/foundation-beam) to the estimated steel-yield strength of the actual structure, 280 MPa. Structure drift is defined as equal to the structure's lateral displacement divided by the height of 4.80 metres from the centreline of the foundation-beam to the centreline of the crossbeam. The lateral-capacity-versus-displacement envelopes of the two plastic-hinge regions are easily combined to give a lateral-capacity envelope for the entire structure.

Figure 8.3 shows the estimated lateral-capacity-versus-displacement envelope of the bridge structure under transverse earthquake loads. For the as-built (ie unretrofitted) structure, the peak lateral capacity is 0.45 times the seismic weight. At a structure drift of 2.7 percent this capacity is diminished by 12%. The 12% reduction reflects the combination of the 8% reduction which occurs in the column-bottom plastic hinge and the 16% reduction which occurs in the column-top plastic hinge.

Anchorage-retrofit Structure

If end-plates are added to the tops of the column-longitudinal bars to retrofit the bar-anchorage condition, the maximum lateral capacity is increased and the rate of degradation of strength is reduced.

The dashed line of Figure 8.3 shows the estimated capacity-versus-displacement envelope of the anchorage-retrofit structure. The lateral capacity is increased to 0.53 times the seismic weight, because of the improved moment strength at the top of the column. The reduction of lateral capacity at 2.7 percent structure drift is 8%.

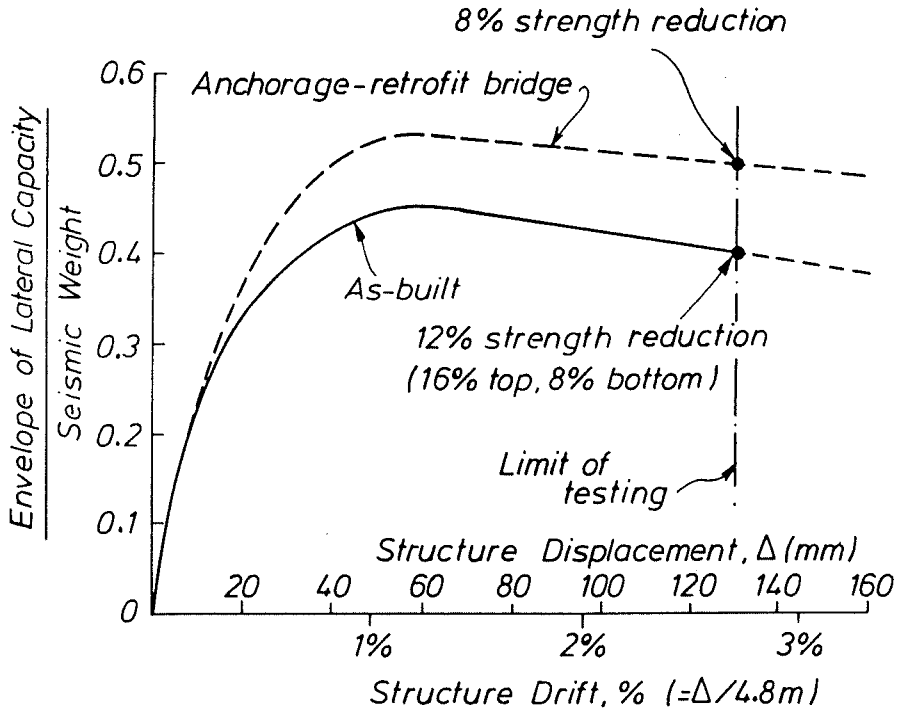

Figure 8.3 **Lateral-strength-versus displacement envelopes for the as-built bridge and anchorage-retrofit bridge.**

The upgraded capacity and strength-degradation characteristics of the anchorage-retrofit structure will improve its earthquake performance. The extent of the improvement is unknown however, and would depend on the particular earthquake characteristics. Having defined the strength-envelopes, stiffness-degradation, and hysteresis-loop-pinching characteristics of the earthquake response, accurate analytical studies of the bridge, using different earthquake records, can now be conducted. Inelastic time-history structural analyses can be carried out to compare the earthquake performance of the as-built bridge structure with that of the proposed anchorage-retrofit structure. Such analyses are presented in Chapter 9.

8.2 Effect of the Diagonal Reinforcing, and Column Shear Capacity

The supplementary diagonal bars at the column haunch contribute to both the shear and flexural strength of the column.

Diagonal Bar Contribution to Flexural Strength

Figure 8.1 shows the diagonal-bar and longitudinal-bar strains in the column plastic-hinge region at ductility, $\mu = 1$. The two diagonal bars which extend past the tension face of the column haunch, bars G and H, carry significant tension due to column flexure, with strains similar to those of the main flexural reinforcement, the longitudinal bars E and F. Thus the diagonal bars make a substantial contribution to the flexural strength of the column, and hence to the lateral capacity of the structure.

The above conclusion is confirmed by the measured strength of the column/foundation-beam specimen. The peak lateral capacity was recorded, at ductility factor $\mu = 2$, to be 138 kN (31.0 kips) in the east direction and 144 kN (32.4 kips) in the west direction. These measured capacities correspond closely to the calculated nominal flexural strength of 135 kN (30.3 kips). The assumption used in calculating the nominal strength—that the two tension-diagonal bars reach yield and fully contribute to the flexural strength—is thus verified.

For the column/crossbeam test specimen, Figure 6.4, diagonal bars are present in both plan directions, anchored into the longitudinal girders and the transverse cross-beam. Thus there are eight diagonal bars at the top of each column. All of these diagonal bars contribute to the flexural strength of the column under earthquake actions. The nominal moment strength of the critical section at the top of the column is calculated as 244 kNm (180 kip-ft). This corresponds closely to the measured maximum moment strength of 236 kNm (174 kip-ft) from the anchorage-retrofit specimen. Thus the assumption used in the calculations—that the diagonal bars in each direction contribute to the column flexural strength—is verified for the top end of the column as well as for the bottom.

Diagonal Bar Contribution to Shear Strength

The diagonal bars also contribute to the shear strength of the column. As shown in Figure 8.1, under lateral forces two of the diagonal bars are subjected to significant tensile strains while the other two bars carry little strain. The two diagonal bars G and H, which extend past the tension face of the column haunch, yield in tension when the column reaches its flexural strength. The horizontal component of the yield force in these two bars provides a substantial portion of the column's shear resistance at the plastic hinge. Meanwhile, the opposite two diagonal bars, bars C and D in Figure 8.1, tend to carry a small compression or tension force which does not significantly increase or decrease the column shear resistance. It is thus considered accurate to assume that two of the diagonal bars contribute to the shear strength while the contribution other two bars can be ignored.

The contribution of the diagonal bars to shear strength is also evident in the crack development of the column/foundation-beam specimen. Unlike the column stirrups which do not contribute to shear strength until diagonal cracking develops, the two tension diagonal bars resist a portion of the column shear even before diagonal cracking. The tension in the diagonal bars reduces the shear stress in the concrete and reduces the amount of diagonal shear cracking.

This effect is evident in the photo of Figure 7.2(c), taken at ductility factor 6 for the column specimen. At the top of the photo is the portion of the column just above the diagonal bars. In this location, flexural cracks in each direction have extended into diagonal shear cracks. Below these two crossing diagonal cracks are the three main flexural cracks in the plastic-hinge region which have extended horizontally across the column and joined up without turning into diagonal shear cracks. Thus the presence of the diagonal bars in this region has reduced the amount of diagonal shear cracking. The reduced diagonal cracking does not affect the overall seismic performance of the bridge, but it re-confirms the assumption that the diagonal bars contribute to the column shear strength.

Calculations of Shear Capacity

Calculations of the shear capacity of the column specimen have been made by the present author. Results of the calculations are shown in Table 8.2. According to the New Zealand code provisions [SANZ 1982, 1995], if the diagonal bars are not considered, the shear capacity of the column plastic-hinge region is deficient. The code assumes $V_C = 0$ and $V_S = 90$ kN to give a shear capacity of only 89% of the shear demand, which is 102 kN. However, if the diagonal-bar contribution is included, the shear capacity is calculated as 161 kN, or 158% of the shear demand.

Furthermore, the code assumption that $V_C = 0$ is a conservative one. The less conservative expression proposed by Paulay and Priestley [1992, page 127] $V_C = 4V_b\sqrt{P_u/A_g f'_c}$, results in $V_C = 58$ kN. Thus a more realistic estimate of the column shear strength at the plastic-hinge regions would be $V_C + V_S + V_{SDIAG} = 58 + 90 + 71 = 218$ kN. This strength is comfortably above the earthquake shear demand of 102 kN. As observed in the tests, column shear failure did not occur. The less conservative calculation for V_C indicates that even without the diagonal bars shear strength will be adequate, $V_C + V_S = 58 + 90 = 148$ kN.

Comparison to Code Provisions

The foregoing comparison of possible calculation assumptions shows that if the shear strength of the subject bridge column is assessed by the *NZS 3101* code [SANZ 1982, 1995], and if an assumption is made to neglect the diagonal bar contribution, then it will be concluded that the column shear capacity is deficient. Such assumptions might be considered conservative, but would not be unreasonable in engineering practice. In fact the pilot-study assessment of the bridge [Chapman 1991] concluded that the shear capacity is marginal. A more detailed evaluation of the column shear capacity, allowing a $V_C > 0$ or some contribution to shear capacity from the diagonal bars, shows, however, that the column shear capacity is in fact adequate.

This example illustrates the point that the assumptions used for the seismic evaluation of existing structures often need to be more accurate than those used for designing new structures. For new bridges conservative design assumptions would only slightly increase construction costs. But for an existing bridge, an overly-conservative assessment of column shear capacity could require that expensive retrofitting, whereas a more detailed and accurate assessment of shear capacity could eliminate the need to retrofit.

Table 8.2 Calculated Shear Demands and Capacities for the Bridge Column

	Test Specimen	Actual Structure
Shear Demand	135 kN	102 kN
Shear Capacity, Steel Contribution:		
f_y	337 MPa	280 MPa
V_S, stirrups	120 kN	90 kN
V_{SD}, 2 diagonal bars	94 kN	71 kN
Shear Capacity, Concrete Contribution:		
f'_c	22 MPa	20 MPa
$P_u/A_g f'_c$	0.074 ($P_u = P_{test}$ = 300 kN)	0.012 (P_u = 0.8 DL-EQ = 46 kN)
<u>NZS 3101 (1982 and 1995)</u>		
V_C at plastic hinge	0	0
V_C outside plastic hinge	$0.226\sqrt{f'_c}$ = 166 kN	$0.192\sqrt{f'_c}$ = 134 kN
<u>Paulay and Priestley (1992)</u>		
V_C at plastic hinge	$0.201\sqrt{f'_c}$ = 147 kN	$0.081\sqrt{f'_c}$ = 58 kN
V_C outside plastic hinge	$0.226\sqrt{f'_c}$ = 166 kN	$0.192\sqrt{f'_c}$ = 134 kN

Paulay has postulated that for members with plain-round bars which undergo significant bond slip, the "entire shear mechanism changes", compared with that for structures with deformed bars. "The reason is that the traditional truss mechanism, relying on perfect bond, cannot develop. Typical 45-degree struts in the concrete will not develop. An arch mechanism must be mobilised" instead. Consequently, the "shear provisions of *NZS 3101*, or *ACI 318* for that matter, are entirely irrelevant" for structures with plain-round reinforcing bars [Paulay pers. comm. 1994].

However, Kordina et al [1989] have tested (monotonically) the shear strength of prestressed concrete beams with unbonded tendons. They conclude that "even for prestress without bond, shear stress can be predicted best on the basis of a truss analogy... a tied-arch model seems less suitable for the determination of the shear-carrying capacity."

Also, engineers evaluating concrete structures with plain-round reinforcement have little choice but to use the shear-strength provisions from design codes or research results, which were developed for structures with deformed reinforcement. Special shear-strength evaluation provisions for concrete structures with plain-round reinforcing have not been developed. Further research in this area would be useful.

8.3 Plastic Hinge Behaviour and Concrete Confinement

Based on the strain readings of the linear potentiometers, the curvature profiles of the plastic-hinge concrete section have been calculated for the column/foundation-beam test. Figure 8.4 shows the column curvature measured over segments of the plastic-hinge region at ductility factors of 1, 3, 5, 6 and 7. As shown in the figure, up to a ductility factor of 5, the curvature was concentrated in one of the 150 mm gauge lengths, which is where the main flexural crack was located, approximately 300 mm above the foundation beam. As shown in Figure 7.7 this crack opened to a maximum width of 10.5 mm at ductility factor of 5.

Beyond ductility 5, the maximum opening widths of the other two flexural cracks began to increase, indicating an increase in curvature further up the column. As shown in Figure 8.4, the curvature began to develop over a greater length of the column at ductilities 6 and 7.

Curvature Ductility

Based on the curvature measurements, the average curvature ductilities can be calculated. The curvature ductility is taken as the maximum measured column curvature, over a 150 mm gauge length, divided by the plastic-hinge curvature measured over the 150 mm gauge length of the main flexural crack during testing to ductility factor 1. Figure 8.5 shows the measured curvature ductilities during testing to increasing displacement ductilities.

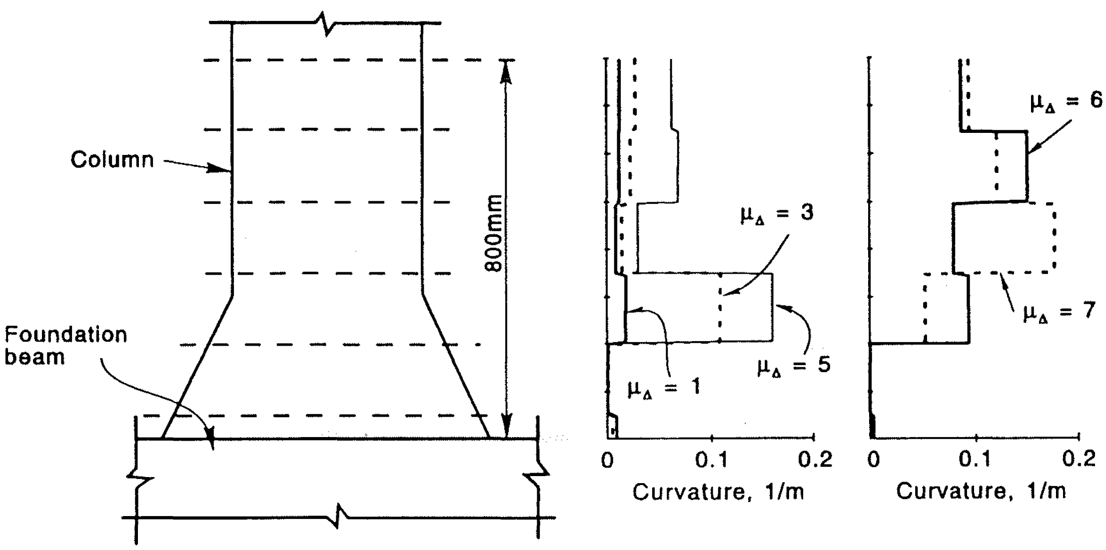

Figure 8.4 **Column curvature profile over the plastic hinge region at displacement ductilities of 1, 3, 5, 6, 7.**

In general, curvature ductilities will increase in step with displacement ductilities. If the plastic-hinge length remains constant, curvature ductility will increase linearly with displacement ductility. However, the column can also accommodate increased displacement ductilities without increased curvature ductilities, if the plastic-hinge length increases.

Plastic Hinge Length

Figure 8.5 shows that initially the column plastic-hinge length, ℓ_p, is about 200 mm, 0.5 times the overall section depth. As the column is tested to cycles of increasing displacement however, the curvature profile over the column length becomes less peaked. At the displacement ductilities 4, 5, and 6 the curvature profile is more even because the plastic-hinge length, ℓ_p, has increased to about 400 mm, 1.0 times the overall section depth. The relationship between plastic-hinge length, curvature ductility, and displacement ductility is given in Park and Paulay [1975, page 553]:

$$\mu_\phi = 1 + \frac{(\mu_\Delta - 1)}{3(\ell_p/\ell)\left[1 - 0.5(\ell_p/\ell)\right]}$$

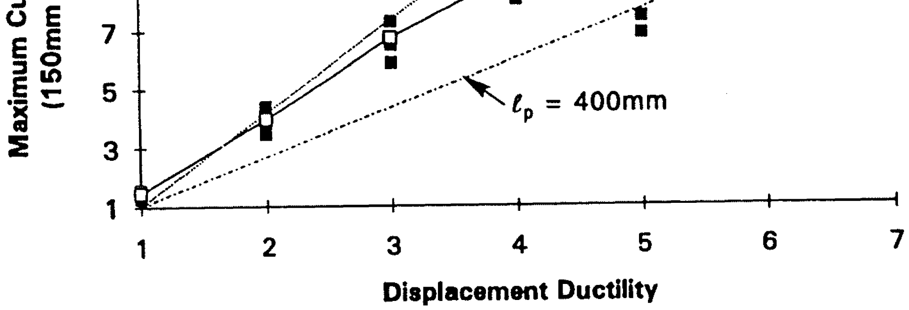

Figure 8.5 Measured concrete curvature ductility, versus displacement ductility, indicating an increase in concrete plastic-hinge length, ℓ_p.

The significance of the concrete-section curvature and plastic-hinge length results for the column is diminished by the extensive bond slip resulting from the use of plain-round reinforcing bars. The bond slip at the reinforcing bars means that the column section behaviour violates the typical assumption of structural mechanics that "plane sections remain plane", and the typical relationship between curvature and material strains is no longer relevant. Because of the bond slip, the length of yielding of the reinforcing bars is much greater than the plastic-hinge length based on concrete-section curvature. Thus the concrete curvature ductility at the plastic hinge does not give an indication of the maximum reinforcing steel strain, as it would do for well-bonded reinforcement. This point is reflected in Figure 8.2 where, under the same column displacement demands the concrete-strain ductility demand is shown to be several times greater than the steel-strain ductility demand.

Column-hinge Lengthening and Degradation

The linear-potentiometer readings were also used to record the axial lengthening of the column specimen during the testing to increased levels of lateral displacement. Figure 8.6 shows the progressive lengthening of the column during testing. The lengthening is substantially restrained by the constant axial load on the column, so that the residual column lengthening, after testing to displacement ductility 7, is only 4.5 mm. Another reason for the small amount of plastic-hinge lengthening is that the inelastic strains which develop in the plain-round column bars are substantially less than those which would develop in deformed column bars.

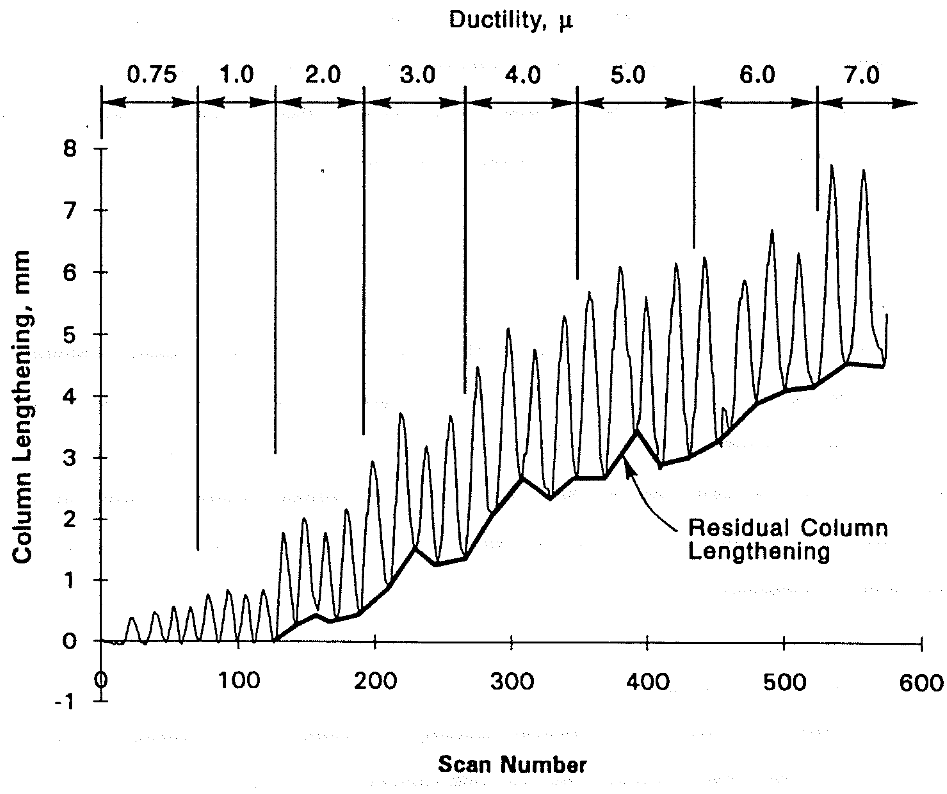

Figure 8.6 Column lengthening during the testing of the column/foundation-beam specimen.

Although the cover concrete of the column specimen began to crack on the compression face at displacement ductilities of 2 to 3, and major spalling began at ductility 5, the strength degradation of the specimen was not pronounced. At a displacement ductility of 5 the column strength had degraded to 88% of its maximum strength, measured at ductility 2. This 12% percent degradation of strength results from to the loss of cover concrete. The amount of strength degradation was small because the core concrete remained intact and was adequately confined by the transverse reinforcing. Figure 7.2(c) shows that the column core was intact at a displacement ductility of 6. Figure 7.2(f) shows a degraded column core, but the degradation occurred only after several cycles to extreme displacements (μ = 12).

Required Transverse Reinforcing Steel Areas

The pilot-study assessment of the bridge had indicated that the "the column-core concrete is poorly confined". This assessment was made based on the requirements for transverse reinforcement in the 1982 New Zealand Concrete Code [SANZ 1982]. For the subject bridge column, the 1982 code requires an area of transverse reinforcing 3.15 times that which is provided by the 9.5 mm (3/8 inch) ties at 152 mm (6-inch) spacing.

Research results over the last ten years have shown, however, that the 1982 concrete confinement requirements are unduly conservative for columns with low to moderate axial loads [Watson et al, 1994] For the subject column with its low axial load level, the revised version of the concrete code [SANZ 1995] requires no transverse reinforcement for concrete confinement. Transverse reinforcement is required to stabilize the longitudinal bars against buckling but not for confinement. The area of transverse reinforcement provided in the subject bridge column is adequate, equal to 1.17 times that required for bar-buckling prevention. Bar buckling did not occur in the tests even after testing to extreme ductility levels.

These points are illustrated in Figure 8.7. The figure shows a comparison of the transverse reinforcement requirements of the 1982 and 1995 versions of the New Zealand concrete code. The figure shows the required transverse steel area for the subject bridge column as a function of axial-load level. The actual axial-load level and transverse steel area of the subject bridge column are also shown on the plot. It can be seen that by the 1982 criteria the subject column is deficient in transverse reinforcement by a factor of 3, but by the 1995 criteria the provided amount of transverse reinforcement is adequate.

Required Column-tie Spacing

Figure 8.7(b) shows the maximum allowable spacing of column ties according to the previous and current versions of the New Zealand concrete code [SANZ 1982 and 1995].

Bar-Buckling Criterion

To stabilize the longitudinal reinforcing against buckling, ties are required at a spacing no greater than $6d_b$, where d_b is the diameter of the longitudinal bars. For the subject bridge this maximum spacing is 6 x 28.6 = 171 mm. Thus the actual tie spacing of 152 mm meets the criteria to prevent longitudinal bar buckling.

Plain-round bars may be less susceptible to buckling under earthquake actions than deformed bars. For the subject test Paulay has pointed out that "inelastic strains in the plain bars were much smaller [than they would be for deformed bars] because of the breakdown of bond". For the columns similar to those of the subject bridge Paulay estimates that "at $\mu = 8$ deformed bars would probably have buckled because much larger reversive inelastic strains would have been sustained" in the steel [Paulay 1994]. This estimate of ductility capacity ($\mu = 8$), and the compliance with the 1995 code criteria for transverse steel area and the $6d_b$ maximum tie spacing, indicate that even with deformed bars the seismic performance of the column with respect to bar-buckling would have been satisfactory.

Although plain-round bars may be less susceptible to buckling, they are not immune to buckling and still need some transverse ties for anti-buckling stability. Rodriguez and Park [1994] tested columns with plain-round longitudinal bars with ties spaced at $13d_b$. This excessive tie spacing allowed the longitudinal bars to buckle and cause significant strength reductions at a displacement ductility of approximately 3.8 (interstory drift of 1.8%).

Confinement and Shear-resistance Criteria

The 1995 draft Concrete Code also requires, for concrete confinement and shear resistance, that column ties be spaced no further apart than h/4, where h is the least dimension of the column section. This requirement is relaxed from the h/5 maximum spacing required by the 1982 code. For the subject bridge, the h/4 criterion equates to a maximum tie spacing of 102 mm. This h/4 criterion governs over the $6d_b$ anti-bar-buckling criterion, and thus the column-tie spacing is deemed inadequate by the 1995 code.

The code requirement for column-tie spacing to be less than h/4 can be conservative for columns with low axial load and shear demand, particularly if diagonal bars are present. The h/4 tie-spacing criteria is appropriate for new construction, because a more detailed criteria would be more complicated and the resulting savings in construction cost would be insignificant. But for the seismic evaluation of an existing structure, a more accurate estimate of required column-tie spacing may be necessary, because it could eliminate the need for expensive retrofitting.

For the subject bridge column, the 1995 code requires no transverse reinforcement for confinement, and the shear capacity of the plastic-hinge region is good due to the contribution of the diagonal bars. However, a tie spacing of h/4 is still required. The issue is illustrated in Figure 8.7. At an axial-load level below that indicated by point "A" in the figure, transverse ties are not needed for concrete confinement; they are only needed for bar-buckling restraint. At axial-load levels less than point "A", then, it is not necessary for concrete confinement to have ties spaced at h/4 (102 mm). And because the two diagonal bars will cross any potential diagonal shear crack in the plastic-hinge region, the shear capacity of the column does not rely on a close spacing of ties.

Outside of the column plastic-hinge region, the New Zealand concrete code [SANZ 1982 and 1995] specifies a maximum tie spacing, for shear resistance, of d/2. For the subject column, d/2 equals 170 mm, thus the tie spacing of 152 mm outside the plastic hinge region complies with the code.

Proposed Requirements for the Subject Bridge

Because the column ties are not heavily relied on for confinement or shear resistance, it should only be necessary in the subject column, even if it had deformed longitudinal bars, to meet the tie-spacing requirement of $6d_b$ (171 mm) so as to prevent longitudinal-bar buckling. This proposed requirement is shown in Figure 8.7(b) by the dash-dot line.

The proposed tie-spacing requirement would then indicate that the column-tie spacing of the subject bridge is acceptable—a conclusion which is validated by the test results. The proposed requirement is recommended as a basis for assessing the ductility capacity of existing columns similar to those of the subject bridge, with either deformed or plain-round reinforcement. The requirement gives a better indication of the true column-tie spacing required for the ductile earthquake response of column plastic-hinge regions. Additional study may be needed, however, to determine the maximum allowable tie spacing for shear resistance.

Additional research is also needed on the performance with respect to shear resistance and bar buckling of concrete members with plain-round reinforcement. It may be that transverse ties are not effective in the shear resistance of such members because an arch mechanism of shear resistance is developed instead of the traditional truss mechanism. It might also be found that less transverse reinforcement is required to prevent bar buckling in such members, compared with members with deformed longitudinal bars.

8.4 Overall Assessment

The testing of the column/foundation-beam specimen and the associated structural analysis reveal several new insights into the seismic behaviour of the 1936-designed New Zealand bridge. The conclusions drawn from the testing and detailed analysis could not have been deduced from a less detailed assessment which relied only on current design codes and practice. The detailed investigation of the present study has, in general, shown that the bridge is less vulnerable to earthquake damage than previously thought.

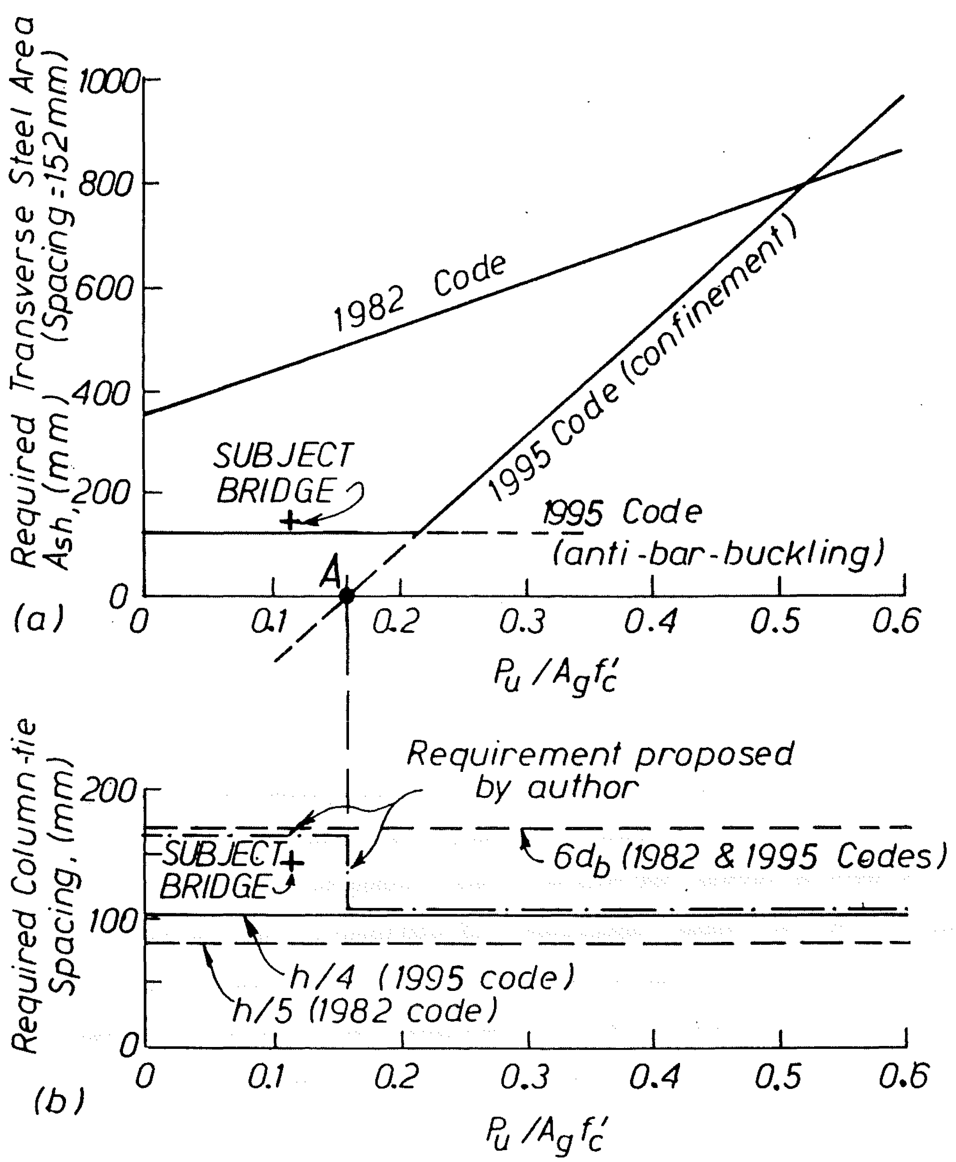

Figure 8.7 **Transverse reinforcement requirements for the subject bridge column, from the current and upcoming New Zealand concrete codes [SANZ 1982 and 1995].**

Seismic Performance

The preliminary seismic assessment of the subject bridge [Chapman 1991] concluded that "the pier-columns are unlikely to tolerate cyclic displacements much exceeding yield ...". This conclusion is generally supported by code provisions and other structural design guidelines. However, the laboratory testing of the column/crossbeam and column/foundation-beam specimens presented here has shown the conclusion to be incorrect.

For the subject bridge to survive a severe earthquake, it needs to have adequate strength and displacement capacity in its transverse direction. The lateral capacity of the bridge is governed by the flexural strength at the top and bottom of each of the bridge columns. The tests and calculations indicate that the lateral capacity is 0.45 times the weight of the structure. This lateral capacity is two or three times greater than that required of many new bridges.

Even with a high lateral capacity, the bridge structure needs to accommodate the displacement demands imposed by a strong earthquake. The lateral displacement capacity of the bridge depends primarily on the inelastic rotation capacity at the plastic-hinge regions at the top and bottom of each of the bridge columns. The lateral-force versus displacement hysteresis loops for both the column/crossbeam test, Figure 6.7, and the column/foundation-beam test, Figure 7.8, indicate a ductile response to earthquake actions. The hysteresis loops show pinching and stiffness degradation, due to bond deterioration, but show only moderate strength degradation. The column/crossbeam and column/foundation-beam tests indicate that at a structure drift of 2.7 percent, the lateral capacity of the bridge will diminish by only 12%.

Thus, the subject bridge has good lateral strength and inelastic displacement capacity to survive earthquake ground motions. This combination of strength and displacement capacity for the bridge means that it is likely to perform well even in a severe earthquake. Considering the earthquake response spectra of the New Zealand loadings code, *NZS 4203* [SANZ 1992], the bridge has adequate strength and ductility capacity to sustain the code-specified level of earthquake shaking. This indicates that the subject bridge will probably perform in an earthquake just as well as a new bridge designed to the 1992 *NZS 4203* criteria. The analytical studies of Chapter 9 confirm this conclusion.

Need to Look Beyond Code Provisions

The prediction of satisfactory earthquake performance from the subject bridge is based on the test results which show good lateral strength and displacement capacity. Using the New Zealand concrete code [SANZ 1982] criteria, the opposite conclusion was reached: poor earthquake performance was predicted for the bridge. However, a detailed seismic evaluation of the structure, which does not rely solely on code implied criteria, verifies the test results and the conclusion that the bridge's seismic performance will be satisfactory. Essential to an accurate seismic assessment of the bridge are the following points:

1 For columns with low axial load, the 1982 New Zealand concrete code [SANZ 1982] is overly-conservative in its requirements for concrete confinement. The 1995 draft code [SANZ 1995] has more accurate requirements.

2 The supplementary diagonal bars at the top and bottom end flares of the subject bridge column contribute significantly to both flexural and shear strength. For such columns, the structural engineer must determine the critical section for moment capacity and plastic hinging, which may or may not be in the flared region of the column. For the subject bridge, a seismic evaluation which neglected the contribution of the diagonal bars would be overly conservative.

3 The code assumption [SANZ 1982 and 1995] that V_c, the column shear capacity of the concrete section, equals zero may be overly conservative for the evaluation of existing structures. Paulay and Priestley [1992] and Priestley et al [1994] offer less conservative criteria.

4 For columns with low axial load, good shear capacity, and large-diameter longitudinal reinforcing, the column-tie spacing requirements of the 1982 and 1995 concrete codes can be conservative. A more accurate requirement, described in Figure 8.7 may be used instead. However, a limit in the maximum tie spacing is still required to ensure that the ties act as efficient shear reinforcement. Currently the code specifies the maximum tie spacing as h/4.

5 Concrete structures with plain-round longitudinal bars can be less susceptible to bar-buckling, shear failures, and loss of confinement—and thus may require less transverse reinforcement—than similar structures with deformed longitudinal bars. The bond slip at plain-round bars makes bar buckling less likely and promotes an arch mechanism of shear resistance rather than the traditional truss mechanism. Bond slip can lessen curvature demands at plastic hinges and thus reduce the need for concrete confinement.

Stiffness Degradation and Pinched Hysteretic Response

Although the hysteretic response of the plastic-hinge regions of the subject bridge column indicate good displacement capacity and little strength degradation, the response also shows pronounced stiffness degradation and pinching. The stiffness degradation and pinching may have an adverse effect on earthquake performance because the energy-dissipation capacity of a structure is reduced. However, the hysteresis-loop shape generally does not have a big effect on seismic response, particularly for structures with longer periods of vibration.

Further insight on expected damage to the bridge for various earthquake scenarios could be gained by conducting inelastic time-history analyses of the structure. Such analyses can be used to check the validity of the code-specified earthquake demands, assess the effect of the pinched hysteretic response, and compare the earthquake performance of the as-built bridge with that of the bridge after seismic retrofitting. Such analyses have been carried out and are discussed in Chapter 9. Mechanically modelling the response of structures which undergo bond slip would also provide insight into the behaviour of structures with plain-round reinforcing.

Confinement Retrofit Unnecessary

The subject bridge is shown by the tests and the detailed evaluation *not* to be vulnerable to earthquake damage related to insufficient transverse reinforcing or shear capacity. Thus there would be no benefit in a confinement-retrofit of the bridge columns, such as adding new column ties or an external column jacket. It had originally been planned to test a confinement-retrofit of the column/foundation-beam specimen, but the idea was discarded once it was concluded that the existing column was not in fact deficient in transverse reinforcing or shear capacity.

Additional Considerations

There are three additional, related considerations concerning how representative the testing is of the actual seismic performance of the prototype bridge. Two issues -- the different detailing at exterior columns and the restraint provided by the test-specimen top-plate -- suggest that the actual bridge will suffer slightly higher stiffness and strength degradation than evident in the response of the test-specimen. The third issue of surface rust on the plain reinforcing bars suggests the opposite effect: less stiffness degradation for the actual bridge compared to the test specimen.

In sum, these additional issues are not considered to have a substantial effect on the validity test results reported here. One or more of the issues could be perhaps be studied as part of some future testing of structures with plain-round reinforcing. The three issues are discussed below.

Interior versus Exterior Column Details

The test has examined the behavior of one of the interior columns of the typical four-column pier of the prototype bridge. As shown in Figure 6.3, the detailing at the base of the exterior column is different than that of the interior column. The seismic performance at this column would probably not be as good as that at the interior column, because of bond slip of foundation beam bars and poorer confinement of the column-bar end hooks.

Based on the test observations and results of Chapter 6 and this chapter, it is possible to estimate the effect of the different detailing at the exterior column. Three observations can be made:

1. The strength of the exterior column base region will initially be the same as that for the interior column. This is because the strength will still be governed by the column-yielding mechanism, since the moment strength of the foundation beam is more than twice that of the column. In fact, the *cracking moment* of the foundation beam is approximately equal to the moment capacity of the column, so that full development of the foundation beam bars is not necessary to force plastic hinging into the column.

2. Upon repeated cycles of seismic forces at moderate to high ductilities, the cracking moment of the foundation beam may be exceeded, after which bond slip at the foundation beam bars is likely to take place. Such bond slip would increase the amount of stiffness degradation in the response of the bridge. Conceivably, the bond slip could eventually degrade the capacity of the foundation beam and joint region to a level less than that required to force plastic hinging into the column. In this case, the response of the bridge would exhibit an increased rate of strength degradation.

3. In the testing of the interior-column/foundation-beam specimen, at high ductility levels, a splitting failure occurred at the column-bar end hooks, as described in Section 7.5. The splitting cracks were first observed at a displacement ductility factor, $\mu = 9$ (structure drift of 6.0 percent). At $\mu = 10$ (structure drift of 6.3 percent), the foundation-beam concrete spalled because of this splitting failure. For the exterior column, there is less concrete surrounding the column-bar end hooks, and it is possible that the spalling and splitting failure could occur at a slightly lower ductility level than for the interior column.

   It is not likely that this difference is significant however, because (a) until the splitting initiates (at $\mu = 8$ or 9 perhaps), the reduced amount of surrounding concrete is not relevant, (b) the effect on bridge seismic response is not crucial since any splitting failure would occur only at such high ductility levels, and (c) bond slip of the beam bars, discussed in item 2 above, may preclude any splitting failure at the column bars.

To completely quantify the effect of the different detailing at the exterior columns, an additional test -- of the *exterior*-column/foundation-beam region -- might be recommended.

Restraint to Bond Slip Provided by Test Set-up

As described in section 7.4, three of the column-bar end welds at the top of the specimen failed at displacement ductility factors, μ, of 5 and 6. The failures attest to a tremendous amount of bond slip, and indicate that the top-plate restraint used in the test set-up does not perfectly model the situation in the actual bridge.

In the actual bridge, once bond along the column bars deteriorates beyond the column inflection point, there would be no restraint similar to the specimen's top plate to prevent further propagation of the bond slip. Thus in the response of the actual bridge, the amount of stiffness degradation may be greater than that shown in the test specimen. Because of the straight anchorages at the tops of the column bars, there could also be a reduction of strength at higher ductility levels, due to bond slip propagating over the entire length of the column bar.

The level of increase in degradation due to this effect is uncertain. However, the load versus displacement hysteresis loops at ductilities, μ of 5 and 6 -- including those labelled A, B, and C, in Figure 7.8 -- give some indication. Considering this evidence, the difference in response of the actual bridge compared to the test specimen, because of the lack of added restraint to bond-slip, could be assessed as follows:

- Presumably there would be little difference in stiffness or strength characteristics up to a ductility, μ of 4.

- Between ductilities, μ of perhaps 4 and 7, there would be an increase in stiffness degradation as bond slip propagates past the column inflection point. An increase strength degradation would not yet be evident.

- At higher ductilities, lower ultimate capacities -- ie., an increase in strength degradation -- would be expected.

- At the expected ductility demands of severe earthquakes (See section 9.4), the difference would not be significant, probably less than 10%. At the ductility demands of code-implied earthquake levels the difference would be negligible.

To more precisely quantify this issue, a test specimen modelling the entire column height could be recommended. Alternatively, more in-depth studies of bond-slip behavior, including attempts at mechanical models, could be undertaken.

Condition of Reinforcing Bars

The reinforcing steel used in the test specimen was in good condition, was delivered directly from the fabricator to the laboratory, and was not corroded. For the actual bridge, the reinforcing steel would have been imported from the UK by ship, and may not have been protected from the weather when transported or stored at the bridge site. Thus the steel for the actual bridge would probably have had surface rust which would increase its bond capacity. It is not known how much effect this surface rust would have in increasing bond resistance, or whether the effect would be significant after several reversed cycles of bond slip. Perhaps simple cyclic testing of the bond of rusted versus pristine reinforcing bars could be recommended.

8.5 Possible Retrofit Measures

It is unlikely that any retrofit of the subject bridge would be economically justified because the earthquake vulnerability of the as-built structure is low. However retrofitting could conceivably be justified in the following circumstances:

(a) if the bridge is extremely important and meant to remain usable even in the largest credible earthquake,

(b) for a bridge of similar details but with a lower lateral-strength/seismic-weight ratio, or

(c) for a bridge of similar appearance to the subject bridge but with poorer detailing and, consequently, a lower displacement capacity.

Three possible seismic retrofit solutions are briefly considered here.

Retrofit of Bar Anchorage

The first possible retrofit would be the addition of anchorage end-plates to the tops of the column-longitudinal bars, as tested on the column/crossbeam specimen. This anchorage retrofit would improve the earthquake performance of the bridge, but the improvement is not likely to be dramatic. As shown in Figure 8.3, the anchorage retrofit improves the lateral strength of the bridge and reduces the degree of strength degradation. This would decrease the likelihood of collapse in a major earthquake, but the level of damage in any smaller earthquake would probably not be much improved. The addition of the anchorage end-plates to all of the column-longitudinal bars would be costly, considering the small improvement in seismic performance that would be expected.

Infill Concrete Wall

The second possible retrofit would provide a more dramatic strength increase to the bridge structure. This retrofit, illustrated in Figure 8.8, involves the addition of a new reinforced-concrete infill wall between the centre two columns of the four-column bent. It is suggested that the reinforcing for the infill wall makes use of diagonal bars as is done in the coupling beams of walls for multi-storey buildings. It is likely that such a big increase in the strength of the multi-column bent will require the strengthening of the foundations, including the addition of new piles and the jacket-strengthening of the foundation beam. However not all piers of a multi-span bridge would need to be strengthened. For example, strengthening two piers in each 5-span segment of the subject bridge may be adequate.

The infill-wall retrofit, which greatly increases the strength and stiffness of the existing bridge, is most appropriate if control of damage is an important retrofit goal, rather than just the prevention of collapse. The retrofit would allow the bridge to respond elastically to large earthquakes.

Added Braces and Energy-dissipation Devices

A third possible retrofit solution would be the addition of supplemental steel braces with energy-dissipation devices, as shown in Figure 8.9. Depending on the chosen properties of the energy-dissipation devices, the foundation of the bridge may not need strengthening. If properly designed, such a retrofit could prevent serious damage to the bridge because less earthquake energy would need to be dissipated in the plastic-hinge regions of the concrete columns. The use of energy-dissipation devices

seems particularly appropriate for structures with plain-round reinforcing (such as the subject bridge), because the energy-dissipation capacity in the as-built structure alone is relatively small due to the pinched hysteretic response resulting from bond slip.

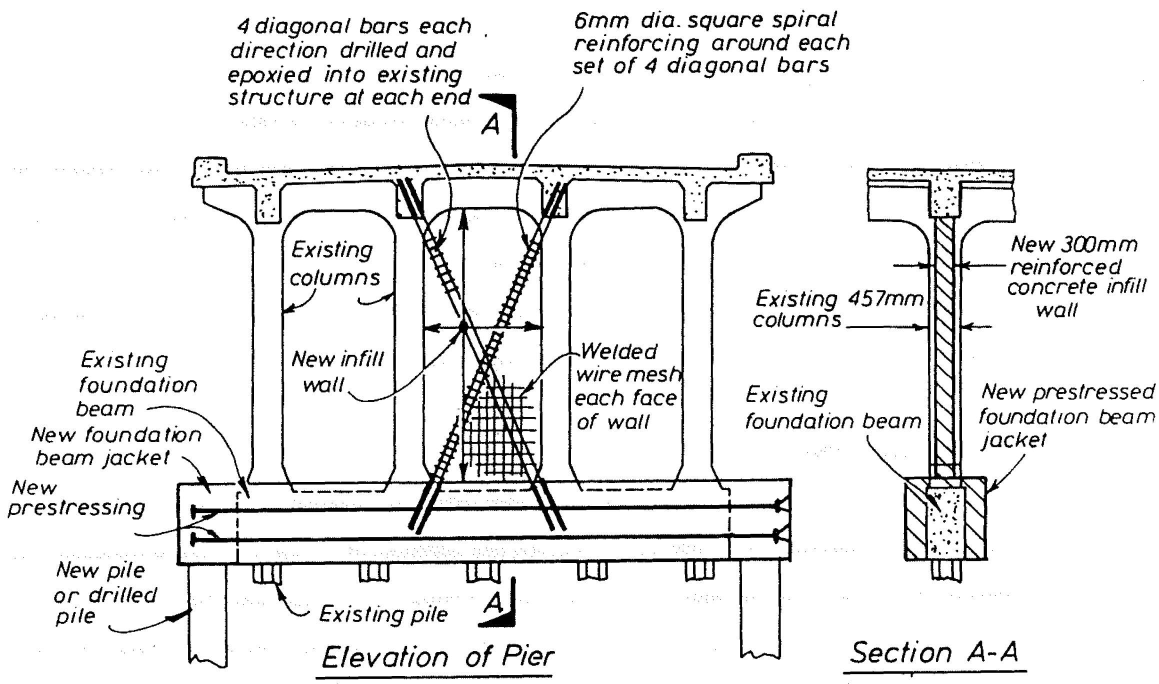

Figure 8.8 **Possible seismic strengthening using a reinforced-concrete infill wall and foundation strengthening.**

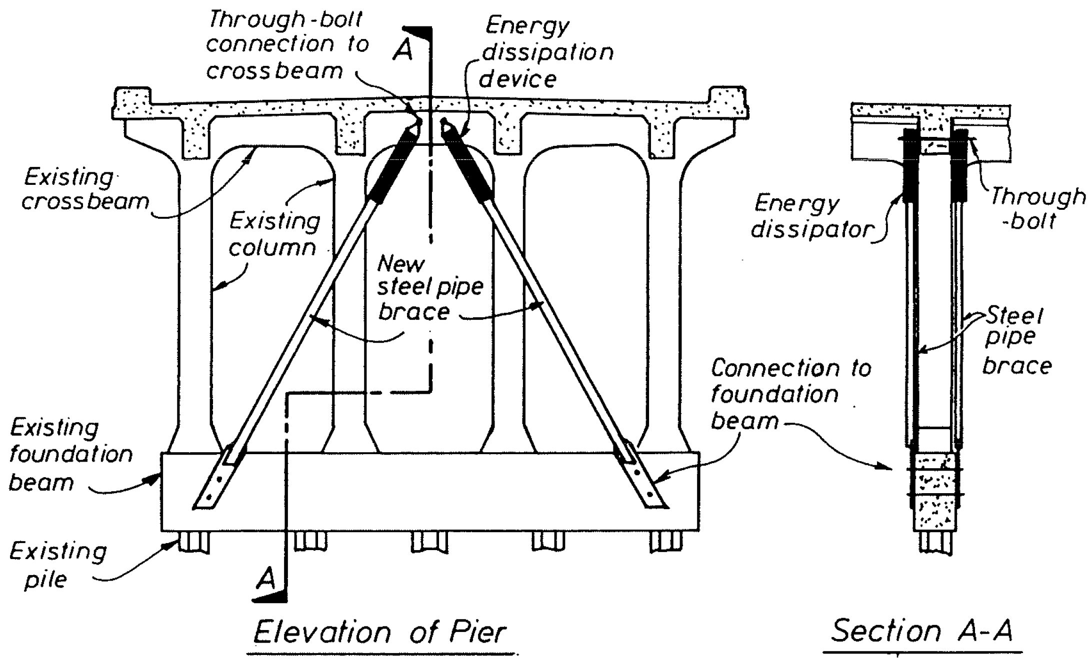

Figure 8.9 **Possible seismic retrofitting using added steel braces with energy- dissipation devices.**

CHAPTER 9

INELASTIC EARTHQUAKE TIME-HISTORY ANALYSES

In Chapter 8, the seismic performance of the 1936-designed New Zealand bridge was predicted to be good, due to the substantial lateral strength and displacement capacity of the structure. In this chapter a series of computer analyses are described which verify that prediction. The analyses also help quantify (a) the benefit of retrofitting bar anchorages, and (b) the effect of the pinched hysteretic response which is characteristic of structures with plain-round reinforcement.

In all, twenty-four inelastic dynamic time history analyses have been run. There are three different structural models, each of which is subjected to eight different earthquake records.

9.1 Modelling of Structure Behaviour

The inelastic frame analysis program *Ruaumoko* [Carr 1995a] is used to model the earthquake response characteristics of the 1936-designed bridge. Three different structures are modelled: (a) the bridge in its unretrofitted condition, (b) the bridge after retrofitting with anchorage end plates at the top of the column bars, as described in Section 6.4, and (c) an ideal structure with the same capacity as the anchorage-retrofit bridge but assumed to have deformed column bars with good bond characteristics.

General Assumptions

As with the previous assessment and experimental studies of the subject bridge, discussed in chapters 6, 7, and 8, only the transverse-direction response of the bridge is considered. A lumped-mass, single-degree-of-freedom model is used, calibrated to the target values of the structural parameters shown in Table 9.1. The target parameters also include a matching of the hysteresis loop shapes and envelopes from the experimental results shown in Figures 6.7, 7.8, and 8.3. The Wayne Stewart hysteresis model [Carr 1995a] is used.

The dynamic, inelastic time history analyses use the Newmark constant average acceleration method, and P-Δ effects are modelled by modifying the member stiffness, given the static dead load [Carr 1995a]. Initial-stiffness Raleigh damping is used at a damping ratio of 2 percent of critical. Earthquake input is in the horizontal direction only. The *Ruaumoko* input data are shown in Table 9.2.

Modelled Hysteresis Loops

The modelled hysteresis loops for the subject bridge are shown in Figure 9.1. The loops were carefully matched to the experimental results and calculated and measured capacities. Figure 9.1(a) shows the pinched hysteresis loops used to model the unretrofitted bridge. Figure 9.1(b) shows similar pinched hysteresis loops, but with a lateral capacity 18 percent higher than the unretrofitted bridge and with a rate of strength degradation (with drift) 1.5 times lower.

Table 9.1 Structural Modelling Parameters

Parameter	Unretrofitted Bridge	Anchorage-Retrofit Bridge	Ideal Structure
Lateral Capacity/Seismic Weight	0.45	0.53	0.53
Hysteresis Loop Shape	Pinched	Pinched	Not Pinched
Initial Stiffness	5.9 kN/mm	5.9 kN/mm	7.8 kN/mm
Strength Degradation at 4% Drift (not including P-Δ)	21%	14%	14%

Table 9.2 Values Used for *Ruaumoko* Input

Input Parameter	Unretrofitted Bridge	Anchorage-Retrofit Bridge	Ideal Structure
Member Length (shear span)	1.80 m	1.54 m	1.54 m
Moment of Inertia	$720(10)^{-6}$ m^4	$450(10)^{-6}$ m^4	$600(10)^{-6}$ m^4
Bi-linear Stiffness Factor	0.4	0.4	0.4
Tri-linear Stiffness Factor	-0.030	-0.020	-0.015
Ultimate Moment	185 kN-m	185 kN-m	185 kN-m
"Yield" Moment	122 kN-m	122 kN-m	122 kN-m
Hysteresis Model	Wayne Stewart	Wayne Stewart	Wayne Stewart
Intercept Moment for Pinching	40 kN-m	40 kN-m	90 kN-m
Pinching Factor, α	0.6	0.6	1.0
Unloading Factor	1.0	1.0	1.0
Factor, β	1.09	1.09	1.09
Strength Degradation Factor after 10 cycles	0.7	0.9	0.9
Damping Ratio	2%	2%	2%

Figure 9.1(c) represents the hysteretic behaviour of an "ideal" structure. The ideal structure has the same lateral strength as the anchorage-retrofit bridge but with a slightly higher initial stiffness and without pinched hysteresis loops. The ideal structure could be considered to be the subject bridge *if* it had deformed column bars with hooks at each end, and assuming that the column transverse reinforcement is adequate to prevent bar buckling. With deformed column bars, significant bond slip

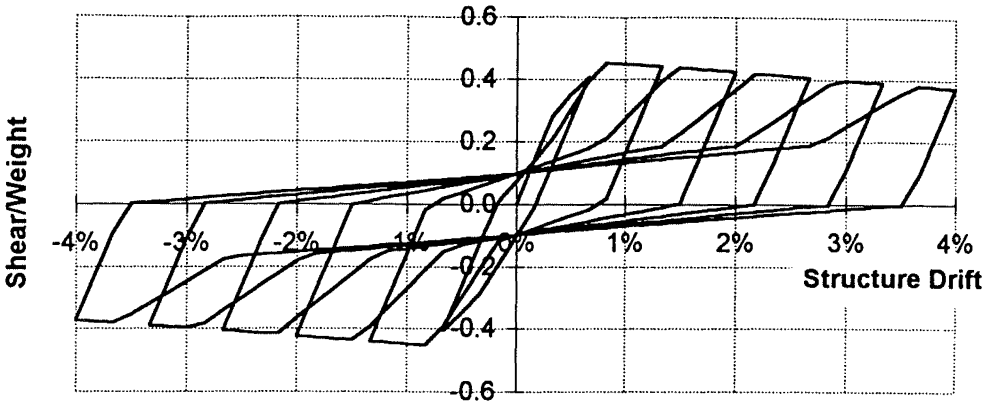

(a) Unretrofitted bridge.

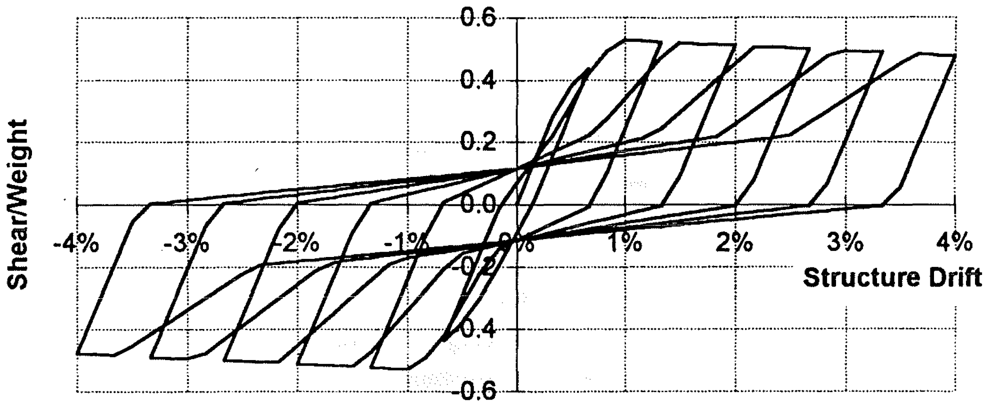

(b) Anchorage-retrofit bridge.

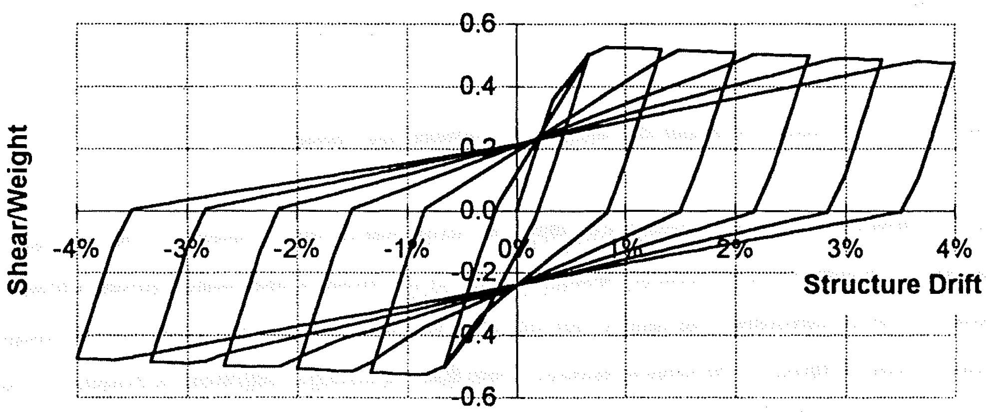

(c) Ideal structure.

Figure 9.1 **Hysteresis Loops to Model Structural Behaviour.**

would not occur and therefore the hysteretic response of the column would not be pinched. The initial stiffness of the ideal structure is modelled to be 1.33 times higher than that of the structures with plain-round bars. This assumption is based on the observation from the test results, discussed in Section 7.3, that the stiffness of the column specimen with plain bars degraded during the first four cycles of testing in each direction, prior to the yielding of the column bars. A column with well-bonded, deformed reinforcement would not be expected to suffer such pre-yield stiffness degradation, therefore its initial stiffness would be somewhat higher.

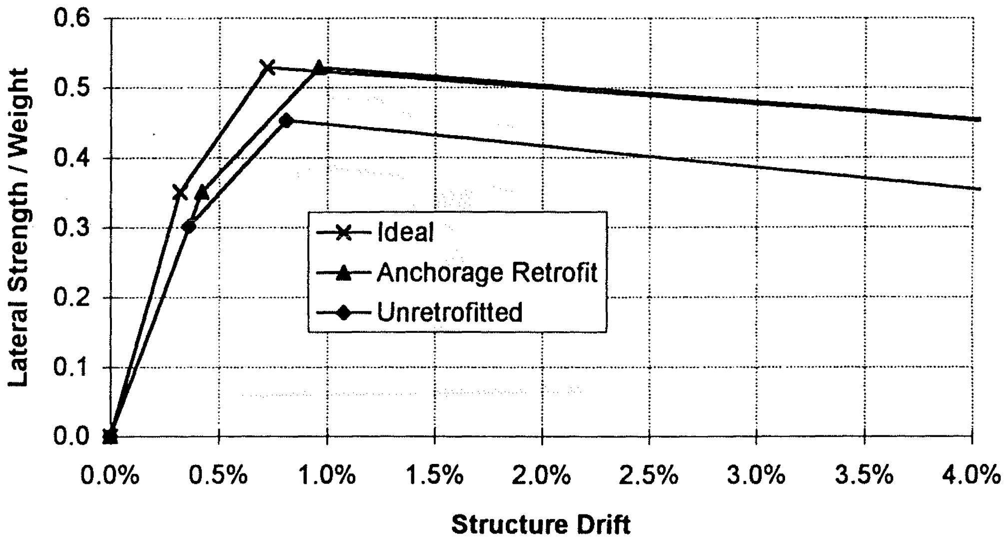

Figure 9.2 Lateral Strength Envelopes for Hysteresis Models.

Figure 9.2 shows the capacity envelopes of the three structural models, plotted on the same graph for comparison. The figure shows clearly the higher capacity of the ideal and anchorage-retrofit structures compared to the unretrofitted, the higher rate of strength degradation of the unretrofitted bridge, and the higher initial stiffness of the ideal structure. Note that the strength degradation evident in the plots of Figures 9.1 and 9.2 does not include a degradation of strength based on number of cycles or the reduction of lateral capacity due to the P-Δ effect, both of which are considered in the *Ruaumoko* analysis. The strength degradation based on number of cycles was not found to be significant in the analysis results.

9.2 Earthquake Input

Eight different earthquake records, as shown in Table 9.3, were used as input to the analysis. The eight records cover a wide range of earthquake characteristics.

Selection of Earthquake Records

The first earthquake record used in the analysis is an artificial record called Bridgeza. This record was created to produce a response spectrum matching that used for the seismic design of bridges in New Zealand's highest seismic zone. Thus, the earthquake record represents the seismic demands which have been considered appropriate for the design of new bridges.

Table 9.3 Earthquake Records Used for the Analysis

Record Name	Filename	Earthquake Date	Direction	Record Duration (seconds)	Peak Ground Accl (g)
Bridgeza	BRIDGEZA.EQC	Artificial	-	20.0	0.50
Pacioma Dam	PACMSW.EQB	9 February 1971	S14W	20.3	1.20
Parkfield	PARKNE.EQB	27 June 1966	N65E	21.1	0.49
El Centro	EL4ONSC.EQB	18 May 1940	N-S	20.06	0.37
Taft	TAFTNW.EQB	21 July 1952	N69W	30	0.16
Bucharest	BUCHNSC.EQB	4 March 1977	N-S	16.22	0.21
Mexico D (Tlahuac Deportivo)	MEXTLHDL.DQ C	19 September 1985	N-S	150	0.12
Mexico S (Sec.Com.y Transportes)	MEXSCT1T.EQC	19 September 1985	E-W	150	0.17

The next four records of Table 9.3—Pacioma, El Centro, Parkfield and Taft—are from California earthquakes and have commonly been used in structural analyses. The last three records, Bucharest and two Mexico records, are included to consider the performance of the bridge if it were located on a soft-soil site.

Naeim and Anderson [1993] provide an excellent classification and evaluation of earthquake records, which was used to help select the records for this study. Table 9.4 shows additional data on the six earthquake records used here which are covered by Naeim and Anderson.

The Pacoima dam record is notable for its high peak ground acceleration, velocity, and displacement. The Parkfield record is notable for its high incremental velocity, and both the Parkfield and Pacoima records are among the records with the largest mean input energy in the period band from 0.5 to 0.8 seconds [Naeim and Anderson 1993, Tables 5-1 and 6-5]. The 1940 El Centro and the 1952 Taft records are considered notable for their reasonably long durations, but Naeim and Anderson [1993, page 156] note that "some of the acceleration records commonly used for earthquake resistant design, such as 1940 El Centro, have very limited damage potential compared to other records contained in the data base."

The Mexico D record was initially selected for the analysis to represent soft-soil earthquake input, however, after the analysis showed it had little effect on the subject structure (response was fully elastic), two other soft-soil records were run: Bucharest and Mexico S. The Mexico S record has the highest peak ground acceleration of any of the 1985 Mexico City records and is considered notable for its peak displacement and incremental velocity [Naeim and Anderson 1993]. (As shown later, both the Mexico S and Bucharest records also had little effect on the subject bridge.)

Response Spectra

The characteristics of each of the eight earthquake records are illustrated by their response spectra, shown in Figures 9.3(a)-(f). The response spectra show a tremendous variation in earthquake characteristics amongst the different records, and compared to the code-assumed response spectrum approximated by the Bridgeza record of Figure 9.3(a). Only the 1940 El Centro record, Figure 9.3(c), even vaguely resembles the Bridgeza record. The Pacoima spectrum, Figure 9.3(b), greatly exceeds the Bridgeza spectrum in most period bands. The Parkfield spectrum, Figure 9.3(d), greatly exceeds the Bridgeza spectrum in the period range of 0.3 to 0.8 seconds, which is critical for the subject bridge. The Taft spectrum, Figure 9.3(e), shows that this record has much lower demands than the Bridgeza record. The soft soil records from Bucharest and Mexico, Figures 9.32(e) and (f), show extremely high demands in the period range around 2 seconds, but much lower demands in the period range of the response of the subject structure, 0.4 to 1.0 seconds.

The spectra shown in Figure 9.3 are plotted on acceleration versus displacement (A-D) axes. This presentation allows the consideration of spectral displacements as well as accelerations. As shown in the figure, lines of constant period extend radially from the origin. Two lines of constant pseudo-velocity are also shown faintly on each of the plots of Figure 9.3. The shape of these lines on the plots is that of an inverse function (ie, $y = kx^{-1}$).

The plotting of the spectra in A-D co-ordinates allows the structure's force-displacement response to be superimposed on the spectrum plot. This has been done in Figure 9.3, using the envelopes of the

Table 9.4 Additional Data on Earthquake Records, from Naeim and Anderson [1993, Table 3-1].

No.	Year	Earthquake Name	Station Name	D	Mag	PA	PV	PD	[D]
147	1971	San Fernando	Pacoima Dam	8	6.6	1125	113.09	38.28	33.9
11	1940	El Centro	El Centro - Imp Vall Irr Dist	12	7.0	338	36.45	10.88	29.3
52	1966	Parkfield CA	Cholame Shandon Array 2	7	6.1	466	77.59	26.74	12.1
29	1952	Kern County	Taft	42	7.4	183	17.80	7.27	15.6
799	1985	Mexico	Sec. Com. Y Transportes	400	8.1	168	60.38	20.57	33.1
805	1985	Mexico	Tlahuac Deportivo	410	8.1	115	34.26	18.53	18.7

D = epicentral distance, km
Mag = magnitude
PA = peak ground acceleration, cm/sec^2
PV = peak ground velocity, cm/sec
PD = peak ground displacement, cm
[D] = 0.05 g bracketed duration, sec

force-displacement response for the unretrofitted bridge. Each bridge response envelope is plotted to the peak displacement reached in the analysis for that particular earthquake record.

9.3 Analysis Results

The results of the 24 computer analyses show a large variation in response depending on the earthquake input, and also point to some differences in seismic performance between the unretrofitted, anchorage-retrofit, and ideal structures.

Structure Drift and Bridge Performance Limit States

Table 9.5 shows the peak levels of structure drift in each direction resulting from the inelastic computer analyses. The structure drift is defined as in Chapters 7 and 8: equal to the lateral displacement of the bridge superstructure with respect to the foundation, divided by the height of 4.80 metres between the centerline of the foundation beam and the centerline of the crossbeam. Figure 9.4 shows a graph of the peak structure drift values resulting from the 24 analysis runs.

The peak structure drift is a fairly good measure of the level of earthquake damage sustained by the bridge. Peak structure drift levels below about 0.7 percent indicate elastic or nearly elastic response.

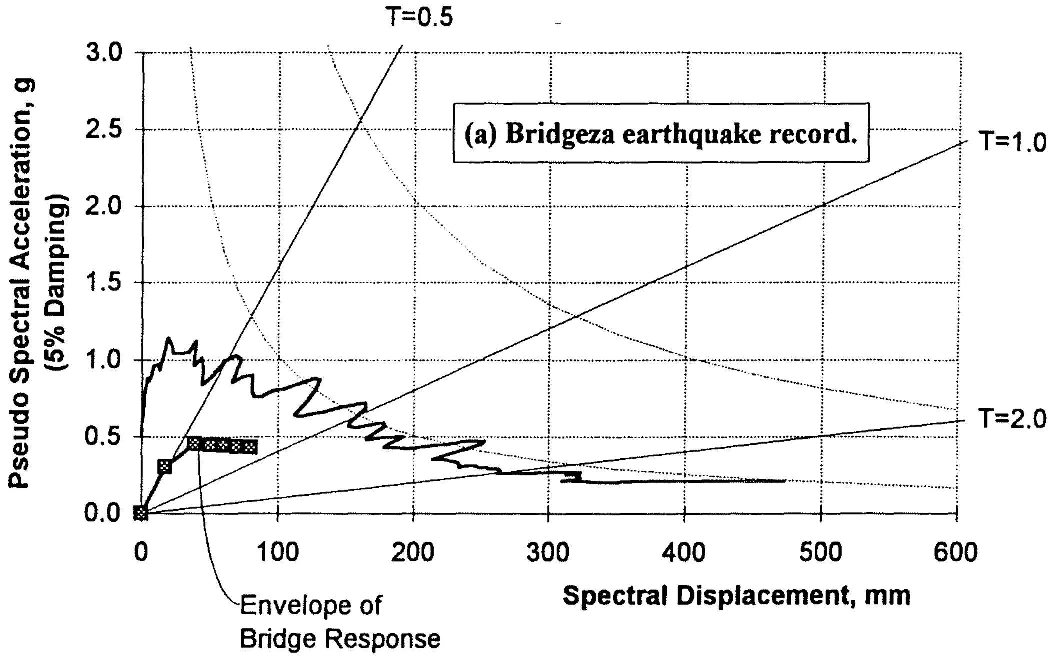

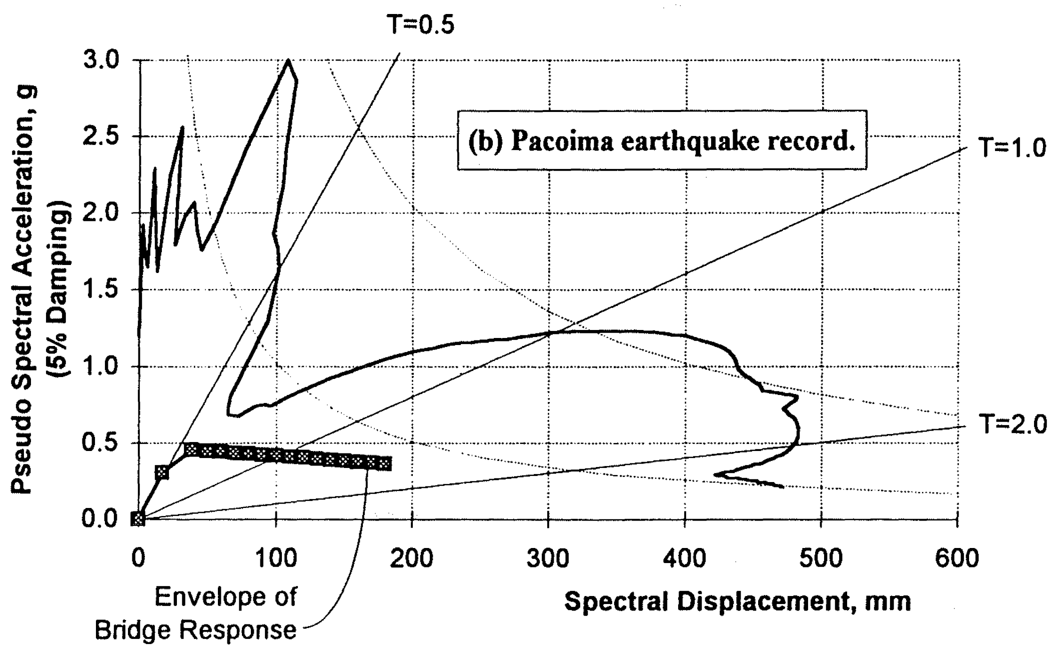

Figure 9.3 **Response Spectra for the Earthquake Records Used as Input to the *Ruaumoko* Analysis.**

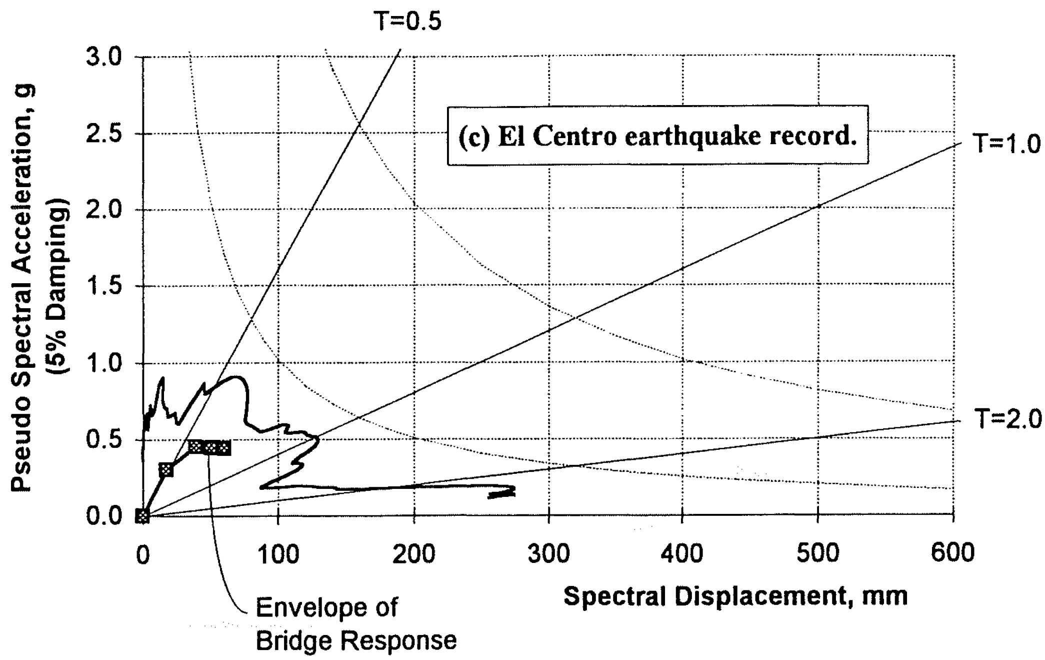

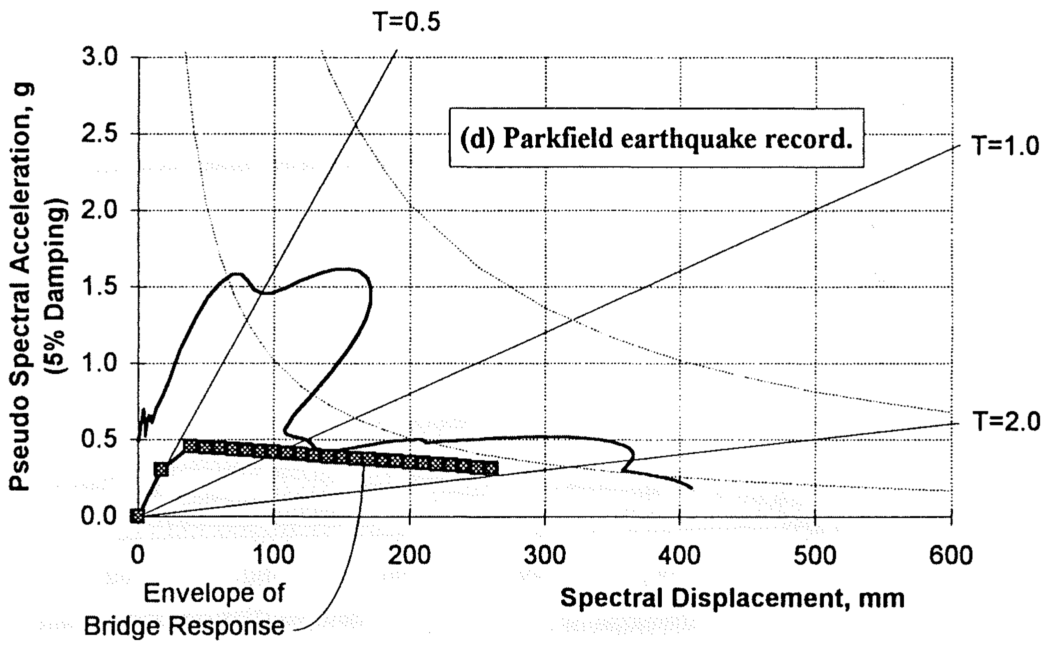

Figure 9.3 (continued) Response Spectra for the Earthquake Records Used as Input to the *Ruaumoko* Analysis.

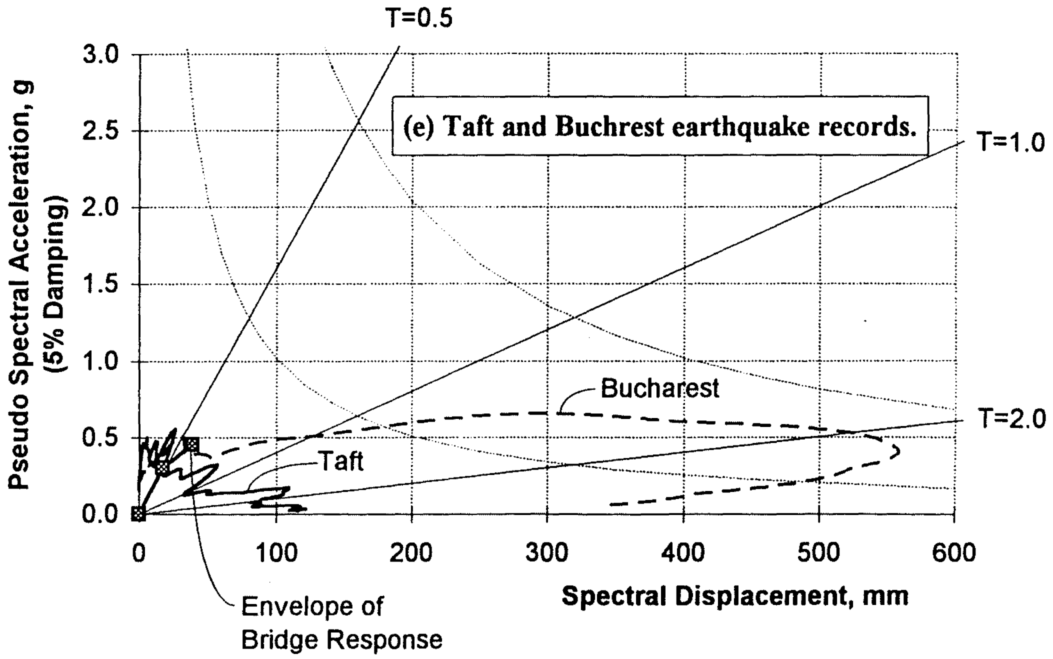

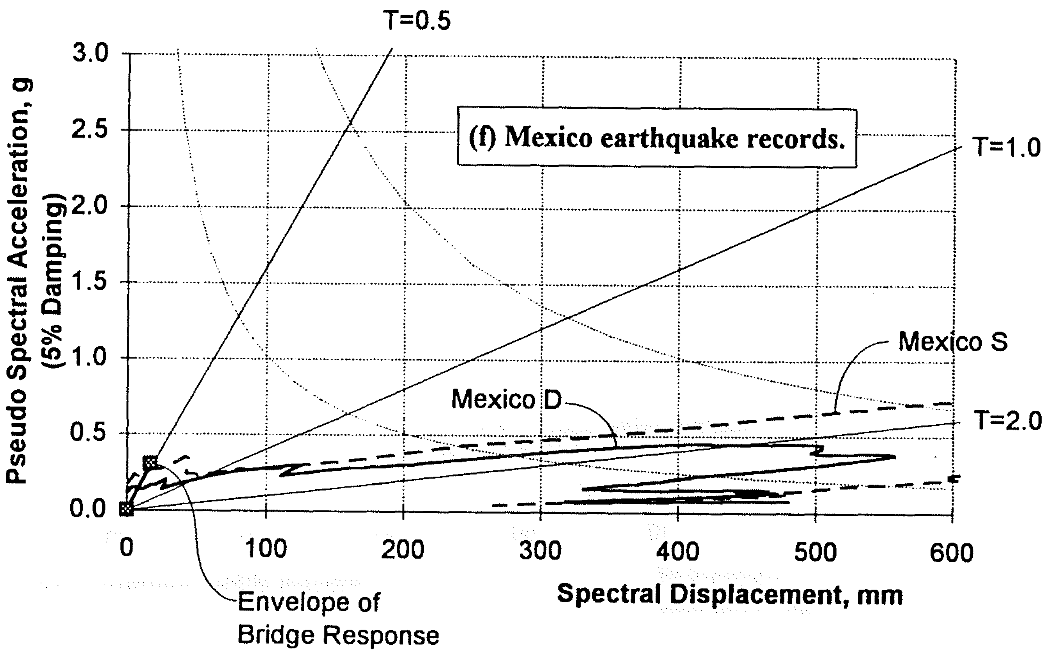

Figure 9.3 (continued) **Response Spectra for the Earthquake Records Used as Input to the *Ruaumoko* Analysis.**

Table 9.5 Maximum Structure Drift Results from the Inelastic Time-History Analyses

Earthquake Record	Peak Structure Drift (Positive and Negative)					
	Unretrofitted Bridge		Anchorage-Retrofit Bridge		Ideal Structure	
Bridgeza	1.76%	-1.45%	1.83%	-1.15%	1.48%	-0.51%
Pacoima	3.76	-1.80	3.11	-1.50	2.06	-1.55
El Centro	1.27	-0.68	1.07	-0.73	0.75	-0.43
Parkfield	5.42	-1.89	4.57	-3.25	2.37	-1.33
Taft	0.51	-0.48	0.56	-0.60	0.58	-0.32
Bucharest	0.44	-0.43	0.45	-0.43	0.23	-0.30
Mexico D	0.22	-0.17	0.22	-0.17	0.20	-0.14
Mexico S	0.26	-0.23	0.26	-0.23	0.18	-0.16

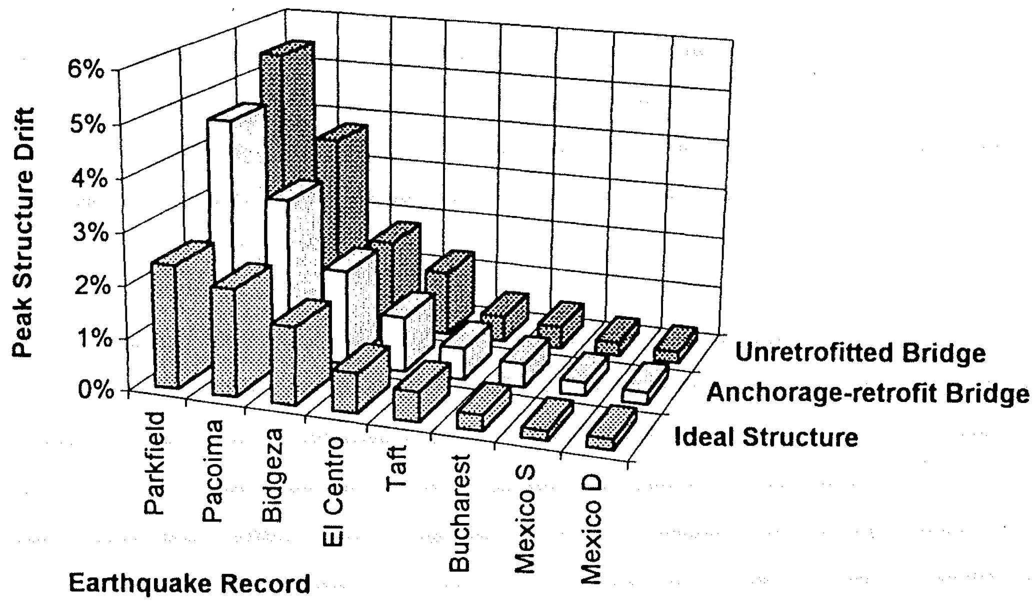

Figure 9.4 Peak Structure Drift Results from the Inelastic Time-History Analyses.

A structure drift level of 4.0 percent indicates a global displacement ductility of 6, sometimes considered [SANZ 1995] to be the upper limit to reliable structural ductility capacity. The level of damage to the test specimen column at a structure drift of 4.0 percent is shown in the photo of Figure 7.2(c). For a structure with deformed column bars at a drift of 4 percent, the level of deterioration in the column could be greater.

Peak drift levels for the bridge could be associated with performance limit states such as those discussed in Section 14.5 of this report, and in Paulay and Priestley [1992]. Table 9.6 outlines the estimated relationship of bridge performance with peak drift levels. The table is based primarily on the test results of Chapters 7 and 8. The table shows that below a drift of 0.7 percent (Limit State A) no bridge damage or repair is expected. Between 0.7 and 1.5 percent drift, cracking and some inelastic behaviour is expected but spalling of the concrete is not expected. Above 1.5 percent drift (Limit State B) concrete spalling is expected.

Limit State C marks the traditional serviceability limit, beyond which a bridge will not remain fully functional for carrying traffic, and beyond which more serious repair or retrofit measures will be required. This limit state may depend more on the residual or permanent drift of the structure after the earthquake than on the peak drift during earthquake shaking. However, the higher the peak drift, the greater the chance that the structure will be left with an unacceptable level of residual drift. Also, a structure with deformed reinforcement, for the same peak drift, may be more likely to have an unacceptable level of residual drift than a structure with plain-round reinforcement. This is because a structure with deformed reinforcing would undergo greater levels of inelastic strain in the column bars. Considering these points, limit state C is estimated to be reached at a peak drift of about 2.5 percent for the bridge with plain bars, and at a drift of about 2 percent for the bridge with deformed bars.

Limit State D marks the traditional damage-control limit state, beyond which damage is not economically repairable. Based on the test results of Chapters 7 and 8, the subject bridge seems to be able to sustain very high drift levels before suffering irreparable damage. Until a drift of 6 percent is reached, damage consists only of cracking and spalling in the column end regions; the reinforcing bars do not buckle. Beyond the 6 percent drift level anchorage splitting failures could occur which would be difficult to repair. Thus a peak drift level of 6 percent is associated with limit state D for the subject bridge with plain-round bars. For the ideal bridge with deformed bars the limit state is estimated to occur at a drift of about 5 percent, when the column bars would be likely to buckle, as discussed in Section 8.3.

Limit State E of Table 9.6 represents the traditional survival or no-collapse limit state. The test results show that the subject bridge with plain-round bars will not collapse even at the extreme drift levels,

Table 9.6 Estimated Relationship of Bridge Drift Level to Performance Limit States

Limit State	Bridge Damage and Likely Repair	Bridge Serviceability	Peak Structure Drift Corresponding to Limit State	
			Unretrofitted or Anchorage-Retrofit Bridge	"Ideal" Structure
	No damage, no repair required	No loss of bridge service		
A			0.7%	0.7%
	Minor damage, epoxy injection of cracks required			
B			1.5%	1.5%
	Moderate damage, epoxy injection and patching of spalled concrete required			
C			2.5%	~2%
	Medium-heavy damage. May need to jack bridge to remove permanent lean and/or add bracing retrofit to restore stiffness. Also patching and epoxy injection required.	Temporary loss of bridge service except for emergency traffic.		
D			6%	~5%
	Heavy damage. Column-bar buckling or anchorage splitting. Not economically repairable.	Bridge unsafe even for emergency traffic		
E			> 8%	Unknown
	Collapse			

Note: Only transverse-direction structural response is considered.

about 8 percent, to which the bridge was tested. For the hypothetical bridge with deformed bars, the peak drift to cause collapse cannot be estimated, due to the lack of specific test results.

Response for Different Earthquake Records

Figure 9.4 clearly illustrates the large variation in structural response depending on the earthquake input. The force-displacement-response envelopes for the unretrofitted bridge are also shown on the spectra plots of Figure 9.3. Four of the earthquake records cause little or no damage to the bridge models. For the two Mexico records the response is fully elastic. For the Bucharest and Taft records the response

is nearly elastic. The structure drift in some cases reaches the bi-linear region of the capacity envelopes shown in Figure 9.2, but does not reach the tri-linear region. Thus none of the four records—Taft, Bucharest, Mexico S, and Mexico D—affect the structures enough to cause them to reach their ultimate strengths. The good lateral strength of the subject structure, as noted in Section 8.4, prevents any damage from occurring under these four earthquake records.

Of more interest are the Bridgeza and El Centro earthquake results. The Bridgeza earthquake causes peak structure drifts of up to 1.8 percent, while the El Centro record causes drifts of up to 1.3 percent. These results confirm that the performance of the modelled structures under a code-implied level of earthquake shaking will be good. The Bridgeza and El Centro earthquakes impart only a limited level of ductility demand on the structures. The maximum displacement-ductility demand for these earthquake inputs is less than 3.

The Pacoima and Parkfield earthquake records impart more extreme demands on the modelled structures. For the Pacoima record the peak structure drift is 3.8 percent; for the Parkfield record it is 5.4 percent. As previously noted, these two earthquakes have very high input energy in the period range of the structural response. For both of these records the earthquake energy is released in a few major pulses, over a duration of just a few seconds.

Naeim [1995] has found these same characteristics in the strongest records from the 1994 Northridge earthquake. Such earthquake records, with a few major pulses of ground motion which greatly exceed code-implied earthquake demands, have also been observed in the 1995 Hyogo-ken Nanbu (Kobe) earthquake, and in the 1992 Petrolia California earthquake. Such earthquake shaking characteristics tend to be found in locations "downstream" from the earthquake source; that is, in the direction of the fault propagation. In this direction the earthquake waves tend to stack up on each other causing larger pulses for shorter durations. For the 1940 El Centro record, the earthquake fault propagation was directed away from the recording station [Carr 1995b] causing a smaller amplitude of shaking with a longer duration. Seismic design codes tend to assume an El Centro type of earthquake response spectrum, although some engineers have proposed to account for more extreme earthquake effects using a near-field factor [SEAONC 1995].

Response for Different Hysteresis Models

As well as showing a strong dependency on earthquake input, the peak displacement results of Table 9.5 and Figure 9.4 show some consistent differences in the response of the three different hysteresis models. Typically, the seismic response of the anchorage-retrofit bridge is slightly improved over that of the unretrofitted bridge, and the response of the ideal structure is further improved over that of the other two models.

For the Taft, Bucharest, and Mexico earthquake records there is, understandably, little difference in the peak displacement response between the three structural models. As previously noted, the behaviour for these earthquake inputs is elastic or nearly elastic, and therefore of little interest.

Bridgeza and El Centro Earthquakes

For the two earthquake records which produce moderate displacement demands, Bridgeza and El Centro, some differences between the three structures are evident. For the El Centro earthquake, the peak drift of the anchorage-retrofit bridge is 16 percent less than for the unretrofitted bridge. For the Bridgeza earthquake the peak drift for these two structures is about the same, but the maximum drift in the negative direction is reduced by about 20 percent for the anchorage-retrofit bridge. (See Tables 9.5 and Figures 9.6a and 9.6b.) Comparing the ideal structure with the anchorage-retrofit bridge, the peak response for the El Centro and Bridgeza earthquakes is reduced by about 20 to 30 percent for the ideal structure.

For the Bridgeza earthquake the structure drift time-histories are shown in Figure 9.5, and the force-versus-displacement hysteresis response is shown in Figure 9.6. The figures again show (a) only a slight reduction in response for the anchorage-retrofit bridge over the unretrofitted, and (b) a more significant reduction in response for the ideal structure over the anchorage-retrofit bridge.

Interestingly, although a peak drift is the least for the ideal structure, the *residual* drift is the greatest. The residual drift is shown at the end of the time-history of Figure 9.5(c) to be about 0.4 percent. This level of residual lean in the bridge may be noticeable but would not compromise the ability of the structure to resist future earthquakes or its design loads. For the unretrofitted and anchorage-retrofit bridges the residual drift is nearly zero.

Pacoima and Parkfield Earthquakes

For the two earthquake records which produce large displacement demands, Pacoima and Parkfield, the differences between the three structural models are more pronounced. Comparing the anchorage-retrofit bridge to the unretrofitted, the results show a reduction of peak displacement by about 16 percent. Comparing the ideal structure with the anchorage-retrofit bridge, a reduction in peak displacements of about 40 percent is evident.

For the Pacoima earthquake, structure drift time histories are shown in Figure 9.7 and force-versus-displacement hysteretic response plots are shown in Figure 9.8. The figures show the significant difference in structural response between the three models.

Figure 9.8(a) shows that the unretrofitted bridge is subjected to most of its inelastic displacement demands in one pulse which pushes the structure to a drift of 3.4 percent. Figure 9.7(a) shows that this is the first major pulse of the Pacoima record, occurring about 3 seconds into the earthquake time history. A similar type of response occurs for the unretrofitted bridge due to the Parkfield earthquake. Naeim [1995] has noted that for such types of earthquake records damping is of little benefit, and the earthquake's energy must be dissipated as hysteretic energy by the structure.

The increased strength of the anchorage-retrofit and ideal structures allows them to dissipate the earthquake energy of the first strong earthquake pulse with less lateral displacement, as shown in Figures 9.8(b) and 9.8(c). The fatter hysteresis loops of the ideal structure allow the structure to dissipate the input energy of the subsequent earthquake pulses with less displacement than that suffered by the anchorage-retrofit bridge.

For the unretrofitted bridge, not only is the peak level of drift considerable, so is the residual drift. As shown in Figure 9.7(a), at the end of the Pacoima earthquake, the structure is left leaning at a drift of about 0.9 percent. For the anchorage-retrofit and ideal structures, the residual drift is about 0.3 percent.

9.4 Final Assessment

The analysis results show that the seismic performance of the bridge depends greatly on the earthquake input. Because of its substantial lateral strength, the bridge is able to respond essentially elastically for a number of earthquake records. Earthquake records with demands similar to those assumed by design codes—eg, the Bridgeza and El Centro records—produce only moderate displacement demands on the structures. More severe earthquake records with extreme ground-motion pulses, such as Pacoima and Parkfield, produce higher displacement demands but do not cause bridge collapse. The performance of each of the three structures is summarized below for both the *code-implied* and *severe* earthquakes.

Performance for Code-implied Earthquake Levels

All of the structures perform very well for code-implied earthquake levels, and the difference in response between the three structures is not dramatic. Considering the limit states of Table 9.6, it is estimated that the structures could survive such earthquakes with only moderate damage which could

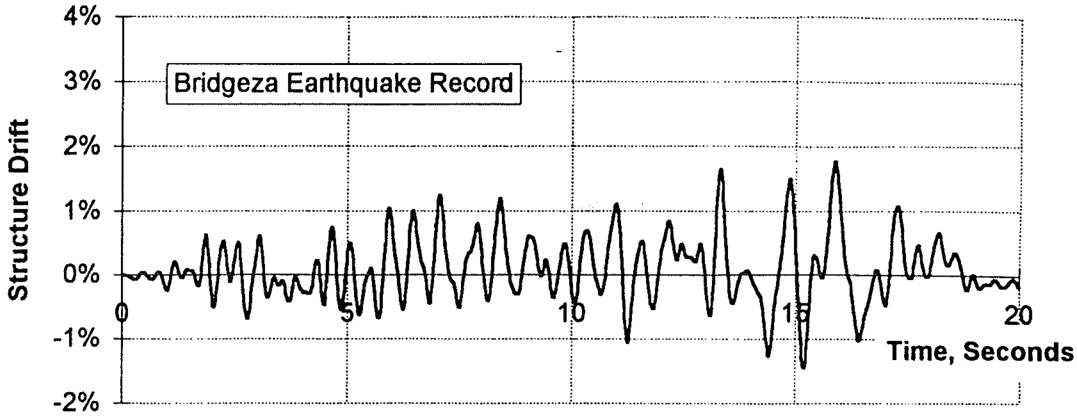

(a) Unretrofitted bridge.

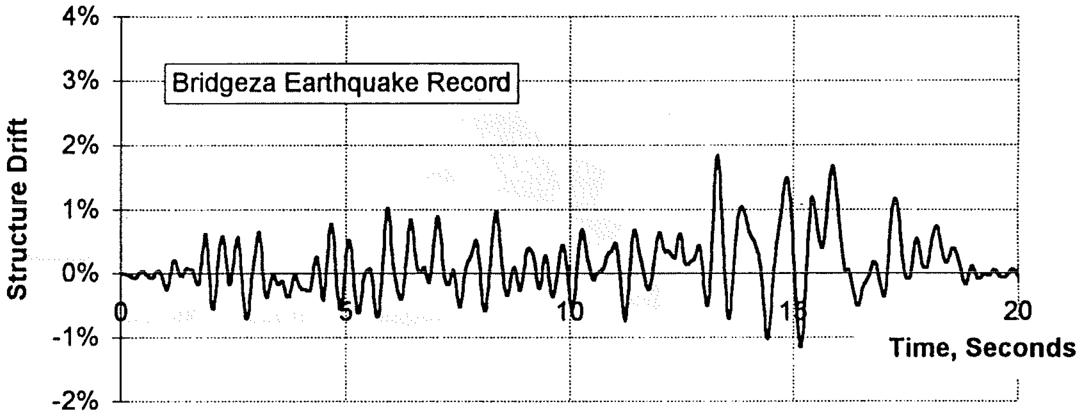

(b) Anchorage-retrofit bridge.

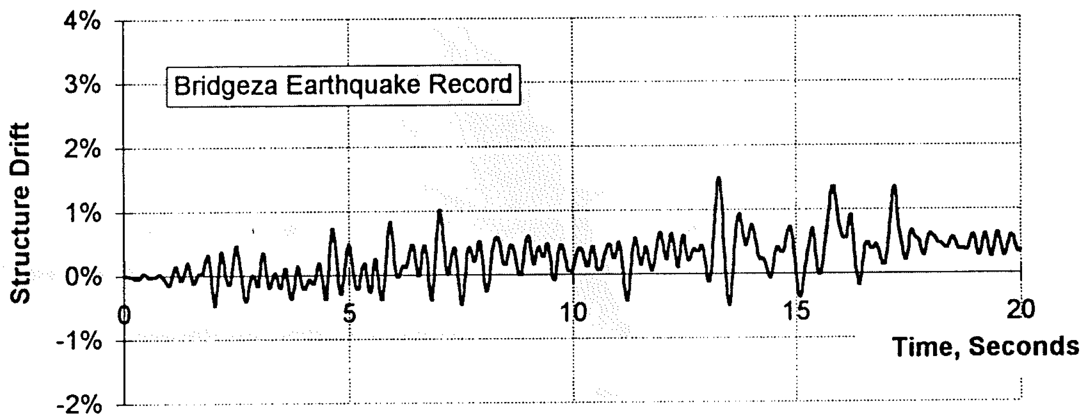

(c) Ideal structure.

Figure 9.5 Structure Drift Time-history Results for the Bridgeza Earthquake Record.

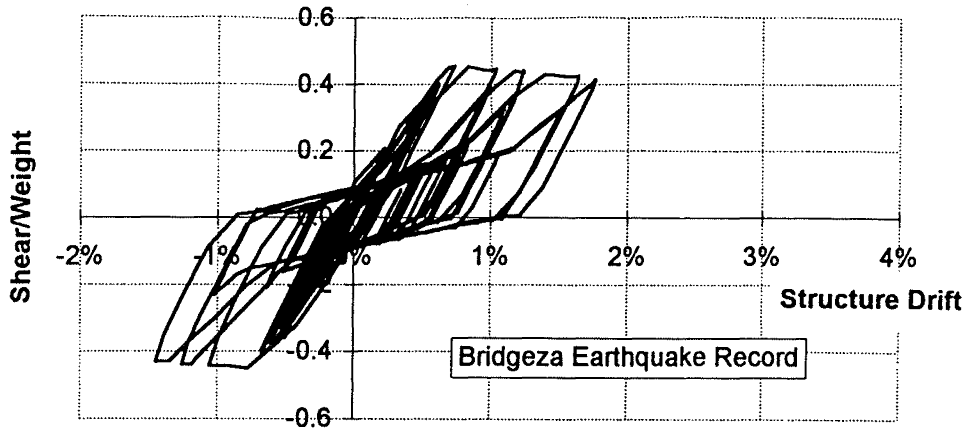

(a) Unretrofitted bridge.

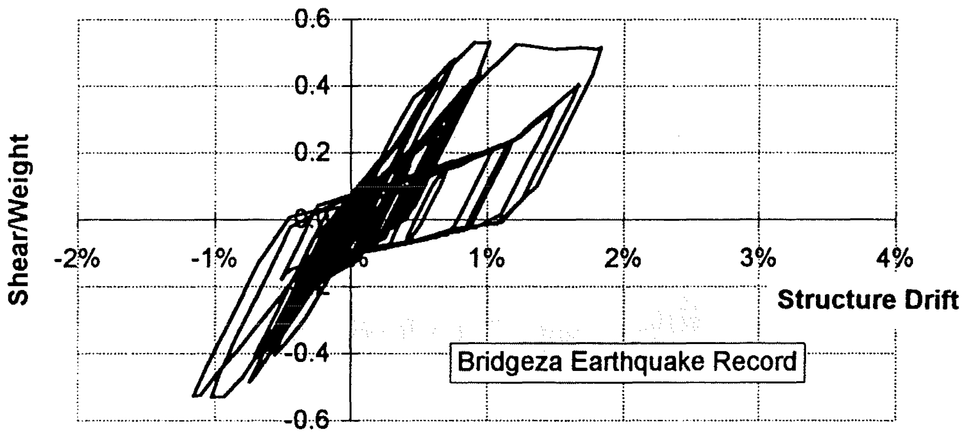

(b) Anchorage-retrofit bridge.

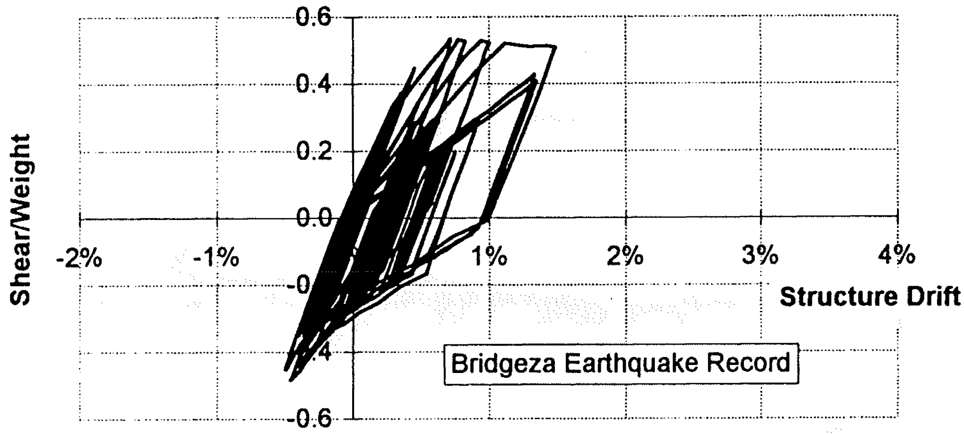

(c) Ideal structure.

Figure 9.6 **Lateral Force Versus Displacement Hysteretic Response for the Bridgeza Earthquake Record.**

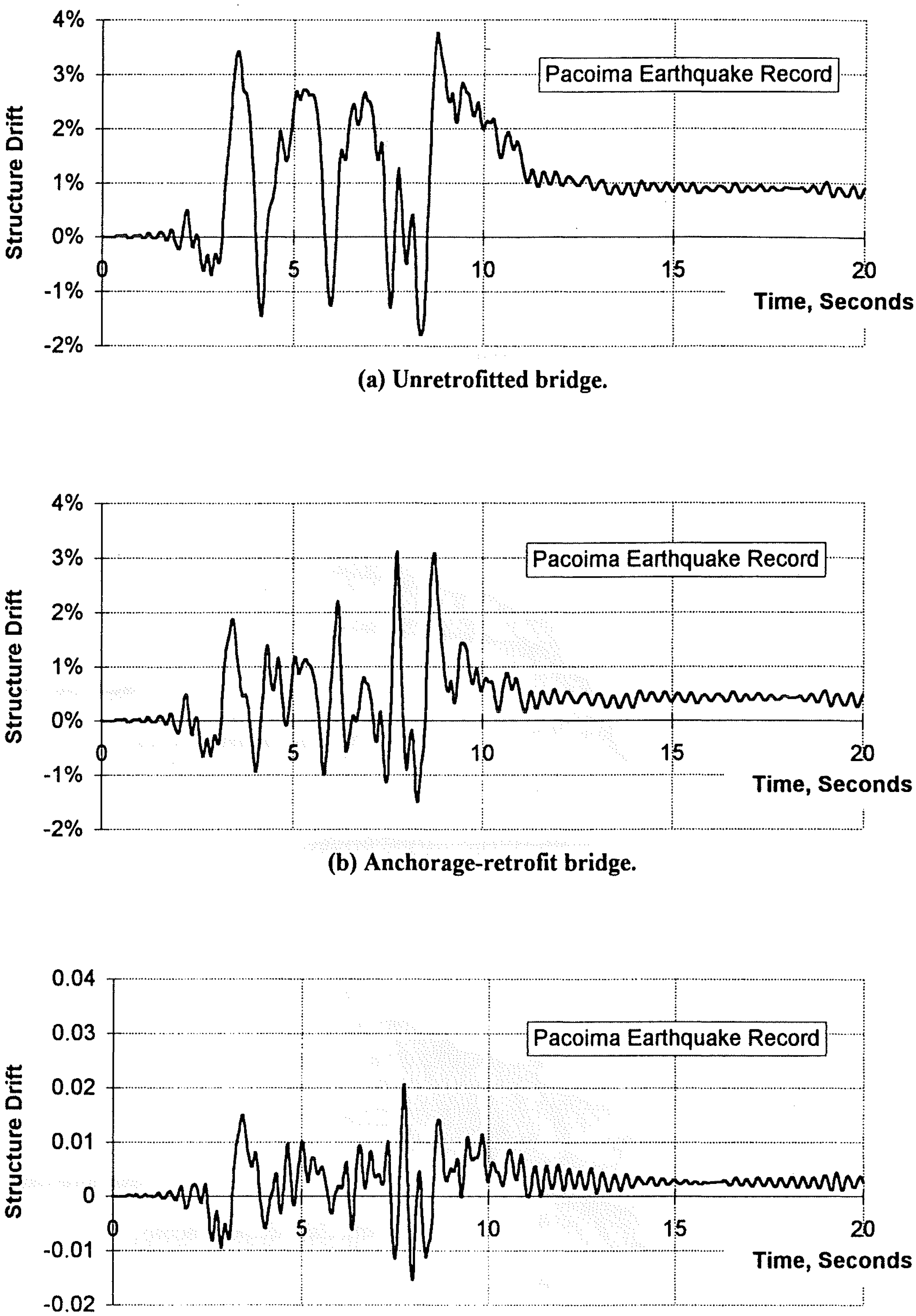

(a) Unretrofitted bridge.

(b) Anchorage-retrofit bridge.

(c) Ideal structure.

Figure 9.7 **Structure Drift Time-History Results for the Pacoima Earthquake Record.**

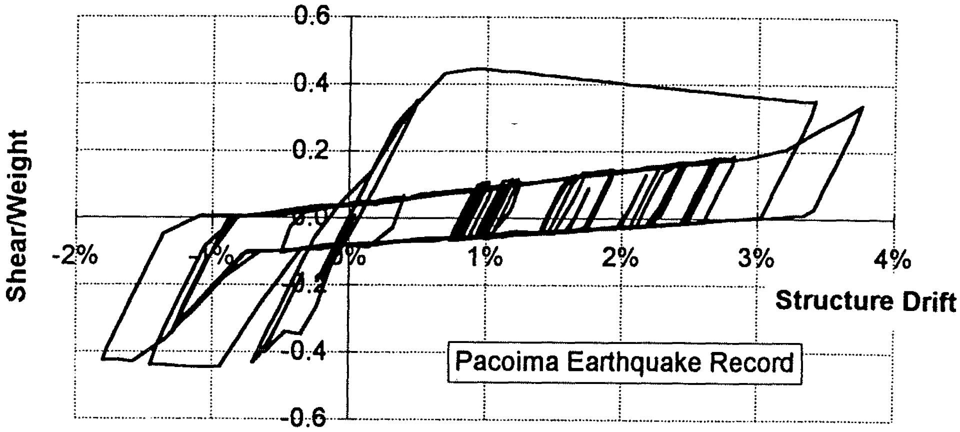

(a) Unretrofitted bridge.

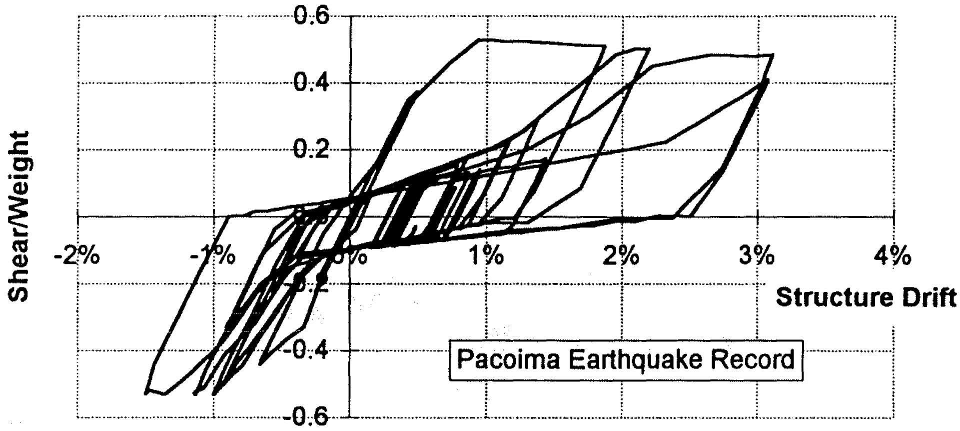

(b) Anchorage-retrofit bridge.

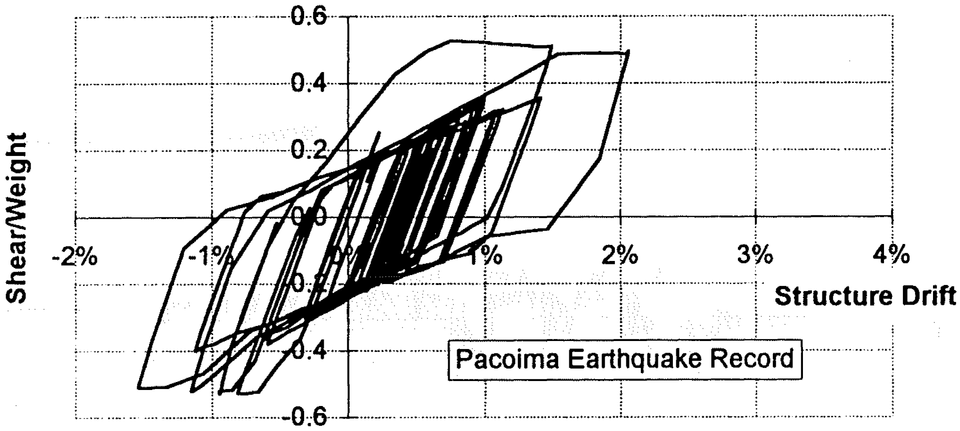

(c) Ideal structure.

Figure 9.8 **Lateral Force Versus Displacement Hysteretic Response for the Pacoima Earthquake Record.**

easily be repaired. The bridges may also be able to survive such earthquakes without loss of service or traffic disruption.

The retrofitting of the column-bar end anchorages can result in a slight decrease in displacement response compared to the unretrofitted bridge. However, the small improvement in bridge performance for this level of earthquake would not justify the cost of the retrofit.

The reduced response for the ideal structure compared to the anchorage-retrofit bridge indicates the better hysteretic energy-dissipating capacity of structures with deformed reinforcing. For the code-implied earthquake level, however, the reduction in response is not dramatic. Also this benefit may be offset by the fact that for the same drift level, greater structural deterioration and residual drift can occur for structures with deformed reinforcing bars.

Performance for Severe Earthquake Levels

For severe earthquake inputs, the differences in structural performance for the three models become magnified. For the unretrofitted and anchorage-retrofit bridge, medium to heavy damage would be suffered and the structure is likely to be left with a noticeable residual drift and a degraded stiffness. Despite the extreme displacement response, the bridge would not collapse and might still be repairable, perhaps by using an added bracing retrofit as shown in Figure 8.9. The new braces could restore the degraded bridge stiffness and also be used, with jacking equipment, to straighten any residual lean in the structure.

The anchorage-retrofit structure shows a consistently reduced response compared to the unretrofitted structure. However, the moderate level of improvement, and the low probability of such extreme earthquake shaking, mean that it would be difficult to justify such a retrofit.

For the severe earthquake input the ideal structure shows a substantial reduction in seismic response. This shows a clear benefit in the use of deformed column bars instead of plain bars. For severe earthquake shaking as represented by the Parkfield and Pacoima records, the structure with deformed reinforcing would suffer less damage than the comparable bridge with plain-round reinforcing.

CHAPTER 10
CONCLUSIONS FOR PART II

The studies of the 1936-designed New Zealand bridge lead to several conclusions regarding the seismic assessment of existing reinforced-concrete structures:

A *Poor Bond Resistance of Plain Reinforcing Bars*

Compared with deformed reinforcement, plain-round reinforcement offers much poorer bond-resistance and undergoes a more rapid degradation of bond under cyclic earthquake actions. The New Zealand concrete code *NZS 3101* [SANZ 1982] specifies that the embedment length of plain-round reinforcement should be twice that required of deformed reinforcement. This factor of two may not be sufficient to account for the poor bond of plain-round reinforcement, particularly at higher ductility levels. The pending 1995 revision to *NZS 3101* prohibits the use of plain-round bars for main longitudinal reinforcement.

B *Stiffness Degradation and Hysteretic Response*

Structures with plain-round reinforcement suffer stiffness degradation under earthquake actions, and a pinching of lateral-force versus displacement hysteretic response, resulting from the bond-slip of the reinforcing. The stiffness degradation and pinched hysteresis loop shape could compromise the earthquake performance of structures with plain-round reinforcing bars, particularly for severe earthquake shaking characterized by a few very strong pulses.

C *Strength, Displacement Capacity, and Seismic Performance*

Despite the pinched hysteretic response, the high lateral strength and displacement capacity of the subject bridge result in excellent seismic performance and allow the structure to survive severe earthquake shaking without collapse.

D *Bar-anchorage Retrofit*

If the bridge is retrofitted by welding anchorage end-plates to the tops of the column longitudinal bars, the peak lateral strength of the bridge increases and the degree of strength degradation reduces. As verified by the inelastic analyses, the anchorage retrofit would improve the seismic performance of the bridge. However, the amount of improvement probably does not justify the expense of such a retrofit.

E *Diagonal Bars*

The supplementary diagonal reinforcing bars at the top and bottom end-flares of the bridge column contribute significantly to both flexural and shear strength of the critical section of the column. A seismic evaluation which neglected the contribution of these bars would under-estimate the earthquake-resisting capacity of the structure.

F *Concrete Confinement*

For columns with low axial load, the 1982 concrete code [SANZ 1982] is conservative in its requirements for concrete confinement. For the subject bridge this code over-estimates the required amount of transverse steel by a factor of 3. The 1995 draft code [SANZ 1995] has more accurate requirements, and is recommended as a basis for seismic assessment criteria.

G *Column-tie Spacing*

For columns with low axial load, good shear capacity, and large-diameter longitudinal reinforcing, the column-tie spacing requirements of the 1982 and 1995 concrete codes [SANZ 1982 and 1995] may be conservative. A more accurate requirement, proposed by the author, is recommended for the seismic evaluation of such columns, except where the requirements of shear reinforcement result in a smaller spacing.

H *Seismic Evaluation Assumptions*

A preliminary seismic assessment of the subject bridge based on current design codes and practice concluded that "the pier-columns are unlikely to tolerate cyclic displacements much exceeding yield ...". The laboratory testing and detailed analyses of the present study have shown this conclusion to be incorrect. This shows that assumptions used for the evaluation of existing structures often need to be more accurate than those used for the design of for new structures.

I *Confinement Retrofit Unwarranted*

The subject bridge is shown by the tests and the detailed evaluation *not* to be vulnerable to earthquake damage related to insufficient transverse reinforcing or shear capacity. Thus there would be no benefit in implementing a confinement-retrofit of the bridge columns such as adding a new column ties or an external column jacket. It had originally been proposed to test a confinement-retrofit of the column/foundation-beam specimen, but because of the above findings the idea was discarded.

J *Research Needed for Structure with Plain Reinforcing Bars*

Concrete structures with plain-round longitudinal bars may require less transverse reinforcement than similar structures with deformed longitudinal bars. Research is needed on (a) bar buckling and (b) mechanisms of shear resistance for such structures. More in-depth studies of bond-slip behavior are recommended.

K *Assumed Earthquake Input*

Inelastic time-history analyses of the subject bridge show that bridge response depends greatly on the earthquake input. Some earthquake records have a much higher damage potential than the earthquake response spectra assumed in design codes.

Part III

MANAGEMENT AND PRIORITIZATION OF BRIDGE SEISMIC UPGRADING

CHAPTER 11
REVIEW OF PRIORITIZATION PROCEDURES FOR BRIDGE SEISMIC UPGRADING

Because of the large number of bridges which need seismic upgrading and the limited resources available to evaluate, design, and carry out bridge retrofits, prioritization of retrofit work is vital. In this chapter bridge retrofit programs are discussed, and procedures for bridge-upgrade prioritization are critically examined.

Prioritization procedures are evaluated in terms of the amount and type of data they consider, and the algorithms used for assessing the data. Proposals for improved methods of bridge upgrade prioritization —for example by using earthquake loss-estimations techniques—are presented. Finally a critique of the prioritization procedures is presented, which identifies some typical shortcomings of the procedures.

11.1 Bridge Retrofit Programs and Established Prioritization Procedures

The bridge upgrade programs in California, New Zealand, and Japan indicate that the task of seismically retrofitting bridges can be an enormous one. In 1986, a survey of Japan's bridges found that 30 percent required some form of retrofitting. A number of US states are beginning retrofitting programs for their bridges, and have developed prioritization procedures.

Retrofit Programs in California and New Zealand

California has approximately 24,500 bridges: 12,500 in the state highway system and 12,000 city and county-owned bridges. After preliminary screening, 7,000 of the 12,500 state highway bridges were identified as being potentially vulnerable to collapse due to earthquakes. On further study, many of these 7,000 bridges are being found to have adequate seismic resistance, so that as of May 1994 about 3,000 state bridges were identified as vulnerable to collapse [Zelinski pers. comm. 1993, 1994].

Approximately 1,000 of California's state bridges have been identified as the highest priority bridges, because of their seismic deficiencies and importance in the transportation network. The design of seismic retrofits for these 1,000 bridges in California was scheduled for completion by the end of 1994. Construction of the projects is expected to be completed by the end of 1995. The program is expected to cost US $2.0 billion. In addition to the state highway bridges, 3,000 of the 12,000 city and county bridges are thought to be potentially vulnerable to seismic collapse, with 200 bridges being in the high-priority category. The retrofit of the city and county bridges is expected to cost US $0.5 billion. Along with the above, a US $1 billion retrofit program is planned for the five large toll bridges crossing the San Francisco Bay. Costs for retrofitting the other five state-owned toll bridges in California are undetermined. The state transportation department, Caltrans, has been made responsible for the seismic assessment and retrofit of all public bridges in California—i.e., the city and county-owned bridges as well as the state highway bridges [Zelinski pers. comm. 1994].

The New Zealand road network comprises approximately 15,500 bridges: 3,300 state highway bridges and 12,200 local authority bridges. The average bridge length is 39 m (130 ft) for state highway bridges and 17 m (56 ft) for local authority bridges. The national body Transit New Zealand is responsible for the state highway bridges, while approximately 50 local authorities are responsible for the remainder of the bridges [TNZ 1992]. Chapman [1991] estimates that nearly 80 percent of the state highway bridges were built before 1970; that is, before modern seismic-resistant design measures were in use. An overall seismic assessment of New Zealand's bridges has yet to be implemented, although studies of possible prioritization procedures are currently underway [Chapman pers. comm. 1993, Chapman and Kirkcaldie 1994].

Established Prioritization Procedures

Several prioritization procedures are discussed here, including the three most established procedures: the *ATC 6-2* screening process [ATC 1983], the Caltrans procedure [Gates and Maroney 1990], and the Japanese Ministry of Construction procedure [Kawashima 1990]. These three procedures are also described by Priestley et al [1992a]. A number of more recently developed procedures are also discussed. The procedures reviewed are listed in Table 11.1. Detailed descriptions of the procedures are not given here. Rather, comparisons and commentary on key aspects of the procedures are given, and suggestions for improved prioritization schemes are presented.

11.2 Data Collection

The task of prioritization can be divided into two steps: (a) collecting data on all of the bridges to be considered, and (b) mathematically (or subjectively) weighing and assessing the data to arrive at a relative priority for each bridge. In the first step of a prioritization procedure it must be decided what information is to be collected and used for each bridge. A comparison of the data used for the three established prioritization schemes, Table 11.2, is revealing.

The *ATC 6-2* Procedure

The ATC procedure [1983] requires the most data, but is less codified in terms of how the information is considered. More judgement and experience is required of the people collecting the data. In fact ATC recommends that "to enhance consistency it is desirable to have the rating of all bridges in one geographical area performed by the same personnel." To collect all of the data recommended by *ATC 6-2*, the transportation network and facilities related to each bridge must be studied. Site-specific soil information must be obtained, drawings must be reviewed, and the reviewer must have a good knowledge of seismic principles in structural engineering. The ATC procedure also requires that a simple calculation be made to estimate column capacities.

Table 11.1 Prioritization Procedures Reviewed

Prioritization Procedure [Reference]	Approx. Number of Data Items			Algorithm Type	Remarks
	Seismicity	Importance	Vulnerability		
ATC 6-2 [1983]	1	8	20	additive, alternative combinations	subjective data used
Caltrans 1990 [Gates and Maroney 1990]	1	4	7	additive	no subjective data
Japan [Kawashima 1990]	0	0	0	mostly multiplicative	based on earthquake damage data
Caltrans 1993 [Gilbert 1993]	3	8	6	additive, seismicity multiplies	
Nevada [Sundstrom and Maroney 1992]	1	4	6	additive	
Missouri [Sundstrom and Maroney 1992]	1	7	2	multiplicative and additive	assumes bridge importance based only on potential casualties
Washington State [Babaei and Hawkins 1991]	*	7	*	multiplicative and additive	*refers to ATC 6-2 for vulnerability and seismicity ratings
New York State [Buckle 1991]	1	8	18	additive	uses ATC 6-2 for structural vulnerability rating
New York St., GIS method [Shinozuka et al 1992]	?	?	14	additive	used regression analysis and damage data
Shelby County, Tennessee [Pezeshk et al 1993]	0	2	13	additive	seismicity considered uniform
Illinois [Cooling et al 1992]	1	5	*	loss-estimation approach, additive for importance	*refers to ATC 6-2 for structural vulnerability
Kentucky [Yu Ouyang et al 1990, Buckle 1992]	1	1	8	additive	importance weighted at only 10%
Oregon [CH2M Hill 1993]	1	8	8	multiplicative and additive	Importance assessed similar to Washington procedure
Canada [Filiatrault et al 1994]	1	5	8	additive, soil and seismicity multiply	tested procedure for dispersion of results and operator sensitivity
Basöz and Kiremidjian [1995]	Numerous			weighted additive	considers fragility curves and network analysis
FHWA [Buckle and Friedland 1995]	1	*	22	multiplicative, additive, and flowchart	subjective data, *importance assessed qualitatively
New Zealand [Chapman and Kirkcaldie 1994]	1	7	17	additive, soil and seismicity multiply	preliminary proposal
Tasman District, NZ [Maffei 1994, 1995]	1	3-7	10	flowchart, loss-estimation and cost-benefit approach	provides for secondary screening

The 1990 Caltrans Procedure

Bridges may also be prioritized based on a more cursory collection of information. The Caltrans first-level prioritization scheme [Gates and Maroney 1990] is based on only those factors shown in the second column of Table 11.2. Caltrans collects a smaller and less subjective set of information for each bridge than that recommended by *ATC 6-2*. The advantage of this approach is that the data collection can be carried out by less experienced engineers or non-engineers without sacrificing consistency. No structural calculations are required. Caltrans used a survey form to solicit the information from local agencies, collecting roughly 12,000 forms from 58 counties and 300 cities.

Subsequent to preliminary screening, Caltrans has collected further information on some of its bridge stock using a "Detailed Seismic Review". The information collected for such a review, as shown in Figure 11.1, is more consistent with the *ATC 6-2* recommendations. However, the detailed review data have yet to be used in an overall prioritization formula.

The Japanese Procedure

Like *ATC 6-2*, the Japanese procedure [Kawashima 1990] considers more information than the Caltrans procedure but unlike *ATC 6-2* has a more codified, less subjective method of determining the numeric values relating to risk factors. The Japanese procedure is likely to be more accurate (and more costly to perform) than the Caltrans procedure. In the Japanese procedure, an assessment is made of soil and structural vulnerability only. Bridge importance is considered in a separate process. A seismicity variable was initially included but was dropped from the final version of the procedure because all areas of Japan have relatively high seismicity [Kawashima 1994]. The Japanese procedure requires a few calculations (and/or engineering judgement) to complete the data on the expected level of damage to piers and fixed supports.

11.3 Weighing and Assessing Data

The second step in a prioritization procedure is putting the bridge data into a formula to assess risk. For the three procedures discussed, numeric values are assigned in various ways to the risk factors collected. The numeric values are then combined in a formula to give a final rating to the bridge. For simple risk-assessment formulas, the factors can be combined in one of three ways: (1) alternative combination, where the worst of two or more factors is entered into combination with the remaining factors, (2) additive combination, where the factors are weighted and added, or (3) multiplicative combination. The combination selected should represent the correct interrelationship between the factors.

The *ATC 6-2* Procedure

The *ATC 6-2* [1983] procedure uses both alternative and additive combinations. The structural vulnerability factor is taken as the largest of separate vulnerability factors for movement joints, columns and footings, abutments, and soil liquefaction. The alternative combination is logical here because, for example, if movement joints are highly vulnerable then span unseating will likely preclude any other type of seismic failure. Thus if the movement joints are rated a 10 on the vulnerability scale of 0-10, that value governs the structural rating and it does not matter if the columns are rated a 2 or an 8 (until the movement joints are retrofitted, then the next highest vulnerability must be considered.)

Table 11.2 Data used for bridge prioritization.

Type of Data	ATC 6-2 [1993]	Caltrans [Gates and Maroney 1990]	Japan Ministry of Construction [Kawashima 1990]
Seismicity	Peak Ground Acceleration	Peak Ground Acceleration	None (All regions have high seismicity)
Importance	FACTORS TO CONSIDER: Traffic/potential casualties. Adjacent facilities which could be damaged. Population and damage vulnerability of neighbourhood. Routing of emergency traffic. Does bridge carry utilities? Evacuation route? Access to critical facilities. Length of alternate route.	FORMULA BASED ON: Route type, Route type crossed, Traffic, Detour length	None (Importance considered in a separate process)
Soil	FACTORS TO CONSIDER: Liquefaction susceptibility based on soil type, density, saturation, profile, and site seismicity. Flexibility and ductility of columns for liquefaction induced displacements. Other structural vulnerability to displacements, such as movement joint details.	Is bridge in a high-risk soil zone?	Soil vulnerability to amplification. Soil vulnerability to liquefaction.
Structure	FACTORS TO CONSIDER: (a) <u>Movement Joints</u> Presence of joints. Abutment type. Bridge skew. Length to width ratio. Type of bearings. Seat continuous transversely? Seat support length compared to span length and height. Presence of shear keys. (b) <u>Columns, Wall Piers and Footings</u> Column transverse reinforcing. Column capacity. Structural continuity. Reinforcing steel grade. Presence of lap splices in hinge regions. (c) <u>Abutments</u> Soil fill height. Is bridge a water crossing? Bridge skew. Depth of abutment foundation.	FORMULA BASED ON: Year of construction, Number of movement joints, Height of bridge, Bridge skew, Presence of single-column bents, Monolithic or seated abutments.	FORMULA BASED ON: Design specification used, Superstructure type, Superstructure material, Bridge skew or curve, Gradient of bridge, Presence of movement-joint restrainers, Presence of single-column bents, Height of bridge, Presence of irregular ground, Scour at river bed, Shear span ratio of piers, Cracking strength of piers, Flexural capacity of piers, Column shear strength, Abutment type, Foundation type, Foundation capacity.

D E T A I L E D   S E I S M I C   R E V I E W   D A T A   S H E E T

B R I D G E # ____________

DEPARTMENT OF TRANSPORTATION
Division of Structures
Special Projects Branch
Seismic Retrofit Program

year designed? ______

SUPERSTRUCTURE DETAILS:

outriggers? ☐YES ☐NO
C-bents? ☐YES ☐NO
any rocker bearings? ☐YES ☐NO
shared columns? ☐YES ☐NO
super/sub conn. type? ☐monolithic joints ☐simple span supports
material type? ☐P.S. concrete ☐C.R. concrete ☐steel ☐timber
section type? ☐I-girder ☐box-girder ☐slab ☐arch ☐T-girder ☐truss ☐suspension
number of spans? ____
maximum span length? ____ minimum span length? ____ average span length? ____
maximum span width? ____ minimum span width? ____ average span width? ____
maximum skew? ____ minimum skew? ____ average skew? ____
overall length measured in feet? ____
curvature:
smallest radius in feet? ____ arc angle in degrees? ____

HINGE DETAILS:

number of hinges? ____ hinge seat width in inches? ____
restrainers? ☐YES ☐NO
seat extenders? ☐YES ☐NO

ABUTMENT DETAILS:

abut. type? ☐seat-type ☐end-diaphragm ☐other (tied down) ☐other (not tied down)
abut. seat width in inches? ____
shear keys? ☐YES ☐NO ☐YES, but very small
retrofit? ☐YES ☐NO

COLUMN DETAILS:

Is column confined in regions of possible yielding (can it behave in a ductile manner)?
☐YES ☐?YES ☐?NO ☐NO
material type? ☐P.S. concrete ☐C.R. concrete ☐steel ☐timber
number of columns per bent? minimum per bent ____ maximum per bent ____
number of single-column bents? ____ number of multi-column bents? ____
maximum columns height? ____ minimum column height? ____ average column height? ____
transverse reinforcement: ☐ spirals #____bars @ ____inches
☐ ties #____bars @ ____inches
trans. reinf. well into footing & superstructure? ☐ YES ☐NO
longitudinal reinforcement:
(to what degree are the columns reinforced?) ---> percent of longitudinal steel in column ____
lap slices in regions of possible yielding? ☐YES ☐NO

FOOTING DETAILS:

top mat of steel? ☐YES ☐NO
pedestal? ☐YES ☐NO
shear reinforcement? ☐YES ☐NO ☐construction only
column/footing connection? ☐ pinned ☐ fixed
piles or spread footings? ☐pile ☐spread ☐shaft
if piles, can they carry tension? ☐YES ☐NO ☐too difficult to judge

SOIL DATA:

log of test borings? ☐YES ☐NO date? ____________
soil type? ☐sand ☐clay ☐silt ☐too difficult to judge
blow count greater than 20 at a depth of 15 feet below the surface? ☐YES ☐NO
depth to rock-like material in feet? ____ ☐too difficult to judge
depth to waterline in feet? ____ date? ________ ☐too difficult to judge
if geology contacted, ARS curve? ____
liquifaction potential? ☐high ☐low ☐none

STATUS: ____________ REASON(#): ____________
REVIEWED NAME: ____________ DATE: ____________
CHECKED NAME: ____________ DATE: ____________
DATA COLLECTOR & DATE NAME: ____________ DATE: ____________

Reviewers and checkers: List suggested retrofit strategies on the back of this sheet.

(Rev 6-22-90)

Figure 11.1 **Caltrans "Detailed Seismic Review Data Sheet"** [Gates and Maroney 1990].

Some interaction of factors, however, is neglected by *ATC 6-2*. Consider the following: if liquefaction occurs, structures with poor column ductility capacities or vulnerable movement joints have a greater risk of failure than monolithic, ductile structures, but if the liquefaction vulnerability of the site is rated a 10, then all types of structures on the site would be given the same vulnerability rating. Conversely, structures with poor column ductility capacity or deficient movement joints are even more vulnerable on a liquefaction-prone site than they would be on a rock site. Thus a more accurate risk formula would consider the interaction of liquefaction risk with structural risk, perhaps by using an additive or multiplicative combination.

The final risk rating used by *ATC 6-2* is calculated on the weighted additive combination of three basic factors: seismicity, importance, and (soil and structure) vulnerability, as shown in Figure 11.2. In this case the additive combination of factors does not seem to be appropriate, especially when one of the factors indicates low risk. Consider an important bridge in a region of high seismicity, on a rock site, detailed to the most recent design requirements with no seismic deficiencies. This bridge would be rated 10 for seismicity, 10 for importance, and 0 for vulnerability. The bridge would have final rating of 6.67 out of 10, despite having been designed to the current state of the art. Meanwhile a bridge of medium to high vulnerability, importance, and seismicity—which would benefit from seismic retrofitting—could end up with a lower final rating, perhaps 6 out of 10. Thus it would be more logical to use a *multiplicative* combination of the three basic factors.

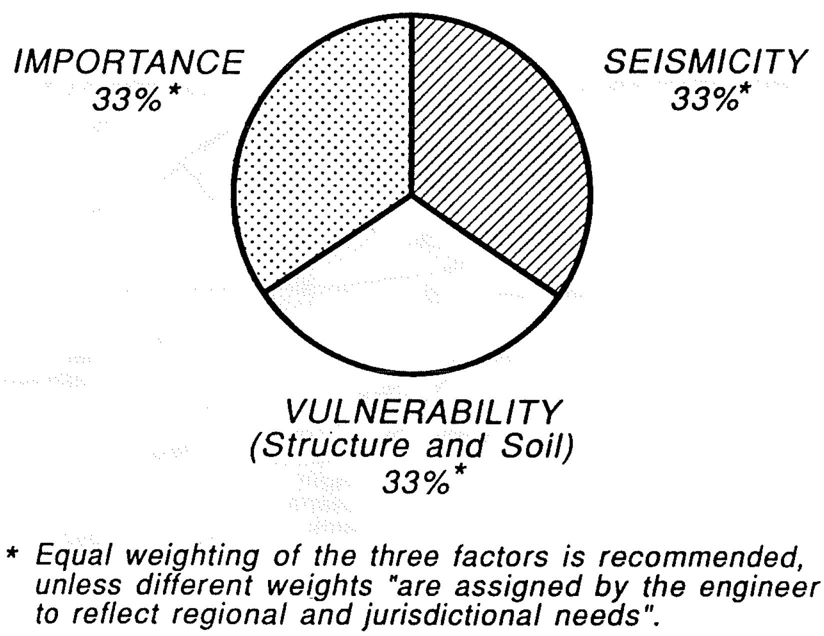

Figure 11.2 *ATC 6-2* **bridge prioritization approach.**

The Caltrans Procedure

The weighted additive formula used by Caltrans is represented by Figure 11.3. The formula gives a priority rating which can be expressed a 0-100 scale, 100 indicating the highest priority to retrofit. Gates and Maroney [1990] note that "Expert judgements by professionals in the field of bridge engineering were used to derive and calibrate a risk algorithm. The survey was used to determine which characteristics would have high correlations to bridge damage or cost to public transportation and what their relative correlations would be. This panel of experts represented hundreds of years of bridge experience". The expert advice was no doubt valuable in assessing the influence of various factors such as year of construction and in assessing the relative importance of the risk factors. The bridge engineering expertise is partly wasted, though, because corresponding expertise in risk analysis appears not to have been used. The strictly additive combination used in the Caltrans algorithm hampers the accuracy and value of the prioritization effort. For example a structurally deficient bridge in an area with *no* seismicity can still be given a rating as high as 88 out of 100, while an important bridge in the highest seismic zone, which is vulnerable to collapse can receive a lower rating, 83 out of 100. This would be the case for a bridge which had severe seismic deficiencies, but which did not include the potential dificiencies of plan skew and single-column belts. According to Priestley et al [1992a] the fact that seismicity only contributes a maximum of 12 percent to the seismic hazard rating "has resulted in some criticism of the Caltrans approach".

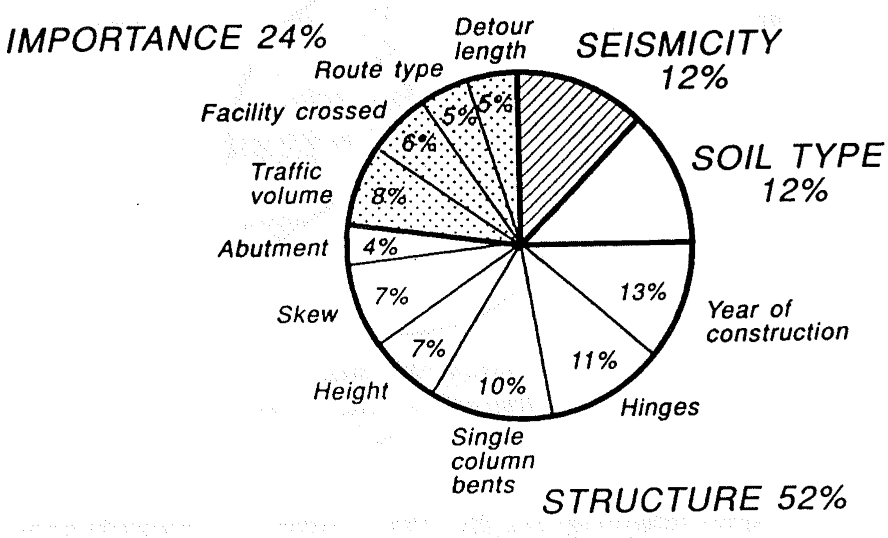

Figure 11.3 Caltrans bridge prioritization rating [Gates and Maroney 1990].

Recently Caltrans has revised its prioritization formula [Gilbert 1993]. The most significant changes are that (a) the overall seismicity variable is now a multiplicative factor, and (b) bridge importance now has more weight than structural vulnerability. The new Caltrans formula weights importance at 0.6 and structure vulnerability at 0.4, adds them together and multiplies by the seismicity. Previously, structural vulnerability was weighted more than twice as much as importance (52% to 24% as shown in Figure 11.3). In the new formula it is weighted at only 66% of the importance weight (0.4 to 0.6). Most of the same risk variables from the previous prioritization data are used in the new formula. However, bridge height has been eliminated as a variable, and the presence of "leased air space" under a bridge is now considered in the importance factor (apparently because of concern over potential lawsuits). Further documentation of leased air spaces for California bridges is now needed to complete the prioritization database.

The Japanese Procedure

The Japanese prioritization formula [Kawashima 1990] seems to be a significant improvement over the additive ATC and Caltrans equations. The procedure was formulated on the statistical analyses of 105 bridges damaged in past earthquakes. Most of the combinations of factors are multiplicative. The procedure was used in 1986 to inspect about 40,000 bridges, 11,700 of which were found to require seismic strengthening. An example of the Caltrans and Japanese procedures, using the 1936-designed New Zealand bridge discussed in Part III of this report, is provided by Dekker and Park [1992].

Procedures Developed for Nevada, Missouri, Washington, and Canada

Sundstrom and Maroney [1992] provide a useful review of prioritization procedures developed for Nevada, Missouri and Washington. The procedures are all simple additive and/or multiplicative algorithms.

Nevada and Missouri

The Nevada procedure is a direct simplification of the *ATC 6-2* method using three additive variables. The seismicity variable is taken as proportional to the seismic acceleration coefficient. The importance variable depends mainly on an additive combination of route type and traffic volume. The structural vulnerability factor depends on the number of vulnerable detail types.

The Missouri procedure is a multiplicative combination of earthquake (rock) acceleration times soil amplification times structure vulnerability times an importance factor. The only structural data required is the classification of the bridge into one of three structure types: simple span, continuous with movement joints, or continuous and monolithic. Thus the structural vulnerability factor can be taken as one of only three possible values. Unlike other prioritization methods which mostly consider the importance of a bridge in terms of transportation disruption, the Missouri procedure considers only the potential casualties. The casualties are assumed to be directly related to the number of vehicles likely to be on the bridge, or within stopping distance of it, at the instant an earthquake strikes. This basis for the importance factor causes the prioritization results to be very sensitive to bridge length [Sundstrom and Maroney 1992].

Washington State

Washington [Babaei and Hawkins 1991a, 1991b uses a mostly multiplicative procedure. "Vulnerability" (including seismicity) is taken as the product of variables for design acceleration coefficient times soil amplification times structural vulnerability times remaining service life. The structural vulnerability factor is the sum of a vulnerability rating for substructure details plus a vulnerability rating for movement joints. (Note that, as previously mentioned, an *alternative* combination would be more appropriate here because if movement joints are likely to fail, the bridge vulnerability is not affected by substructure details.)

The factor for remaining service life is unique to the Washington procedure. It reflects the decreased likelihood of strong earthquakes occurring over a shorter service life. Note that remaining service life could also be considered in another way: if a bridge will need replacement or substantial repair soon, it may not make sense to seismically retrofit the structure until that time. Thus the seismic retrofit prioritization of the bridges in a jurisdiction should (ideally) be considered in conjunction with other bridge upgrade, repair, and maintenance priorities.

The Washington state procedure multiplies the vulnerability factor times a criticality (ie, importance) factor. The criticality factor is an additive combination of variables used for (a) the traffic importance of the bridge (equal to route type times traffic volume times detour length variables), plus (b) essential utility lines carried by the bridge, plus (c) the traffic importance of the route which is crossed, plus (d) a function of traffic volume times length, which apparently accounts for potential casualties. This formula for the criticality factor seems to be a well-considered mixing of the combination types which are appropriate and logical for each of the variables involved.

Canada

Filiatrault et al [1994] have proposed a seismic screening procedure for existing bridges in Canada. The procedure is an adaptation of the revised Caltrans procedure. Filiatrault et al tested their procedure on 17 bridges in the Montreal area, and concluded that the procedure showed a "good dispersion in the score obtained", but they did not compare the scores to actual seismic vulnerability, such as would be determined in a detailed analysis.

Filiatrault et al had three different operators use the procedure on their sample group of bridges, to show that the procedure was not sensitive to who carried out the evaluation. This consistency of results by different operators is a necessary attribute of a prioritization procedure. Such consistency derives from (a) minimizing subjective data, and (b) providing clear instructions for the procedure.

Comparisons of Procedures

Buckle [1991, 1992] has reviewed the *ATC 6-2* and 1990 Caltrans methods, and the methods proposed for Washington, Kentucky, and Illinois, and has proposed his own additive procedure.

Sundstrom and Maroney [1992] have compared the Nevada, Missouri, and Washington procedures with the Caltrans procedures using a sample of 100 California bridges. Their comparison shows disparities between the results of the different prioritization procedures, but further conclusions are not made. Further studies of this type would be very useful in validating or improving prioritization procedures. Comparisons with experts' opinions of the bridge rankings, with the results of detailed seismic evaluations, and with actual bridge damage data, would also be useful.

11.4 Concepts for Improved Prioritization Methods

The prioritization formulas discussed may each have different strengths and weaknesses. In general, however, the procedures seem rather arbitrary and poorly verified. None of the prioritization procedures reviewed above use cost-benefit analyses or take advantage of available seismic-risk analysis techniques.

Besides providing better information on relative risk, a more sophisticated probability-based risk analysis has the benefit that overall risk and expected earthquake losses can be determined. Thus for a given magnitude earthquake on a given fault, an estimate of probable economic losses, transportation disruption, and casualties can be made. Combined with the probabilities of various levels of earthquakes occurring, overall risks for a jurisdiction can be determined, and the cost effectiveness of different bridge retrofit programs can be evaluated. Gates and Maroney [1990] state that "such analyses generally require vast collections of data to define statistical distributions for all, or at least the most important, elements of some form of analysis, design, and/or decision equations. The acquisition of this information can be extremely costly if obtainable at all". Priestley et al [1992a] echo similar doubts about the feasibility of probability-based risk analyses. These statements are not well founded. With proper application, probability-based risk analysis techniques can be used even with the most limited of data sets. In fact, if the depth of bridge data is limited, it is *more* important that they be analysed properly than if the data were extensive.

Seismic Risk-assessment Method Proposed by Lizundia

An example of a probability-based seismic risk analysis of a large group of structures is provided by Rutherford and Chekene Consulting Engineers [1990] in a study of San Francisco's unreinforced masonry (URM) buildings. In this study limited data such as number of stories, plan area, building use, and structural irregularities were collected from each of the 2007 URM buildings in the study area. A probability-based procedure was used to determine, among other things: (a) the likely casualties and property damage losses resulting from specified scenario earthquakes (eg, magnitude 7.0 on the Hayward fault or magnitude 8.3 on the San Andreas fault), (b) the overall costs, damage savings, and casualty savings associated with three different proposed city-wide retrofit ordinances, considering probabilistic seismicity, and (c) the relative seismic vulnerabilities of 15 different types of URM buildings.

A similar approach can be used to prioritize bridge retrofit work. The basic steps of a probability-based seismic risk analysis of bridges could be as follows [Lizundia pers. comm. 1993]:

1 Separate the bridge structures into five to ten basic categories such as:

- Bridges less than three spans, monolithic or with restrainers.
- Bridges less than three spans with unrestrained movement joints.
- Bridges ≥ three spans with restrainers.
- Bridges ≥ three spans with unrestrained movement joints.
- Bridges ≥ three spans with single column bents.
- Bridges designed after 1980.

2 Based on damage data from past earthquakes and expert opinion, develop damage versus modified mercalli earthquake intensity (MMI) curves, as shown in Figures 11.4 and 11.6, taken from *ATC 13* [1985]. (Instead of using MMI, peak ground acceleration, PGA, or some other measure of earthquake shaking could be used.)

3 For each bridge site determine the probable seismicity, which can be expressed as a curve of annual probability of exceedance versus earthquake intensity (or versus peak ground acceleration) as shown in Figure 11.5. The seismicity is adjusted based on the site soil conditions.

4 Based on the combination of damage curves and probable seismic intensity curves, determine the "baseline" expected damage to each class of bridge.

5 For each bridge, adjust the baseline damage for the individual risk factors of that bridge, such as skew, curvature, pier height, etc.

6 Over the time period of interest, say the next 30 years, compute the earthquake loss results, for example: final dollar loss resulting from bridge damage, probability of loss of bridge use, and estimated casualties.

7 Consider bridge importance by estimating equivalent dollar losses resulting from bridges being closed. Note that plots of "restoration time" versus damage state have been developed by *ATC-13* [1985], as shown in Figure 11.7. Such plots can be the first step in quantifying the cost of losing the use of a bridge.

8 For each bridge, add the cost of bridge damage to the cost of loss of use. The bridges with the highest sum of these two factors are the highest priority bridges to retrofit.

A few points on the procedure are important to note:

(a) In step (1) the given categories are for example only; the proper selection of categories involves consideration of how distinct the damage curves for each category will be.

(b) In step (2) it should be noted that significant work on developing damage curves has already been done. *ATC-13, Earthquake Damage Evaluation Data for California* [1985] presents such curves, in graphical and matrix form, for 78 different classes of structures including three categories of bridges. These damage curves are shown in Figure 11.5 and tabulated in Figure 11.8. *ATC-13* also describes the methodology for deriving damage curves.

(c) As shown in step (3), with the current sophistication of obtaining seismological data, seismicity need not be considered as just one factor. Site specific curves of probability versus intensity can be derived from identification of causative earthquake faults, probable earthquake magnitudes, distances to faults and attenuation relationships. In many areas of the world, seismological studies have been done which make this information available in the form of seismic hazard maps.

In California such information can be obtained, and conveniently used in computer analyses, from computer seismicity models. One such program [Rutherford and Chekene Consulting Engineers 1990] uses a geometric model of all fault sources, their maximum earthquake, and probabilities of lesser earthquakes, to predict earthquake shaking intensity (by either MMI or PGA) at any given location in California. The intensity can be predicted for any given scenario earthquake, or a probable seismicity curve can be generated considering all possible faults and earthquakes.

(d) Although the procedure is probabilistic, expert opinion is relied upon to provide data for the basic assumptions in steps 1, 2, 5, and 7 of the analysis (defining bridge categories, developing damage curves, adjusting damage for individual risk factors, and estimating the costs of bridge damage). The procedure is designed so that the assumptions are easily checked and calibrated; thus the engineering expertise is used to maximum benefit.

(e) With little added effort, the risk analysis program can provide additional useful information to bridge jurisdictions. For example, the annual probability of closure for any given bridge or the probable damage along a given route or in a given area could be determined.

(f) The use of additional data could further increase the accuracy of the risk model. Expected remaining service life for a bridge could be factored into the model, adjusting the importance factor. A rough estimate of retrofit cost, perhaps based on bridge size and type, could also be

used as data. This would allow prioritization on a cost-benefit basis: cheaper-to-fix bridges would get pushed up on the priority scale.

(g) Finally, if damage curves for post-retrofit structures are developed, the effectiveness of various retrofit programs could be assessed by comparing pre-retrofit and post-retrofit damage predictions.

In their theoretical study of bridge-upgrade prioritization, Basoz and Kiremidjian [1995] also advocate the use of bridge damage curves (or fragility curves) combined with probable seismicity curves to estimate bridge vulnerability. Their assumption in defining damage curves, that bridge structural vulnerability depends mainly on construction materials and overall structure type, rather than detailing and the presence of specific seismic deficiencies, is, however questionable.

Seismic Risk Survey for Illinois

Cooling et al [1992] have carried out a bridge seismic risk study for the Illinois Department of Transportation. They have used an approach based partly on risk-analysis methods which has similarities to several of the recommendations given in the previous section. Cooling et al summarize the risk-based approach with the following formula:

$$Risk = (Probability\ of\ failure)\ X\ (Consequences\ of\ failure)$$

A bridge vulnerability factor is used as a measure of probability of failure, and an importance factor is used as a measure of consequences of failure.

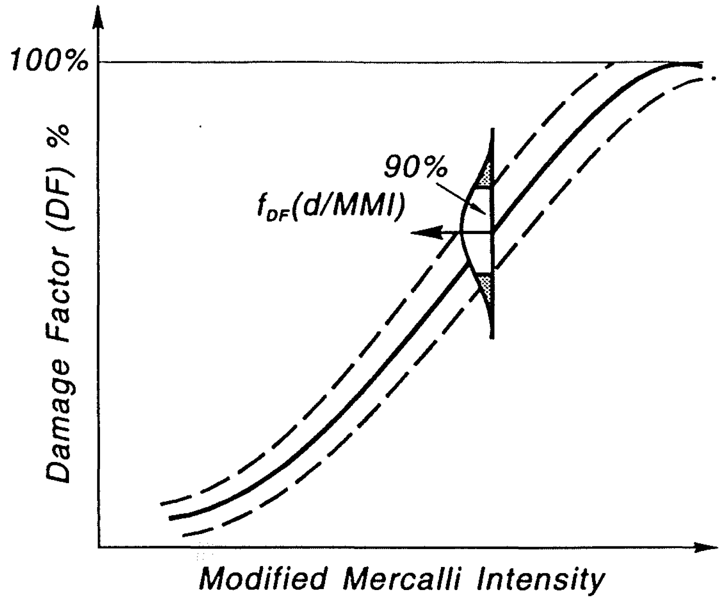

Figure 11.4 **Example damage factor versus earthquake intensity curve** [ATC 1985].

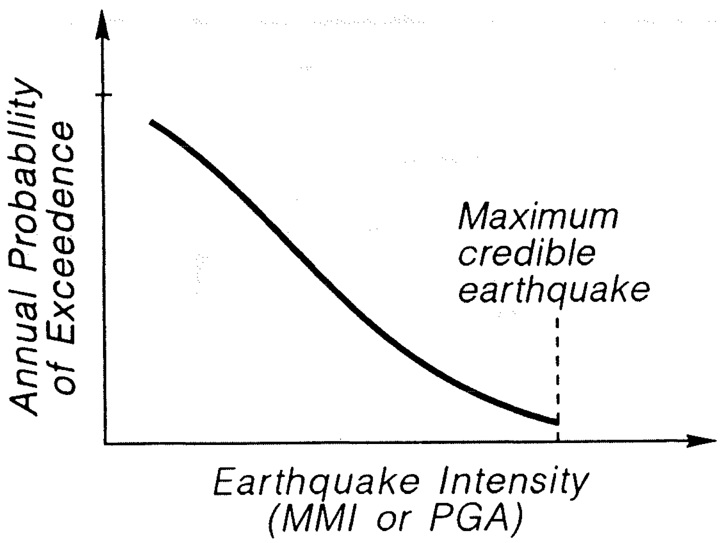

Figure 11.5 **Example probabilistic seismicity curve.**

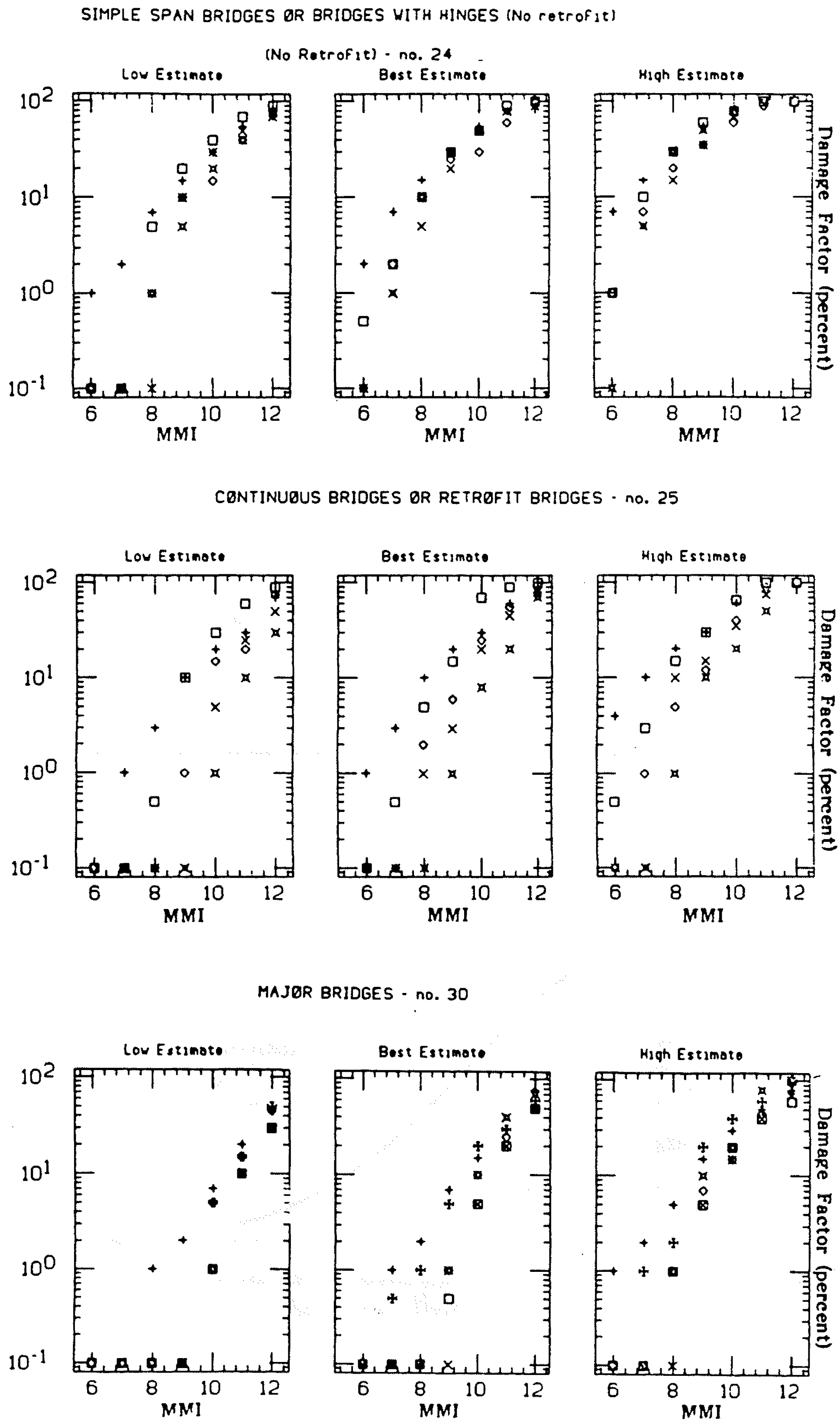

Figure 11.6 Damage versus intensity curves for bridges based on expert opinion, [ATC 1985].

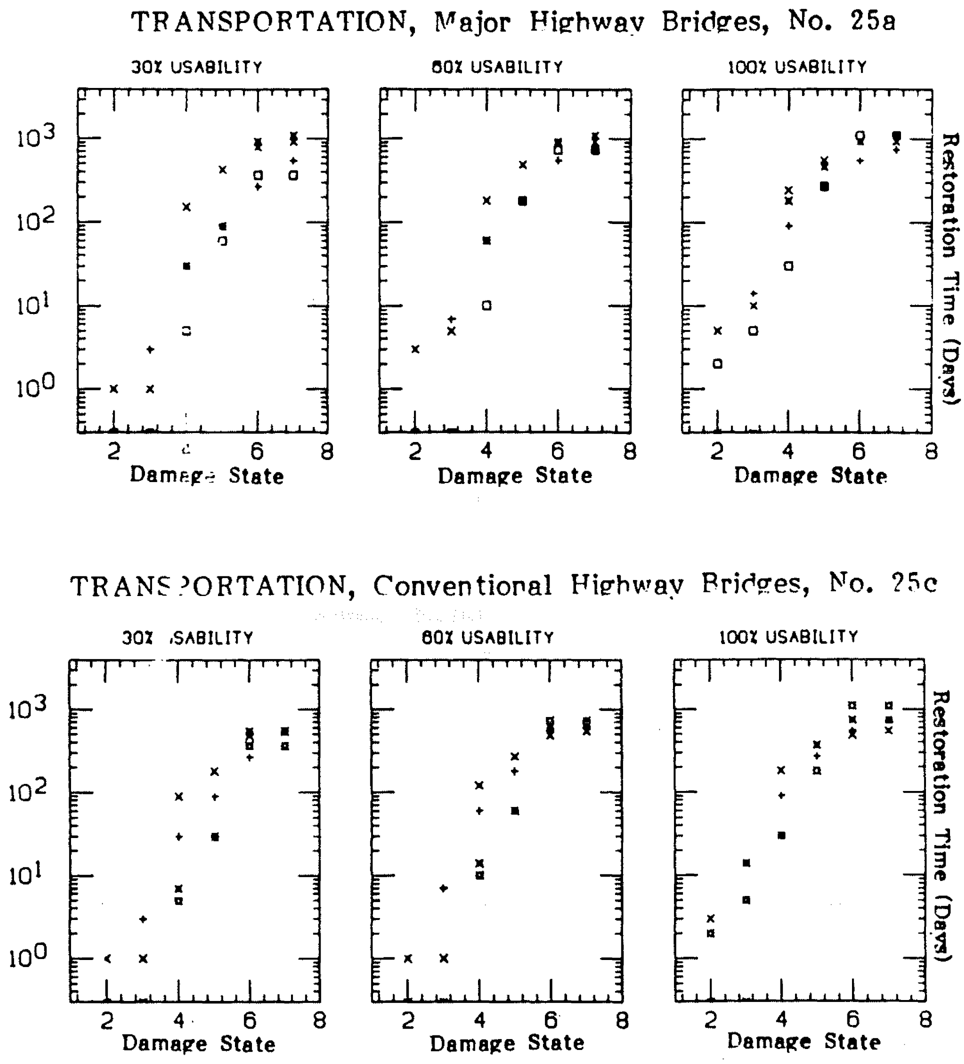

Figure 11.7 Loss of function versus damage curves based on expert opinion [ATC, 1985].

Central Damage Factor	Modified Mercalli Intensity						
FACILITY CLASS=24							
	VI	VII	VIII	IX	X	XI	XII
0.00	3.0	***	***	***	***	***	***
0.50	97.0	12.3	***	***	***	***	***
5.00	***	85.7	70.9	***	***	***	***
20.00	***	***	29.1	71.1	***	***	***
45.00	***	***	***	28.9	82.4	***	***
80.00	***	***	***	***	16.9	100.0	***
100.00	***	***	***	***	***	***	100.0
FACILITY CLASS=25							
	VI	VII	VIII	IX	X	XI	XII
0.00	93.6	8.1	0.9	***	***	***	***
0.50	6.4	77.8	17.6	***	***	***	***
5.00	***	14.1	78.6	56.5	***	***	***
20.00	***	***	2.9	43.5	1.8	1.2	0.7
45.00	***	***	***	***	98.2	36.8	5.7
80.00	***	***	***	***	***	61.9	39.1
100.00	***	***	***	***	***	0.1	54.5
FACILITY CLASS=30							
	VI	VII	VIII	IX	X	XI	XII
0.00	100.0	58.0	33.2	15.8	***	***	***
0.50	***	42.0	66.5	39.9	0.7	***	***
5.00	***	***	0.3	43.7	55.2	5.0	***
20.00	***	***	***	0.6	43.4	53.0	3.6
45.00	***	***	***	***	0.7	40.8	39.9
80.00	***	***	***	***	***	1.2	56.0
100.00	***	***	***	***	***	***	0.5

***Very small probability

Figure 11.8 **Matrix representation of probabilistic damage versus earthquake intensity (MMI) relationships [ATC 1985].**

In assessing the vulnerability factor, the Illinois procedure uses a probability-based approach. In assessing the consequence of failure, the Illinois procedure is somewhat more arbitrary, using weighted-additive combination of bridge importance variables. The variables and their weighting factors are as shown below:

Traffic Volume	69%
Emergency Route	15%
Detour Length	10%
Defence Route	5%
Utilities Carried	1%
	100%

In establishing the bridge vulnerability factor, the Illinois procedure uses a form of damage-versus-earthquake intensity curve called a fragility curve. Peak ground acceleration is used on the horizontal axis as the measure of earthquake-shaking intensity; probability of failure is plotted on the vertical axis. Fragility curves are developed for different structural ratings and then combined with the probable seismicity curve for the bridge site to arrive at a *structural vulnerability factor.* This factor is meant to reflect the "probability of failure caused by shaking alone, independent of liquefaction failure". A second set of fragility curves is developed for different soil conditions to arrive at a *ground vulnerability factor*, which reflects the "probability of failure caused by liquefaction alone, independent of failure due to shaking". The structural and ground vulnerability factors are "combined according to the rules of probability" to give a bridge vulnerability factor. (The reference does not make clear what interdependence is assumed between structural and liquefaction failures.)

The bridge vulnerability factor is multiplied by the importance factor to give the bridge priority score.

The structural assessment procedures of the Illinois method are "based primarily on *ATC 6-2*". A structural rating is assigned, on a scale of 0 to 100, by taking the worst of either the substructure or superstructure rating and combining it with factors related to bridge geometry, stiffness, and mass. Different fragility curves are assumed, based on the structural rating.

Before carrying out any structural assessments, the Illinois bridges were preliminarily ranked based on (a) the importance factor, (b) expected seismic accelerations, (c) soil zone for amplification, and (d) soil zone for liquification. For this preliminary step, all 6,700 bridges were assumed to have the same structural rating. Statewide maps of expected bedrock acceleration and soil categories were digitized and put into the database used for bridge ranking. After this preliminary ranking, structural assessments were made, looking at the highest-ranked bridges first.

Seismic-Risk Study for the Tasman District

Although a probabilistic risk analysis can be complex, it is not necessarily a difficult undertaking. For preliminary screening, the procedure should be based on a minimum amount of data from each bridge. Useful information already exists on damage versus intensity curves, probabilistic seismicity, and the costs of losing a bridge. This information can be specifically adapted to the bridge stock being screened. For the remainder of the procedure the computer does the work. A risk-based model of bridge upgrade prioritization is well within current analysis capabilities.

In New Zealand's Tasman District, an overview seismic assessment and bridge-upgrade management study has been conducted by the present author [Maffei 1994]. Risk analysis techniques similar to those described in the above sections have been used in the study. The study introduces a new method of (a) ranking the seismic vulnerability of bridges related to damage curves, and (b) estimating the likely seismic damage, the cost of damage, and benefit/cost ratios for seismic upgrading. The method allows the prioritization of bridge-upgrading according to the estimated benefit/cost ratio of each project. The Tasman study also includes a quick method of estimating the seismic vulnerability of typical New Zealand bridges. The method is described in Chapter 12.

Future Developments

Additional levels of sophistication in bridge-upgrade prioritization are also worth considering. Evaluation of the transportation routes using network theory—with links and nodes of the transportation system modelled onto computer along with bridge locations—could more accurately account for the importance of a particular bridge. Such an analysis could consider for example that the priority to retrofit bridge "A" depends partly on the seismic vulnerability of bridges "B" and "C" which are in series with it, and of bridges "D", "E", "F", etc, which may be on the potential alternate routes should bridge "A" collapse. Thus the interrelationship of bridge importance is considered. Network theory has been used to evaluate efficiencies and problem scenarios in telecommunication networks. However, its application to transportation networks is relatively new [Du and Nicholson 1993]. Recently Basöz and Kiremidjian [1995] have studied highway lifeline network analysis for bridges damaged in earthquakes, considering both the disruption to emergency access routes occurring immediately following an earthquake and the longer-term transportation disruption effects.

The developing technology called geographical information systems (GIS) may prove useful for bridge retrofit prioritization analysis. GIS programs are computer databases which include spatial data and have cartographic capabilities. They have been used for studies of land use, development planning, environment and wildlife, and other applications where the data is partly geographical (or spatial). Road networks, bridges, and associated data can be entered into, and manipulated by, GIS programs. For many bridge jurisdictions, it may be preferable to integrate bridge seismic retrofit programs with other bridge-upgrade and maintenance programs. A GIS method may be one way to accomplish this overall bridge management. A preliminary effort to integrate bridge seismic risk assessment with GIS technology is proposed by Shinozuka et al [1992]. The topic is also discussed by Bosöz and Kiremidjian [1995].

The level of effort which is appropriate for the prioritization of bridge retrofitting needs to be considered. Some of the above suggestions might be unjustifiably complex for smaller jurisdictions. However, in many places the number of vulnerable bridges is substantial, and it is unlikely that all bridges will be retrofitted in time to escape the next damaging earthquake. California, for example, will spend multiple *billions* of dollars on bridge retrofitting in the coming decades. Even the most complex risk analysis would cost only a fraction of a percent of the total seismic retrofit cost.

11.5 Critique of Prioritization Procedures

After reviewing numerous prioritization procedures, then developing the Tasman District procedures (see Chapters 12 and 13), and then re-examining the established prioritization procedures, the author has found a number of questionable aspects in the established procedures. When tested by comparing the prioritization of different hypothetical bridges, the procedures can give illogical results.

Table 11.3 summarizes some of the major shortcomings of many of the prioritization procedures which have been reviewed here. As shown in the table, flaws are evident in several aspects of typical prioritization procedures. These aspects include (a) the assessment of structural vulnerability, (b) the assessment of bridge importance, (c) the overall prioritization algorithm, and (d) the verification and implementation of the procedures. These aspects of the prioritization procedures are considered below:

Assessment of Structural Vulnerability

Many of the procedures reviewed here assess the structural vulnerability of bridges by using additive combinations of variables which each relate to vulnerable structural aspects or seismic deficiencies. The basic problem with this approach is that in reality bridges can be extremely vulnerable to earthquake damage even if they have only one type of seismic deficiency.

For example a bridge with reinforced-concrete columns which (due to their proportions and detailing) are prone to brittle shear failure can be extremely vulnerable. But if the variable for column detailing is only one of several variables in an additive combination, such a bridge is not likely to be given a high priority rating. Hwang [1994] has noted that "the seismic vulnerability of a bridge is not caused by the summation of minor defects; instead, a single major defect may cause the bridge to fail. Thus, the additive form is not suitable for screening procedures". The *ATC 6-2* procedure, using an *alternative* combination of three structural vulnerability ratings, is less susceptible to this problem.

For bridges with reinforced-concrete columns, a close-spacing of column ties is essential to good earthquake performance. Prior to the early 1970s such ductile detailing was rarely provided in bridge columns. The extreme influence of this single variable is often neglected or under emphasised in prioritization procedures.

Conversely, the effect of the number of columns in a bridge pier may be over-emphasised by prioritization procedures. Some procedures consider bridges with single-column bents to be twice as vulnerable as those with multiple-column bents. Past earthquakes have shown however that the "redundancy" of a multi-column bent is of little help if the columns are not ductile. The failure of one column often coincides with the failure of other columns in the pier and results in the bridge's collapse. In some cases multi-column piers can be *more* vulnerable than single-column piers because shear demands are higher due to double-curvature, rather than cantilever, bending.

Prioritization procedures often consider the number of superstructure movement joints to be a significant variable affecting the vulnerability of a bridge to drop-type span collapses. In reality, the span seating length and the presence of linkage bolts or restrainers seem to be more important variables than the number of movement joints. A bridge with two movement joints (eg, at the abutments only) having poor seating and linkage is more vulnerable than a bridge with 50 movement joints having good seating and linkage.

The effect of skew on seismic vulnerability is usually modelled poorly in prioritization procedures. For bridges with movement joints, the presence of skewed supports can greatly magnify the likelihood of drop-type failures, even for relatively small skew angles. By contrast, skew has little or no detrimental effect on monolithic bridges. None of the prioritization procedures reviewed recognise this distinction; the same skew rating is applied regardless of whether or not movement joints are present. For bridges with movement joints, the typical skew variable seems to have too little of an effect on the bridge priority rating.

The more general weakness of prioritization procedures in assessing the structural vulnerability of a bridge seems to be that they are too arbitrary. Many of the specific shortcomings of procedures, as described above, could be eliminated if the assessment of structural vulnerability were derived from seismic damage estimates using risk analysis techniques. Such a method relates bridge seismic deficiencies, structural characteristics, and various combinations of deficiencies and characteristics to a damage versus earthquake-intensity curve, as discussed in Section 11.4, and as used in the Illinois procedure and the Tasman District method. (See section 12.6.)

Table 11.3 Typical Flaws Found in Prioritization Procedures

Component of the Procedure	Typical Flaws
Structural Vulnerability	Additive combinations of variables for seismic deficiencies, can overlook bridges with a single critical deficiency.
	Underemphasis on detailing or year of construction for reinforced concrete columns.
	Overemphasis of single-column vulnerability compared to multi-column.
	Emphasis on number of movement joints rather than span seating details or year of construction.
	Underemphasis of skew for bridges with movement joints; overemphasis of skew in other cases.
	Neglect seismic damage-estimation and risk analysis techniques.
Bridge Importance	Neglect expected bridge service-life variable.
	Neglect variable of whether temporary access can be provided in place of the bridge.
	Underemphasize traffic volume (ADT).
	Possibly unnecessary variables (eg, route-type, utilities) included.
	Additive combinations used where multiplicative are more logical (eg, transportation disruption should be proportional to ADT *times* detour length).
	Neglect loss-estimation and cost-benefit techniques.
Overall Algorithm	Single-formula algorithms used rather than flow-chart algorithms—do not allow "if-statements".
	Additive or partially additive combinations— are apparently arbitrary and can give illogical results.
	Over-use of step functions, rather than continuous ratings.
	Some data too subjective.
	Formulas are abstract, not transparent.
Verification	Poorly verified. Results not compared to actual bridge damage data or results from detailed seismic-evaluations or cost-benefit studies.
	Engineering expertise used abstractly—not used to verify results.
Implementation	Secondary screening procedures not provided.
	Procedures poorly integrated with computer-database capabilities.

Assessment of Bridge Importance

Most of the prioritization procedures reviewed (the Washington state procedure being an exception) do not consider expected bridge service life as a variable. And none of the procedures consider the important variable of whether temporary access can be provided in place of the bridge during its reconstruction after earthquake damage. This variable depends on the type of obstacle crossed by the bridge. Most New Zealand bridges are water crossings. Those which cross small streams would probably be temporarily replaced by a ford following earthquake damage. Bridges which cross large rivers cannot be temporarily replaced in this way and it is thus more important to protect them from earthquake damage. In developing the prioritization method described in Chapter 12, the service life and temporary-access variables were found to be significant factors in the importance of a bridge.

Some of the prioritization procedures reviewed may underemphasise the significance of traffic volume (average daily traffic, ADT) in the bridge importance assessment. Other, seemingly less significant variables are often given more prominence. It seems that a "route-type" variable should only be used if it is impossible to get an estimate of the ADT of the route. Route-type is a somewhat artificial variable, unlike ADT which for practical purposes is directly proportional to the potential transportation-disruption and road-user casualties due to bridge damage. Such a relationship implies that ADT should be a multiplicative factor. In many procedures however, the ADT variable is only one of a number of variables used in an additive combination; thus its significance is diminished. (The Illinois procedure is somewhat of an exception, with ADT weighted at 69 percent.)

Many prioritization procedures include a variable to consider whether the bridge carries important utilities. This variable may be unnecessary. Compared to the cost of transportation disruption and structural repairs, the cost of restoring utilities across a bridge site is probably small enough that it can be neglected in a preliminary prioritization procedure.

As with structural vulnerability, bridge importance is poorly assessed by many prioritization procedures because earthquake loss-estimation techniques are not used. Instead of the somewhat arbitrary procedures commonly proposed, the importance of a bridge could be estimated by an approximate cost-benefit analysis, as is described in Chapter 12.

Algorithms for Bridge-Priority Ratings

All of the prioritization procedures reviewed use a single-formula type of algorithm to determine bridge priority ratings. As shown in Chapter 12, a flowchart type of algorithm could be used instead.

The flowchart method has the advantage of allowing "if statements" to be incorporated into the algorithm. For example, using a flowchart algorithm, a skew factor can be applied *if* the bridge has movement joints. If the bridge does not have movement joints the skew factor can be reduced or left out. Similarly, a significant year-of-construction factor can be applied *if* the bridge has reinforced-concrete columns. For other pier types the year-of-construction factor can be changed. With a single-formula algorithm, it is difficult to include such options.

Many procedures use an additive or partially additive combination of ratings for structural vulnerability, bridge importance, and seismicity to arrive at a final priority rating. In Section 11.2 it was shown that additive combinations, used in the *ATC 6-2* and 1990 Caltrans procedures, can produce illogical results. A revised combination is used in the 1992 Caltrans procedure and in some other procedures, where the priority rating is taken as the seismicity rating times the sum of 0.6 times the importance rating plus 0.4 times the structural vulnerability rating, as shown below (the terminology here is changed from that used by Caltrans):

$$\textit{Priority Rating} = \textit{Seismicity} \times [0.6 \times \textit{Importance} + 0.4 \times \textit{Vulnerability}]$$

This combination formula can also produce illogical results. Assume that the *seismicity, importance,* and *vulnerability ratings* range between 0 and 1.0 and consider the following example of two bridges: Bridge A is in a relatively high seismic zone, *seismicity* = 0.8, has a medium *importance,* = 0.5 and has extreme structural deficiencies, *vulnerability* = 1.0. This bridge is assigned a *priority rating* of 0.56. Bridge B has high *seismicity* and *importance* ratings, 1.0 each, but has no structural deficiencies, *vulnerability* = 0. This bridge is assigned a higher priority rating, 0.60, than the fragile Bridge A, despite the fact that it contains no seismic deficiencies, and its earthquake performance cannot be improved by seismic retrofitting.

Comparisons between different procedures can demonstrate their arbitrary nature. In the original Caltrans procedures [Gates and Maroney 1990] bridge importance was weighted at 24% of the total additive index and had 46% of the weight that structural vulnerability had. In the revised Caltrans procedure [Gilbert 1993] importance was given 150% more weight than structural vulnerability. A justification for this major change (from 46 to 150%) was not given. This can be compared to the Kentucky procedure [Yu Ouyang et al 1990] where bridge importance is only weighted at 10% of the total additive index, and only has one third the weight that structural vulnerability has.

Another weakness of some prioritization procedures is that they have imposed step functions on data in which there is actually a gradation of conditions, for example soil-profile type or span seating lengths. In addition, some procedures include too much subjective data to obtain consistent results from different bridge evaluators. The amount of subjective data and judgement required in preliminary screening procedures should be minimized.

In general, the weakness of most prioritization algorithms is that the combination formulas are too arbitrarily chosen. The formulas seem like "black boxes" where basic bridge data is input and a priority rating is output, but where the workings in between are mysterious. Often there is no clear logic or rationale to the combination rules, weighting, or inclusion of the variables used. For the Illinois study, Cooling et al [1992] note that the *ATC 6-2* and Caltrans algorithms are both "based on subjective weighting factors". For their study, Cooling et al tried to avoid such subjective factors and instead chose "to base the systems on a set of logical defensible criteria (including soil effects), without presupposing the outcome".

Thus it is preferable to use more transparent methods, such as those proposed in Chapter 12, where the intermediate results, such as probability of earthquake damage or transportation-disruption cost, have a physical meaning are thus easier to verify. An earthquake loss-estimation approach and cost-benefit criteria would seem to be much more direct and transparent than the abstract algorithms commonly used.

Buckle [1991] has recommended weighted-additive combinations with the following explanation:

> "Multiplication, instead of addition, gives more emphasis to extreme values of each parameter, and this may distort the ranking procedure. It also amplifies the error or uncertainty inherent in each factor such that the error in the overall index is significantly higher than would otherwise be the case, if the same factors were added together. However, addition methods can be insensitive and it may be difficult to separate a large group of bridges which have average scores. This may be overcome to a certain extent by using unequal weighting factors."

The present author disagrees with the conclusion that additive procedures are preferable because they are less error sensitive. Procedures using multiplicative combinations may be erroneous, but it seems that this would only be so because the multiplicative factors themselves have been poorly chosen.

A possible analogy (perhaps over-simplified) could be the determination of bending moment in a simply supported span, based on its load per length, w and its length l. The direct and transparent calculation of maximum bending moment is, of course, $wl^2/8$.

Some prioritization procedures it seems, would attempt to predict this value by a weighted-additive combination of the two variables w and l. The weighted-additive formula for this problem would be:

"*moment rating*" = $k_1w + k_2l$, which would be justified by the knowledge that bending moment will increase with increasing load and/or increasing span length. Some might even argue that the weighted additive calculation is preferable to the $wl^2/8$ solution because it is less sensitive to errors in the span length l.

This seems to be a fallacy. Three important conclusions are illustrated by the analogy:

1 It can be shown that no matter what values are selected for the weighting factors k_1 and k_2, the weighted-additive formula $k_1w + k_2l$ can only be roughly accurate for a limited range of loads, w and span lengths, l. Extreme errors can result for w or l outside this range of accuracy.

2 Even if the likely range of w and l is limited and well understood, a thorough analysis is required to determine the appropriate weighting factors k_1 and k_2. It would not be wise to choose the factors arbitrarily. Therefore, the proposed formula must be carefully verified for the entire possible ranges of the input variables w and l.

3 To attempt to make an algorithm less error-sensitive by making it less sensitive overall does not improve the algorithm. At the extreme case, one could remove the variable l from the prediction of bending moment, (ie, make the weighting factor $k_2 = 0$) so that the moment rating is independent of span length. While this would make the procedure insensitive to uncertainties in span length, it would not improve accuracy of the result.

This is not to say that uncertainties in prioritization procedures and their input data should not be a concern. Such uncertainties should be investigated. The best way to do this would be by using risk-analysis methods.

Verification of Prioritization Procedures

Although some of the prioritization procedures reviewed here have been established for several years, none of the procedures seem to have been well verified. (The Japanese procedure, based on earthquake damage data, may be somewhat of an exception.) It is not sufficient merely to show that a prioritization procedure produces a good dispersion of results, as was done by Filiatrault et al [1994], or to compare the results of two or more procedures without a reference to which procedure is more accurate, as was done by Gilbert [1993] and Sundstrom and Maroney [1992]. A proper verification should compare the results of the prioritization algorithm with the results produced by detailed seismic evaluations and economic (eg cost-benefit) studies. The best use of engineering expertise would be in comparing and interpreting the results of the prioritization algorithm with those of the more detailed evaluations. Similarly, a comparison of actual damage with the assessment of seismic vulnerability, for bridges which have been damaged in earthquakes, would be useful.

Implementation of Prioritization Procedures

Most prioritization procedures are not well co-ordinated with the overall program of bridge upgrading for a jurisdiction. It appears that some bridge authorities may rely too heavily on the accuracy of initial prioritization procedures. Hwang [1994] has noted that, "An exaggerated statement about the usefulness of preliminary screening results may lead other persons such as emergency planners to misuse the screening results". Where screening procedures have been implemented (such as in California), the initial, approximate prioritization list generally has not been updated by secondary, follow-up seismic assessments. Instead, fully-detailed seismic evaluations are carried out on all bridges identified in the preliminary screening. The number of such evaluations required could be greatly reduced if a secondary screening procedure is used (as proposed in Chapter 12).

Some bridge jurisdictions seem to ignore the "bridge-importance" variable after the preliminary screening stage. After preliminary screening, a bridge-retrofit program should proceed with not only more detailed structural evaluations of potentially vulnerable bridges, but also more detailed assessments of bridge importance, using better estimates of transportation-disruption effects, etc.

Finally, attention needs to be given to integrating prioritization procedures with computer databases. Many authors proposing prioritization procedures have developed forms for hand-calculating priority ratings. These may be useful for illustration; but in practice, where authorities will be evaluating hundreds or thousands of bridges, it is clearly most efficient to have a computer database program do all calculations.

CHAPTER 12

RECOMMENDED METHOD OF PRIORITIZING BRIDGES FOR SEISMIC UPGRADING

To produce a more accurate and more flexible bridge screening process, the author has developed a method based on earthquake-loss estimation and cost-benefit criteria. The method has been implemented on a stock of 445 bridges in New Zealand's Tasman District [Maffei 1994]. The main features of the new method are described in this chapter, beginning with the overall approach.

12.1 Overall Approach to Bridge-upgrade Prioritization

Figure 12.1 presents a diagram of the proposed method for prioritizing bridges for seismic upgrading. The method prioritizes bridges according to the approximate benefit/cost ratio for upgrading. The methodology illustrated in the diagram applies to the initial preliminary screening step of the bridge upgrade process. However, the same methodology is applicable to more detailed assessments of bridge seismic vulnerability and importance.

Bridge Seismic Vulnerability and Expected Damage

The top half of the diagram of Figure 12.1 describes the engineering side of the recommended method; that is, the procedure for estimating the likely seismic damage to a bridge. The likely damage is a function of the bridge structural vulnerability and soil condition, and of the probable seismicity over the expected service life of the bridge. The vulnerability characteristics of the bridge can be expressed by a damage versus earthquake-intensity curve as was described in Figures 11.4 and 11.6. Such a curve shows what level of damage can be expected in a particular bridge or group of bridges, depending on the strength of the earthquake.

The data for creating the damage curve could be expert judgement, earthquake damage data, or brief or detailed seismic assessments. As discussed in Section 11.4, damage-versus-intensity curves for 78 different classes of structures, including 3 categories of bridges, are presented in the Applied Technology Council publication *ATC-13* [1985]. The *ATC-13* curves are based on expert opinion and are presented in both graphical and matrix form. For the Tasman District project, damage curves were developed for different values on a seismic vulnerability rating scale, which will be described in Section 12.3. The damage curve is combined with a probable seismicity curve, such as that shown in Figure 11.5, to give the expected seismic damage to a particular bridge or class of bridges.

Bridge Importance and Asset Value

The bottom half of the Figure 12.1 diagram describes the economic side of the method, ie, the estimation of bridge-asset value, which is taken as the sum of structure value plus loss-of-use value. Structure value equals the cost of replacing a bridge after complete earthquake damage, and can be assumed to be a function of the bridge length, number of lanes, and factors to account for rough terrain and remote locations. Loss-of-use value of a bridge is more difficult to quantify; it should consider all of the additional costs to a community of losing a bridge in an earthquake, including transportation disruption, casualties, and lifeline dependencies such as ambulance and firefighting access. The loss-of-use value of a bridge depends on the likely time that would be required to restore the bridge to service after earthquake damage. After estimating likely bridge damage and bridge-asset value, estimates of bridge-upgrade costs can be used to determine the benefit/cost ratio for seismic upgrading. The highest priority bridges to retrofit are those with the highest benefit/cost ratios.

In the Tasman District this new prioritization method was implemented on a sample of 56 bridges [Maffei 1994]. Each bridge was given a seismic vulnerability rating related to a damage curve, which was then combined with the probable seismicity in the region to calculate the expected damage for that bridge. A computer database was used to record the input data on seismic vulnerability and asset value for each bridge. The calculations of expected earthquake losses and benefit/cost ratio for upgrading are made within the database.

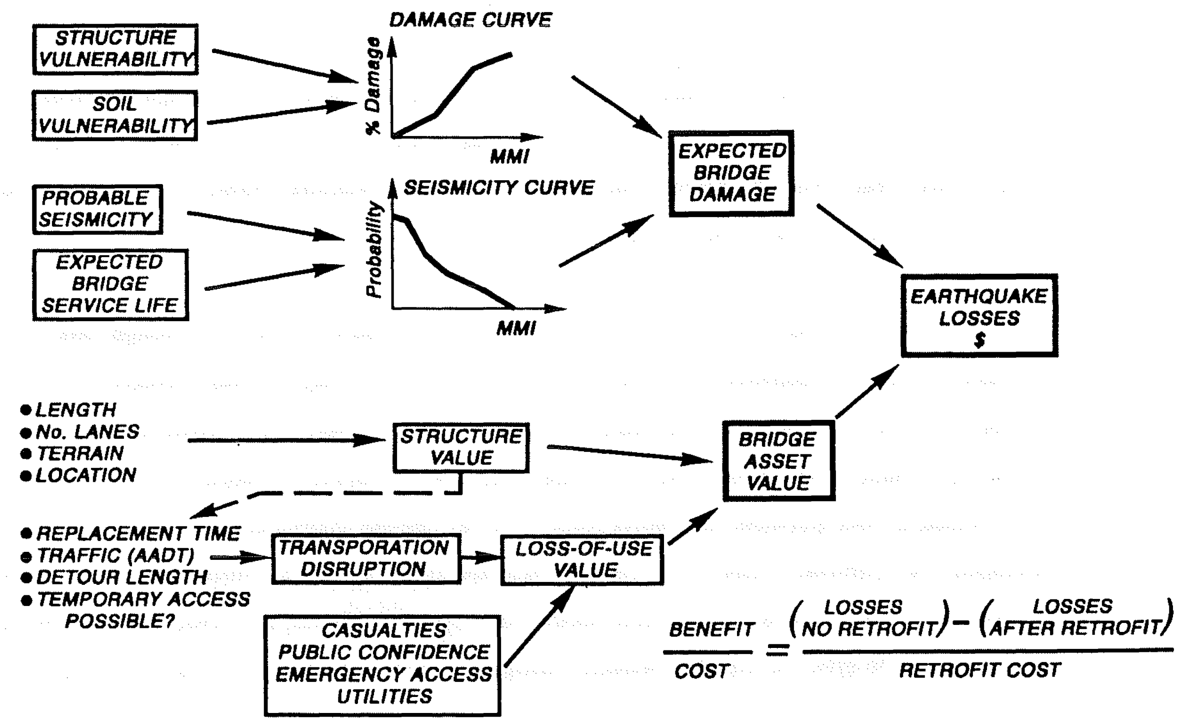

Figure 12.1 **Diagram of the proposed prioritization method for bridge seismic upgrading.**

12.2 Levels of Seismic/Structural Assessment

To assess seismic vulnerability, a rating is assigned to each bridge based on its structural features and seismic deficiencies. The rating is drawn from a seismic/structural assessment at various possible levels of detail.

For a first-pass identification of potentially vulnerable bridges, a brief structural assessment is usually appropriate. This assessment may be based on only a handful of risk factors such as year of construction, bridge length and skew, soil type, and seismic zone. At the other end of the spectrum, a detailed evaluation involving the verification of as-built conditions, dynamic analyses, and calculation of plastic-mechanism strengths and ductility capacities is appropriate once the actual seismic retrofit of the bridge is planned. In between, investigations involving, for example, only quick hand calculations of seismic demand and capacities, using static forces, may be required. In managing and prioritizing seismic upgrade work, structural assessments of low to medium detail are usually the most useful.

For the first screening of a large group of bridges, a prioritization procedure should be based on a brief assessment of seismic vulnerability and bridge-asset value. The first screening should be accurate enough to identify a number of clearly non-vulnerable bridges, which can then be eliminated from further consideration. For subsequent screenings of bridges, more detailed assessments of both bridge vulnerability and asset value should be made. Thus a process of increasingly detailed seismic and value assessments is used to finally determine (a) which bridges should be upgraded and (b) the appropriate seismic retrofit level.

According to this approach, the author has outlined four different levels of bridge seismic/structural assessments. These include three levels of engineering assessment: a *level-one* visual assessment, a *level-two* schematic assessment, and a complete *level-three* engineering evaluation. In addition, a simple preliminary screening procedure using flowcharts, called a *level-zero* assessment, has been developed. The four levels of investigation are described further in Table 12.1. Ideally, the less-detailed investigations should yield more conservative results, and as more-detailed investigations are carried out, the conservative assumptions can be reviewed, and a number of bridges can be eliminated from further consideration.

The recommended implementation sequence of the different levels of seismic evaluation is shown in Figure 12.2. The figure shows that an initial study, using level-one assessments of a sample of bridges, is recommended before proceeding with the level-zero preliminary screening procedure. The purpose of the initial study is to verify and calibrate the level-zero procedure according to the particular needs and characteristics of the bridge jurisdiction.

Table 12.1 Levels of Seismic/Structural Assessment

	Level of Assessment	Assessment Conducted by:	Estimated time required for investigation each bridge:	
			Simple bridge eg < 10 m long	Moderately complicated bridge eg 20-60 m long
FLOWCHART PROCEDURE	**LEVEL 0 - FLOWCHART ASSESSMENT** Approximate procedure following simple flow charts	Engineering Technician, Draughtsperson, or Student	5-15 minutes	10-15 minutes
ENGINEERING ASSESSMENTS	**LEVEL 1 VISUAL ASSESSMENT** - Field inspection and brief review of drawings. No calculations. Consideration of seismic-force path and likely vulnerabilities. Comparison to typical earthquake performance of similar structures.	Experienced Engineer familiar with research on the seismic behaviour of bridges	½ hr at site 0-½ hr review drawings ½-1 hr assessment 1-2 hrs total	1 hr at bridge site 1 hr to review drawings 2 hrs to write assessment 4 hrs total
	LEVEL 2 - SCHEMATIC ASSESSMENT Level 1 plus approximate calculations. Perhaps a further investigation of the soil type and structure condition.	Experienced Engineer	Usually not necessary	Level 1, +1-3 days
	LEVEL 3 - COMPLETE EVALUATION More detailed engineering calculations and evaluation. Computer analysis and material testing if required.	Experienced Engineer	Level 1, + 1-2 days	Level 2 + 2-10 days

Figure 12.2 also shows that the actual retrofit work need not wait until all bridges have been fully evaluated. If the early stages of preliminary screening identify bridges which are clearly vulnerable, retrofit work can begin on those bridges while the rest of the bridge stock is still being investigated.

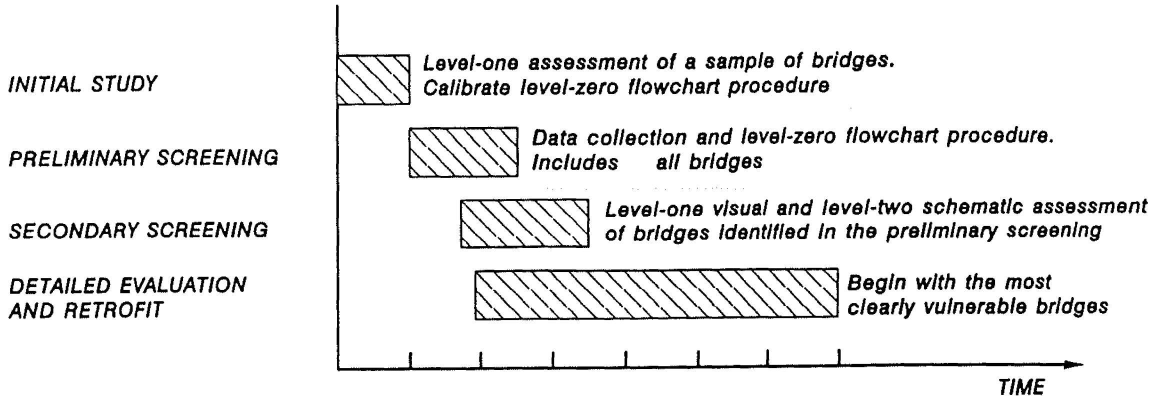

Figure 12.2 **Recommended implementation sequence for a program of bridge seismic screening, assessment, and retrofit.**

In the Tasman District, the initial study phase involved level-one assessments of 56 bridges. The results of these assessments were used to calibrate the level-zero assessment procedure, which was implemented on the remainder of the 445 district bridges.

12.3 Bridge Seismic Vulnerability Ratings

As part of the proposed method of bridge-upgrade prioritization, a system of seismic-vulnerability ratings has been developed. The ratings are on a scale of 0 to 10, similar to those of the *ATC 6-2* [1983] method, as shown in Table 12.2. The rating for a bridge can be derived from either a brief or detailed seismic assessment.

The vulnerability ratings are somewhat subjective but can be quantified by the series of damage curves shown in Figure 12.3. The damage curves relate the vulnerability ratings to the expected bridge damage at different earthquake intensities. The use of the damage curves is discussed in Section 12.6.

Table 12.2 **Seismic Vulnerability Rating**

Rating	Meaning
0	Not applicable, therefore not vulnerable
1 2 3 4	Low vulnerability
5 6 7	Medium vulnerability
8 9 10	High vulnerability

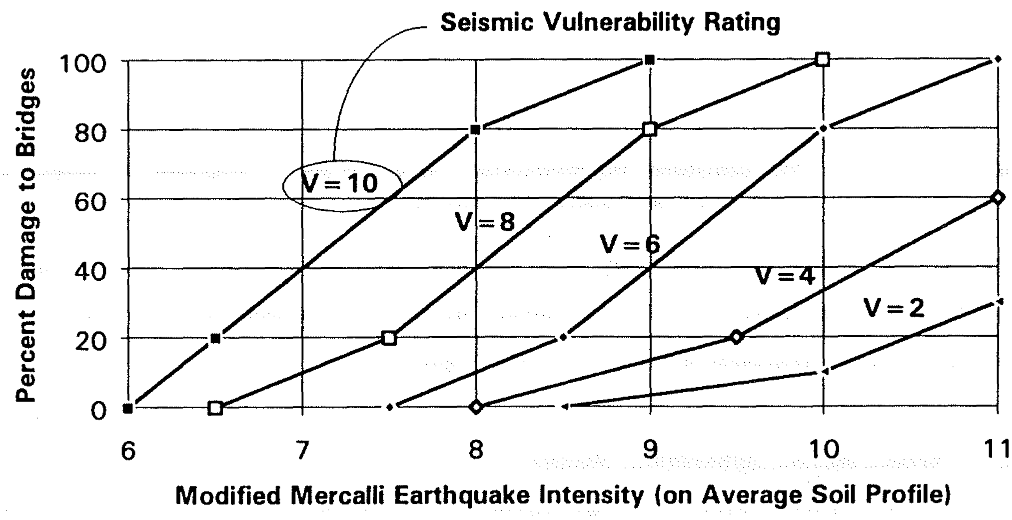

Figure 12.3 **Damage-versus-intensity curves for different seismic vulnerability ratings.**

Even for detailed structural evaluations these ratings are based partly on subjective engineering judgement. To reflect the appropriate uncertainty, the seismic vulnerability ratings should not be reported to more than one decimal place. (For example, if V = 6.73 results from one of the vulnerability formulas given below it should be rounded to V = 6.7.)

Component Vulnerability Ratings

For brief (level-one or level-zero) seismic assessments, separate structural vulnerability ratings are determined in three areas of potential seismic deficiency: (a) superstructure movement joints, bearings, and support seats, (b) substructure columns or pier-walls, and (c) foundations and abutments. The worst of these three ratings is taken as the overall structure vulnerability rating as shown in the following formula:

$$V_{STRUCT} = \text{MAX}\ (V_{MJ},\ V_{CW},\ V_{FA})$$

where:

V_{STRUCT} = Structure vulnerability rating.

V_{MJ} = Vulnerability rating for superstructure movement joints and related seismic deficiencies.

V_{CW} = Vulnerability rating for substructure columns, pierwalls, or other type of intermediate supports.

V_{FA} = Vulnerability rating for foundations and abutments.

The alternative combination—ie, taking only the largest of the three factors and ignoring the other two—is used because if a bridge fails in one of these areas, that weak area generally governs the overall capacity of the bridge, and the bridge's capacity in the other two areas is somewhat irrelevant. This is similar to the combination used in *ATC 6-2* [1983].

Considering the uncertainties in the brief seismic assessments, and the potential for partial damage in different areas of the same structure, a more sophisticated combination formula of the three separate vulnerabilities could also be considered.

Soil Effects

In addition to structural deficiencies, soil conditions influence seismic vulnerability. A factor to consider soil-profile type and liquefaction vulnerability is defined based on Uniform Building Code (UBC) [ICBO 1994] soil types. The soil factor ranges from 1.0 for firm or rock soil profiles to 2.0 for deep soft clays, as shown in Table 12.3. The soil profile definitions of the New Zealand code [SANZ 1992] differ from those of the UBC, but can be interpolated between the UBC values as shown in the table.

Liquefaction potential is not strictly related to soil type, but should be included by increasing the soil factor where liquefaction is possible.

The soil factor is combined with the structural vulnerability rating to give an overall seismic vulnerability rating. The following formula is recommended:

$$V = (V_{STRUCTURE} \times \text{soil factor})^{0.85}$$

Table 12.3 Soil Risk Factor

Soil Factor	Description
1.0	UBC soil type S_1 or NZS 4203 Soil A (firm or rock-like)
1.2	UBC soil type S_2
1.4	NZS 4203 Soil B
1.5	UBC soil type S_3 or unknown soil or medium liquefaction potential
1.8	NZS 4203 Soil C
2.0	UBC soil type S_4 (very deep clay) or high liquefaction potential

The 0.85 exponent is used to bring the $V_{SEISMIC}$ rating into line with the vulnerability definitions of Table 12.2. A structure on a type S_3 soil profile or an unknown soil profile will have an overall vulnerability rating equal to or slightly higher than its structural vulnerability rating. On more competent soil profiles (Type S_1 and S_2) the overall vulnerability rating is less than the structural vulnerability rating. On deep clays or liquefiable sites, the vulnerability is increased, sometimes to a result greater than 10. As this would happen only for highly deficient structures on highly vulnerable sites, the meanings given for the 0-10 scale are still valid. Conceivably though (and deservedly) an extremely vulnerable bridge could be rated an 11 or 12 out of 10. Sample results of the formula are given in Table 12.4.

Orthogonal Combination Formula

Separate vulnerability factors may be assigned for transverse-direction and longitudinal-direction earthquake shaking, with respect to the bridge axis. The two vulnerability ratings can be combined using the following formula, developed by the author:

$$V = \frac{V_1^2 + V_2}{V_1 + 1}$$

Where V_1 is the larger of the vulnerability ratings V_1 and V_2 which have been assigned to the two orthogonal directions. The formula recognizes that the final vulnerability for a bridge is dominated by its "weaker" direction, but that the vulnerability in the "stronger" direction should also have an effect on the overall rating. Sample results of this formula are given in Table 12.5.

Table 12.4 Sample Results of the Soil Factor Combination Formula

V Structure	Soil Factor	V
9	1.5	9.1
9	1.2	7.6
9	1.0	6.5
5	1.5	5.5
2	1.5	2.5
9	2.0	11.7

Table 12.5 Sample Results of the Orthogonal Risk Combination Formula

Transverse Vulnerability Rating	Longitudinal Vulnerability Rating	V
9	9	9
9	3	8.4
3	9	8.4
9	7	8.8
8	8	8
2	1	1.7

12.4 Level-One Visual Seismic Assessment Method

The level-one visual assessment procedure requires a brief site inspection and review of the bridge drawings by an experienced engineer. In the Tasman District, a bridge maintenance inspection was carried out at the same time that the seismic-risk data were collected.

A one-page, double-sided form was used to collect data from the bridge site and drawings. The front side of the form is a modification of the Transit New Zealand *Bridge Inspection Report* [TNZ 1991a]. It records information on the bridge condition and recommended maintenance, and is discussed in Section 13.5.

The overleaf of the form, shown in Figure 12.4, is designed to record the level-one seismic evaluation data. Since information on bridge identification, location, and geometry is recorded on the maintenance-inspection side of the form, it is not repeated on the seismic-evaluation side shown in Figure 12.4. The seismic-risk data include year of construction, structure type, and movement-joint (span seating) and load-path descriptions.

The structure type is described using a multiple-choice table defining the construction type of six basic components of the bridge. The six data items allow a great number of possible bridge-structure types to be concisely described. The structure-type information can be used in the database not only for bridge seismic-risk assessments but also for bridge maintenance and inspection purposes.

If there are movement joints in the bridge structure, a sketch of the support conditions at the movement joints, and measurements of the support overlap lengths are recorded. If bearings are present the type of bearing and the bearing overlap lengths are recorded. The definitions of support and bearing overlap distances at the movement joints are taken from the Transit New Zealand *Bridge Manual* [TNZ 1991b].

The seismic-force path of the bridge in the transverse and longitudinal directions is outlined diagrammatically on the seismic evaluation form. The force-path description should draw the attention of the engineer to the likely mechanism of seismic response for the bridge, and help him or her identify any potential seismic deficiencies in the structure. The approach of first describing the seismic-force path is taken from the evaluation procedure contained in the NEHRP *Seismic Evaluation Handbook for Buildings* [14].

Based on the seismic-force path, observed deficiencies, and the judgements of the structural engineer assessing the bridge, the seismic vulnerability ratings for movement joints, columns or walls, and foundations or abutments are assigned. These ratings are assigned separately for longitudinal- and transverse-direction earthquake effects.

At the bottom of the form for seismic evaluation data, the engineer can calculate the final vulnerability rating. This is done by first taking the maximum of the component vulnerability ratings in each direction, then by applying the soil factor, and then by applying the orthogonal combination formula. When conducting level-one evaluations on a large number of bridges, these calculations can be carried out by the computer database program.

At the bottom of the data form, the engineer can also record preliminary suggestions for seismic retrofitting. Finally, the engineer should make a recommendation as to whether a more detailed (level-two or level-three) investigation of the bridge is warranted.

LEVEL 1 Seismic Evaluation Data

Bridge No ....615...... Year of Construction....1935....

Movement Joints ....NO...............................

	Longitudinal	Transverse
Support Overlap Length		
Bearing Overlap Length		
Restraint		

Sketch:

SPAN LENGTHS :
45' - 192' - 36'
13.7m - 58.5m - 11.0 m

Seismic Load Path and Suspected Critical Elements

Transverse:

DECK → TIMBER DECK BRACING → PIER WALL → FDNS
↘ HORIZONTAL CABLE STAYS ↗
*

Longitudinal:

DECK → PIER WALLS → FDNS
↘ ABUTMENTS

BRIDGE STRUCTURE TYPE

Component	Type
Deck	■ Timber ■ R/C ■ P/C ■ Other
Beam/Girder/Truss	■ None (i.e. slab only) ■ P/S girders ■ Monolithic R/C Beams ■ R/C Arch ■ Steel Beams ■ Steel Truss ■ Suspension ■ Timber Truss ■ Timber Beams ■ Other
Column/Pier. Wall	■ None (i.e. single span) ■ R/C pier-wall ■ R/C multi-column bents ■ R/C simple-column bents ■ Other
Column/Pier Foundation	■ None (i.e. single span) ■ R/C spread footings ■ R/C cylinders (CIP) ■ P/C piles ■ Steel piles ■ Timber piles ■ Unknown
Abutment	■ R/C ■ P/C sleepers ■ R/C multi ■ Timber ■ R/C box culvert ■ U culvert
Abutment Foundation	■ R/C box culvert ■ R/C spread footings ■ R/C cylinders ■ P/C piles ■ Steel piles ■ Timber piles ■ Unknown
Structure Details:	
Drawing Nos Used:	95 SHEET 2

	Transv	Longit
Movement Joint Risk Factor	5-7	1-3
Column or Wall Risk Factor	3-4	2-3
Fdn or Abutment Risk Factor	4	3-4
Structure Risk Factor	7	4

Soil Profile Type .....

Soil Factor...... Zone Factor Z..1.2

Structure Factor...6.6.

Final Vulnerability Rating ....

FEROS : 1.5

Conclusions and Possible Upgrade Measures

SUSPENSION BRIDGES ARE TYPICALLY NOT HIGHLY VULNERABLE TO EARTHQUAKES. HOWEVER, THE POOR CONDITION OF THE BRIDGE AND THE STAYS BEING MISSING MAKE THE BRIDGE ~~VA~~ VULNERABLE TO TRANVERSE SHAKING.

POSSIBLE UPGRADE WITH NEW CABLE STAYS IN CONJUNCTION WITH CONDITION UPGRADE.

Further Evaluation Recommended: None Level 2 Level 3 Full Evaluation and Upgrade

Figure 12.4 **Bridge seismic-assessment and condition-inspection field form, side two, with the level-one assessment of the Peninsula Bridge.**

12.5 Level-Zero Method of Seismic Assessment

After conducting numerous level-one visual assessments in the Tasman District, the author recognized the possibility and need for developing an even simpler procedure for bridge seismic assessments. A *level-zero* procedure was devised to approximate, on the conservative side, the results of the level-one assessment. The goal of the procedure is for a quick first-pass screening to identify bridges for further prioritization.

The procedure follows a series of flowcharts, so that the assessment does not need to be performed by an engineer. An engineering technician or drafter would have the necessary skills to collect the required data from the drawings and calculate the bridge vulnerability ratings. If drawings or photos of the bridge are available, a site visit is not needed.

The procedure follows the vulnerability-rating scale described in Section 12.3. As explained in that section, the structural vulnerability is taken as the worst of three vulnerability ratings: that for movement-joint failures, that for column or pier wall failures, and that for foundation or abutment failures.

The *level-zero* procedure uses three flowcharts as shown in Figures 12.5, 12.6, and 12.7, one each for the vulnerability ratings of (a) movement joints or support seats, (b) columns or pier-walls, and (c) foundations and abutments. The procedure is specifically derived for the types of bridges prevalent in rural New Zealand. For application to different bridge stocks, the factors in the flowcharts can be adjusted.

Movement-Joint Vulnerability

The first step in the simplified assessment procedure is to determine the seismic vulnerability rating for the bridge superstructure movement joints. The flowchart in Figure 12.5 describes the procedure. Structures with no movement joints (ie, those with monolithic, integral superstructures) are given a vulnerability rating V_{MJ} of zero. For bridges with movement joints, the technician then looks at the seating conditions for the superstructure spans.

For bridges with movement joints, Figure 12.5 shows that the movement-joint vulnerability rating is based on a multiplication of factors to account for superstructure seating length (f_{SEAT}), the presence of earthquake linkage bolts (f_{LINK}), bridge skew (f_{SKEW}), and construction type (precast concrete or steel).

Superstructure Seating Length

The seating length factor is based on the ratio of actual seating length N, to the ideal seating length N_D, which, as a minimum, should be taken as that recommended in the Transit New Zealand *Bridge Manual* [TNZ 1991b] or in *ATC 6-2* [1983]. The following formula is used:

$$f_{SEAT} = 1.4 - \frac{N}{N_D}$$

The factor is limited to a maximum value of 1.0 for structures with poor seating conditions, ie, short seating lengths, and can be limited to a minimum value of 0.4 for structures with satisfactory seating lengths. Where support overlap lengths vary among different girders or span ends of the same bridge, the worst condition should be selected.

A conservative approximation of the ideal support overlap length, N_D, could be defined as 500 mm + 3 x L, where L is the bridge length in metres. N_D need not be assumed greater than 800 mm. This seat-length criterion, tentatively proposed by the present author, is more stringent than that which is recommended by the Transit New Zealand Bridge *Bridge Manual* [TNZ 1991] or by *ATC 6-2* [1983]. The criterion is based on the observation that in recent moderate earthquakes large displacements have occurred at bridge movement joints. It seems that more research is necessary to establish a reliable formulation for satisfactory bridge seating lengths.

If the support overlap length, N, cannot be established or estimated from the drawings and has not been measured from a site visit—or if a quick assessment needs to be done without gaining this information—the seat factor can be based simply on the year of bridge construction. New Zealand bridges constructed before 1973 tend to have shorter seat lengths and the factor is set at 1.0. Bridges constructed after 1973 have somewhat longer seat lengths and the factor is set at 0.8.

Superstructure Linkages

Bridges that have horizontal earthquake-linkage bolts or cable restrainers are expected to perform better in earthquakes and be less likely to suffer movement-joint support failures. The linkage bolts reduce the risk of superstructure collapses during an earthquake. Accordingly, the movement-joint vulnerability rating is reduced by a factor, f_{LINK}, equal to 0.8 when linkage bolts or restrainers are present. For structures without horizontal linkage bolts or restrainers, f_{LINK} is set equal to 1.0.

Note that the presence of hold-down bolts has not been included in the assessment of bridge movement-joint vulnerability. Although it is likely that hold-down bolts increase a bridge's chance of surviving an earthquake without movement-joint failures, many hold-down bolts for typical New Zealand bridges have only a small capacity to resist lateral earthquake forces. Such bolts will likely fail early in the sequence of earthquake shaking so that the bridge structure will still need to rely on adequate seat-support length or horizontal linkage bolts or restrainers.

Skewed Supports

The factor f_{SKEW} describes the increased risk of seismic collapse for skew bridges. The factor is 1.0 for a bridge with no skew and increases to a factor of 2.0 for bridges with vulnerable skew geometries. Evidence from past earthquakes justifies the assumption that skewed bridges can be twice as vulnerable to movement joint-failures as right-angle bridges. The skew factor is calculated from the following formula:

$$f_{SKEW} = 1 + 2 \cos\theta \sin\theta, \text{ for } 0 \le \theta \le 45°$$

$$f_{SKEW} = 2.0 \quad , \text{ for } \theta \ge 45°$$

where θ = the skew angle for the bridge.

The formula for skew factor is based loosely on a geometrical study of the likelihood of span drop-off for different skew angles. The skew factor has a significant effect on the vulnerability rating even for relatively small skew angles. For example, $f_{SKEW} = 1.5$ for $\theta = 15°$.

Calculation of V_{MJ}

The final vulnerability rating for movement joints then depends on the multiplication of three factors $f_{SEAT} \times f_{LINK} \times f_{SKEW}$. The first two factors f_{SEAT} and f_{LINK} are set at 1.0 for the most vulnerable case and are less than 1.0 for situations with reduced vulnerability. The skew factor is 1.0 for the least vulnerable situation and is larger for more vulnerable geometries.

The last factor in the flowchart of Figure 12.5 is specific to the common bridge types prevalent in New Zealand. It is based on the observation, from the seismic assessments of the Tasman District bridges, that precast-concrete-girder bridges in New Zealand tend to have reasonably long seat lengths and substantial horizontal earthquake-linkage bolts compared to typical steel-beam bridges. The final value for V_{MJ} need not be taken greater than 10.

A possible modification to the procedure could be made to consider more distinctly the span seating and linkage characteristics related to *transverse-direction* earthquake effects. This would require additional data and factors in the movement-joint vulnerability flowchart. To avoid over-complication, such a modification has not been attempted.

Column/Pier Wall Vulnerability

As shown in Figure 12.6, the procedure for determining column or pier wall vulnerability rating is the simplest of the three flowcharts. For single-span bridges there would be no intermediate column or pier wall supports so this vulnerability rating would be zero.

For multi-span bridges, the algorithm recognises that older non-ductile concrete columns are a clear seismic deficiency. Bridges with pre-1973 reinforced concrete columns are assigned the maximum vulnerability rating of 10. This reflects the experience of past earthquakes where reinforced-concrete columns with non-ductile detailing have resulted in a number of catastrophic bridge collapses. Conversely, post-1973 columns generally perform well in earthquakes due to detailing for ductile response. These columns are assigned a low vulnerability rating, $V_{CW} = 3$.

Other types of intermediate supports used in New Zealand, principally reinforced-concrete pier walls and occasionally timber-pile bents, are assumed to have medium to low seismic vulnerability, $V_{CW} = 5$. The seismic capacity of concrete pier walls or other types of intermediate supports with high lateral strength is often determined by the foundations. This is accounted for with a separate vulnerability factor, V_{FA}, as discussed below.

Foundation/Abutment Vulnerability

As shown in Figure 12.7 the vulnerability rating for foundations and abutments depends largely on whether or not there has been erosion or scour at the foundations. This assumption is particularly applicable to New Zealand bridges, which commonly cross granular river or stream beds. An example of erosion seriously compromising the seismic resistance of a bridge would be a reinforced-concrete pier wall founded on pile foundations for which the supporting soil has been eroded. If a large enough length of the piles has been exposed, then the piles become the weak link in the lateral-force resistance of the structure.

As shown in Figure 12.7, the principal variable in the assessment of foundation or abutment seismic vulnerability is the erosion factor, f_{EROS}. As shown in the figure, this factor ranges from 1.0 for bridges not susceptible to erosion or scour to 2.0 to 2.5 for cases where erosion has seriously compromised the ability of the foundations to resist lateral earthquake forces. The foundation/abutment vulnerability rating, V_{FA}, is taken as 4 times the erosion factor for multi-span bridges, 3 times the erosion factor for single-span bridges more than 5 metres long, and 2 times the erosion factor for shorter single-span bridges.

Unless there has been serious erosion, the foundation/abutment rating will not indicate a high vulnerability in this area. Thus, for many bridges, the foundation/abutment vulnerability rating may be unlikely to govern over the ratings for superstructure movement joints or columns/pier walls.

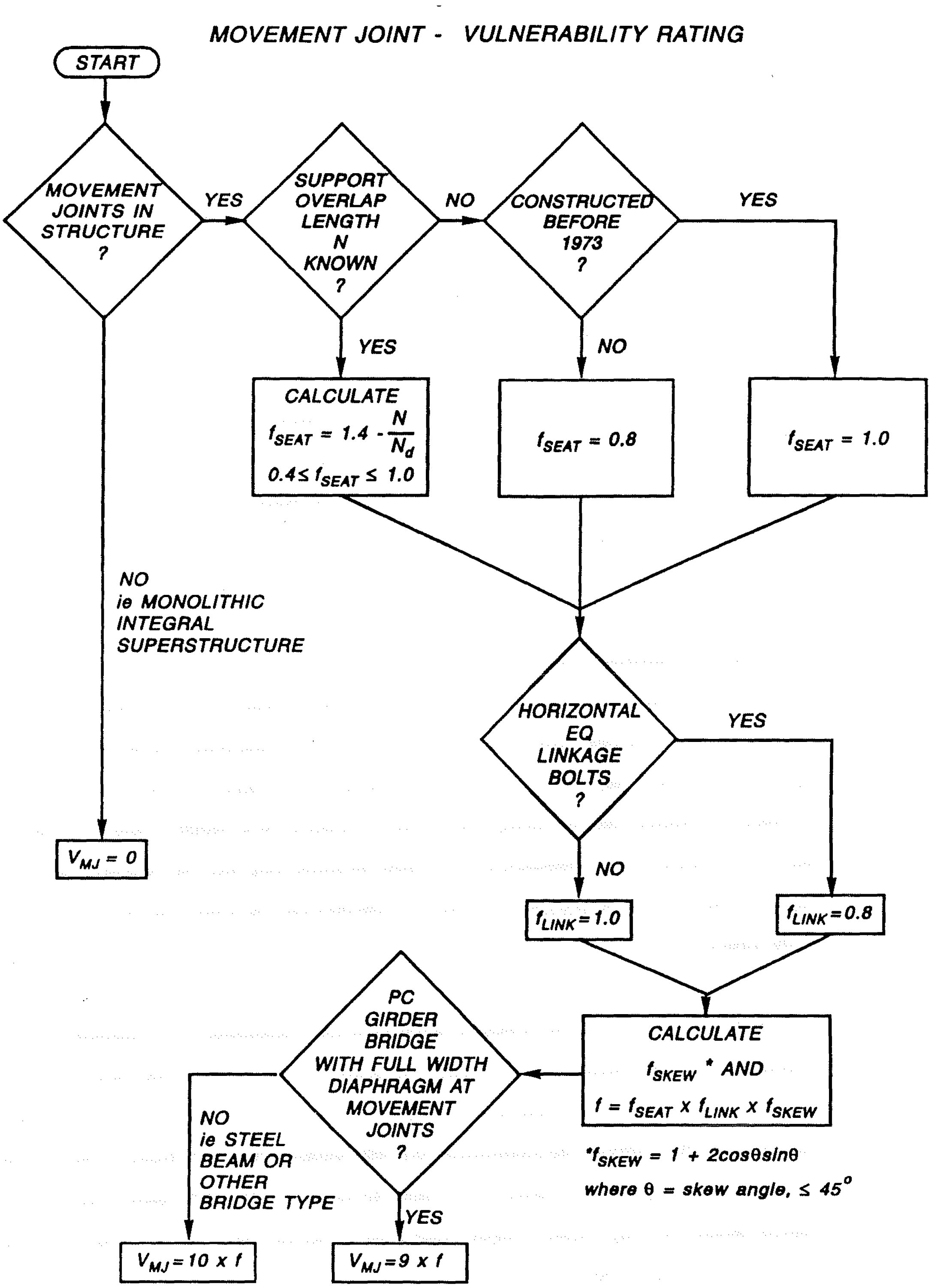

Figure 12.5 *Level-zero* **seismic-assessment flowchart for movement-joint vulnerability rating, V_{MJ}.**

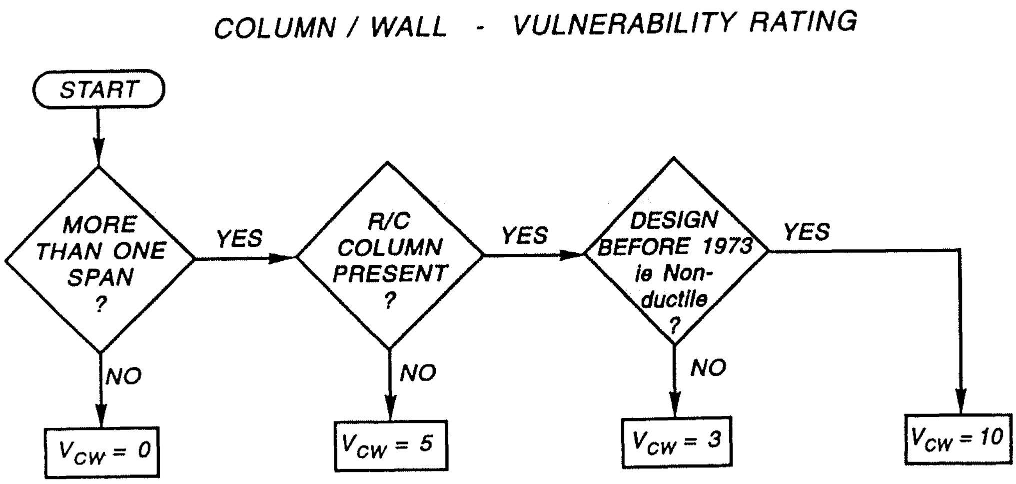

Figure 12.6 ***Level-zero*** **seismic assessment flowchart for column or pier wall vulnerability, V_{CW}.**

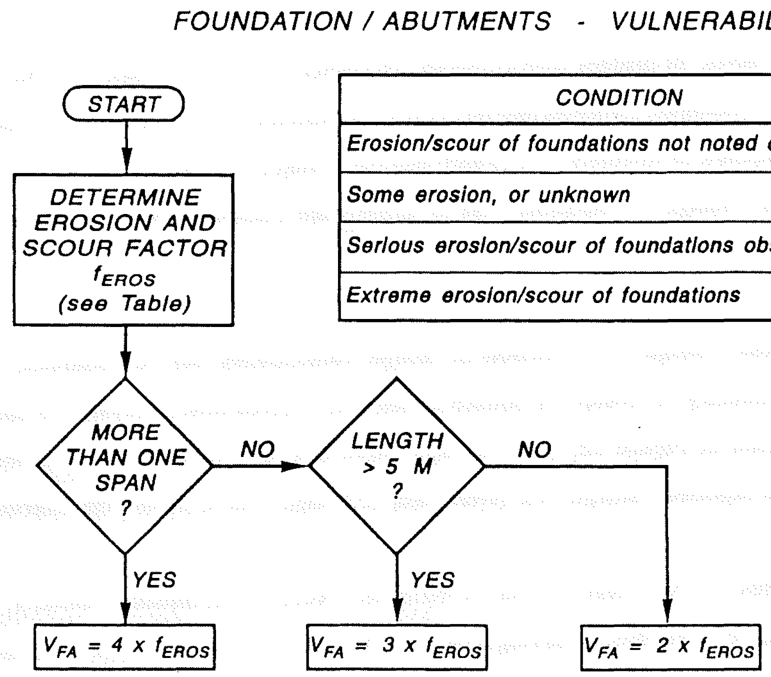

CONDITION	f_{EROS}
Erosion/scour of foundations not noted or expected	1.0
Some erosion, or unknown	1.5
Serious erosion/scour of foundations observed	2.0
Extreme erosion/scour of foundations	2.5

Figure 12.7 ***Level-zero*** **seismic assessment flowchart for foundation and abutment vulnerability, V_{FA}.**

The foundation-risk algorithm is based on conclusions and judgements drawn from the *level-one* assessments in the Tasman District, many of which were for small bridges. Single-span bridges are assumed to be less vulnerable than multiple-span bridges, for which the foundations of the intermediate supports provide an additional source of seismic vulnerability. For single-span bridges, short bridges tend to have better integral connections with the supporting soil, and there will be less seismic-force demand at the foundations of shorter bridges.

12.6 Expected Seismic Damage as a Function of Vulnerability Rating and Seismicity

In Section 12.3, it was proposed that the seismic vulnerability ratings can be associated with damage versus earthquake-intensity curves as shown in Figure 12.3. The horizontal axis for the damage curves is the earthquake intensity from the Modified Mercali scale. The vertical axis indicates the percent of damage to the bridges.

The percent damage can be interpreted in two ways. For a single structure it can be assumed that with increasing earthquake intensity an increasing level of damage would occur to the bridge, and that the damage can be expressed as a percentage of the replacement cost of the bridge, so that a bridge with 20 percent damage requires 20 percent of the replacement cost of the bridge to repair that earthquake damage. A bridge with 100 percent earthquake damage is judged to be non-repairable. Alternatively, when a number of bridges are being considered, the damage curve gives an indication of the percentage of bridges which will be seriously damaged.

Figure 12.3 gives damage curves for bridges with vulnerability ratings of 10, 8, 6, 4 and 2. The curve for vulnerability rating 8, for example, indicates that no damage is expected for earthquakes of intensity less than 6.5. For an earthquake of intensity 7.5, twenty percent damage is expected. At earthquake intensity 8, eighty percent damage is expected, and at earthquake intensity 10, total damage is expected.

The information on expected damage as a function of bridge vulnerability can be combined with information on expected seismicity to predict earthquake losses over a given time interval. As shown in the top half of the diagram of Figure 12.1, the damage curve can be combined with a probable seismicity curve to give the expected damage to a given class of bridge over a given time interval.

From seismological estimates of the return period of different levels of earthquake intensity, the probability of those earthquake intensities occurring over the lifespan of a bridge can be calculated. For two different bridge lifespans, 65 years and 100 years, Figure 12.8 shows the probabilities of different levels of earthquake intensities occurring, based on assumed return periods. This probable seismicity curve can then be combined with the damage curves for different vulnerability ratings, shown in Figure 12.3.

Figure 12.9 shows the relationship of expected bridge damage as a function of seismic vulnerability. This curve is derived from Figures 12.3 and 12.8 by numerically integrating the probability versus earthquake-intensity curve times each damage versus earthquake-intensity curve.

This curve of damage versus vulnerability rating, Figure 12.9, indicates for each vulnerability level the amount of damage that can be expected. The curve for a 65 year bridge service life is closely approximated by the quadratic function $0.01 * (V - 1.5)^2$. In the vulnerability range of 2-3 almost no damage is expected. In the vulnerability range of 3-4, only 4% of the value of bridges in that category is expected to be damaged. For vulnerability 5-6, 16% damage is expected; for vulnerability 6-7, 25% damage; for vulnerability 7-8, 36% damage; for vulnerability 8-9, 49% damage; and for vulnerability 9-10, 64% damage.

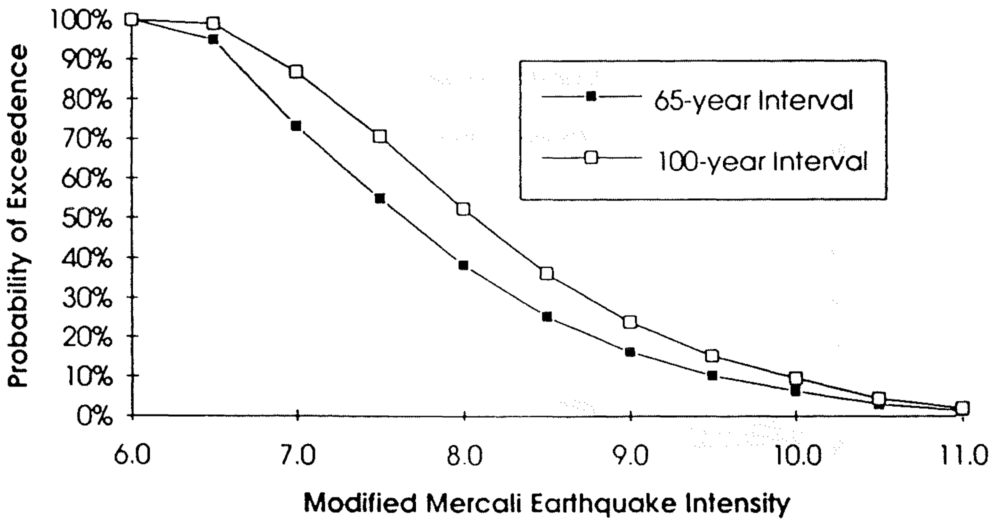

Figure 12.8 **Estimated probability of a given-intensity earthquake occurring during a typical 65-or 100-year bridge service life.**

The Modified Mercali index is used as the measure of earthquake intensity because it is the parameter that correlates best with damage to structures. Although it is a subjective parameter rather than a measured parameter from seismographic records, it is a valuable index for seismic damage estimation. Measured parameters such as peak ground acceleration or spectral acceleration, could also be used at the measure of earthquake level, however, these parameters have been shown not to correlate well with earthquake damage. [Naeim and Andersen 1993].

The earthquake-intensity scale for both the damage-versus intensity curves and the return-period-versus-intensity curve assume a structure situated on an average soil profile. Structures on a very stiff or rock-like soil profiles tend to experience lower earthquake intensities. Structures situated on deeper and softer soil profiles experience a higher earthquake intensity, often on the order of one intensity-level higher, due to the amplification of ground motion in the soil. Since the seismic vulnerability rating already takes into account the factor for soil profile, the earthquake intensity of the damage curves is defined to be independent of soil-profile properties.

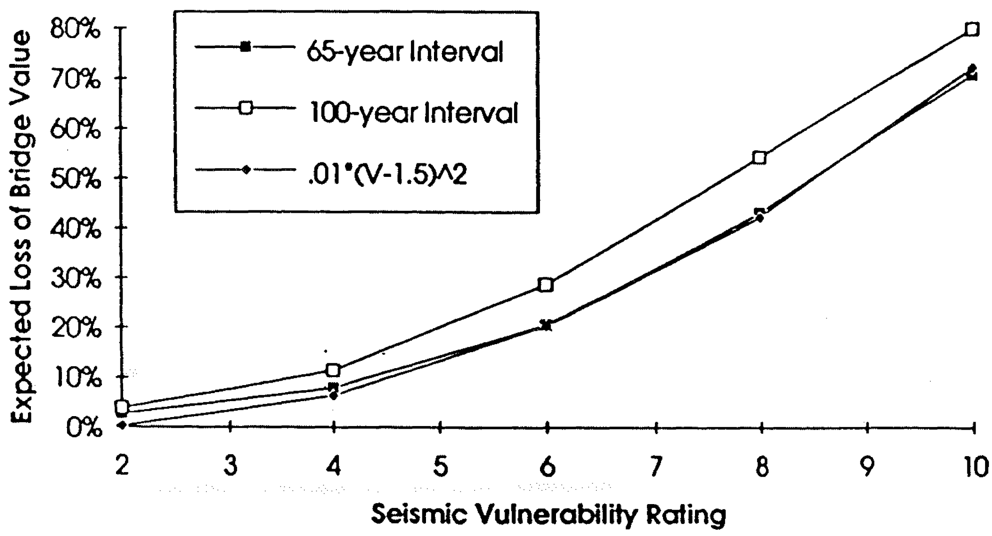

Figure 12.9 Expected bridge damage based on probable seismicity and bridge-vulnerability characteristics.

12.7 Bridge Asset Value

As shown in Figure 12.1, the expected level of damage to the bridge can be combined with an estimate of bridge asset value to predict the monetary value of earthquake losses for a group of bridges.

Typically, a computer database would be used to record the seismic vulnerability ratings for each bridge along with other basic bridge information such as length, number of lanes, detour length, and traffic volume. Given this data, bridge asset values and benefit/cost ratios for seismic upgrading can be automatically calculated.

As shown in the bottom half of the Figure 12.1 diagram, a bridge's value can be considered as the sum of:

(a) Its *structural value* (or replacement cost)—ie, the cost to construct a new bridge in its place, and

(b) Its *loss-of-use value*, ie, the total cost that would be suffered by bridge users during the time that it takes to rebuild the bridge.

The loss-of-use costs result primarily from transportation disruption, but can include other factors such as casualties resulting from bridge collapse.

Bridge Structure Value

The structure value (replacement cost) of a rural New Zealand bridge can be estimated as a function of its length, L, and number of lanes, according to the following formulas:

$$\textit{Struct. value} = \$15{,}000 + \$5{,}500/m*L$$
for one-lane bridges

$$\textit{Struct. value} = \$20{,}000 + \$8{,}000/m*L$$
for two-lane bridges

The formulas are based on a linear-regression analysis of construction costs (in 1994 dollars) for 69 bridges built in the Tasman District between 1975 and 1993. Sample results of the formulas are shown in Table 12.6.

The bridge replacement cost is calculated without reference to the type or cost of construction of the *existing* bridge. The reason for this approach is that if a bridge is destroyed by an earthquake, it is unlikely that the bridge will be rebuilt in the same structural form in which it was originally built.

Regression Analysis

The regression analysis of construction costs for two-lane bridges used a sample of 33 bridges varying in length from 2 metres to 190 metres. The sample for one-lane bridges included 36 bridges varying in length from 5 metres to 110 metres. As can be seen from Table 12.6, a one-lane bridge is projected to cost approximately 70% of the cost of a two lane bridge of the same length.

Table 12.6 Estimated Bridge Replacement Costs

BRIDGE LENGTH	ONE LANE BRIDGE C = 15,000+5,500 L	TWO LANE BRIDGE C = 20,000+8,000 L	RATIO $\frac{\text{one lane}}{\text{two lane}}$
5 m	$42,500	$60,000	0.71
10 m	70,000	100,000	0.70
20 m	125,000	180,000	0.69
50 m	290,000	420,000	0.69
100 m	565,000	820,000	0.69

There is a significant amount of scatter in the cost data used for the regression analysis. A major source of the scatter is that the construction of new bridges involves different levels of re-use of existing bridge components. For example, some of the bridges in the cost study made use of existing bridge substructures and simply added a new superstructure to the existing abutments or piers, or perhaps strengthened the existing abutments or piers. In other cases the construction of the new bridge required the demolition of the old bridge with no re-use of the substructure, and thus was more expensive.

After an earthquake, a similar uncertainty in bridge reconstruction costs is likely, since for some bridges only the superstructure may be damaged, and the piles, piers, and abutments can be reused; whereas for other bridges the earthquake damage may require that the bridge be entirely replaced including the substructures and foundations. Thus the bridge cost formulas developed here are not necessarily accurate on a bridge-by-bridge basis but are meant to be accurate when considering a group of bridges that have suffered damage due to an earthquake.

The bridge costs are intended to be on the slightly conservative side to reflect that in the period after a damaging earthquake there is a much greater demand for construction equipment and labour so that construction costs will be higher. The costs are meant to include design and inspection costs as well as construction costs.

Terrain and Location Factors

The estimate of bridge structure value based on only two variables, bridge length and number of lanes, may be sufficiently accurate for preliminary seismic screening. If a more refined estimate of bridge value is wanted, two additional factors can be used to adjust the value. The first is a terrain factor which accounts for bridges which must cross difficult obstacles, for example a wide river where intermediate piers would be required, or a steep ravine where construction would be difficult. The second is a location factor which reflects the fact that it is more expensive to build a bridge in a remote location than it would be to build the same bridge in an easily accessible location.

Thus, the bridge costs calculated by the cost-versus-length formulas can be subsequently multiplied by a terrain factor, which is 1.0 for typical terrain such a short stream crossings, and increases to perhaps 1.2 to 1.3 for more difficult terrain, eg, multiple-span bridges or deep ravines; then multiplied by a location factor, which is 1.0 for easy-access locations close to major towns and construction facilities, and increases to perhaps 1.3 for remote sites for which construction is more expensive.

Bridge Loss-of-Use Value

Bridge Replacement Time

The first step in determining the loss-of-use costs due to transportation disruption is to estimate the time that it would take to replace the bridge structure if it has been damaged or it has collapsed in an earthquake. This bridge replacement time is estimated to vary in a linear relationship with the replacement cost of the bridge. Since the formula for replacement cost includes number of lanes, bridge length, and terrain and location factors, the replacement time for the bridge depends on these factors as well. Replacement time is calculated to be 7 weeks plus 1 additional week for every $40,000 of bridge construction (ie, replacement) cost, as shown below:

$$Repl.Time = 7\ weeks + \frac{Struct.Value}{\$40{,}000/week}$$

Sample results of this formula are shown in Table 12.7.

Table 12.7 Estimated Bridge Loss-of-Use Times

BRIDGE REPLACEMENT COST	BRIDGE REPLACEMENT TIME
\$40,000	8 weeks
\$100,000	9.5 weeks
\$200,000	12 weeks
\$500,000	19.5 weeks
\$1,000,000	32 weeks

Transportation Disruption Costs

For the sparsely populated Tasman district, transportation disruption was considered to be the main component of loss-of-use cost. It was assumed to depend on traffic volume, detour length, bridge reconstruction time, and the feasibility of providing a temporary detour such as ford. Loss-of-use costs were estimated according to the formulas shown in Table 12.8.

Table 12.8 Formulas for Calculating Loss-of-Use Costs

SCENARIO	ITEM	FORMULA
Detour all traffic to alternate route	Detouring costs	= (Replacement time for bridge) x (ADT x 7 days/weeks) x (Detour length x 0.7) x \$0.60/km
No alternate route	Ferrying or other costs	= (Replacement time for bridge) x (ADT x 7) x \$100
Build a ford during bridge replacement	Cost to build ford	= (\$4,000 + \$200/m x L) x f_{terr}^2
	Cost to maintain	= (Replacement time for bridge, weeks) x (\$300 + \$4/m x L) f_{terr}
	Time to build ford	$= 0.5 \text{ weeks} + \dfrac{\text{cost-to-build}}{\$7{,}0000/\text{week}}$
	Detouring costs when building ford	= (Time to build x (ADT x 7) x (Det. length x 0.7) x \$0.60/km
	Vehicle costs to negotiate ford	= (Replacement time for bridge x (ADT x 7)x \$0.50/crossing

where ADT = Average daily traffic
L = Bridge Length
f_{terr} = Terrain factor, typically between 1.0 and 1.2

The costs of transportation are considered according to two possible scenarios. The first scenario assumes that until the bridge has been reconstructed all traffic must be detoured to the shortest alternate route. The second scenario assumes that a ford or other temporary access can be built in the location of the bridge, and be used by all traffic during the bridge reconstruction.

The cost of taking a detour is calculated based on the following assumptions.

(a) That the typical traveller needs to increase his driving distance by 70 percent of the full-circular detour length, which is recorded for all bridges. (The full-circular detour length is the distance from one bridge end to the other, travelling along the shortest route if the bridge itself cannot be crossed.) This factor of 0.7 in actuality depends on the intended route of the traveller. Several bridge-detour routes were reviewed in comparison to the intended routes for most of the traffic over the bridge. From this review it was found that the average detour for a traveller was about 0.5 to 0.7 times the full circular detour length.

(b) That the cost to the road user is 60¢ per km of additional travel distance. This number should account for both vehicle costs—fuel usage, vehicle maintenance, etc—plus the value of the time spent by the driver and passengers of the vehicle. The second factor of the traveller's time value is difficult to assess. The order of magnitude can be estimated, however, by considering that if a vehicle travels at 60km/hr and contains one person whose time is worth $10/hr, then the value of that extra time is calculated to be 17¢/km.

    The figure of 60¢/km can be compared to values from the Transit New Zealand method for estimating benefit/cost ratios. That method indicates that $1.25 is the cost in 1991 dollars of operating a Class 1 heavy vehicle at 70 km/hr for one km, and that $1.61 is the cost in 1991 dollars of operating a Class 2 heavy vehicle at 70km/hr for one km.

The disruption cost for the present study is then calculated as 60¢/km x 0.7 x detour length x the number of vehicles which must be detoured around the bridge during the time that it takes to reconstruct the bridge.

For several of the roads of the Tasman District there is no alternative route for possible detour. In such a case, disruption costs can be taken as some fixed amount, say $100, per every vehicle that would have used the bridge. This could be considered as the cost of making other transportation arrangements for essential trips across the river (or other obstacle).

Temporary Access (Ford) in Place of the Bridge

The second scenario for considering disruption costs is to assume that a ford is built across the river. For most obstacles where it is possible to build a ford, the savings in transportation-disruption costs more than balance the cost of building and maintaining the ford for the time that it takes to build the bridge. The loss-of-use cost for the build-a-ford scenario considers four separate costs. The first is the initial construction cost for the ford which is assumed to be a function of the bridge length and the terrain factor. The variation of construction cost of the ford with bridge length is assumed to be linear and is taken as $4,000 plus $200 per metre of bridge length. The cost is then adjusted to account for site conditions using the terrain factor discussed in the previous section. The terrain factor for most bridges is 1.0 causing no adjustment. For bridges with difficult crossing conditions such as steep ravines the terrain factor is increased to a value of perhaps 1.2. The ford construction cost is adjusted by the terrain factor *squared*. This reflects that the cost of building a ford is affected more by terrain than is the cost of building a bridge.

The second cost component is the cost to maintain the ford. Again a linear relationship with length is assumed, the weekly maintenance cost being $300 plus $4 per metre of bridge length. This cost is then multiplied by the terrain factor. These formulas are shown in Table 12.8.

The third component of costs associated with loss of use of the bridge and construction of a ford is the cost of detouring traffic during the time that it takes to build the ford. This cost is calculated in the same way as the detour costs previously described. In the case of constructing a ford, the time required to build the ford is estimated to be a linear relationship with the cost to build the ford, and is taken as 0.5 weeks + 1 week for every $1,000 of construction cost. The cost for detouring traffic for the time that it takes to build the ford then is equal to that time in weeks times the detour length, adjusted by the 0.7 factor, times 60¢/km, times the weekly traffic volume.

The fourth and final component of the cost to build a ford is the transportation disruption caused by vehicles having to slow down to negotiate the ford (and to wait for opposing traffic). This cost is assumed equal to 50¢ per crossing per vehicle. This fourth component of loss-of-use cost is then equal to the average daily traffic x 7 days per week x the number of weeks required to replace the bridge x 50¢. The 50¢ per crossing per vehicle is meant to be an average for all vehicles and can be compared to the figure of $1.70 (in 1991 dollars) per Class 1 heavy vehicle, and $1.93 (in 1991 dollars) per Class 2 heavy vehicle, assumed in the Transit New Zealand cost-benefit method.

Thus for each bridge there are two options for calculating the loss-of-use cost. One is to assume that a ford or other temporary access is built and the other is to assume that all traffic must be routed over the detour route for the whole time that it takes to reconstruct the bridge. The benefit/cost ratio of building a ford then can be calculated as the cost of detouring traffic divided by the total cost of having a ford, both costs calculated for the duration of the time that it takes to reconstruct the bridge after earthquake damage. For the pilot study sample of 56 bridges it was found that it makes economic sense to build the ford in all situations where it is physically possible to do so. Typically the benefit/cost ratio (calculated as indicated above) of building a ford is between 3 and 7.

The loss-of-use value of the bridge then is taken as the lowest cost of the two options, detour or build-a-ford.

Additional Considerations

The formulas given above for estimating bridge structure value and loss-of-use value are intended as guidelines only. The procedures were developed for the sparsely populated Tasman District, where most bridges carry low traffic volumes and cross streams or rivers. The procedures can still be used for different types of bridge jurisdictions, but in some cases the formulas may need to be adjusted, or additional factors may need to be considered.

Although no specific guidelines are given here for estimating potential losses due to earthquake casualties, such losses should be considered. Typically, casualties can be assumed proportional to the traffic volume, ADT, carried by the bridge. For bridges with roadways passing underneath, the ADT under the bridge should be included. For bridges which have buildings, parking, or other uses underneath, the replacement cost and potential casualties related to the facilities under the bridge should be estimated.

Benefit/Cost Ratio for Seismic Upgrading

Using the computer database, bridge-upgrading can be prioritized based on calculations of the bridge asset value and benefit/cost ratio for upgrading. The highest priority bridges to retrofit are those with the highest benefit/cost ratio.

The calculation of benefit/cost ratio requires an estimate of the cost of seismic retrofitting for each bridge. For preliminary screening, an approximate estimate—for example a proportion of bridge structure value—may be used.

It may also be possible to roughly estimate the cost of retrofitting based on the nature of the seismic deficiencies, as indicated by the relative value of the component vulnerability ratings for superstructure movement joints, columns or pier walls, or foundations or abutments. For example, retrofitting cost can be estimated at 15 percent of structure value for bridges in which the seismic vulnerability rating is governed by the rating for superstructure movement joints, and estimated at 25 percent of structure value for all other bridges. This would reflect that movement joint seismic deficiencies are generally easier to retrofit than substructure seismic deficiencies.

The benefit/cost ratio for upgrading can be calculated as shown in Figure 12.1, according to the following formula:

$$\frac{Benefit}{Cost} = \frac{(Losses,\ No\ Retrofit) - (Losses,\ After\ Retrofit)}{Retrofit\ Cost}$$

The losses after retrofit can be calculated by estimating what the vulnerability rating of the bridge will be after retrofitting. If retrofits are done to a high standard of earthquake performance, eg, to the same criteria as for new bridges, this term could be neglected. More typically, however, a retrofit programme may be carried out only to address the worst seismic deficiencies, so that a less stringent earthquake performance criteria is used compared to that for new bridges. For example, a bridge with a high vulnerability rating of 9.5 may, after retrofitting, still have a medium vulnerability rating of 5.5. For this bridge, the benefit/cost ratio is based on the difference between losses calculated for V = 9.5 and those calculated for V = 5.5.

In calculating benefit/cost ratios, three additional points should be noted:

1 The expected seismic losses are calculated over the estimated remaining service life for the bridge. The time value of money should be accounted for in the calculations of benefit/cost ratio, so that the present worth of the benefits is compared with the present worth of costs.

2 The benefits calculated are the *expected value* of benefits. Clearly there is a tremendous possible range of the actual value of benefits for any given bridge, depending on what level of earthquake, if any, actually occurs, and on numerous uncertainties in damage estimation and asset value determinations.

3 Part of the benefits of retrofitting come from avoiding the costs of bridge repair or replacement due to earthquake damage. As shown in Figure 12.1, this portion of the benefits is derived from the structure value portion of bridge asset value. Another possible formulation of benefit/cost ratio would consider the avoided costs of bridge repair as negative costs rather than positive benefits. In such a case the benefit/cost ratio would be formulated as follows:

$$\frac{\text{Benefit}}{\text{Cost}} = \frac{\left[\frac{\text{Expected User Losses}}{\text{No Retrofit}}\right] - \left[\frac{\text{Expected User Losses}}{\text{After Retrofit}}\right]}{\text{Refrofit Cost} + \left[\frac{\text{Expected Repair Costs}}{\text{After Retrofit}}\right] - \left[\frac{\text{Expected Repair Costs}}{\text{No Retrofit}}\right]}$$

Application of Cost-benefit Results

The benefit/cost ratios calculated above can be used as a relative measure to compare retrofit options. As previously emphasized, the ratios are only approximate. If they are to be considered as an absolute measure of the worth of retrofitting, several cautions must be observed:

- Not all of the benefits of seismic retrofitting can be easily quantified. For example, a major benefit of retrofitting might be to avoid the bad publicity and loss of public confidence in the transportation authority, such as occurred in California after the 1989 Loma Prieta earthquake.

- Numerous assumptions and uncertainties are inherent in estimating benefit/cost ratios, including probabilities of earthquake occurrence, estimated damage at different earthquake levels, loss-of-service times, costs of disruption, and probabilities of collapse, injuries, fatalities, and associated costs. Different assumptions can result in significant differences in the computed benefit/cost ratios. However if the assumptions are made consistently for all bridges evaluated, the benefit/cost ratio will still be an accurate measure for the prioritization for seismic upgrading within the group of bridges.

12.8 Simplified Prioritization Formula

It is also possible for the preliminary screening stage, to use a single prioritization formula instead of explicit calculations of benefit/cost ratio. The recommended formula is based on the seismic vulnerability rating and three additional variables:

$$B/C = (V - 1.5)^2 \left[0.1 + \frac{ADT\,(DET * K_{FORD} + 5)}{500{,}000}\right]$$

where:

B/C	=	Approximate Benefit/Cost Ratio for Upgrade.
V	=	Seismic Vulnerability Rating, 2-10.
ADT	=	Average Daily Traffic (Vehicles/Day).
DET	=	Detour Length (km).
K_{FORD}	=	1 if it is possible to construct a temporary ford in place of the bridge; 5 = otherwise

The formula was developed by the author to approximate the cost-benefit results which were calculated for 56 bridges in the Tasman district. The term $(V - 1.5)^2$ reflects the likely amount of bridge damage due to an earthquake, as shown in Figure 12.9. The term 0.1 reflects the structure-value portion of bridge-asset value; it is a constant because retrofit costs are assumed proportional to structure value. The remaining term reflects the loss-of-use value of the bridge, which is proportional to ADT. Within this term, the quantity $DET{*}K_{FORD}$ reflects the loss-of-use costs coming from transportation disruption, while the constant 5 reflects the costs of casualties or other losses.

The formula assumes all bridges are in the same seismic zone. When applied to a group of bridges in different seismic zones, the formula should be modified. This can be done by multiplying the vulnerability rating, V, by a seismicity factor. For New Zealand's seismic zones, the formula can be assumed applicable to the highest seismic zone, $Z = 1.2$. For other seismic zones V should be multiplied by $Z/1.2$, where Z is the seismic zone coefficient for structural design [SANZ 1992].

CHAPTER 13
BRIDGE SEISMIC RISK AND UPGRADE MANAGEMENT RESULTS FOR NEW ZEALAND'S TASMAN DISTRICT

This chapter presents selected results from the seismic risk and bridge asset management study conducted for New Zealand's Tasman District [Maffei 1994]. The purpose of the chapter is to show some of the applications of the recommended evaluation and prioritization methods described in Chapter 12.

In the Tasman District, a pilot-study sample of 56 bridges was evaluated with a visual structural assessment and an approximate cost-benefit analysis. The seismic vulnerability results for these bridges are presented in Section 13.1. In Section 13.2 the results are extrapolated so that the vulnerability of the entire stock of 445 bridges is considered. Sections 13.3 and 13.4 use the results to assess, in economic terms, different possible bridge-upgrade programs.

An important part of implementing a seismic evaluation and upgrade program in a bridge jurisdiction is a computer database for bridge information. Section 13.5 presents several recommendations for bridge databases.

The results presented in this chapter are meant to be illustrative only; in some cases they are based only on preliminary findings from the Tasman District. The benefit/cost ratios presented should be considered as an approximate and relative measure of the worth or seismic upgrading, rather than as an absolute economic indicator.

13.1 Vulnerability Rating Results

For the Tasman District, each of the 56 pilot-study bridges was seismically evaluated with a level-one assessment, and a vulnerability rating on the 0-10 scale was assigned to each structure. The rating scale and procedure for these evaluations is described in Sections 12.3 and 12.4. For most of the bridges the soil profile condition was not studied, so final vulnerability ratings have not been used; rather the structural-vulnerability rating has been used.

Figure 13.1, graph (a), shows the distribution of results of the seismic assessments of the pilot study bridges. The structural vulnerability ratings for these 56 bridges fall between the values of 1 and 10, with many bridges having vulnerabilities in the range of 2 to 4, and a number of more vulnerable bridges having ratings in the range of 5 to 9. The mean vulnerability rating is 4.8; the median rating is 3.8.

Bridge structural vulnerability was found to vary with bridge length. Figure 13.2 shows a plot of structural vulnerability rating versus bridge length. It can be seen that nearly all of the bridges with low vulnerability ratings of 2 or 3 are less than 15 m in length, and that as bridges get longer, particularly in the 30-50 m range, bridge seismic vulnerability tends to be higher. This is not to say that short bridges cannot be also be vulnerable. There are a few short bridges which were found to have high seismic vulnerability.

The association of seismic vulnerability with bridge length is important for two reasons. The first is that the value of a bridge greatly increases with bridge length, so that even though the number of vulnerable bridges may be low the asset value of those bridges can still be significant. Second, the typical length of the pilot-study bridges is greater than that of the overall bridge stock for the Tasman District so that the vulnerability characteristics of the pilot study need to be adjusted somewhat to be representative of the entire bridge stock.

The distribution of bridge asset value as a function of seismic vulnerability rating is shown in Figure 13.1, graph (b). In comparison with Figure 13.1(a), Figure 13.1(b) demonstrates that a substantial portion of the asset value of the Tasman District bridges fall within the medium to high seismic vulnerability range. The mean structural-vulnerability rating of the bridges based on asset value is 5.7, significantly higher than the mean based on number of bridges. The *median* vulnerability based on asset value is approximately 5.9 (ie, 50 percent of the asset value of the pilot study bridges have a vulnerability greater than 5.9).

13.2 Extrapolation to the Entire Bridge Sample

Before extrapolating the results for the pilot study bridges to the total Tasman District bridge stock, the variables characterising the two bridge samples were studied. The most important of these variables are listed in Table 13.1. There are 56 bridges in the pilot study and 445 bridges total in the district. The average bridge length is 24.3 m for the pilot-study bridges and 15.7 m for the total bridge stock. The pilot study bridges include several long crossings of the Motueka river which push up the average bridge length. The *median* bridge length for the pilot study is also higher than that for the total bridge stock. The percentage of one lane bridges is smaller for the pilot-study bridges than for the total bridge stock. Of the pilot-study bridges 48 percent are one-lane bridges, while of all of the district bridges, 65 percent are one-lane bridges.

Bridge Structure Value

The structural value of the pilot-study bridges, calculated as described in Section 4.2, averages \$200,000 per bridge, giving a total value of \$11.2 million for the 56 pilot-study bridges. The structural value per metre of length of the pilot study bridges is \$8,240. To estimate the structural value of the entire bridge stock, it is necessary to account for (a) the shorter average bridge length, and (b) the greater predominance of one-lane bridges amongst the entire bridge stock. Assuming that the structural value

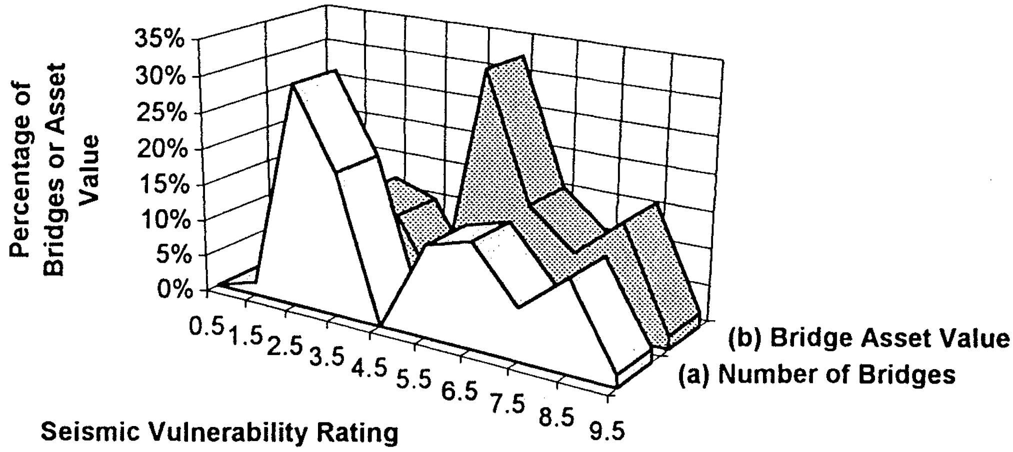

Figure 13.1 Distribution of bridge seismic vulnerability for the 56 pilot-study bridges: (a), by number of bridges, and (b) by asset value of the bridges.

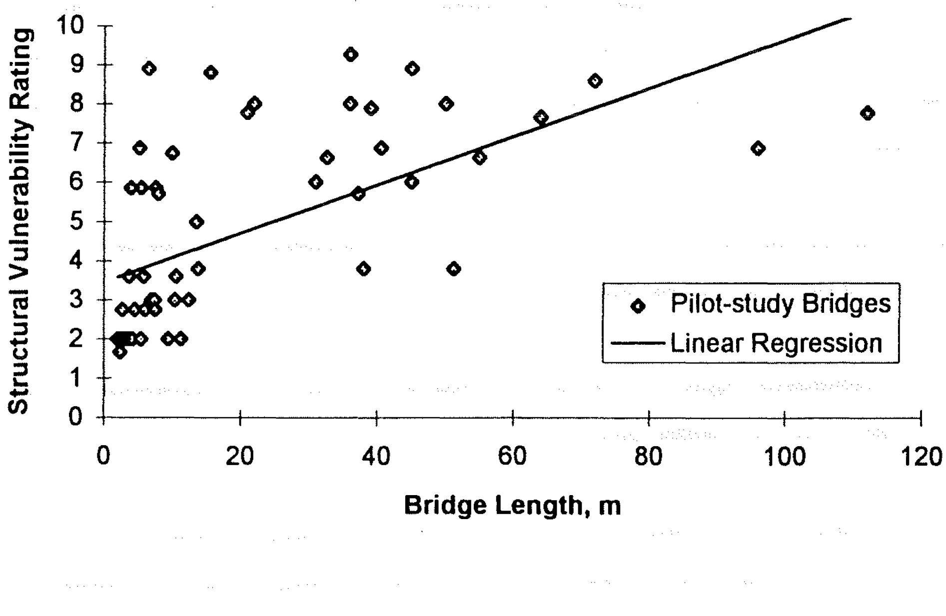

Figure 13.2 Relationship between seismic vulnerability and bridge length for the 56 pilot-study bridges.

of one-lane bridges is 70 percent of that of two-lane bridges, a linear interpolation is used to calculate an average structural value per length for the entire bridge stock. The result of this interpolation calculation is $7,750 per metre of bridge length. This value is multiplied by the total bridge length for the Tasman District to give a structural value of $54.2 million for the district bridges.

Bridge Loss-of-Use Value

The loss-of-use value of the bridges is calculated according to the method described in Section 12.7. For the pilot-study bridges the average loss-of-use value was found to be $177,000 per bridge (in 1994 dollars), giving a total loss-of-use value for the 56 pilot-study bridges of $9.9 million. The ratio of loss-of-use value to structural value for the bridges is 0.88. This ratio is thought to be roughly independent of bridge length, number of lanes, or any other variables which differ between the pilot-study bridge sample and the entire bridge stock. Therefore the ratio 0.88 is used to estimate the loss-of-use value for the entire bridge stock. The resulting loss-of-use value for all of the Tasman District bridges is $48 million. The resulting *total asset value* of the Tasman District bridges then is $54.2 million structural value plus $48 million loss-of-use value, equal to $102 million asset value. The estimate of bridge loss-of-use value can depend greatly on the discount factor assumed in converting future values into present worths. The results given here assume a relatively low discount factor.

Seismic Vulnerability Ratings

As discussed in the previous section, the distribution of bridge vulnerability is expected to be slightly different for the entire bridge stock than it is for the pilot-study bridges due to the predominance of longer bridges in the pilot-study sample. The distribution of vulnerability ratings for the pilot-study bridges shown in Figure 13.1 shows a significant amount of unevenness, due to the small sample size of 56 bridges. For a larger sample of bridges, a smoother distribution of seismic vulnerability ratings would be expected.

To estimate a realistic distribution of the asset-value versus vulnerability rating for the entire stock of 445 bridges, a two-step process was used.

1 The distribution of Figure 13.1(b) was simplified to a smoother distribution with approximately the same mean and median values.

2 The distribution was shifted towards a lower mean and median vulnerability, to account for the greater predominance of shorter bridges in the 445-bridge sample compared to the 56-bridge sample. The shift of mean vulnerability was calculated to roughly correspond to the shift of mean bridge length between the pilot-study and total bridge sample considering the vulnerability-versus-length regression line shown in Figure 13.2.

Table 13.1 Comparison Of Pilot-study Bridge Sample With Total Bridge Stock

Category	Item		Pilot-study Bridges	All Bridges
Basic Data	Number of bridges		56 (12.2%)	445
	Bridge Length	Average	24.3 m	15.7 m
		Median	10.4 m	9.0 m
		Total Length	1360 (19.5%)	6990
	Percentage one lane bridges		48.2%	65.4%
Asset Value	Average Traffic AADT		349 vpd	Unknown
	Average Terrain Factor		1.06	Unknown
	Average Location Factor		1.08	Unknown
	Average Bridge Replacement Time		12.0 weeks	Unknown
	Average Benefit/Cost to build Ford during bridge replacement		3.9	Unknown
	Structure Value	Average	$199,700	$122,000 *
		Total	$11,200,000	$54,200,000 *
		Value/Length	$8,240/m	$7,750/m *
	Loss-of-use Value	Average	$177,000	$108,000 *
		Total	$9,910,000	$48,000,000 *
	Loss-of-use Value ÷ Structure Value		0.88	0.88 *
	Total Asset Value	Average	$377,000	$230,000
		Total	$2,100,000 (20.7%)	$102,000,000
Seismic Vulnerability	Structural Vulnerability Rating:			
	Average by number of bridges		4.8	4.4 *
	Median by number of bridges		3.8	3.5 *
	Average by Asset Value		5.7	5.4 *
	Median by Asset Value		5.9	5.2 *

* Extrapolated from pilot-study sample.

For simplification, the minimum vulnerability rating was taken as 2.0.

The resulting distribution of asset value versus seismic-vulnerability rating is shown in Figure 13.3, graph (a). This distribution indicates that 35% of the bridges have low seismic vulnerabilities between 2 and 4, and that 65% of the bridges have moderate to high seismic vulnerabilities, with ratings between 4 and 10.

13.3 Expected Seismic Damage and Effect of Upgrading

The seismic vulnerability distribution as shown in Figure 13.3(a) for the Tasman District bridges is used to give an estimate of the likely earthquake damage to district bridges over the next 65 years. The 65-year period is equal to the assumed average remaining service life of the bridges in the district. The typical lifespan of a bridge is assumed to be 100 years, according to Transit New Zealand guidelines. Among the pilot-study bridges the average bridge age is approximately 35 years. Thus on average, the Tasman District bridges could be expected to have 65 years of service life remaining.

The expected seismic damage is calculated by combining the distribution of asset value versus seismic vulnerability, Figure 13.3(a), with the expected bridge damage versus vulnerability curve shown in Figure 12.9. The combination of these damage estimates with the asset value of the bridges in each vulnerability category indicates an earthquake loss of 20.3% of the bridge asset value over the next 65 years. This equates to a loss of $20.7 million in bridge reconstruction costs and disruption costs to the bridge users.

Effect of Seismic Upgrading

Three possible levels of seismic-upgrade programs are considered here for illustration. A stage-one program which retrofits the most critical 19% of bridge-asset value, a stage-two program which retrofits an additional 14% of the bridge-asset value, and a hypothetical stage-three seismic upgrade program which retrofits all bridges with vulnerability ratings above 4. The benefit of implementing a bridge seismic upgrade program is considered by adjusting the bridge asset value versus vulnerability distribution to account for seismic upgrades which would be carried out. This is illustrated in Figure 13.3.

It is expected that the seismic retrofit criteria for an upgrading program would be flexible, allowing different retrofit options to be considered for each bridge. (See Chapter 14 for recommended methods of deciding between various retrofit options). A complete retrofit -- ie, to a seismic performance level equivalent to that of a new bridge -- would reduce the vulnerability rating of a bridge to around 2. A minimal seismic retrofit, addressing only the worst seismic deficiencies, would reduce the vulnerability rating of a bridge to perhaps 5. In the stage-one and stage-two retrofit programs, it is assumed that bridges would be retrofitted to somewhere between these two standards.

Stage-one Retrofit Program

Figure 13.3(b) shows a plot of the new asset value versus vulnerability distribution upon completion of a "stage-one" seismic upgrade program which retrofits the most critical 19% of the bridge asset value. The most critical bridges would be those with the worst combination of high vulnerability ratings and high importance variables such as traffic volume. The upgrading of each bridge would be

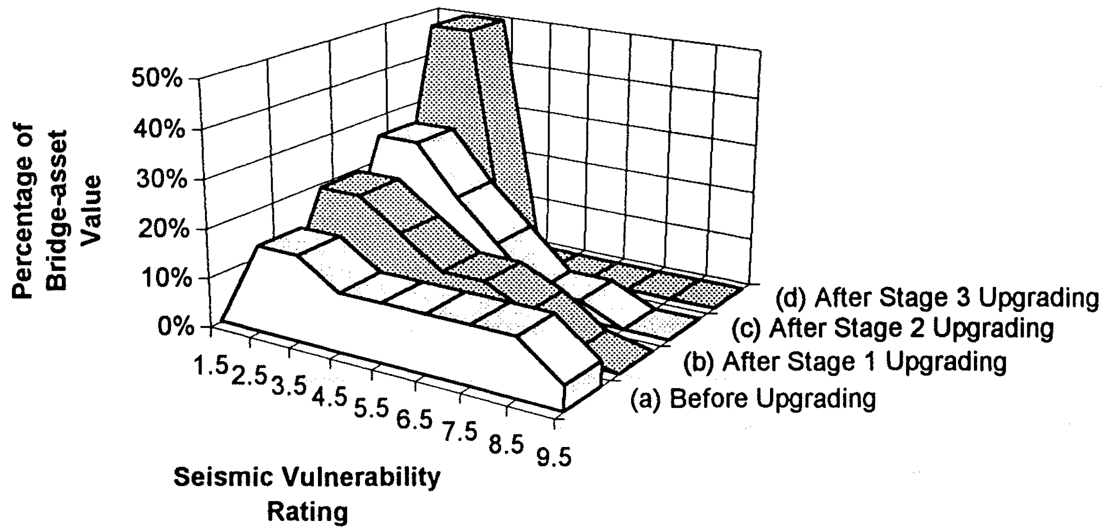

Figure 13.3 Assumed distribution of asset value versus vulnerability rating for the Tasman District bridge stock: (a) before upgrading, (b) after stage-one upgrading, (c) after stage-two upgrading, and (d) after an idealistic stage-three upgrading.

considered individually using structural and economic evaluations. After completion of the evaluations and stage-one seismic upgrading it is expected that most of the bridges in vulnerability categories from 8-10 would be upgraded and a few bridges in vulnerability category 7-8 would be upgraded. After upgrading, these bridges would have an improved seismic vulnerability rating, in the range of 2-5 for typical seismic-retrofit criteria. Thus the distribution of asset value versus vulnerability is shifted, with a portion of the asset value coming from the rating levels 7-10 and being moved down to the rating levels 2-5. The assumed vulnerability distribution after such an upgrade program is shown in Figure 13.3(b).

Having postulated this new vulnerability distribution, the expected earthquake losses over the next 65 years are calculated in the same manner as before. The expected earthquake losses after stage-one upgrading are 11.6% of the bridge asset value or $11.8 million. Compared to the earthquake losses with no upgrading, $8.8 million is saved in earthquake damage costs.

Stage-two Retrofit Program

If further seismic upgrading is contemplated, additional vulnerable bridges can be seismically retrofitted. It can be assumed that in the second stage of upgrading a number of the bridges with vulnerability ratings from 6-8 will be seismically retrofitted and that the asset-value versus vulnerability distribution will be shifted to an even more favourable distribution as shown in Figure 13.3(c). This stage-two program would seismically upgrade an additional 14% of the bridge asset value. Assuming such a vulnerability distribution after stage-two upgrading, the predicted earthquake losses are again calculated. The results indicate that after a stage-two upgrading only 7.7% of the bridge asset value will be lost due to earthquake damage over the next 65 years. This equates to a loss of $7.8 million.

Stage-three Retrofit Program

A hypothetical stage-three upgrading program is also considered, Figure 13.3(d), where all bridges with structural vulnerability ratings above 4 were seismically retrofitted. Such an extensive retrofitting program generally would not be economically justified, however it is considered here for illustration. As a result of this complete upgrading of district bridges, the expected seismic loss to the Tasman District bridges over the next 65 years would be only 2.5% of the bridge asset value, or $2.5 million.

13.4 Benefit/Cost Ratios for Seismic Upgrading.

Estimates of benefit and cost have been calculated for the three possible seismic upgrading programs described in Figure 13.3. The benefit of each stage of seismic upgrading is calculated as an incremental benefit equal to the savings in seismic damage due to carrying out that stage of the upgrade program.

For the stage-one upgrade program, addressing the most vulnerable bridges, it is estimated that seismic upgrading will cost on average, 20 percent of the structural value (or replacement cost) of each upgraded bridge. For some bridges the cost of upgrading will be less because perhaps only superstructure restrainers or hold-down devices would need to be added to the structure, however for other bridges the cost of upgrade could be more than 20 percent of replacement value. This may be the case if column jacketing or foundation strengthening were required. Based on the 20 percent of replacement-cost figure, the cost of the stage-one seismic upgrade program is estimated to be $2.6 million. The benefit of the stage-one upgrading program is calculated to be the earthquake losses with no upgrading, $20.7 million, minus the earthquake losses assuming the upgrading has been carried out, $11.8 million. The difference, equal to the savings in earthquake losses, is $8.8 million. This number divided by the cost of the upgrading program gives the benefit/cost ratio of 4.3 for carrying out the seismic upgrading of these bridges.

For the stage-two seismic upgrading program it is assumed that the cost of upgrading is somewhat higher per bridge than for the stage-one seismic upgrading. This is because in the stage-one program some of the more vulnerable details are the easier-to-fix details, the restraint and hold-down of bridge movement joints for example. It is estimated that for the stage 2 upgrading, the average upgrade cost would be 35% of the replacement cost of each upgraded bridge. This results in a cost of $2.7 million for the stage-two seismic upgrading program.

In calculating the potential benefit of the stage-two seismic upgrade program, it is assumed that the stage-one upgrading has been completely carried out, so that if no further upgrading is done earthquake losses of $11.8 million are anticipated. If the additional bridges of stage-two are upgraded, then the expected earthquake losses will reduce to $7.8 million. Thus the incremental benefit is the difference between $11.8 million and $7.8 million, equal to $4.0 million. The benefit/cost ratio, then, of the stage-two upgrading is equal to $4.0 million divided by $2.7 million, and is equal to 1.5.

For illustrative purposes the benefit/cost ratio for an idealistic stage-three seismic upgrade program is calculated. The costs of such a complete seismic upgrading is estimated to be 50% of the replacement cost of each bridge, resulting in an upgrade cost of $10.8 million. The incremental benefit of such an upgrade program, equal to the savings in damage over that already achieved in the stage-one and stage-two seismic upgrade programs, is calculated to be $5.3 million. This yields a benefit/cost ratio of 0.61.

These calculations confirm that it would not be economically justified to carry out such an extensive bridge-seismic upgrade program.

The cost-benefit results of the three seismic-upgrade scenarios are each plotted as a point in Figure 13.4. In the figure, a line is drawn through the three points to show the estimated distribution of the benefit/cost ratios for the seismic upgrading of the Tasman District bridges. Note that this distribution is based on rough extrapolations from the pilot-study bridge sample. As the bridge database input and preliminary screening program is completed, benefit/cost ratios for each bridge can be calculated and a better estimate of the distribution of the benefit/cost ratios can be made.

The distribution of Figure 13.4 indicates that 45 percent of the district's bridge assets have a benefit/cost ratio for seismic upgrading which is greater than one. The figure shows that 15 percent of the bridge-asset value is vulnerable enough to have a benefit/cost ratio for seismic upgrading greater than 5.

As emphasised in Section 12.7, the benefit/cost ratios should not be interpreted as an absolute measure of the worth of seismic retrofitting, because the values of the benefit/cost ratios can be significantly changed by changing the assumptions used in the bridge evaluation. The benefit/cost ratio is however very useful as a relative measure, and although the actual values of the ratios could be debated, the *shape* of the distribution shown in Figure 13.4 is thought to be illustrative of the typical economic characteristics of bridge seismic upgrading.

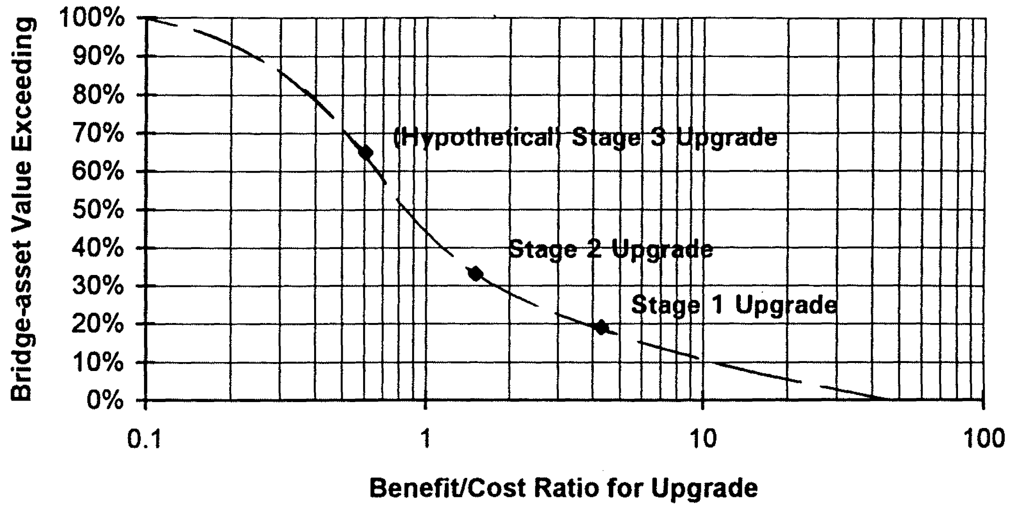

Figure 13.4 Estimated distribution among the Tasman District bridges of benefit/cost ratio for seismic upgrade.

13.5 The Bridge Database

An important component of implementing a bridge seismic-retrofit program is to establish a system for the bridge inventory or database. The bridge database for many jurisdictions can be used for more than just seismic-assessment data. This was the case in the Tasman District where it was requested that the database be designed to eventually contain all of the information necessary for calculating bridge-asset values, determining and recording bridge seismic risk and flood risk, recording vehicle load ratings and speed and safety ratings, and finally, recording bridge condition data including inspection records and maintenance records.

This section describes the objectives and recommended content and organization of such a database, and also briefly outlines an improved inspection procedure for bridges.

Objectives of the Database

The bridge database for a jurisdiction should be designed to (1) contain all of the important information for each bridge, (2) provide the capability to analyze the data to determine results such as asset values, benefit/cost ratios of upgrades, and seismic vulnerability ratings, and (3) be flexible so that it can be revised and built upon in the future. The database should also be organized for ease of use.

In the Tasman District, the bridge inventory and database is designed to record and save important data on:

(a) factors related to the asset value of the bridge, such as daily traffic (ADT) and structural replacement cost,

(b) condition records and maintenance requirements for each bridge,

(c) seismic assessment variables, such as structural features, year of construction, and seismic assessment results and vulnerability ratings,

(d) vehicle-load ratings so that applications for overweight permits can be quickly checked,

(e) an assessment of the speed and safety condition of the bridge, and

(f) variables and assessment results associated with flood risk to a bridge.

Much of this data is used for the bridge asset-value determinations, as discussed in Section 12.7, and for the management of bridge maintenance and upgrade work.

As shown in item (b) above, part of the Tasman District Council bridge database involves bridge maintenance. A study of bridge maintenance management has been carried out in New Zealand by J H Wood [1993]. The study concisely defines the goals of a bridge maintenance management system, and considers more specifically eighteen capabilities that can be provided in a bridge maintenance-management system.

Content and Organisation of the Database

As part of the bridge seismic-risk and asset-management study for the Tasman District [Maffei 1994], recommendations have been made for the content and organization of the bridge computer database. Some of the recommendations for bridge databases are summarized here. The recommendations are intended as guidelines only, realizing that different bridge jurisdictions will use their databases in different ways, and will use different computer software.

The lists of data items given below are intended to be neither completely exhaustive, nor minimized. In many cases more data items are listed than would be recommended to use for a specific purpose (such as calculating a seismic vulnerability rating). This is because often it is worthwhile to include extra data items which require little additional effort to record but which may turn out to be useful.

Bridge data items can be organized by either the purpose or the source of the data:

Organization by Purpose of the Data

When reviewing bridge inventory information, it is best to have the information grouped according to the purpose of the data. Tables 13.2 through 13.5 show some of the data items that may be needed for purposes such as asset value determination and seismic risk assessment.

Table 13.2 Basic Bridge Data

CATEGORY	DATA ITEM	SOURCE OF DATA	NOTES
Identification and Location	Bridge File No	Input	
	Bridge Name	Input	
	Old Bridge No	Input	
	Name of Road	Input	
	Obstacles crossed	Input	
	Route Point of:		
	Bridge	Input	Meters
	Start Segment	Input	Meters
	Finish Segment	Input	Meters
	Drawing Nos and No of drawing sheets	Input	
	Notes	Input	
Geometry	No Lanes	Input	
	Length	Input	Meters
	No Spans	Input	
	Span Length	Input	Meters
	Width - kerb	Input	Meters
	Width - from RAMM	Input	Meters
Structure	Structure type:		See table of structure types.
	Deck	Input	
	Beam/Truss	Input	
	Column/Pier	Input	
	Col/Pier Foundation	Input	
	Abutment	Input	
	Abutment	Input	
	Foundation	Input	
	Year of construction	Input	
	Year of major upgrade	Input	
	Structure description	Input	

The last column in each of the Tables 13.2 through 13.5 is titled "Notes" and describes some of the details of data items which are not self explanatory. In some cases the notes indicate the possible range of values assigned to data items, or formulas used to calculate asset values, vulnerability ratings, or costs and benefits of upgrade proposals.

The basic bridge data shown in Table 13.2 contains information to identify the bridge and its location, data on the geometry of the bridge such as number of lanes and length, and data on the structure of the bridge, which includes the year of construction and the categories of structure type as described in Section 12.4.

The asset value data shown in Table 13.3 includes information relating to the replacement cost of the bridge, to the importance of the bridge as a transportation link, and consequently to the loss-of-use value of the bridge

Table 13.3 Asset Value Data

CATEGORY	DATA ITEM	SOURCE OF DATA	NOTES
Structure Value	Length No Lanes Terrain Factor Location Factor Replacement Cost	Prev. Input Prev. Input Input Input Calculate	 1.0 avg Terrain, > 1.0 difficult. 1.0 accessible, > 1.0 remote. Function of length, lanes, terrain, location.
Route Importance	ADT Route Hierarchy % Heavy Vehicles Detour Length Detour Routes Detour Route Hierarchy Detour Cost Factor Possibility of Temporary Access (eg ford) Utilities Carried Utilities Factor Access to Critical Facilities Critical Access Factor	Input Input Calculate Input Input Input Calculate Input Input Input Input Input	 5 = Arterial, 3 = Collector, 1 = Access Depends on route hierarchy. Complete length from one side of the bridge to the other. Yes, No, type of utilities. 1.0 = no utility, 1.05-1.2 utility Type of facilities 1.0 = no crit.fac 1.1-2.0 crit.fac
Loss-of-use Value	Replacement Time, weeks Disruption Cost	Calculate Calculate	Linear function of cost. Function of ADT, % heavy veh, detour costs.
Total Value	Total Value	Calculate	Replacement + Disruption cost.
Construction Cost Data	Year of Construction Cost of Construction CCI in year built Cost per Current CCI Compare cost to replacement cost	Prev. Input Input Input Input Calculate	

as described in Section 12.7 of this report. The total value of the bridge is considered to be the sum of the structure value (or replacement cost) of the bridge plus the loss-of-use value (or disruption cost) of the bridge.

The seismic risk assessment data is outlined in Table 13.4. These data include the seismic vulnerability ratings which are described in Section 12.3, and information on the seismicity and soil profile at the site. The database can automatically calculate a final seismic vulnerability rating based on formulas presented in Chapter 12. Additionally, the database can use the total bridge value, previously calculated, in an estimate of the benefit/cost ratio of proposed seismic upgrading.

Table 13.4 Seismic Risk Data

CATEGORY	DATA ITEM	SOURCE OF DATA	NOTES
Structure Risk	Structure type No Lanes Length No Spans Span Lengths Year of construction Year of major upgrade Structure description Presence of movement joints Support lengths Movement joint risk factor Column/wall risk factor Foundation/abutment risk factor Structure risk factor	Prev. Input Prev. Input Prev. Input Prev. Input Prev. Input Prev. Input Input Input Input Input Input Input Input Calculate	 Yes, no, restrained. mm O = no movement joints, 10 = vulnerable. 0 = not vulnerable, 10 = vulnerable. 0 = not vulnerable, 10 = vulnerable. Highest of above 3 factors.
Soil and seismicity	Soil Profile type Liquefaction potential Soil factor Seismic zone coefficient Seismicity factor	Input Input Input Input Calculate	1,2,3, or 4 corresponding to UBC. No, maybe, yes, high. 1.0, 1.2, 1.5, 2.0 per UBC, also high liquefaction = 2.0. From NZS 4203 1992. = zone coefficient ÷ 1.2
Seismic Risk Rating	Rating	Calculate	= (structure x soil x seismicity)$^{0.85}$
Recommended Upgrade	Upgrade Measure Estimated cost Total value of bridge Seismic damage probability Estimated benefit Benefit/cost	Input Input Prev. Input Calculate Calculate Calculate	 Based on seismic risk rating. Based on damage probability and bridge value.

Table 13.5 Condition and Maintenance Data

CATEGORY	DATA ITEM	SOURCE OF DATA	NOTES
Structure	Structure Type Year of Construction Year of major upgrade Structure description	Prev. Input Prev. Input Prev. Input Prev. Input	
Inspection Record	Date of last Gen.Inspection. Findings. Date of last Detailed Inspn. Findings.	Input Input Input Input	
Maintenance Record	Date of Maintenance Description of Maintenance Estimated vs Actual costs, unit costs	Input Input Input	
Recommended Maintenance	Condition Summary	Input	
	Vulnerability to Scour	Input	None, low, medium, high.
	Recom maintenance Items	Input	
	Date by which maintenance item should be completed	Input	
	Est remaining Serv.Life Est costs of maintenance	Input Input	Assuming Maintn is carried out $/year
	Est benefit of maintenance	Input	In years of increased service life provided.
	Total asset value of bridge	Prev. Input Calculate	
	Est $ benefit of maintenance		$ based on asset value depreciation and increase service life.
	Benefit/cost	Calculate	

As shown in Table 13.5, a fourth category of data can be defined, relating to the condition and maintenance of each bridge. Such data would include information from the inspection and maintenance records of each bridge, and calculated benefits and costs of specific proposed maintenance measures.

Additional blocks of data which relate to different specific purposes can also be included in the database. For example, vehicle overweight load ratings can be input into the database along with the source and date of the vehicle-load rating information. Information on the flood potential at the bridge site, and information on safe crossing speed and records of accidents, could also be included.

Organisation by Source of Data

The items of the bridge database can also be grouped according to the source of the data. It is recommended that data items be grouped in this way for the input to the database. For some computer database programs input forms which are structured by data source can be created, while output forms can be structured around the purpose of the data. The sources of bridge data for the Tasman District were the following:

1 bridge drawings,
2 bridge files,
3 topographic maps of bridge locations and terrain,
4 field inspection reports, and
5 the road-analysis computer program RAMM which provides traffic data.

Data items coming from the drawings include: drawing numbers, number of drawing sheets, which drawings are structural drawings, number of lanes, bridge length, number of spans, span length, bridge width, structure type, year of construction, year of major upgrades, structural details, soil-profile type, and information regarding seismic risk variables. The terrain factor for asset value can also be estimated from the drawings.

Input from bridge files includes dates of inspections and findings, and dates of maintenance carried out and associated costs and descriptions of maintenance. The presence of structural calculations in the files should also be noted in the database.

Input from map data includes the name of the waterway or other obstacle which is crossed by the bridge, the location factor for bridge cost, and the detour length for the bridge. (Note that detour length is computed as the complete circular length from one side of the bridge to the other when the bridge itself cannot be crossed. In this way, detour length is computed consistently for all bridges and does not vary depending on the intended route or destination of the traveller). Names of the routes making up the detour length are also input to the database. Often it can be judged from a topographic map whether a bridge can be replaced by a temporary ford during construction. If the bridge provides access to a critical facility such as a hospital or police station, that can also be recorded with the map data.

The bridge inventory and database relies on the RAMM output for the average daily traffic estimate (ADT) for each bridge, for the hierarchy of the bridge route, and for the hierarchy of the detour route. There are five route hierarchies used by the Tasman District Council. In the database the hierarchies are given numbers from one to five so that route hierarchy can be mathematically related to the percentage of heavy vehicles on the route, and to the cost to bridge users of having to take the detour route. The five route hierarchies are: arterial = 5, main distributor = 4, collector = 3, access/collector = 2, and access = 1.

Data from the site inspection of the bridge can be used to fill in the gaps in the bridge inventory, particularly if drawings for the bridges are not available as is the case with a number of the Tasman District bridges.

Bridge Inspection Data and Procedure

As part of the study for the Tasman District, the form used to record bridge-inspection results was reviewed. From this review and the experience of inspecting the 56 pilot-study bridges, a new version of the bridge inspection data sheet and report form was recommended.

The recommended form is taken from the Transit New Zealand *Bridge Maintenance and Inspection Manual* [1991], with some modifications for the data specifically required by the Tasman District Council.

The new form is less ambiguous than the form used previously and is easier to complete, with less additional writing and less subjective judgements necessary. In the Transit New Zealand form the inspection items of the bridge should be marked either "satisfactory," "routine maintenance required," or "urgent maintenance required." In customizing the form, an intermediate marking has been added to indicate items that are "marginally satisfactory."

CHAPTER 14
EVALUATION OF SEISMIC RETROFIT OPTIONS FOR THE THORNDON BRIDGE

Chapter 13 showed the application of the recommended methods of bridge-upgrade management to a large group of bridges, based on a minimum level of evaluation; this chapter illustrates the application of the methods to a single major bridge, based on in-depth structural and economic evaluations. The study of retrofit concepts for the Thorndon bridge [BCHF 1994b] provides a unique example of the assessment of various seismic retrofit options for a major structure. To the author's knowledge, no other bridge retrofit project has used the in-depth evaluation methods summarized here.

This chapter shows the application of some of the general methods described in Chapter 12, such as the use of a probable seismicity curve combined with damage curves to estimate earthquake losses, and ultimately benefit/cost ratios for seismic upgrading. A probabilistic analysis of earthquake performance with respect to *limit states* is also presented. Such methods provide valuable information for choosing between different retrofit options.

This chapter focuses on those aspects of the Thorndon bridge study [BCHF 1994b] which were developed and proposed by the present author. These aspects include (a) the presentation of probable seismicity results and the need to separate Wellington fault seismicity from the seismicity from other sources, (b) the derivation of damage curves (and tables) from seismic evaluation results, (c) the consideration of seismic performance in terms of limit states, (d) the probabilistic assessment of limit-state performance, and (e) the presentation of economic analysis results.

Although these aspects of the Thorndon bridge study were conceived by the present author, the study of retrofit concepts was a team effort by BCHF consulting engineers, as indicated in the acknowledgements.

14.1 Background

A description of the structural features of the Thorndon bridge was given in Chapter 4, along with descriptions of some of the proposed retrofit measures. There are other important features of the bridge and its environment which affect the possible seismic retrofit options for the bridge, and the evaluation of the retrofit options, which are presented in this section.

Four basic retrofit options were defined for the bridge, as discussed in Section 14.3. The retrofit options range from a minimal scheme which addresses only the most vulnerable structural details, to extensive retrofit schemes which bring the bridge up to standards similar to those for new construction.

A major passenger ferry terminal and its parking lot are located near to and partially underneath the bridge. At certain times, a large number of ferry passengers could be under the bridge and would be at physical risk if the bridge were to collapse. In addition, railway yards are located near to and underneath the bridge. Regular passenger and freight trains pass under the bridge, and two busy urban streets also cross under the bridge.

The main bridge structure and the bridge off-ramp cross the Wellington fault. Because the fault offset can cause additional structural damage, the study of probable seismicity discussed in Section 14.2 considers the Wellington fault separately from other potential earthquake sources.

Since the purpose of this chapter is to illustrate the general principles and methods of evaluating different seismic retrofit options, not all aspects of the detailed study of retrofit concepts done by BCHF [1994b] are presented here. Some simplifications have been made. The retrofit costs and seismic performance discussed in Sections 14.3 and 14.5 are for the main bridge and on-ramp only, and exclude the off-ramp. The damage estimates and economic analyses of Sections 14.4 and 14.6, however, include the off-ramp.

14.2 Probable Seismicity

The seismic assessment of the Thorndon bridge [BCHF 1994a] included a detailed study of the seismicity at the bridge site. The study identified the known earthquake faults that could affect the bridge and used attenuation relationships and a probabilistic analysis to calculate return periods for different levels of earthquake shaking at the site. The return periods can be converted into probabilities of exceedance over any given interval, for example 50 years. Although the contributions of a number of earthquake faults were combined in the probabilistic seismicity analysis, it was found that the higher levels of earthquake accelerations were most likely to come from the Wellington fault, which crosses directly underneath a section of the bridge.

Earthquake damage to the Thorndon bridge can be caused by (1) the level of ground shaking, which can cause both structural failure and ground liquefaction, and (2) the permanent movement (up to a five-meter offset) of the Wellington fault, which is crossed by both the main structure and the off-ramp. The first effect, ground shaking, occurs for all possible earthquake sources, while the second effect, fault offset, occurs at the bridge only for a Wellington fault earthquake. Thus various levels of earthquake accelerations can occur with or without fault offset occurring.

To estimate the probability of a given level of damage to the bridge, then, the probabilities of Wellington fault ground shaking must be separated from the probabilities of distant-fault ground shaking. (Note that the relative term "distant-fault" is used in this chapter to denote all known earthquake sources other than the Wellington fault; some of these sources are within 20 or 30 km of the Thorndon bridge). Table 14.1 shows the approximate probabilities of different levels of ground shaking occurring from either the Wellington fault or distant faults. The dominance of the Wellington fault for the higher acceleration levels is evident from the last column of the table. The probabilities of exceedance can be plotted versus the level of earthquake spectral acceleration, as shown in Figure 14.1. This is similar to the probabilistic seismicity curves described in Figures 11.5 and 12.8.

Table 14.1 Probabilities of Various Earthquake Levels [BCHF 1994b]

Spectral Acceleration at T = 1.0 s	Probability of Exceedance in 50 Years, of the Spectral Acceleration			Probability that if given acceleration is exceeded it will be due to Wgtn Fault
	All Earthquake Sources	Wellington Fault Only	Distant Faults Only	
0.34 g	24%	11%	15%	42%
0.50 g	19%	11%	9.5%	54%
0.84 g	13%	9%	4.5%	67%
1.3 g	10%	7%	3%	70%
2.0 g	6%	5%	1%	83%

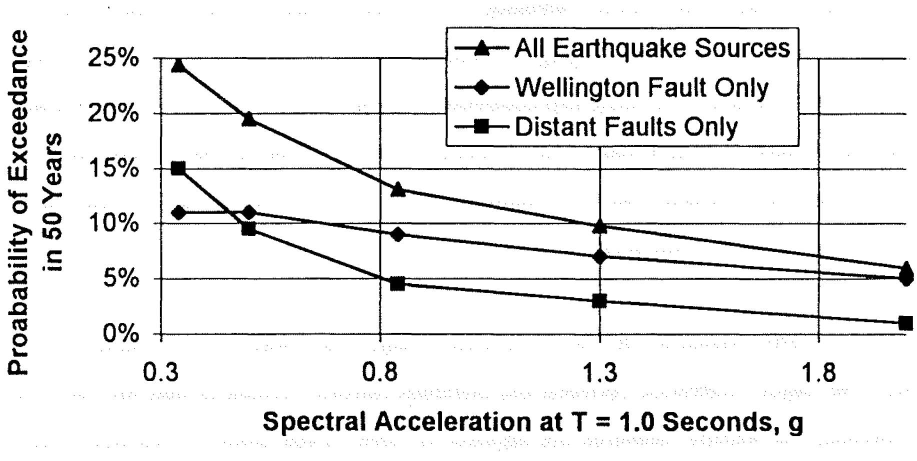

Figure 14.1 Probable seismicity curve for the Thorndon bridge.

14.3 Proposed Retrofit Options

Four different retrofit options were proposed for the Thorndon bridge, based roughly on different design earthquake levels [BCHF 1994b]. The four retrofit options are described in Table 14.2.

Table 14.2 Retrofit Options for the Thorndon Bridge

Retrofit Option	Cost	Description of Retrofit Measures
A	\$2.6M	Jacket columns at 15% of piers, strengthen pilecaps at 20% of piers
B	\$4.6M	Retrofit superstructure linkages at 30% of piers, jacket columns at 40% of piers, strengthen pilecaps at 45% of piers
C	\$14M	Retrofit superstructure linkages at all piers, add support frames for Wellington fault offset, jacket columns at 60% of piers, strengthen pilecaps at 80% of piers.
D	\$54M	Same as option C, but strengthen ground against liquefaction with stone columns (vibro-replacement) and jet grouting.

Retrofit Option A is a minimal or interim retrofit scheme designed for an earthquake shaking level with a 200-year return period. Thus, this option addresses only those areas of the bridge which are susceptible to damage in moderate ground shaking. Retrofit Option B is an intermediate level of strengthening, and Retrofit Option C is a relatively complete retrofit of the structure, which includes measures to prevent the collapse of spans due to the potential 5-meter offset of the Wellington fault. Retrofit Option D includes the structural retrofit measures of Option C, plus expensive measures to improve the soil at the site to resist liquefaction.

Some of the individual retrofit measures for the Thorndon Bridge are discussed in Chapter 4. As shown in Table 14.2, the major difference between the different retrofit options is that for the more extensive retrofit schemes, the retrofit measures are applied to more of the piers. Typically there is little difference in the retrofit measures themselves for the different retrofit schemes. For example the steel column jackets used for Retrofit Option A would be similar in design to those used for Retrofit Option D. Conceivably, though, a thinner steel jacket might be justified for Option A compared to Option D because the column ductility demands will be less for the design earthquake level of Option A.

14.4 Expected Seismic Damage

For each of the different retrofit options, and for the unretrofitted bridge, the expected damage to the structure for various earthquake levels has been estimated. The level of damage is represented by the earthquake repair costs and loss of use times shown in Tables 14.3 and 14.4. In the evaluation of retrofit options for the Thorndon bridge [BCHF 1994b], tables such as these were used as input for the assessment of (a) bridge functionality and safety, (b) earthquake fatalities and economic losses, and (c) the cost-benefit characteristics of retrofitting.

In Tables 14.3 and 14.4, eight earthquake scenarios are considered, which correspond to the spectral acceleration levels of Table 14.1. As shown in Table 14.1, there are five acceleration levels that have been considered for both Wellington fault and distant-fault earthquake scenarios. However, one acceleration level for each scenario can be eliminated from consideration. For distant-fault earthquakes the 2.0g acceleration need not be considered because its probability of exceedance is low; for the Wellington fault earthquake, the 0.34g acceleration need not be considered because accelerations at the site are almost certain to exceed 0.50g for the characteristic earthquake on this fault.

Thus, Table 14.3 shows a matrix of 5 retrofit possibilities (4 retrofit schemes plus unretrofitted) times 4 acceleration levels for the Wellington fault earthquake. Table 14.4 shows a similar matrix, of 5 retrofit possibilities times 4 acceleration levels, for distant-fault earthquakes. The earthquake repair costs in each cell of the tables are derived from a consideration of the likely damage to different areas of the bridge under the scenario represented by that cell.

For example, for the scenario of a distant-fault earthquake causing an 0.84g acceleration for the unretrofitted bridge, it is estimated that extensive pile-cap damage would occur in several areas of the bridge, spans would collapse in one area of the bridge, and ramps to the bridge would collapse. For this damage scenario, a structural repair cost of $37 million is estimated to be needed to bring the bridge back to its original state. This value is shown in the relevant row and column of Table 14.4. The loss-of-service time for the bridge is also estimated, based on the predicted damage and the time required for repair and rebuilding. For the example scenario, the loss of service time is estimated as 30 months, as shown in Table 14.4 [BCHF 1994b].

The Wellington-fault earthquake scenarios need to be considered separately from distant-fault earthquakes because the Wellington-fault ground displacement—the potential five-meter fault offset—causes damage in addition to that caused by ground shaking. For the Wellington-fault earthquake, additional damage or span collapses will generally occur in the area of the bridge that crosses the fault. Thus, for the same level of spectral acceleration, greater earthquake losses will occur if that acceleration comes from the Wellington fault rather than a distant fault. This can be seen by comparing the repair costs and loss-of-service times of Table 14.3 with those of Table 14.4. For the same acceleration level, particularly at 0.50 and 0.84g, the values of Table 14.3 are higher than those of Table 14.4.

Table 14.3 Estimated Earthquake Repair Costs and Loss-of-Service Times, Due to a Wellington-fault Earthquake [BCHF 1994b].

Earthquake Spectral Acceleration (at T = 1.0 seconds)	Earthquake Repair costs and *Loss of Service Times*				
	Unretrofitted	**Retrofit A**	**Retrofit B**	**Retrofit C**	**Retrofit D**
0.50 g	$27M *20 months*	$15M *12 months*	$10M *12 months*	$7M *9 months*	$7M *9 months*
0.84 g	$44M *30 months*	$24M *14 months*	$17M *14 months*	$8M *9 months*	$7M *9 months*
1.3 g	$55M *42 months*	$55M *42 months*	$55M *42 months*	$55M *42 months*	$8M *9 months*
2.0 g	$55M *42 months*	$55M *42 months*	$55M *42 months*	$55M *42 months*	$55M *42 months*

Table 14.4 Estimated Earthquake Repair Costs and Loss-of-Use Times, Due to a Distant-fault Earthquake [BCHF 1994b].

Earthquake Spectral Acceleration (at T = 1.0 seconds)	Earthquake Repair costs and *Loss of Service Times*				
	Unretrofitted	**Retrofit A**	**Retrofit B**	**Retrofit C**	**Retrofit D**
0.34 g	$3 *9 months*	$0 *0 months*	$0 *0 months*	$0 *0 months*	$0 *0 months*
0.50 g	$20 *12 months*	$6M *4 months*	$1M *0 months*	$0 *0 months*	$0 *0 months*
0.84 g	$37M *21 months*	$15M *6 months*	$8M *6 months*	$1M *0 months*	$0 *0 months*
1.3 g	$55M *42 months*	$55M *42 months*	$55M *42 months*	$55M *42 months*	$1M *0 months*

Damage Curves

The values of earthquake repair costs in Table 14.3 and 14.4 can be used to create a series of damage versus earthquake acceleration curves, as shown in Figure 14.2. Such curves are similar to those described in the previous chapters, and shown in Figure 11.4 and 12.3.

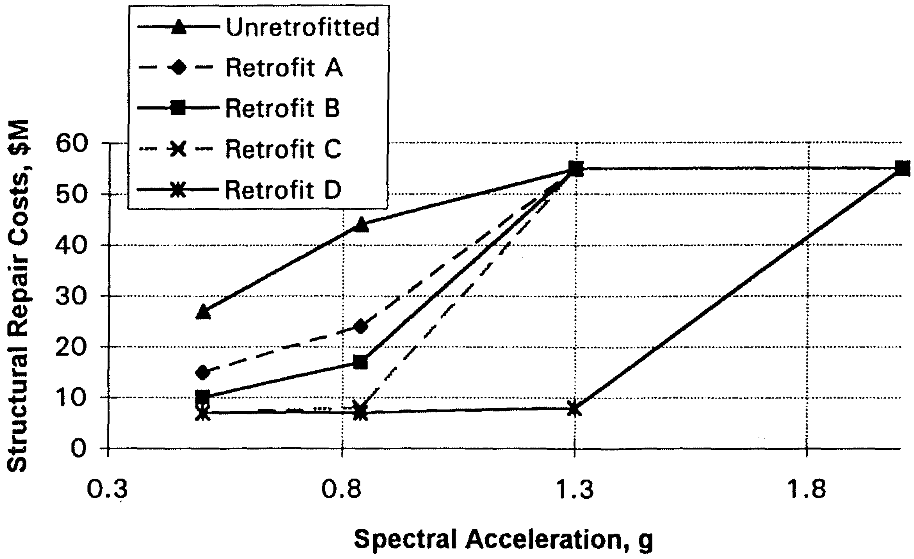

(a) Wellington-fault Earthquake

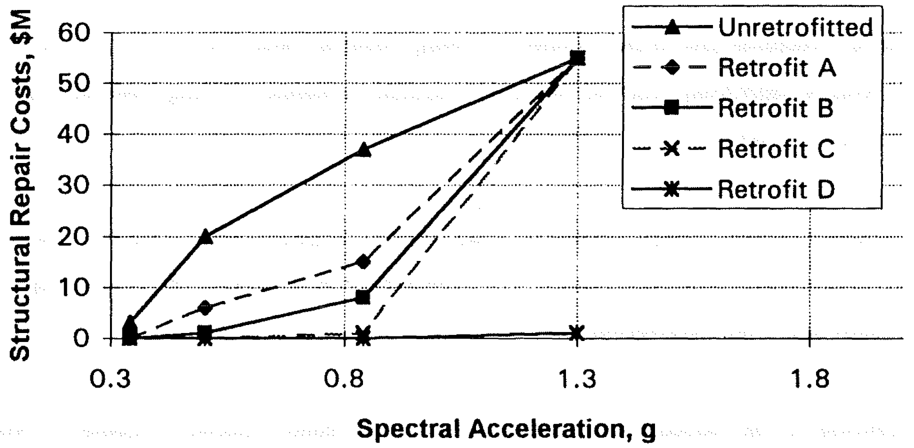

(b) Distant-fault Earthquake

Figure 14.2 **Damage versus earthquake acceleration curves for the Thorndon bridge.**

14.5 Limit States for Seismic Performance

Besides earthquake damage costs, another way to quantify seismic performance is by defining limit states. For important, heavily trafficked bridges the loss of service of the bridge is likely to be a more significant consequence of an earthquake than the actual structural damage. Limit states are a customary way to consider consequences such as loss-of-service.

Definition of Three Performance Levels

For the seismic performance of buildings, three limit states have traditionally been defined: the *serviceability* limit state, the *damage-control* limit state, and the *survival* (or no-collapse) limit state. A good explanation of these limit states is given by Paulay and Priestley [1992].

The limit state criteria for bridges can be slightly different from that for buildings. Three limit states were defined for the Thorndon bridge, which are labelled as:

1 Fully serviceable
2 Can restore limited service, and
3 No collapse

In the study of the Thorndon bridge [BCHF 1994b], the performance requirements were defined for each of the above limit states as follows:

1 "the bridge structures are to be capable of remaining fully serviceable with only minor repairs being necessitated",

2 "the bridge structures are to be capable of being brought back into service (albeit at a reduced level) a short time after the event, and capable thereafter of being repaired to a full level of service", and

3 "the response of the bridge structures shall be investigated and measures that may significantly improve their performance and reduce the risk to human life on and adjacent to the bridge are to be investigated".

Note that the definition of the second limit state includes two different criteria: *capable of being quickly brought back into service*, and *capable of being fully repaired*. For buildings, only the second criteria is traditionally used to define the "damage-control" limit state. According to Paulay and Priestley [1992], the second limit state "may be defined [to mark] the boundary between economically repairable damage and damage that is irreparable or which cannot be repaired economically". For bridges the ability to quickly bring a structure back into service, particularly for emergency vehicles, is crucial. For most bridge structures this criterion would be more stringent than the repairability criterion. In other words the *restore limited service* criterion would be exceeded at a lower level of earthquake damage than the *repairability* criterion. Thus for the Thorndon bridge the *restore limited service* criterion is assumed to govern limit state 2. (Note that the repairability criterion could be made as an additional limit state for the Thorndon bridge, between limit states 2 and 3).

For the third limit state, the goal is to minimise the risk to human life. This is typically interpreted to mean that collapse of the structure is to be prevented. This interpretation was used for the assessment of the Thorndon bridge.

Seismic performance at Different Earthquake Accelerations

Based on the seismic damage and loss-of-service estimates which were summarised in Section 14.4, an assessment of bridge performance has been made with respect to the defined limit states. Figure 14.3 shows the expected limit-state performance for various spectral acceleration levels for each of the retrofit options. As was the case in Section 14.4, the seismic performance will depend on whether the earthquake accelerations are produced by the Wellington fault or distant faults. Performance for the Wellington fault earthquake will be worse, due to increased damage at the section of the bridge which crosses the fault.

Figure 14.3 considers only the main bridge structure and on-ramp for the Thorndon bridge. The off-ramp of the bridge requires a separate assessment, and for simplification is excluded from consideration here.

Figure 14.3(a) shows that for a Wellington fault earthquake, collapse will occur at all acceleration levels for the unretrofitted bridge, and for the bridge retrofitted according to Options A and B. Note that the collapse limit state is considered to be exceeded even if only one or two spans collapse. For the bridge retrofitted to Option C, at an acceleration of 0.50 to 0.84g there is expected to be damage which requires a temporary or partial shut down of bridge traffic, but limited service to the bridge can soon be restored. At an acceleration level of 1.3g there will be more severe damage. This damage would prevent a restoration of limited service; however, the damage would not cause collapse of the bridge and the risk to human life would still be minimised. At an acceleration of 2.0g collapse has occurred. For retrofit Option D, limited service can be restored to the bridge for accelerations up to 1.3g, and collapse is prevented even at 2.0g.

Figure 14.3(b) shows the limit-state performance for distant-fault earthquakes. For the unretrofitted bridge, limited service can be restored for a 0.34g acceleration, but collapse occurs for accelerations of

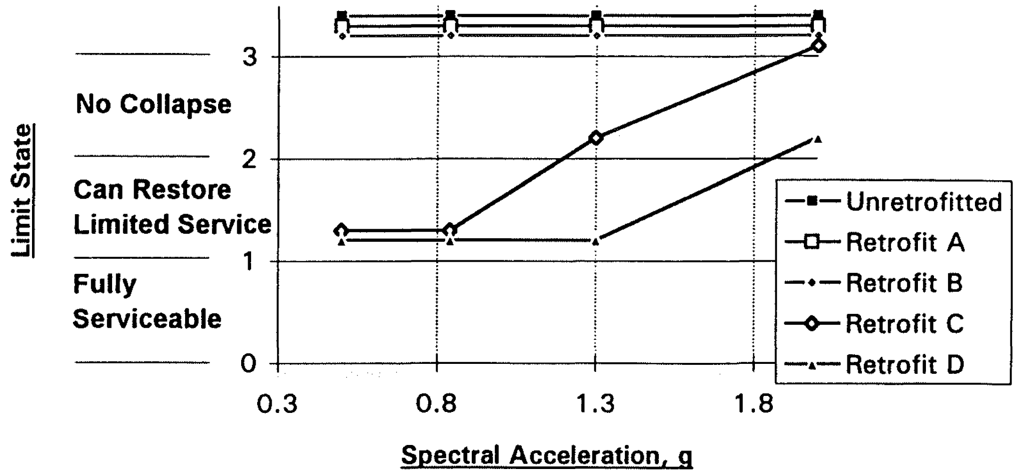

(a) Wellington-fault Earthquake

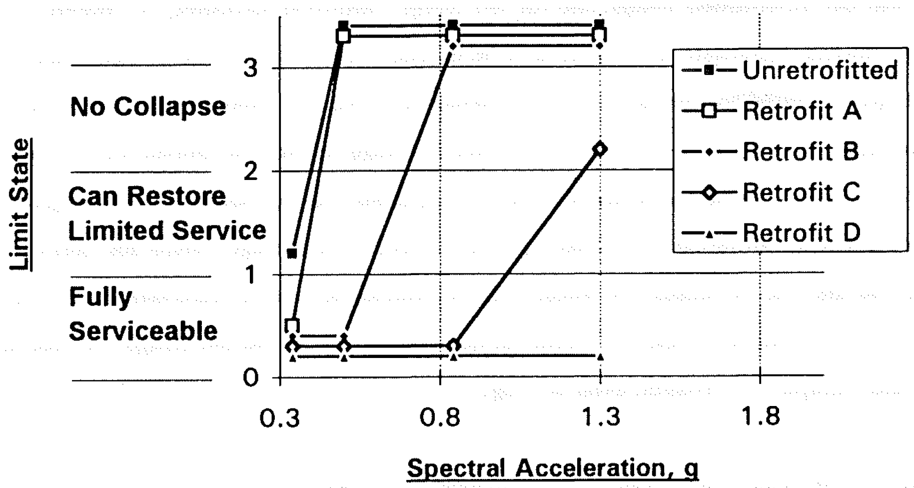

(b) Distant-fault Earthquake

Figure 14.3 **Seismic performance with respect to limit states, versus earthquake acceleration.**

0.50g and higher. The benefit of Retrofit A is that is allows the bridge to remain fully serviceable for the 0.34g earthquake, but collapse is still expected for higher acceleration levels. The bridge with Retrofit B is expected to remain fully serviceable at 0.50g and below and collapse at 0.84g and above. The bridge with Retrofit C will remain fully serviceable at 0.84g and below, and at 1.3g will suffer severe damage but not collapse. The bridge with Retrofit D is expected to remain fully serviceable for all likely levels of acceleration from distant-faults.

Probability-Based Assessment

Combining the limit-state versus acceleration curves of Figure 14.3 with the probable seismicity curves of Figure 14.1 allows a calculation of the probability of exceedance of the defined limit states over the expected life of the bridge. The results of these calculations are shown in Figure 14.4. The figure presents the probability of exceedance, over 50 years, of the defined performance levels. The 50 year period approximates the estimated remaining service life of the bridge.

This figure provides a clear basis for understanding and comparing the expected seismic performance of the various retrofit options. The figures shows for example, that for Retrofit Option C, it is expected that retrofitting the main bridge and on-ramp will cost $14 million. If the retrofitting has been carried out, the following seismic performance over the next 50 years can be expected [BCHF 1994b]:

- There is a 15% chance that an earthquake will occur which exceeds the Full-service level. That is, after the earthquake at least some of the traffic-carrying capacity of the bridge must be shut down.

- There is a 10% chance that an earthquake will occur which exceeds the Limited-service level. That is, after the earthquake no traffic can pass over the bridge, not even temporary or emergency traffic.

- There is a 5% chance that some portion of the bridge will collapse.

Conclusions

Based on the results presented in Figure 14.4 the following conclusions can be drawn regarding the functionality and safety performance of the proposed retrofit options for the main bridge [BCHF 1994b]:

- Retrofit Scheme A provides little benefit over the option of not retrofitting the bridge.

- Retrofit Scheme B provides some improvement in bridge performance: the probability of collapse over 50 years is reduced from 20 to 15%. The probability of loss of service is similarly reduced.

- Retrofit Scheme C provides a dramatic improvement in bridge safety and a substantial improvement in functionality. The probability of collapse over 50 years is reduced to 5%.

- Retrofit Scheme D which includes extensive ground strengthening, further reduces the probability of collapse and the probability of loss of service.

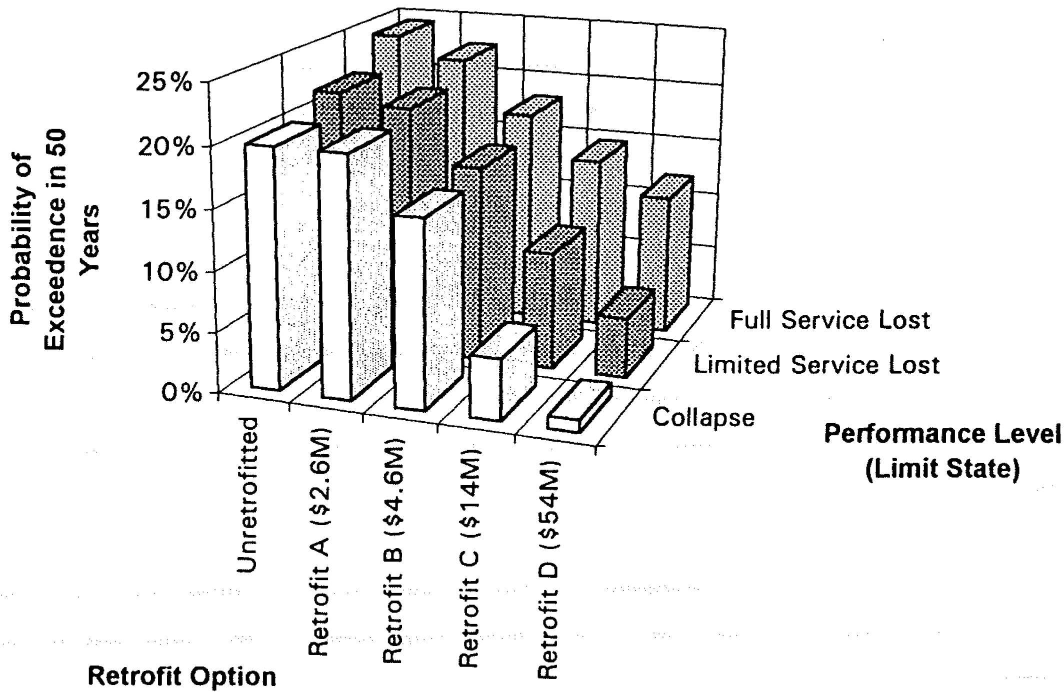

Figure 14.4 **Probabilities of exceedance of bridge performance limit states** [BCHF 1994b].

14.6 Economic Analysis

The benefits of seismic retrofitting for the Thorndon Overbridge can be quantified in more specific terms than the performance levels discussed in the previous section. Using a probabilistic simulation analysis, estimates of potential earthquake injuries, fatalities, and economic losses can be made for each of the different retrofit options.

The methodology and some of the most illustrative results of the economic analysis are briefly discussed here, summarised from the detailed report by BCHF consulting engineers [BCHF 1994b]. It should be remembered that a large number of assumptions are necessary for the analysis and there are many ways in which the probabilities of coincident events can affect the economic loss outcome. However, the analysis gives a good comparison of the retrofit schemes.

Methodology

The economic analysis of retrofit options for the Thorndon bridge is based on a probabilistic computer simulation of outcomes. The analysis was

> "carried out using a Lotus 123 spreadsheet and proprietary risk analysis software add-in *@RISK*. This allowed a Monte Carlo simulation to be carried out for a large number of calculations taking account of the following probabilities of occurrence:
>
> - the probability of an earthquake occurring in any one year and the acceleration level of that earthquake; distant and Wellington fault earthquakes are modelled separately;
> - given that an earthquake occurs, the probability that it strikes in morning or evening peak, interpeak, evening, night time or weekend [for both road and rail traffic];
> - given that an earthquake occurs, the probability that it occurs in the season of peak Cook Straight ferry traffic and whether it occurs at a peak arrival time for ferry passengers, on the shoulder of the peak arrival, or at a time away from the ferry arrival;
> - given that an earthquake occurs of sufficient magnitude to dislodge one span on each of the east and west side viaduct in areas 9 and 10 (includes piers 24-34 & 61-71), the probability that any particular span is dislodged - this is needed as the damage outcome varies depending on which spans fall; and
> - the probability that passenger and/or freight trains are passing under the bridge at the time of the earthquake; the [two principal railway] lines being considered independently" [BCHF 1994b].

The economic analysis was used to give (a) estimates of damage costs for different scenarios of earthquakes and retrofit levels, and (b) cost-benefit results for each of the different retrofit options in comparison to the unretrofitted bridge.

The earthquake damage costs were considered to come from:

- "initial damage and personal injury costs to vehicles, rolling stock, buildings, trackwork and personnel at the time of the earthquake; and
- road traffic delays ensuing during the period of reinstatement of the viaduct" [BCHF 1994b].

In calculating benefit/cost ratios, benefits were taken as the damage costs avoided by retrofitting; costs were taken as the retrofit construction costs minus the expected savings between the earthquake repair costs for an unretrofitted bridge and a retrofitted bridge. As discussed in Section 12.7, it could be debated whether the expected repair cost savings should be treated as a project cost (denominator of the benefit/cost ratio) or as a project benefit (numerator of the benefit/cost ratio).

Results

The probabilistic analysis of outcomes for the Thorndon bridge produces predictions of earthquake fatalities and the economic consequences for the different seismic retrofit options.

Fatalities

One of the principal reasons to retrofit the Thorndon bridge is to protect against injuries and fatalities that could result from the bridge's collapse. In the study of retrofit options [BCHF 1994b], worst-case type scenarios for earthquake fatalities have been estimated.

Time of day has a great influence on the expected number of casualties. The worst time for a damaging earthquake to occur would be during peak traffic hours and during the peak arrival time for ferry passengers. If the same earthquake were to occur during interpeak traffic levels and during medium ferry activity, the expected earthquake fatalities due to bridge collapse would be about a third of the number for the worst time, and if the earthquake were to occur at night during low ferry activity, the expected earthquake fatalities would be less than a tenth the number for the worst time. These results are shown in Figure 14.5.

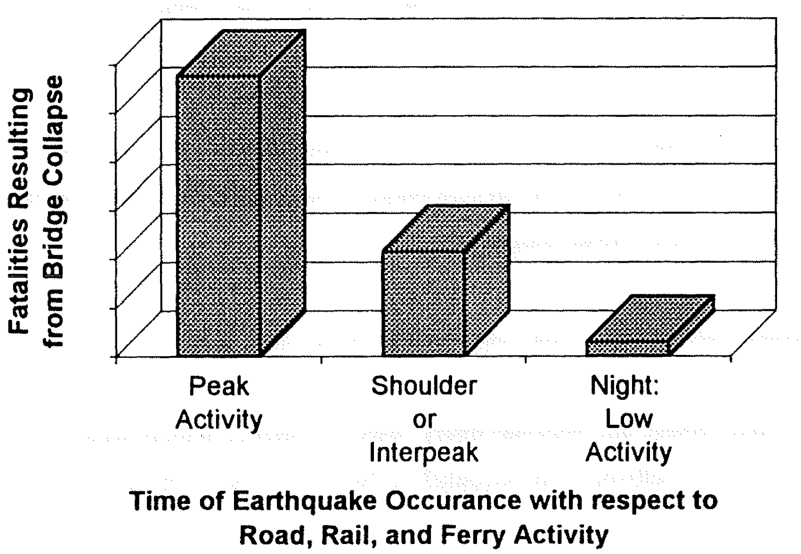

Figure 14.5 **Fatalities resulting from bridge collapse versus time of earthquake occurrence [BCHF 1994b].**

To effectively reduce the risk of earthquake casualties for the Thorndon bridge, one of the more extensive retrofit options, C or D, must be chosen. As was shown in Figure 14.4, only these options greatly reduce the probability of collapse of the bridge. The point is also made evident by considering the *expected value* of earthquake fatalities, as shown in Figure 14.6. This figure shows the expected values of earthquake fatalities over 50 years for the unretrofitted bridge and each of the four retrofit options. The expected value (EV) of fatalities can be a deceptively low number because of the high probability that no strong earthquake will occur in the next 50 years, or that it will occur at night or when few people are near or under the bridge. Nevertheless, Figure 14.6 shows that Retrofit Schemes C and D reduce the EV of fatalities due to earthquakes at the Thorndon bridge by more than 90%. Schemes A and B provide only a small reduction in the expected fatalities [BCHF 1994b].

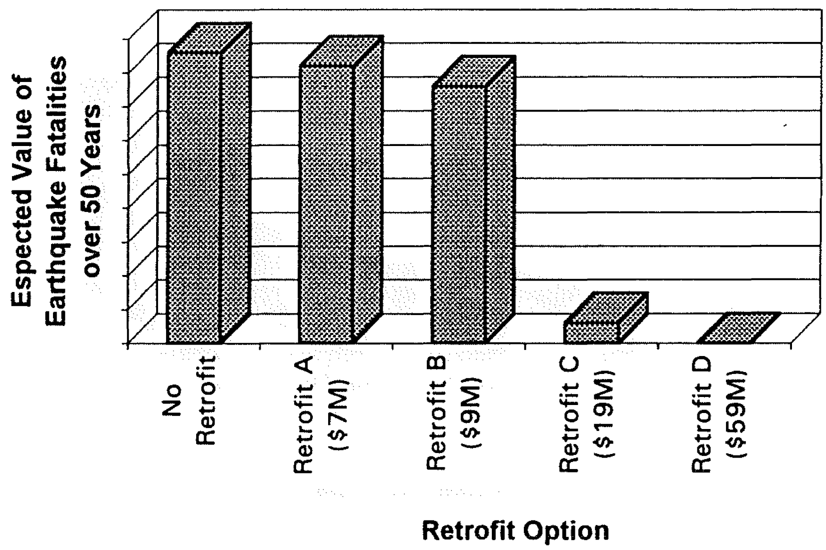

Figure 14.6 **Expected value of earthquake fatalities [BCHF 1994b].**

Economic Losses and Benefit/Cost Ratios

If the Thorndon bridge is damaged in an earthquake, economic losses could occur due to the disruption to road, rail, and ferry traffic, fatalities, injuries, or other effects. Using the probabilistic analysis, the expected value of these economic losses has been approximately quantified.

For each retrofit option, the *avoided* losses can be calculated as the difference between the losses which would occur for the unretrofitted bridge and those for the retrofitted bridge. Figure 14.7(a) shows the expected value of avoided losses for each of the four retrofit schemes, considered over a 25 year period. The figure shows that the economic benefits of Retrofit C are expected to be approximately

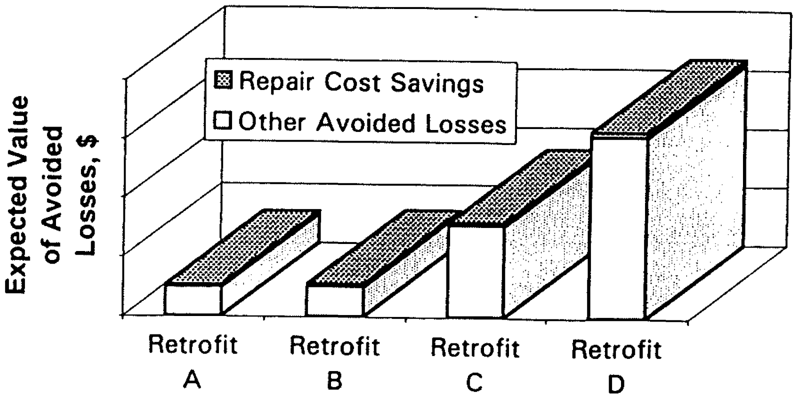

(a) Avoided losses due to seismic retrofitting (i.e. benefits).

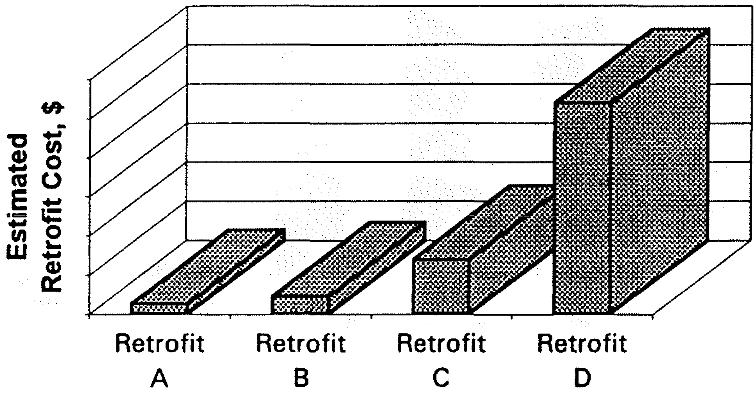

(b) Retrofit Costs.

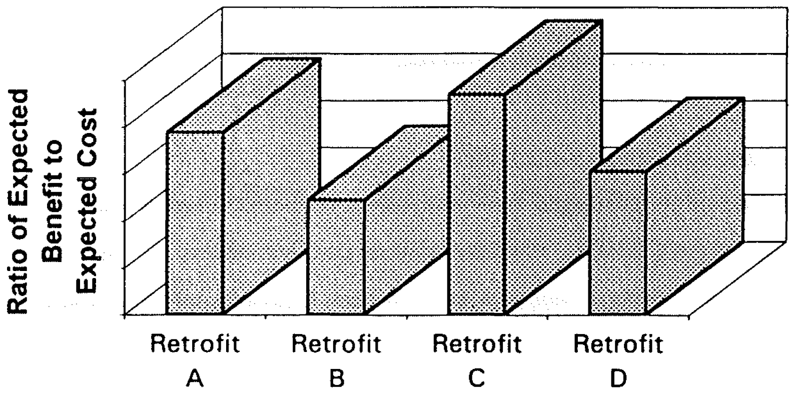

(c) Benefit/cost ratios.

Figure 14.7 **Expected benefits, costs, and benefit/cost ratios of retrofit options for the Thorndon bridge** [BCHF 1994b].

three times those of Retrofits A or B; the expected benefits of Retrofit D are approximately six times those of Retrofits A or B.

Figure 14.7(a) also shows that the benefits of retrofitting lie primarily in avoiding losses due to transportation disruption and casualties, rather than in avoiding the costs of repairing the earthquake damage to the bridge. The repair cost savings are only a small fraction of the avoided losses.

Although 50 years is a better estimate of the remaining service life of the bridge, 25 years is used in the economic analysis. Due to the discounted value of money beyond 25 years there is little difference between results over a 25 year period and over a 50 year period.

By comparing the expected value of benefits, shown in Figure 14.7(a), with the estimated retrofit costs, shown in Figure 14.7(b), benefit/cost ratios for the various retrofit options can be calculated. The benefit/cost ratios are shown in Figure 14.7(c). Note that the repair cost savings of Figure 14.7(a) were considered as negative costs rather than positive benefits, as previously discussed. Figure 14.7(c) shows that Retrofit Scheme C is estimated to have the highest benefit/cost ratio.

While the benefit/cost ratio provides useful information for bridge-upgrade decision-making, it should not be used as the sole criteria, or even the main criteria, for such decisions. As noted in Section 12.7, it is impossible to completely quantify all of the benefits of seismic retrofitting. One somewhat questionable and simplistic aspect of cost-benefit analyses is that a dollar value is assigned to each expected earthquake fatality. The Thorndon bridge study noted that "Society seems to be much less tolerant of risk [of loss of life] from engineered structures than from other documented involuntary risks". In recommending a retrofit scheme for the Thorndon bridge, the study considered the customarily accepted levels of earthquake performance defined in the design codes and retrofit policies of various jurisdictions [BCHF 1994b].

CHAPTER 15
CONCLUSIONS FOR PART III

Chapters 11 through 14 represent an in-depth study of methods for the management and prioritization of bridge seismic upgrading work. The following conclusions can be drawn from the study:

A. *Importance of Prioritizing Bridge-retrofit Work*

Bridge seismic evaluation studies and retrofit programmes in California, New Zealand, and Japan indicate that the task of upgrading seismically deficient bridges represents an enormous undertaking. In Japan, 30 percent of bridges required some form of retrofitting. In California, a similar percentage of bridges is being retrofitted, at a total cost which is likely to exceed US $4 billion. In New Zealand, nearly 80 percent of the state-highway bridges were built before 1970—ie, before the use of modern seismic-resistant design practices. Because of the large number of bridges which need retrofitting, and the limited funds available, the prioritization and management of bridge-upgrade work is vital.

B. *Limitations of Previous Prioritization Procedure*

Procedures used to date for prioritizing bridges for seismic retrofitting have been of limited accuracy and usefulness. Critical examination of these procedures reveals a great many questionable aspects, such as the use of additive combinations, the poor representation of column structural vulnerabilities, and the underemphasis of traffic volume, bridge service life, and the possibility of temporary access in place of an earthquake-damaged bridge. None of the procedures used to date have been verified for accuracy.

C. *Advantages of Proposed Prioritization Method*

Bridge-upgrade prioritization methods based on earthquake loss-estimation techniques would offer a more rational and verifiable means of screening bridges. Such an approach was used by the author to develop a new prioritization method. There are several advantages to the new method:

- Different levels of seismic evaluation are defined, including a simple flow-chart procedure for the preliminary screening of bridges.

- A system of seismic vulnerability ratings is defined and correlated to earthquake damage curves.

- Formulas are given for estimating the economic impact of earthquake damage to bridges.

- After preliminary screening, secondary seismic assessments are used to refine the priority ratings for borderline bridges and reduce the number of detailed seismic assessments necessary.

- In the level-zero preliminary screening procedure, the amount of data—particularly subjective data—is minimized, resulting in a more consistent and cost-efficient procedure.

- Although the amount of data is limited, it is analysed in a thorough and relatively transparent manner. All variables and intermediate results relate to a physical meaning, such as probability of earthquake damage or transportation-disruption cost, so that the accuracy of the method's assumptions can be judged at each step of the procedure. This should make the procedure more accurate and verifiable than previous methods.

- The method is flexible and can be modified for regions with different bridge characteristics, seismicity, or retrofit priorities.

D. *Application of Recommended Method Using Minimal Data*

The recommended approach for bridge-upgrade management and prioritization can be applied to the study of a large group of bridges based on a minimum of data. The recommended methods have been successfully implemented on a stock of 445 bridges in New Zealand's Tasman district. Structural evaluations of 56 bridges, and basic data on all bridges, were used to draw conclusions about the distribution of seismic vulnerability, the expected seismic damage, and the benefits and costs of seismic upgrading for the district's bridges.

E. *Application of Recommended Concepts Using In-depth Data*

The recommended approach for bridge-upgrade management can also be applied to in-depth studies of a single seismic-retrofit project. The recommended methods were used for the detailed evaluation of retrofit options for a major elevated highway structure, the Thorndon bridge in Wellington. The evaluation used the results of a probabilistic seismicity study and estimated damage curves for different retrofit options. Seismic performance was considered in terms of structural behaviour limit states, expected fatalities, and expected economic losses due to bridge damage.

ADDENDUM TO PART III

TESTING OF THE RECOMMENDED BRIDGE-UPGRADE PRIORITIZATION METHOD BY COMPARISON TO THE 1993 CALTRANS PROCEDURE

Summary of Addendum

This addendum describes a comparison of the recommended method of prioritizing bridges for seismic upgrading, the Tasman District method, with the 1993 Caltrans procedure. The comparison is made by considering a number of examples for each of the five main component areas of the prioritization procedures: structural vulnerability, seismicity, soil type, bridge importance, and the overall formulation of the priority rating.

The comparison shows great differences between the two procedures, but reveals no erroneous aspects or unintended results in the Tasman District method. The comparison also shows that the Tasman District method is more easily modified than other additive-type procedures, and reinforces several of the conclusions made in Chapter 15.

A1 Introduction

Part III of this report reviews procedures which have been used for the prioritization of bridges for seismic retrofitting and proposes a new method, which has been applied in New Zealand's Tasman District [Maffei 1994]. In Part III, several features of existing procedures and the new method are discussed. To make these features and their possible advantages more apparent, the Tasman District procedure is applied here to a number of example bridges and conditions.

For the purposes of comparison, the 1993 Caltrans procedure [Gilbert 1993] is applied to the same examples. The Caltrans procedure has been selected because it has been one of the more influential of the prioritization procedures, and it has been considered for application in New Zealand [Chapman and Kircaldie 1994].

Objectives

The objectives of this addendum are to:

A. Further illustrate the main features of the Tasman District method through comparison to the 1993 Caltrans procedure, and to establish the extent of the differences between the procedures.

B. Look for areas in which the Tasman District method might produce erroneous or unintended results.

C. Comment on the relative advantages of either of the two procedures.

Organization

Section A2 of this addendum covers the methodology used in the comparison of prioritization procedures. Sections A3 through A7 cover, respectively, comparisons of structural vulnerability, seismicity, soil type, bridge importance, and the overall formulation of the priority rating. Section A8 presents the conclusions for the addendum.

A2 Methodology

Several possible methodologies were considered for the testing of the recommended prioritization procedure. The methodology used is described below, followed by additional considerations and possible alternate methodologies which could be used for testing prioritization procedures.

Methodology Used

The Tasman District method and the Caltrans procedure are each applied to a set of example bridges and conditions. The comparisons are made in five component areas of the prioritization procedures: structural vulnerability, seismicity, soil type, bridge importance, and the overall formulation of the priority rating. Examining the prioritization procedures component by component allows specific conclusions to be drawn about the strengths and weaknesses of different parts of the procedures.

Assessment of Structural Vulnerability

In comparing the assessment of structural vulnerability, 12 example bridges are considered. The examples were selected to give the best illustration of the differences between the two procedures. The structural vulnerability results of the two procedures are compared not only to each other, but also to a "judgement-based" vulnerability rating, which is taken as a benchmark. The judgement-based rating has been assigned to each bridge by the author based on his experience as a structural engineer and on his research into bridge seismic deficiencies and observed earthquake damage.

There is the potential for an unintended bias in this aspect of the comparison methodology, because the same author's judgement which was used to develop the Tasman district procedure is also used to define the benchmark. However it is not expected that other experienced engineers or researchers would disagree markedly with the judgement-based vulnerability levels assigned in Section A3.

As discussed later, it might be preferable for future comparison studies to have detailed seismic/structural evaluations of actual bridges as a benchmark, or to use a consensus ranking from a number of engineers and researchers. It might also be preferable to use bridges from an actual jurisdiction. Two problems with this approach would be (a) the likelihood that not all of the data required by both procedures would already by collected for the bridge sample (since different prioritization procedures tend to require different data), and (b) that a larger bridge sample would be required to cover the extremes of the ranges of the significant variables involved.

Assessment of Other Components of the Prioritization Procedures

For the assessment of seismicity, soil type, bridge importance, and overall formulation of the priority rating, many additional examples of bridge conditions are considered. Comparisons between the two procedures are focused on determining where differences arise. Then brief comments are made on the implications of these differences.

Alternate Methodologies of Testing Prioritization Procedures

Section 11.5 discusses the issue of the verification of prioritization procedures. Ideally, any prioritization procedure, before being applied, would be tested by comparing the results of the prioritization with those produced by detailed seismic/structural evaluations and economic (cost-benefit) studies. Preferably, the procedure would be tested on actual bridges within the jurisdiction where the procedure is proposed to be applied. The sample of bridges in such a case should attempt to include the widest possible variety of conditions, eg, the extreme categories of seismic zone and soil profile type, high and low traffic volumes and detour lengths, and bridges which represent all prominent structural characteristics.

Point-by-point Comparisons versus Final-result Comparisons

The component-by-component comparison of prioritization procedures used in this addendum offers the advantage of clearly identifying which parts of a prioritization procedure may result in discrepancies or be in need of improvement. The effects of specific variables are also more easily seen. The disadvantage of a component-by-component comparison is that some prioritization procedures differ from others in their form, so that in order to make direct comparisons a number of assumptions must be made for one or both of the procedures being compared.

An alternative might be to compare only of the final priority results rather comparing procedures point by point. In using such a methodology several recommendations should be followed:

1. A relatively large sample of bridges must be considered in order to cover as many different conditions and combinations of conditions as possible. Otherwise the comparison will not be as comprehensive as a component-by-component comparison. (As an illustration, the 12 example bridges, 8 seismicity examples, and 4 soil types considered in this addendum imply 384 possible combinations of conditions, before even considering different conditions related to bridge importance.)

2. The comparison of final priority ratings should be supplemented with studies of the effects of individual variables and assumptions. Otherwise, little insight will be gained into the reasons for differences or agreements between results. For instance, it is possible that the final priority rating may be considered correct, but only because two or more major sources of error cancel each other out.

3. Priority-rating results should be compared to an accurate benchmark of what the correct prioritization is considered to be. Preferably this would be based on detailed seismic/structural evaluations and cost-benefit studies and would make use of a consensus of expert judgements in the areas of structural engineering, seismology, geotechnical engineering, economics, and risk analysis.

Verification of the Explicit Cost-benefit Procedure

For consideration of the bridge-importance component of the Tasman District method, the simplified prioritization formula of Section 12.8 was used. This makes possible a more direct comparison between the Tasman District method and the Caltrans procedure. If a final-result type of comparison were to be conducted instead, the method of explicitly calculating benefit/cost ratios could be tested.

This would be advantageous, since the author recommends the use of the explicit method over the simplified formula. Such an exercise would also allow the testing of some of the assumptions of the cost-benefit procedure. As emphasised in Section 12.7, these assumptions are numerous; however, the same assumptions are applied to each bridge and thus their effect on the *relative* priority ranking is probably not critical.

This is illustrated by the simplified formula itself which requires only 3 variables related to bridge importance. Any additional variables and assumptions tend to cancel each other out and do not have a large effect on a bridge's priority rating. It should also be noted that a testing of the explicit cost-benefit method could not easily be done in a comparative way to another prioritization procedure. Nevertheless, testing of the explicit cost-benefit method would be useful and could be recommended as part of future verification studies.

A3 Comparison of Structural Vulnerability Ratings

One of the marked differences between the Tasman District method of prioritizing bridges and the Caltrans procedure is in the assessment of structural vulnerability. The differences between the two procedures can be explored by considering a number of example bridges.

Tasman District Method

As discussed in Section 12.3, the Tasman District method assesses structural vulnerability on a scale of zero to ten. In Section 12.5, a level-zero flowchart procedure is proposed for quickly assigning a vulnerability rating to a bridge. The flowcharts for this procedure are shown in Figures 12.5, 12.6, and 12.7.

Caltrans Procedure

The Caltrans procedure uses an additive combination of 6 variables to arrive at a structural vulnerability rating, which theoretically could range between 0 and 1.0. The six variables and the corresponding weighting factors are shown in Figure A1.

Example Bridges

Twelve example bridges have been selected by the author. The bridges were chosen to:

1. represent a range of structural vulnerability levels from high to low,
2. cover a variety of structural features and combinations of structural features,
3. be representative of real bridges, including those which have been damaged in earthquakes, and
4. illustrate several of the differences between the Tasman District method and the Caltrans procedure.

For each of the example bridges, the seismic/structural vulnerability is assessed (a) by the judgement of the author, (b) by the level-zero flowchart procedure of the Tasman District method, and (c) by the 1993 Caltrans seismic prioritization procedure.

Descriptions of each Example Bridge

The data and brief descriptions for each of the example bridges are listed in Table A1. A further description of each example bridge is given below:

- *Example Bridge 1* is a multi-column reinforced-concrete bridge with a monolithic superstructure, built in 1955. The seismic deficiency which governs the structure's vulnerability is the poor detailing of the columns. The columns are susceptible to shear failures because of an inadequate amount of transverse reinforcement.

  This bridge is representative of a great number of structures which have collapsed because of shear failures in their columns. These include four major bridges which completely or partially collapsed in the 1994 Northridge California earthquake: the Mission-Gothic, LaCienega-Venice, and Fairfax-Washington undercrossing bridges, and the Bull Creek Canyon Channel bridge [Caltrans 1994]. The last of these bridges had a monolithic superstructure, as in the example bridge.

  The author judges the vulnerability of Example Bridge 1 to be *high*.

GLOBAL UTILITY FUNCTION DEFINITIONS

ACTIVITY CRITERION	
Seismic Activity	1.00*(0.25=low;0.50=moderate;0.75=active; 1.00=high)
HAZARD CRITERION	
Soil Conditions	0.33*(1=high risk zone; else 0)
Peak Rock Acceleration	0.38*(linear, normalized to 0.7g)
Seismic Duration	0.29*(0.5=short;0.75=intermediate;1=long)
IMPACT CRITERION	
ADT on Structure	0.28*(parabola for a max ADT of 200000)
ADT Under/Over Structure	0.12*(see ADT above)
Detour Length	0.14*(linear, normalized to 100 miles)
Leased Air Space (Residential, Office)	0.15*(1=present; else 0)
Leased Air Space (Parking, Storage)	0.07*(1=present; else 0)
Rte Type on Bridge	0.07*(1.0=interstate; 0.8=US , ST rte, or stream; 0.7=RR; 0.5=fed funded Co rte or city str; 0.2=nonfed funded Co rte of city str; 0.0=fed land, ST land, other)
Critical Utility	0.10*(1=present; else 0)
Facility Crossed	0.07*(see Rte Type on Bridge)
VULNERABILITY CRITERION	
Year Designed (Constructed)	0.25*(0.5=yr<1946; 1.0=1946≤yr≤1971; 0.25=1972≤yr≤1979; 0.0=yr>1979)
Hinges (Drop Type Failure)	0.165*(0.0=no hinge; 0.5=1 hinge; 1.0=2 or more hinges)
Outriggers, Shared Column	0.22*(1=present; else 0)
Bent Redundancy	0.165*(0.0=no col.;0.25=pier walls;0.5 multi-col bents;1.0=single col bents)
Skew	0.12*(linear, normalized to 90)
Abutment Type	0.08*(0=monolithic;1=nonmonolithic)

Figure A1 Variables and weighting factors for the Caltrans prioritization procedure [Gilbert 1993].

Table A1 Data and vulnerability ratings for example bridges.

Bridge Example Number:			**1**	**2**	**3**
Description:			Multicolumn r/c bridge with monolithic superstructure.	Multicolumn r/c bridge with well-designed movement joints.	Bridge with vulnerable movement joints (short seats and weak linkages) and well-confined columns.
Governing Deficiency:			Shear failure in r/c columns.	Shear failure in r/c columns.	Unseating at movement joints.
Judgement-based vulnerability:			**High**	**High**	**High**
Data Item	**Tas.**[1]	**Cal.**[2]			
Year of Construction	✓	✓	1955	1955	1977
Number of Spans	✓		multiple	multiple	multiple
R/C Columns Present	✓	✓	yes	yes	yes
Movement Joints Present	✓	✓	no	yes	yes
Seat Length	✓[3]		n/a	500 mm	200 mm
Ideal Seat Length	✓[3]		n/a	500 mm	500 mm
Linkage Bolts Present	✓[3]		n/a	yes	yes
Skew Angle at Supports	✓[3]	✓	0	0	22°
Girders with Typically Good Linkages	✓[3]		n/a	yes	no
Erosion Factor	✓		1.0	1.0	1.0
Span Length			>>5 m	>>5 m	>>5 m
Number of In-span Movement Joints		✓	0	≥ 2	≥ 2
Outrigger or Shared Column Present		✓	no	no	no
Number of Columns per Pier		✓	2	2	2
Movement Joints at Abutments		✓	no	yes	no
Vulnerability Ratings for Tasman District Method [Maffei 1994]					
$V_{MOVEMENT\ JOINT}$			0	2.9	10.8
$V_{COLUMN/WALL}$			10	10	3
$V_{FOUNDATION/ABUTMENT}$			4	4	4
V_{STRUCT}			**10**	**10**	**10**
Vulnerability Ratings for Caltrans Procedure [Gilbert 1993]					
a_{41} (year)			0.25	0.25	0.062
a_{42} (hinges)			0	0.165	0.165
a_{43} (outrigger col.)			0	0	0
a_{44} (redundancy)			0.082	0.082	0.082
a_{45} (skew)			0	0	0.03
a_{46} (abutment type)			0	0.08	0
c_4			**0.33**	**0.58**	**0.34**

Notes: [1]Indicates data items used in the Tasman District method [Maffei 1994].
[2]Indicates data items used in the Caltrans procedure [Gilbert 1993].
[3]Data item used only if movement joints are present.

Table A1 Continued

Bridge Example Number:			4	5	6
Description:			Single-span bridge with vulnerable movement joints.	River crossing with r/c pier-walls with pile foundation suffering severe erosion.	Multicolumn, monolithic bridge, having vulnerable outrigger columns.
Governing Deficiency:			Unseating at movement joints (at abutments).	Shear failure of foundation piles.	Outrigger column joint failure
Judgement-based vulnerability:			**High**	**High**	**Medium-high**
Data Item	**Tas.**[1]	**Cal.**[2]			
Year of Construction	✓	✓	1977	1935	1984
Number of Spans	✓		1	multiple	multiple
R/C Columns Present	✓	✓	no	no	yes
Movement Joints Present	✓	✓	yes	no	no
Seat Length	✓[3]		300 mm	n/a	n/a
Ideal Seat Length	✓[3]		500 mm	n/a	n/a
Linkage Bolts Present	✓[3]		yes	n/a	n/a
Skew Angle at Supports	✓[3]	✓	22°	0	0
Girders with Typically Good Linkages	✓[3]		no	n/a	n/a
Erosion Factor	✓		1.0	2.0	2.0
Span Length			>>5 m	>>5 m	>>5 m
Number of In-span Movement Joints		✓	0	0	0
Outrigger or Shared Column Present		✓	no	no	yes
Number of Columns per Pier		✓	0	pier-wall	2
Movement Joints at Abutments		✓	yes	no	no
Vulnerability Ratings for Tasman District Method [Maffei 1994]					
$V_{MOVEMENT\ JOINT}$			8.6	0	0
$V_{COLUMN/WALL}$			0	5	3
$V_{FOUNDATION/ABUTMENT}$			4	8	4
V_{STRUCT}			**8.6**	**8**	**4**
Vulnerability Ratings for Caltrans Procedure [Gilbert 1993]					
a_{41} (year)			0.062	0.125	0
a_{42} (hinges)			0	0	0
a_{43} (outrigger col.)			0	0	0.22
a_{44} (redundancy)			0	0.041	0.082
a_{45} (skew)			0.03	0	0
a_{46} (abutment type)			0.08	0	0
c_4			**0.17**	**0.17**	**0.32**

See first page of table for notes.

Table A1 Continued

Bridge Example Number:			7	8	9
Description:			New multicolumn bridge with large skew and movement joints, having outrigger columns.	Single-span new bridge with large skew and movement joints.	Pier-wall bridge with monolithic superstructure and large skew.
Governing Vulnerability:			Unseating at movement joints.	Unseating at movement joints (at abutments).	--
Judgement-based vulnerability:			**Medium**	**Medium-low**	**Medium-low**
Data Item	**Tas.**[1]	**Cal.**[2]			
Year of Construction	✓	✓	1992	1992	1965
Number of Spans	✓		multiple	1	multiple
R/C Columns Present	✓	✓	yes	yes	no
Movement Joints Present	✓	✓	yes	yes	no
Seat Length	✓[3]		500 mm	500 mm	n/a
Ideal Seat Length	✓[3]		500 mm	500 mm	n/a
Linkage Bolts Present	✓[3]		yes	yes	n/a
Skew Angle at Supports	✓[3]	✓	45°	45°	45°
Girders with Typically Good Linkages	✓[3]		no	no	n/a
Erosion Factor	✓		1.0	1.0	1.0
Span Length			>>5 m	>> 5 m	>> 5 m
Number of In-span Movement Joints		✓	≥ 2	0	0
Outrigger or Shared Column Present		✓	yes	yes	no
Number of Columns per Pier		✓	≥ 2	0	0
Movement Joints at Abutments		✓	yes	yes	no
Vulnerability Ratings for Tasman District Method [Maffei 1994]					
$V_{MOVEMENT\ JOINT}$			6.4	6.4	0
$V_{COLUMN/WALL}$			3	3	5
$V_{FOUNDATION/ABUTMENT}$			4	3	4
V_{STRUCT}			**6.4**	**6.4**	**5**
Vulnerability Ratings for Caltrans Procedure [Gilbert 1993]					
a_{41} (year)			0	0	0.25
a_{42} (hinges)			0.165	0	0
a_{43} (outrigger col.)			0.22	0	0
a_{44} (redundancy)			0.082	0	0.041
a_{45} (skew)			0.06	0.06	0.06
a_{46} (abutment type)			0.08	0.08	0
c_4			**0.61**	**0.14**	**0.35**

See first page of table for notes.

Table A1 Continued

Bridge Example Number:			**10**	**11**	**12**
Description:			New bridge with movement joints, zero skew, and single-column-piers, except for one outrigger pier.	Monolithic single-span bridge with a large skew at abutments	Small culvert-type monolithic single-span bridge with a large skew at abutments
Governing Deficiency:			--	--	--
Judgement-based vulnerability:			**Low**	**Low**	**Low**
Data Item	**Tas.[1]**	**Cal.[2]**			
Year of Construction	✓	✓	1992	1965	1965
Number of Spans	✓		multiple	1	1
R/C Columns Present	✓	✓	yes	no	no
Movement Joints Present	✓	✓	yes	no	no
Seat Length	✓[3]		500 mm	n/a	n/a
Ideal Seat Length	✓[3]		500 mm	n/a	n/a
Linkage Bolts Present	✓[3]		yes	n/a	n/a
Skew Angle at Supports	✓[3]	✓	45°	45°	45°
Girders with Typically Good Linkages	✓[3]		no	n/a	n/a
Erosion Factor	✓		1.0	1.0	1.0
Span Length			>> 5 m	>>5 m	4 m
Number of In-span Movement Joints		✓	≥ 2	0	0
Outrigger or Shared Column Present		✓	yes	no	no
Number of Columns per Pier		✓	1 and 2	o	o
Movement Joints at Abutments		✓	yes	no	no
Vulnerability Ratings for Tasman District Method [Maffei 1994]					
$V_{MOVEMENT\ JOINT}$			3.2	0	0
$V_{COLUMN/WALL}$			3	0	0
$V_{FOUNDATION/ABUTMENT}$			4	3	2
$\mathbf{V_{STRUCT}}$			**4**	**3**	**2**
Vulnerability Ratings for Caltrans Procedure [Gilbert 1993]					
a_{41} (year)			0	0.25	0.25
a_{42} (hinges)			0.165	0	0
a_{43} (outrigger col.)			0.22	0	0
a_{44} (redundancy)			0.165	0	0
a_{45} (skew)			0	0.06	0.06
a_{46} (abutment type)			0.08	0	0
c_4			**0.63**	**0.31**	**0.31**

See first page of table for notes.

- *Example Bridge 2* is similar to Example Bridge 1 except that it does not have a continuous, monolithic superstructure. Instead it has movement joints in the superstructure, which are well designed with good seating lengths, no skew angle, and competent linkages. The seismic deficiency which governs the structure's vulnerability is the same as for Example Bridge 1: poor detailing of the columns which are prone to shear failure. The movement joints of Example Bridge 2 represent significantly less seismic vulnerability than the columns.

  The bridge is representative of several bridge structures found in New Zealand and California. In California, bridges similar to this example can have much shorter seating lengths, and can therefore be possibly vulnerable in their superstructures as well as in their columns. However, most such bridges in California have had their movement joints retrofitted with cable restrainers or other linkages. This was the case for the Mission-Gothic, LaCienega-Venice, and Fairfax-Washington undercrossing bridges which suffered catastrophic column shear failures in the Northridge earthquake [Caltrans 1994].

  The vulnerability of Example Bridge 2 is judged to be *high*, generally the same as that for Example Bridge 1.

- *Example Bridge 3* has vulnerable details at the superstructure movement joints, but columns which were designed after early 1970s and are thus well reinforced for confinement and shear strength. The movement joints are vulnerable because of short seating lengths, moderate skew angle, and questionable linkage strength and details.

  The example is representative of a bridge which has cable restrainers or other linkages at its movement joints, which were designed for a much lower strength criteria than is considered appropriate by today's standards. This has been a common situation with California bridges. The performance of Example Bridge 3 would be similar to that of the Gavin Canyon undercrossing bridge which collapsed in the 1994 Northridge California Earthquake. As with Example Bridge 3, the Gavin Canyon bridge had skewed supports, short 200 mm (8-inch) support seats, and reinforced-concrete columns in which the column strength or ductility were not factors in the bridge's earthquake vulnerability. The Gavin Canyon bridge also had cable restrainers at the movement joints of the superstructure, and these restrainers failed to prevent the unseating of the superstructure spans which resulted in the bridge's collapse.

  The vulnerability of Example Bridge 3 is judged to be *high*.

- *Example Bridge 4* is similar to Example Bridge 3 except that it is a single-span bridge, with its superstructure movement joints at the abutments instead of within the bridge spans. A 300 mm (12-inch) seating length is assumed rather than 200 mm (8 inches), since seating lengths at abutments are typically somewhat longer than at in-span movement joints.

The vulnerability of Example Bridge 4 is judged to be *high*, only slightly less than that for Example Bridge 3.

- Example Bridge 5 is a reinforced-concrete bridge with pier-wall intermediate supports, which are supported on driven foundation piles. The bridge crosses a river which has caused severe erosion and scour around the pile foundations, so that the weak link to the seismic resistance of the structure is in the pile foundation.

  Example Bridge 5 is typical of many bridges in New Zealand, and is based on one of the Tasman District bridges. The vulnerability of Example Bridge 5 is judged to be *high*.

- Example Bridge 6 is a multi-column, monolithic bridge which has outrigger columns. The outrigger columns represent the governing seismic deficiency of the structure. As discussed in Section 2.2, outrigger columns were shown to be a vulnerable structural feature in bridges affected by the 1989 Loma Prieta California earthquake. The date of construction of Example Bridge 6, 1984, is taken to be the same as that for the I-980 bridge structure in Oakland California, which was shown by the Loma Prieta earthquake to have vulnerable outrigger column details.

  Outrigger columns are relatively common in California bridges but are rare in New Zealand. None of the 445 bridges in New Zealand's Tasman district have outrigger columns.

  The vulnerability of Example Bridge 6 is judged to be *medium-high*.

- Example Bridge 7 is a new multi-column bridge with a large skew angle at supports and movement joints within the bridge superstructure and at the abutments. The bridge also has outrigger columns, but they do not represent a seismic deficiency because of the late construction date. Although the length of the support seat meets code requirements and some type of linkages are provided, unseating of the superstructure spans is considered to be the governing seismic deficiency for this bridge.

  Although such a bridge would probably meet the letter of current bridge design codes, the use of movement joints in a bridge with large skew is not recommended by the author. Thus, the vulnerability of Example Bridge 6 is judged to be *medium*

- Example Bridge 8 is similar to Example Bridge 7 except that it is a single-span bridge. Thus, the only movement joints are at the abutments, and there are no outrigger columns.

Movement joints at abutments may be somewhat less vulnerable than similar movement joint details within a bridge span, because relative earthquake displacements could be less. Thus the vulnerability of Example Bridge 8 is judged to be *medium-low*, slightly less than the vulnerability of Example Bridge 7.

- *Example Bridge 9* has reinforced-concrete pier-walls and a monolithic superstructure with a large skew angle. The bridge has no clear seismic deficiencies, and its response is likely to be governed by rocking at the foundations of the pier-walls. Because the superstructure is monolithic, the skew of the supports is not a significant factor in the structure's vulnerability. The bridge is typical of many older bridges in New Zealand and elsewhere.

  The bridge is judged to have a *medium-low* seismic vulnerability.

- *Example Bridge 10* is a new bridge with movement joints, zero skew, and single-column piers with one multi-column outrigger pier. It is similar to Example Bridge 7, except for the single-column piers and zero skew at the movement joints. The bridge has no clear seismic deficiencies, despite having some features which might be suspect if they were in an older bridge. Unseating of the movement joints for Example Bridge 10 is much less likely than for Example Bridge 7 which has a 45° skew angle at the span supports.

  The vulnerability of Example Bridge 10 is judged to be *low*.

- *Example Bridge 11* is a monolithic single span bridge with a large skew at the abutments. The example represents a common type of bridge which is generally not vulnerable to earthquake damage. As with Example Bridge 9, the skew of the supports is not a significant factor in the structure's vulnerability because the superstructure is monolithic.

  The vulnerability of this bridge is judged to be *low*.

- *Example Bridge 12* is similar to Example Bridge 11 except that its span is shorter. It is a culvert-type bridge with a span of 4 meters (13 feet). Such bridges are common in New Zealand.

  The vulnerability of Example Bridge 12 is judged to be *low*, even lower than that of Bridge 11.

Vulnerability Rating Results

Table A1 shows the results of the calculated vulnerability ratings, including some of the intermediate values calculated. Figure A2 shows the results for each example bridge on a bar chart. The results show very little agreement between the Tasman District method and the Caltrans procedure.

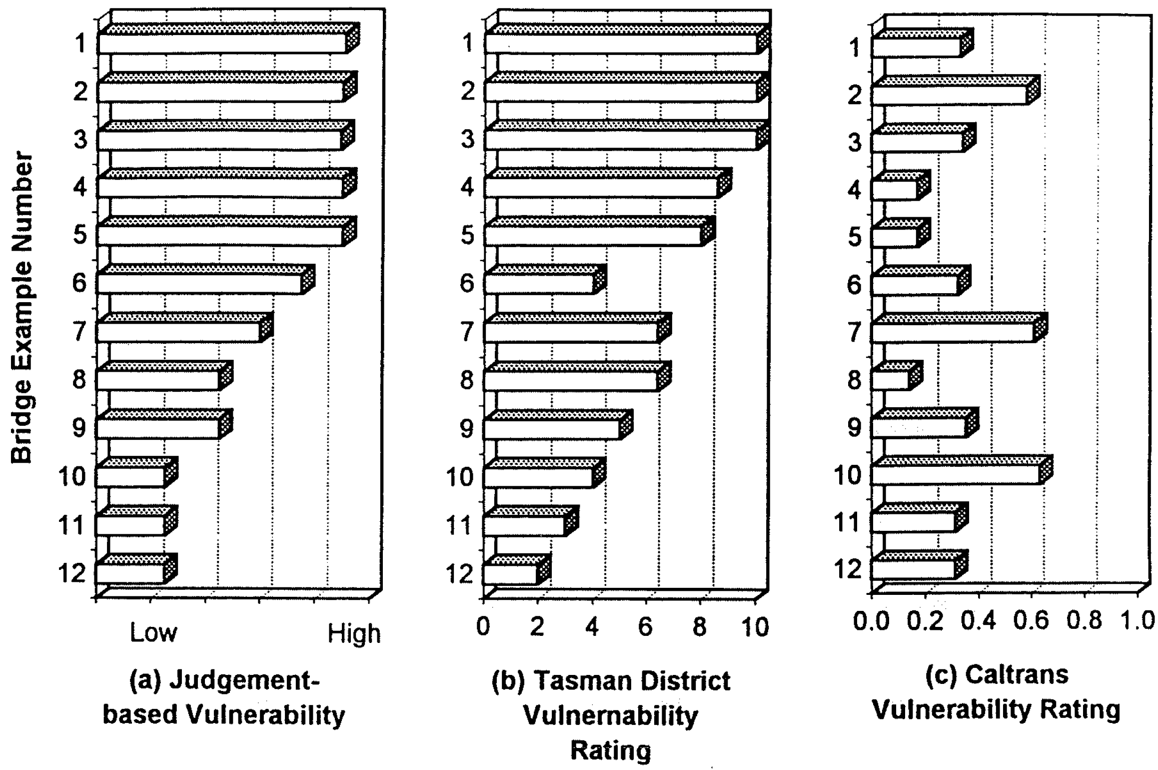

Figure A2 Structural vulnerability ratings for the example bridges.

Figure A2(a) shows the judgement-based vulnerability for each example bridge. Figure A2(b) shows the structural vulnerability ratings assigned by the Tasman District method. These ratings correspond closely to the judgement-based vulnerability. Except for Example Bridge 6, the bridges are put in the same order of structural vulnerability. For the Tasman District method, the mean value of structural vulnerability rating for the 12 example bridges is 6.4; the median rating is also 6.4.

Figure A2(c) shows the ratings assigned by the Caltrans procedure. The ratings do not correlate well with the judgement-based vulnerability shown in Figure A2(c). The order of ranking for the Caltrans procedure is very different from that based on the author's judgment or that given by the Tasman District method. The mean Caltrans rating for the 12 bridge sample is 0.36; the median rating is 0.32.

Discussion of Results for Each Example Bridge

The vulnerability ratings calculated for the example bridges illustrate several important points. The results for each bridge are discussed below:

Example Bridges 1 and 2

The vulnerability rating of 10 assigned by the Tasman District method for each of these bridges reflects the high seismic vulnerability of bridges which are prone to column shear failures.

The Caltrans procedure applies a relatively high rating, 0.58, to Bridge 2 only, and applies an average rating, 0.33, to Bridge 1. Thus the vulnerability of Bridge 1 seems to be under-predicted by the Caltrans procedure. The vulnerability of Bridge 2 seems to be more accurately predicted, but only because the bridge happens to have some potentially vulnerable features which are in fact unrelated to its governing seismic deficiency. This illustrates three points which were made in Section 11.5:

1. The under-influence of variables related to the non-ductile failure of concrete columns allows some prioritization procedures to overlook clearly vulnerable bridges.

2. Some additive prioritization procedures implicitly assume that the vulnerability of a bridge is caused by the summation of several minor defects, where in reality a single major defect can cause a bridge to fail.

3. The effect of the number of columns per pier (or bent) may be overemphasized in many procedures.

Example Bridges 3 and 4

The Tasman District method assigns a vulnerability rating of 10 to Bridge 3, and a rating of 8.6 to Bridge 4. The ratings reflect the high vulnerability for these bridges of span unseating at the superstructure movement joints.

The Caltrans procedure applies an average rating, 0.34, to Bridge 3, and a below-average rating, 0.24, to Bridge 4. This again seems to be an under-prediction of the actual vulnerability of these two structures, and further illustrates point 2 above, that many prioritization procedures tend to under-emphasize the vulnerability of bridges with a single major type of seismic deficiency.

Example Bridge 5

The Tasman District method assigns a vulnerability rating of 8 to Bridge 5. This reflects the high susceptibility to collapse from pile shear failure for this bridge.

The Caltrans procedure assigns a low rating, 0.17, to Example Bridge 5 and under-predicts the actual vulnerability of the structure. This under-prediction occurs because the Caltrans procedure does not consider seismic deficiencies in foundations, foundation erosion, or river scour. The Caltrans procedure seems to be derived more for freeway overcrossing and undercrossing bridges than for river-crossing bridges. Nevertheless there may be bridges in California which are susceptible to shear failures in foundation piles.

Example Bridge 6

The Tasman District method assigns a vulnerability rating of 4 to Bridge 6. This under-predicts the actual vulnerability of the bridge. The reason for the under-prediction is that outrigger columns are not considered in the Tasman District method. None of the bridges in the Tasman District have outrigger columns.

This illustrates the point made in Section 12.2 that before applying the Tasman District method to a new jurisdiction, the level-zero procedure should be calibrated using a brief initial study. This initial study should reveal any bridge characteristics or other issues which are particular to the new jurisdiction.

Possible Modification of the Tasman District Level-zero Procedure

For application in a jurisdiction such as California, the Tasman District method can easily be modified to include outrigger columns. This can be accomplished by changing the flowchart of Figure 12.6 to that of Figure A3. As can be seen by comparing the two figures, outrigger columns are covered by adding two question boxes to the flowchart.

For non-outrigger columns, those constructed after the early 1970s are markedly better than those constructed before. For outrigger columns, deficiencies persist even for construction through the 1980s. The flowchart in Figure A3 indicates that a separate cut-off date, 1992, is used for outrigger columns, while for all other columns the cut-off date remains 1973.

Caltrans Procedure

The Caltrans procedure also under-predicts the vulnerability of Example Bridge 6, assigning an average rating of 0.32. This again illustrates the point that additive prioritization procedures often underestimate the vulnerability of a bridge which has a single major type of seismic deficiency.

Another reason that the Caltrans procedure under-predicts the vulnerability of Example Bridge 6 is that the year of construction variable is not as appropriate to outrigger columns as it is to other seismic deficiencies. Compared to the Tasman District method, the Caltrans procedure cannot be as easily modified to consider a separate cut-off date for outrigger columns. If the weighting factors of the additive Caltrans procedure are modified in an attempt to account for this issue, the prioritization rating given to all other bridges can be affected.

Example Bridges 7 and 8

The Tasman District method assigns a vulnerability rating of 6.4 to each of these bridges, indicating a medium vulnerability. The rating is considered appropriate for Bridge 7 and somewhat conservative for the single-span Bridge 8.

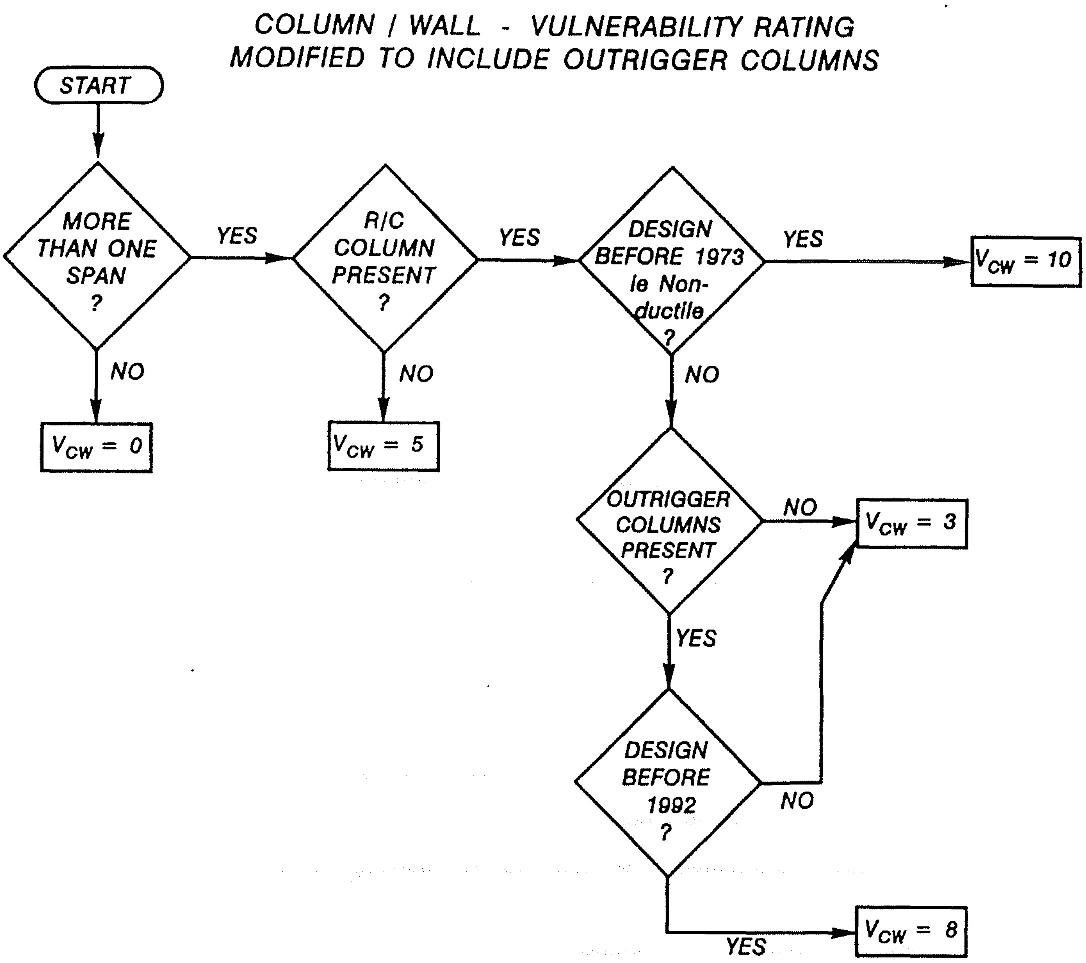

Figure A3 Level-zero seismic assessment flowchart for column or pier-wall vulnerability, V_{cw}, modified to account for outrigger columns.

Conservatism Related to Superstructure Deficiencies

There is an intentional conservatism in the Tasman District method related to superstructure movement joints. The conservatism is based on the following issues:

- The procedures which have customarily been used for calculating the force and displacement demands at superstructure movement joints may be inadequate (as mentioned in Section 2.3 and Chapter 5). Therefore, even new bridges may have shorter seating lengths than would be desirable.

- Related to the above issue, linkages or cable restrainers may not have adequate strength, and could fracture in earthquake shaking and become ineffective.

- Procedures used for designing new bridges typically do not contain any formal provisions for increasing seating lengths where supports are skewed.

Note that these example bridges have superstructure linkages but they are not necessarily assumed to have good linkage details or linkage strength. If the bridges were of a construction type which can be correlated with good linkage details, the Tasman District vulnerability rating of the bridge would be reduced by the last factor shown in Figure 12.5. To include this factor, the construction would have to be of a type which could be easily identified by the inexperienced technicians conducting the level-zero procedure.

Additionally, the Tasman District procedure does not distinguish between movement joints at abutments and movement joints within the bridge span. This is done for simplicity. If the distinction were considered important for a bridge jurisdiction, the vulnerability rating could be refined by adding an additional step to the Figure 12.5 flowchart.

Caltrans Procedure

The Caltrans procedure gives a high rating of 0.61 to Example Bridge 7, which seems to over-predict the actual vulnerability. The procedure gives an extremely low rating of 0.14 to Example Bridge 8, under-predicting the actual vulnerability. This illustrates the following points:

- The additive combination of vulnerability factors can result in major inconsistencies, as previously discussed.

- Prioritization procedures such as the Caltrans procedure underestimate the effect of skew on bridges with movement joints, as discussed in Section 11.5.

- The Caltrans procedure seems to make too great a distinction between movement joints at abutments and those within a bridge span, and inappropriately uses an additive combination of the two variables for these attributes. (For example, a bridge with 4 movement joints has 0.165 added to its rating if all of the joints are within the span and 0.245 added to its rating if two of the joints are at the abutments, when in reality one would expect little difference in the vulnerability of the two structures.)

<u>*Example Bridge 9*</u>

The Tasman District method assigns a vulnerability rating of 5 to this pier-wall structure. This reflects the medium to low vulnerability of the bridge.

The Caltrans procedure assigns an average rating of 0.35 to Bridge 9. This is may be somewhat conservative, considering that several of the more vulnerable example bridges previously discussed are given a lower rating.

The vulnerability of pier-wall bridges is not strongly related to year of construction, as it is for bridges with reinforced-concrete columns. The Caltrans procedure does not make such a distinction, and applies the same year-of-construction factor to all bridges. The flowchart algorithm used in the Tasman District method is more suited to making such distinctions, as discussed in Section 11.5.

Example Bridge 10

The Tasman District method applies a vulnerability rating of 4 to Bridge 10, reflecting the low vulnerability of the structure.

The Caltrans procedure over-predicts the vulnerability of this bridge, giving it the highest rating, 0.63, of all 12 example bridges. This again illustrates the shortcomings of an additive combination of structural vulnerability variables. It also confirms that prioritization procedures often disregard important distinctions within the consideration of certain seismic deficiencies (in this case, the distinction between vulnerable and non-vulnerable movement-joint details). Such distinctions are most easily made in a flowchart algorithm.

Example Bridges 11 and 12

The Tasman District method assigns a vulnerability rating of 3 to Bridge 11, and a rating of 2 to Bridge 12. These ratings reflect the very low vulnerability of these bridges.

The Caltrans procedure assigns an average rating of 0.31 to each of these bridges. This rating seems to over-predict the vulnerability of the two bridges. Furthermore, the rating is similar to that assigned to a number of the example bridges which the author would judge to be much more vulnerable. This reinforces the observation reported in Section 11.5 that additive combinations can be insensitive and that it can be difficult to separate a large group of bridges which have average scores [Buckle 1991].

Correlation of Results to Judgement-based Vulnerability

Figure A4 shows the correlation of the vulnerability rating results with the judgement-based vulnerability. As was shown in Figure A2, the correlation plots of Figure A4 show a large disagreement between the results of the Tasman District method and those of the Caltrans procedure.

Figure A4(a) shows the correlation of the Tasman District vulnerability rating with the judgment-based vulnerability. The correlation is good, with the exception of one bridge — Example 6 — which is judged to have a medium-high vulnerability because of its outrigger columns, but is given a rating of only 4 in the Tasman District method, as discussed in the previous section.

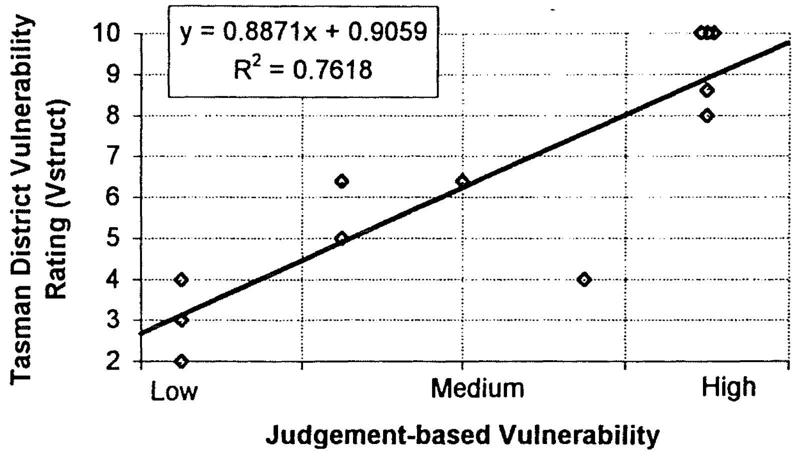

(a) Tasman District method.

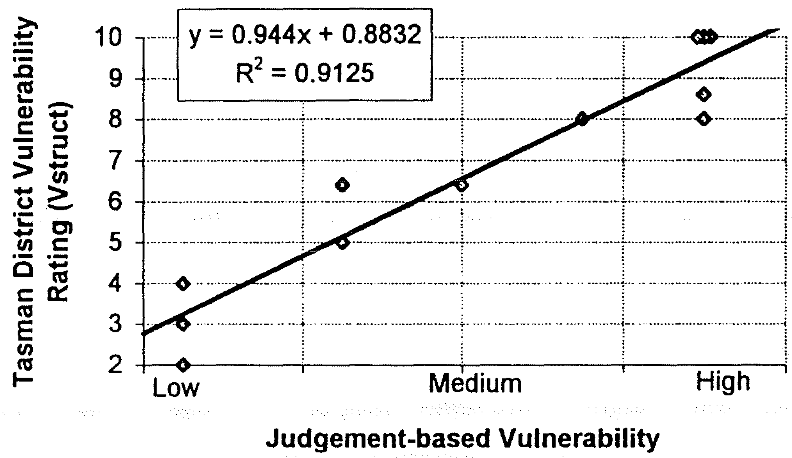

(b) Tasman District method modified for outrigger columns.

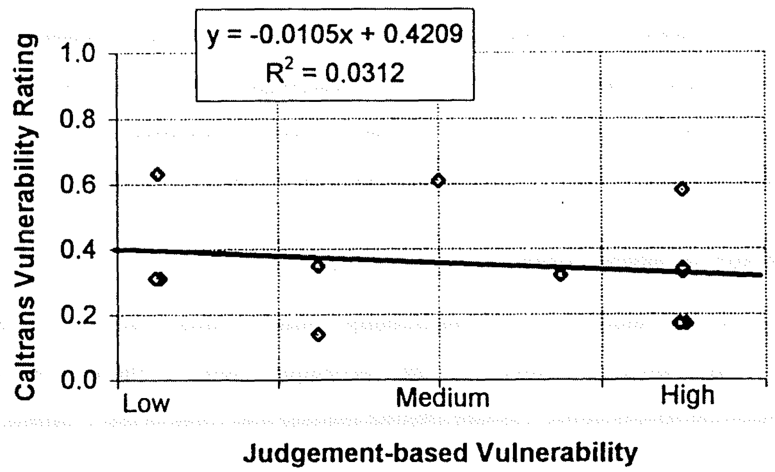

(c) Caltrans procedure.

Figure A4 Correlations of structural vulnerability ratings with judgement-based vulnerability.

If the level-zero procedure of the Tasman District were modified to account for outrigger columns, as shown in Figure A3, then Example Bridge 6 is given a rating of 8 and the correlation improves. This is shown in Figure A4(b).

The correlation of the Caltrans ratings with the judgement-based vulnerability is shown in Figure A4(c). The correlation is poor, and the regression line actually trends in the wrong direction. That is, as the judgement-based vulnerability increases, the Caltrans rating (for these 12 bridges) tends to decrease.

A4 Comparison of Seismicity Ratings

There are major differences between the Tasman District method and the Caltrans procedure in how the seismicity at a bridge site is assessed. These differences are explored by considering eight seismicity examples.

Tasman District Method

The Tasman District method uses a single factor to account for the seismicity at a bridge site. For New Zealand, this is taken as proportional to the seismic zone coefficient which ranges from a minimum of 0.5 to a maximum of 1.2. The seismic zones reflect the expected earthquake acceleration levels for a given return period.

Caltrans Procedure

The Caltrans procedure uses three seismicity variables as shown in Figure A1. The three variables account for peak ground acceleration (on rock), seismic duration, and seismic activity. Presumably the seismic duration is assumed to be high when the seismicity at the site is controlled by faults capable of generating large-magnitude earthquakes, and presumably the seismic activity is assumed to be high when the controlling earthquake faults have a high slip rate.

The seismic duration and activity factors have a great effect on the priority ratings assigned to bridges. It is not clear whether the full range of factors for these two variables can be applied regardless of seismic zone.

For the examples considered below it is assumed that at peak ground acceleration (PGA) levels of 0.3g and 0.7g, seismic duration can be either short, intermediate, or long. For example, a site may have a 0.3g PGA based on a large, long-duration earthquake fault some distance away, or may have a 0.7g PGA based on being very close to a smaller, short-duration earthquake fault.

For seismic activity, it is assumed that there would not be complete independence of this variable with PGA. Therefore, in the examples considered below, it is assumed that for a PGA of 0.3g, seismic activity can be low, moderate or active, but is unlikely to be high. Similarly, for a PGA of 0.7g, it is assumed that seismic activity can be moderate, active, or high, but is unlikely to be low.

Seismicity Examples

Considering the three seismicity variables used by Caltrans, eight examples have been developed by the author to cover the range of possible conditions. These eight seismicity examples are shown in Table A2. In the examples, the New Zealand zone factor of 1.2 is considered to correspond to the Caltrans PGA of 0.7g, while the New Zealand zone factor of 0.5 is considered to correspond to the Caltrans PGA of 0.3g.

Table A2 Data and multipliers for seismicity examples.

Seismicity Example:	**A**	**B**	**C**	**D**	**E**	**F**	**G**	**H**
New Zealand Zone Factor	1.2				0.5			
Tasman District Seismicity Multiplier [1]	**1.0**				**0.42**			
Caltrans Seismicity Data								
Peak Ground Acceleration	0.7g				0.3g			
Seismic Duration	Long		Short		Long		Short	
Seismic Activity	High	Mod.	High	Mod.	Active	Low	Active	Low
Caltrans Seismicity "Attributes"								
a_{22}(PGA)	0.38				0.16			
a_{23}(duration)	0.29		.0145		.0.29		0.145	
a_{11}(activity)	1.0	0.5	1.0	0.5	0.75	0.25	0.75	0.25
Caltrans Seismicity Multiplier [2]	**0.67**	**0.34**	**0.53**	**0.26**	**0.34**	**0.11**	**0.23**	**0.076**

[1] [Maffei 1994].
[2] [Gilbert 1993].

Comparison of Seismicity Multiplier for Examples

Table A2 and Figure A5 show the seismicity multipliers which result for the eight examples. The results show large differences between the multipliers of the Tasman District and Caltrans procedures.

Comparison of Examples E, D, and H.

The multipliers of the Caltrans procedure are strongly affected by the seismic duration and activity factors, which are not considered in the Tasman District method. Depending on the values of these two factors, the priority rating of a bridge can be changed by a factor as high as 4.5. This is the most extreme case, and is seen in the comparison between Examples E and H. While the Caltrans procedure applies such different seismicity multipliers to these two example bridges, the Tasman District method would apply equal seismicity factors, as shown in Figure A5.

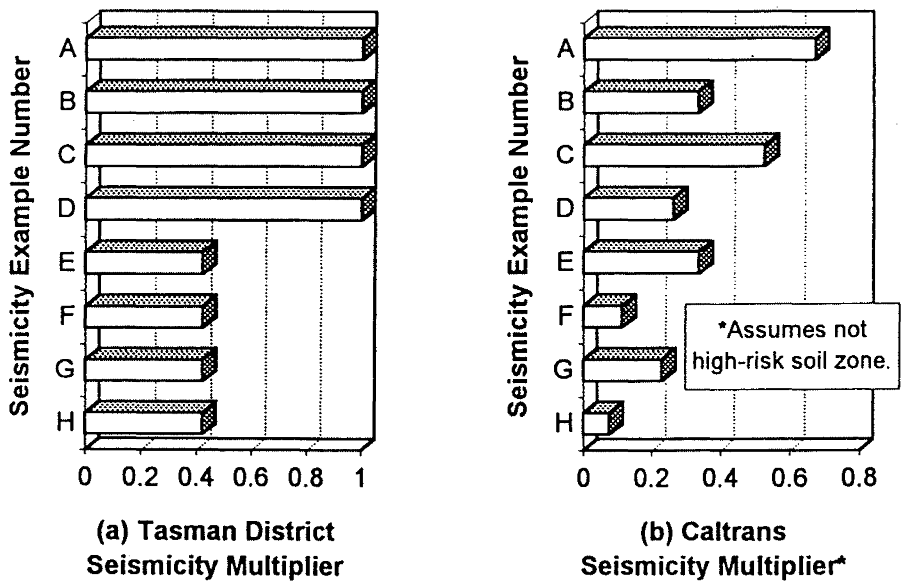

Figure A5 Resulting multipliers for seismicity examples.

A great difference between the two procedures is also shown in the comparison of Seismicity Example D with Example E. In the Tasman District, the seismicity multiplier of site E is 2.4 times higher than that for site D, based directly on the different (PGA-based) seismic zones of each site. In the Caltrans procedure, site D is given a higher seismicity multiplier than site E, by a factor of 1.3. Thus in the Caltrans procedure, the site with 0.3 PGA is assigned a seismicity multiplier 30% higher than the site with 0.7 PGA.

Comparison of Examples A and H

The above results rely on the assumption that there is a degree of independence between the three Caltrans seismicity variables, ie, that a high PGA factor does not always imply a high duration and a high seismic activity. If in fact the variables are not assumed to be independent, then it seems that the difference between high and low seismic zones will be over emphasized. This is illustrated by comparing Example A with Example H. In the Caltrans procedure Bridge A has a seismicity multiplier 8.8 times higher than Bridge H, even though the expected PGA at Bridge A is only 2.4 times higher.

Discussion of Results

Based on these results, it seems that the Caltrans seismicity multiplier is poorly formulated. The multiplicative factors for seismic activity in particular seem to be poorly chosen in that they have too great an effect on a bridge's priority rating. The additive variable for seismic duration also seems to have too great an effect. There also seems to be no apparent logic in why the duration variable is additive while the activity variable is multiplicative. These points are particularly pertinent considering that there are large uncertainties in the typical data which is available on fault locations, seismic activity, and expected earthquake duration.

This illustrates the conclusion made in Section 11.5 that some prioritization procedures seem to use poorly chosen multiplicative factors.

Note that the seismicity results given here for the Caltrans procedure assume that the bridge is not in a high-risk soil zone. (Not being in a high-risk zone would be the more common case.) Because the Caltrans soil factor is additive with the seismicity factors, the effect of the seismicity factors cannot be evaluated without assuming a soil factor.

A5 Soil Factor

The Tasman District method and the Caltrans procedure differ in the ways in which they consider the effect of the soil profile at a bridge site. These differences are explored using additional examples.

Tasman District Method

The Tasman District method uses a multiplicative factor to account for soil-profile type and liquefaction potential as described in Section 12.3 and Table 12.3. The factor follows the soil-profile definitions of the Uniform Building Code (UBC) [ICBO 1994].

Caltrans Procedure

The Caltrans procedure uses an additive soil variable which puts all sites into one of two categories, either a "high risk zone" or not. The comparison of soil factors applied by the two procedures is shown in Table A3. Because the soil variable is additive to seismicity variables, its effect on the priority ratings cannot be judged unless values are assumed for the seismicity variables.

Table A3 Soil Factors

Soil Profile Type from the Uniform Building Code [ICBO 1994].	**IV**	**III**	**II**	**I**
Tasman District Soil Factor [Maffei 1994]	2.0	1.5	1.2	1.0
Caltrans Additive Soil Attribute [Gilbert 1993]	0.33	0	0	0

Soil/Seismicity Examples

Eight examples of combined soil and seismicity variables are presented in Table A4. The examples are intended to cover the widest range of likely combinations of the variables. Four of the seismicity examples from Table A2 are used in combination with the two extreme ranges of UBC soil types, type I and type IV.

Table A4 Examples of combined soil and seismicity factors.

Soil/Seismicity Example	**A-IV**	**A-I**	**D-IV**	**D-I**	**E-IV**	**E-I**	**H-IV**	**H-I**
Seismicity Example (See Table A2)	A		D		E		H	
UBC Soil Type	IV	I	IV	I	IV	I	IV	I
Tasman District Multiplier	**2.0**	**1.0**	**2.0**	**1.0**	**0.84**	**0.42**	**0.84**	**0.42**
Caltrans Multiplier	**1.0**	**0.67**	**0.43**	**0.26**	**0.59**	**0.34**	**0.16**	**0.076**

Comparison of Combined Soil/Seismicity Multipliers

The resulting multipliers to the priority ratings are given in Table A4 and illustrated in Figure A6. The figure shows large differences between the multipliers of the Tasman District method and Caltrans procedures. These differences, however, result mainly from the differences in seismicity factors as previously discussed, not from large differences in the effect of the soil type variable.

The effect of the different soil type in each of the two procedures can be observed by considering the difference between Example A-IV and A-I, between Example D-IV and D-I, etc. The Tasman District method always results in a multiplier 2.0 times higher for soil type IV, compared to soil type I. The Caltrans procedure results in a multiplier between 1.5 and 2.1 times higher for soil type IV compared to soil type I. The two procedures could be considered to be roughly in agreement in this instance, but the Caltrans procedure tends to give somewhat less emphasis to high-risk soil sites than the Tasman District.

In considering the intermediate soil types II and III defined in the UBC [ICBO 1994], some additional differences between the two procedures would be likely to emerge. This is because the Caltrans procedure does not consider such a gradation of soil types, as is indicated in Table A3.

A6 Comparison of Bridge Importance Ratings.

A large part of any prioritization procedure concerns how bridge importance is considered. The Tasman District method considers bridge importance in a very different way to the Caltrans procedure. The differences are such that it is difficult to make direct comparisons between the two

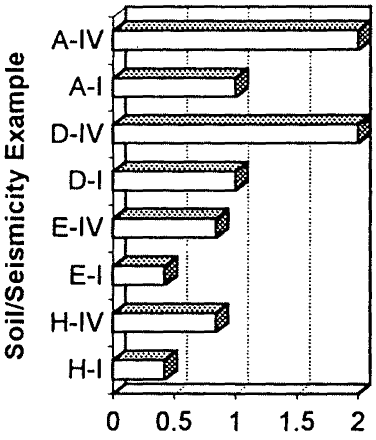

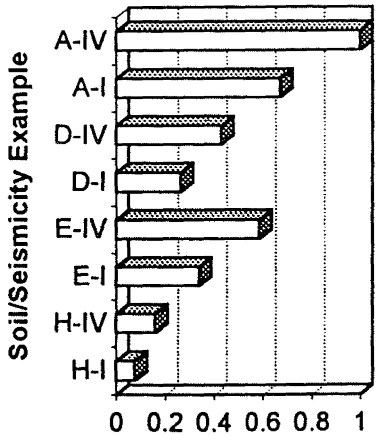

Figure A6 Resulting multipliers for combined soil/seismicity examples.

procedures. However the effect of two major variables—detour length and traffic volume—on the importance ratings of the two procedures can be compared.

Tasman District Method

As is discussed in Section 12.7, it is recommended in the Tasman District method that the importance of a bridge be assessed by calculating benefit/cost ratios for seismic upgrading. It is noted in Section 12.8 that it is also possible for the preliminary screening stage to use the following formula instead of explicit calculations of benefit/cost ratios:

$$B/C = (V - 1.5)^2 \left[0.1 + \frac{ADT(DET \times K_{FORD} + 5)}{500{,}000} \right]$$

where:

B/C	=	Approximate Benefit/Cost Ratio for Upgrade.
V	=	Seismic Vulnerability Rating, 2-10.
ADT	=	Average Daily Traffic (Vehicles/Day).
DET	=	Detour Length (km).
K_{FORD}	=	1 if it is possible to construct a temporary ford or other access in place of the bridge; = 5 otherwise

In the following sections the results given by this formula are compared to results of the Caltrans procedure.

Caltrans Procedure

As shown in Figure A1, the Caltrans procedure uses an additive combination of 8 variables to assess bridge importance. (The term "importance" is used here rather than the term "impact" or "impact criterion" as used by Caltrans and shown in Figure A1.) The bridge importance is combined additively with the structural vulnerability rating and then multiplied by the seismicity and soil multipliers (called activity and hazard by Caltrans), as shown below:

$$\textit{Priority Rating} = \textit{Seismicity} \times [0.6 \times \textit{Importance} + 0.4 \times \textit{Vulnerability}]$$

Comparisons of Importance Rating

The Tasman District method considers the importance of a bridge to be affected by 3 major variables. These are detour length, average daily traffic (ADT), and whether temporary access can be provided in place of the bridge. The Caltrans procedure does not consider the temporary access variable; thus there are only two importance variables which are common to both procedures: detour length and ADT. The effects of these two variables in each of the procedures are considered below.

Effect of Detour Length on the Importance Rating

The effect of varying detour length on the importance rating of the two procedures has been considered for typical examples. The results, shown in Figure A7, indicate that the Tasman District method is much more sensitive to changes in detour length than the Caltrans procedure.

Figure A7(a) shows that the Tasman District importance multiplier for a bridge increases significantly as detour length increases. This is particularly true if temporary access cannot be provided in place of the bridge during the bridge reconstruction. For an increase in detour length from 10 to 50 km, the Tasman District importance rating increases by a factor of 2.9 if temporary access is not possible, and by a factor of 1.6 if temporary access is possible.

Figure A7(b) shows that the Caltrans procedure is relatively insensitive to changes in detour length. For a five-fold increase in detour length, from 10 to 50 km, the Caltrans importance rating increases by a factor of only 1.09. The effect of this increase will be further diminished by the subsequent additive combination of the importance rating with the vulnerability rating.

The Tasman District example assumes an ADT of 1000, which is typical of bridges in the district. The Caltrans example is based on the assumptions shown in Figure A7(b). Because the Caltrans procedure uses an additive combination of importance variables, the effect of one particular variable can only be assessed if values are assumed for the other variables.

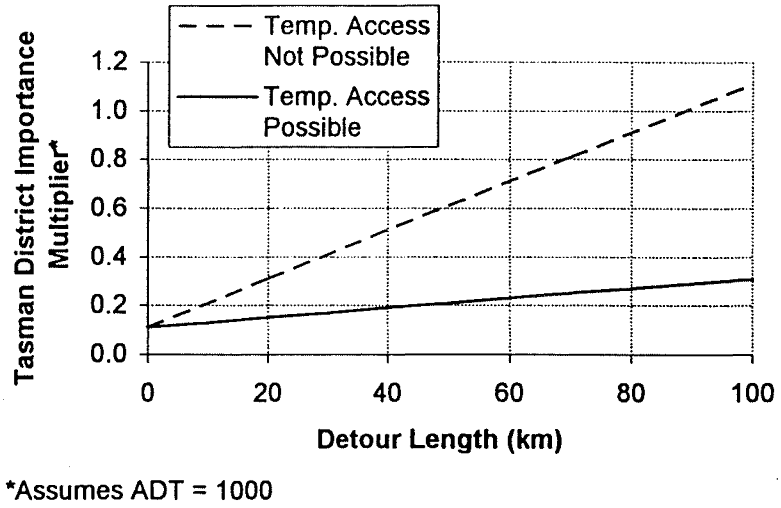

(a) Tasman District Procedure

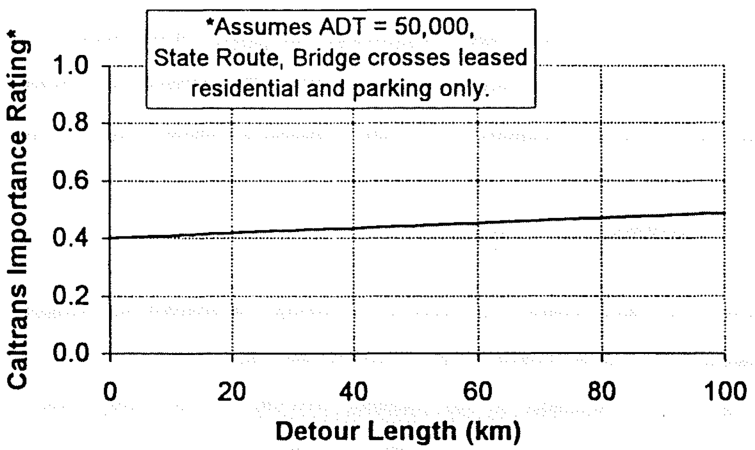

(b) Caltrans Procedure

Figure A7 Effect of detour length on ratings for bridge importance.

Effect of Average Daily Traffic (ADT) on Importance Rating

The effect of varying traffic volume on the importance rating of the two procedures has also been considered. The results are shown in Figure A8. The results indicate that the Tasman District method is much more sensitive than the Caltrans procedure to changes in traffic volume.

Figure A8(a) shows that the Tasman District importance multiplier for a bridge increases significantly as ADT increases. As with the detour-length variable, this is particularly true if temporary access cannot be provided in place of the bridge during the bridge reconstruction. For an increase in ADT from 500 to 2500 vpd, the Tasman District importance rating increases by a factor of 3.0 if temporary access is not possible, and by a factor of 1.8 if temporary access is possible. The range of ADT levels considered in Figure 8(a) — 0 - 5000 vehicles per day — covers the range of traffic levels on the roads in the Tasman District.

Figure A8(b) shows that the Caltrans procedure is relatively insensitive to changes in ADT. For a five-fold increase in ADT — from 20,000 to 100,000 vpd — the Caltrans importance rating increases by a factor of only 1.44. The effect of this increase will be further diminished by the subsequent additive combination of the importance rating with the vulnerability rating. The range of ADT levels considered in Figure 8(b) — 0 - 100,000 vpd — is thought to be typical of California bridges.

Both the Tasman District and Caltrans example assume a detour length of 20 km. The Caltrans example includes the additional assumptions shown in Figure A8(b).

A7 Effect of Vulnerability Rating on Overall Priority Rating

As with other aspects of the two prioritization procedures, there are major differences in the formulation of overall priority ratings between the Tasman District method and Caltrans procedure. Again, direct comparisons are difficult. However, one issue — the effect of structural vulnerability on the overall priority rating — can be examined.

Tasman District Method

As discussed in Chapter 12, the Tasman District method uses a multiplicative combination of a damage function (based on the seismic vulnerability rating) times an importance multiplier to arrive at an overall priority rating (which is considered to be an approximate benefit/cost ratio). As shown in Figure 12.9, the damage function can be assumed to be parabolic in form. Thus the Tasman District priority rating relates to the seismic/structural vulnerability rating (on the zero to ten scale) according to the vulnerability multiplier shown in Figure A9(a).

Caltrans Procedure

The Caltrans procedure combines the vulnerability rating in a weighted additive manner with the

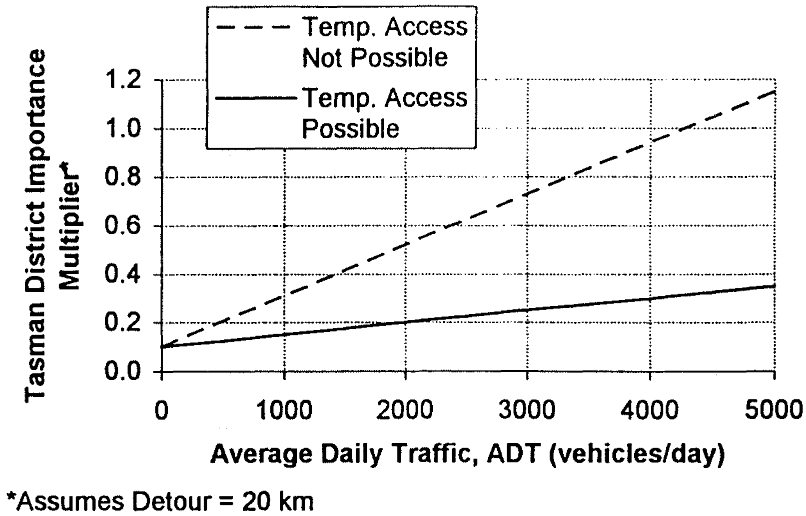

(a) Tasman District Procedure

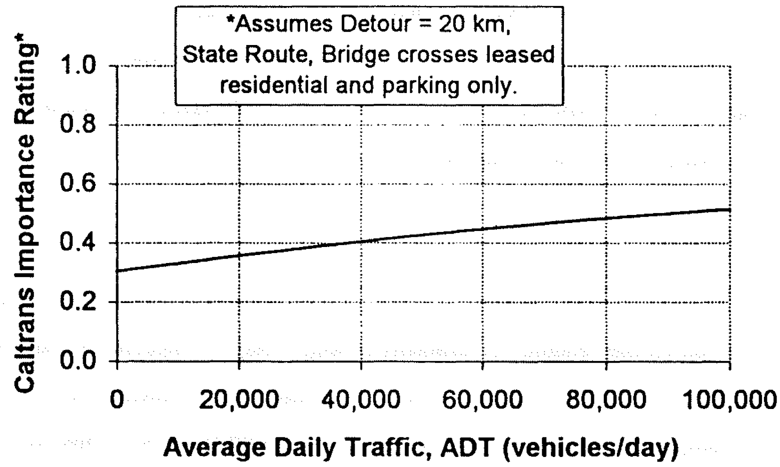

(b) Caltrans Procedure

Figure A8 **Effect of ADT on ratings for bridge importance.**

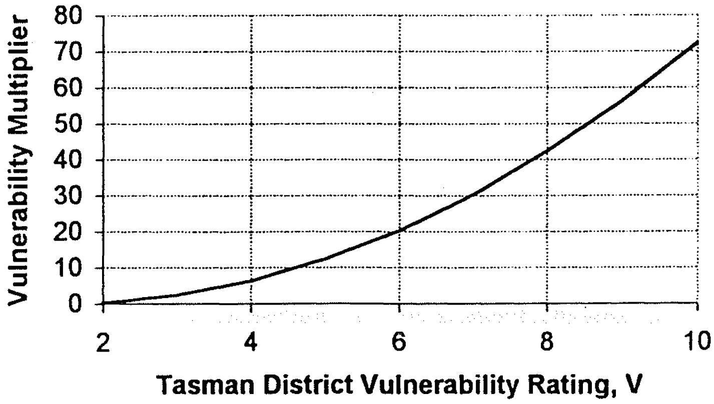

(a) Tasman District Procedure

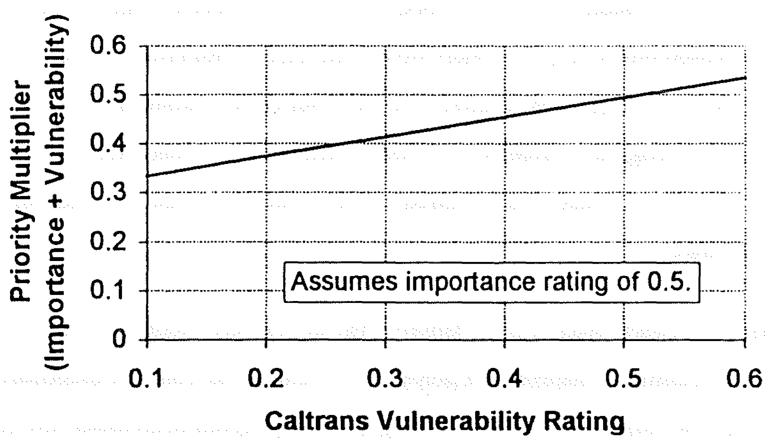

(b) Caltrans Procedure

Figure A9 Effect of structural vulnerability rating on bridge-retrofit priority ratings.

importance rating, as discussed in Sections 11.5 and A6. Assuming an average importance rating of 0.5, the effect of the vulnerability rating on the overall Caltrans priority rating is shown in Figure A9(b). The range of vulnerability ratings is taken from a minimum of 0.1 to a maximum of 0.6. The studies in Section A1 showed that the Caltrans procedure is unlikely to produce vulnerability ratings much outside this range.

Comparison of Tasman District and Caltrans Results.

The comparison of Figures A9(a) and A9(b) shows that the Tasman District priority rating of a bridge is more heavily affected by structural vulnerability than the Caltrans priority rating. For the Tasman District method, if the vulnerability rating increases from an average value of 6 to the maximum value of 10, the overall priority rating is increased by a factor of 3.6. For the Caltrans procedure, if the vulnerability rating increases from an average value of 0.35 to a high value of 0.60, the overall priority rating is increased only by a factor of 1.23

A8 Conclusions and Recommendations for the Addendum to Part III

The comparison studies of this addendum lead to and reinforce several conclusions:

A. There are great differences between the Tasman District method and the Caltrans procedure for the prioritization of bridges for seismic-upgrading. These differences are evident in nearly every component of the procedures and lead to a different priority ranking for the same bridge examples.

B. The findings for the Tasman District method reveal no erroneous aspects, and no unintended results. The method tends to give conservative structural vulnerability ratings to bridges with movement joints and large skew angles, and the level-zero procedure does not consider the vulnerability of outrigger columns. These features are intentional, however, and if modifications in these areas were desired, they would be easy to incorporate into the flowchart procedure.

C. The flowchart procedure used in the Tasman District is easily modified to account for added variables. With additive prioritization procedures such as the Caltrans procedure, it is more difficult to add new variables without affecting the ratings given to all other bridges.

D. There are a number of questionable aspects in the 1993 Caltrans procedure for bridge-retrofit prioritization. For example, the multiplicative seismicity factors seem to be poorly chosen, the additive combinations make the procedure insensitive to major changes in important variables, and bridges with critical seismic deficiencies could be overlooked. Many of the questionable aspects are discussed in Section 11.5 and are also evident in other prioritization procedures.

Recommendations

For the management and prioritization of bridge-seismic retrofit work, the Tasman District method is recommended. The method should be implemented according to Figure 12.2, which recommends an initial study and verification before applying the level-zero preliminary screening procedure to a new jurisdiction.

In cases where researchers disagree about the advantages of various prioritization procedures, perhaps cooperative efforts at testing, verifying, and/or modifying procedures should be recommended.

REFERENCES

Aguilar, Jorge, Hugón Juárez, Rodolfo Ortega, and Jesus Iglesias, "Statistics of Damage and Retrofitting Techniques in Reinforced Concrete Buildings", *Earthquake Spectra*, Volume 5, Number 1, Earthquake Engineering Research Institute (EERI), El Cerrito California, February 1989.

ATC, Applied Technology Council, Seismic Design Guidelines for Highway Bridges, Report No. ATC-6, Palo Alto, California, October 1981.

ATC, Applied Technology Council, *Seismic Retrofitting Guidelines for Highway Bridges*, Report ATC 6-2, Palo Alto California, August 1983. (Also published by US Department of Transportation, Federal Highway Administration, Research Development and Technology, McLean Virginia, December 1983.)

ATC, Applied Technology Council/Federal Emergency Management Agency, *Earthquake Damage Evaluation Data for California*, Report ATC-13, Redwood City California, 1985.

Babaei, Khossrow and Neil M Hawkins, *Bridge Seismic Retrofit Planning Program* Report WA-RD 217.1, National Technical Information Service, Springfield Virginia 22616, December 1991.

Babaei, Khossrow and Neil M Hawkins, "Bridge Seismic Retrofit Prioritisation", *Lifeline Earthquake Engineering*, Monograph Number 4, Technical Council on Lifeline Engineering, pages 149-155, August 1991.

BCHF, Beca Carter Hollings and Ferner Ltd, *Thordon Overbridge Seismic Retrofit, Assessment Report*, Auckland New Zealand, May 1994 [1994a].

BCHF, Beca Carter Hollings and Ferner Ltd (A Powell, J Maffei, J Marsh, I J Billings, D V Toan, L G Cormack), *Thorndon Overbridge Seismic Retrofit, Draft Retrofit Concepts Report*, Auckland New Zealand, October 1994 [1994b].

Billings, I J and A J Powell, "Thorndon Overbridge Seismic Assessment", Proceedings of the Second International Workshop on the Seismic Design of Bridges, Queenstown New Zealand, August 1994.

Bollo, Martin E, Stephen A Mahin, Jack P Moehle, Ray M Stephen, and Xiaoxuan Qi, *Observations and Implications of Tests on the Cypress Street Viaduct Test Structure*, Research report UCB/EERC-90/20, Earthquake Engineering Research Center, University of California Berkeley, December 1990.

Buckle, Ian G, "Screening Procedures for the Retrofit of Bridges", *Lifeline Earthquake Engineering*, Monograph Number 4, Technical Council on Lifeline Engineering, pages 156-165, August 1991.

Buckle, Ian G, "Screening Procedures for the Seismic Retrofit of Bridges," *Proceedings of the 3rd International Workshop on Bridge Rehabilitation*, Dormstadt Germany, June 1992.

Buckle, Ian G and Ian M Friedland (Editors), *Seismic Retrofitting Manual for Highway Bridges*, Report FHWA-RD-94-052, US Department of Transportation, Federal Highway Administration, McLean Virginia, May 1995.

BSSC, Building Seismic Safety Council, *NEHRP Handbook for the Seismic Evaluation of Buildings*, Ballot Copy, Washington DC, 1991.

Bull, Des, Department of Civil Engineering, University of Canterbury, Christchurch New Zealand, personal communication, 1994-1995.

Caltrans, California Department of Transportation, Division of Structures, *Seismic Design References*, Sacramento California, June 1990.

Caltrans, California Department of Transportation, Division of Structures, *Interim Memo to Designers 20-4*, Sacramento California, April 1992.

Caltrans, California Department of Transportation, Division of Structures, *Proceedings of the Second Annual Seismic Research Workshop*, Sacramento California, March 1993.

Caltrans, California Department of Transportation, Division of Structures, *The Northridge Earthquake Post-earthquake Investigation Report*, Sacramento California, January 1994.

Calvi, G M and M J N Priestley editors, *Proceedings of the International Workshop on Seismic Design and Retrofitting of Reinforced Concrete Bridges*, Bormio Italy, April 1991.

Carr, Athol J, *RUAUMOKO Inelastic Frame Analysis Program*, Department of Civil Engineering Computer Program Library, University of Canterbury, Christchurch New Zealand, March 1995 [1995a].

Carr, Athol, Department of Civil Engineering, University of Canterbury, Christchurch New Zealand, personal communication, 1995 [1995b].

Chapman, H E, "Retrofitting - New Zealand," *Proceedings of the International Workshop on Seismic Design and Retrofitting of Reinforced Concrete Bridges*, G M Calvi and M J N Priestley editors, Bormio Italy, pages 505-527, April 1991.

Chapman, H E, Works Consultancy Services, Wellington New Zealand, personal communication, 1993-1994.

Chapman, H E and D K Kirdaldie, "Earthquake Resistance Evaluation and Upgrading of Bridges", *New Zealand Concrete Society Annual Technical Conference*, Wairakei New Zealand, October 1992.

Chapman, H E and D K Kirkaldie, "Assessment of Highway Bridges in New Zealand", *Seismic Design and Retrofitting of Reinforced Concrete Bridges, Proceedings of the Second International Workshop*, Queenstown New Zealand, August 1994.

CH2M Hill Engineers, *Oregon Department of Transportation Bridge Seismic Retrofit Prioritization Model*, Final Report, Oregon Department of Transportation, Salem Oregon, October 1993.

Cooling, Thomas L, Ralph E Anderson, and Mary Shore, "Illinois Department of Transportation Seismic Condition Survey", Paper Number IBC 92-21, *9th Annual International Bridge Conference*, Pittsburgh Pennsylvania, June 1992.

Dekker, D R and R Park, *The Repair and Strengthening of Reinforced Concrete Bridge Piers, Civil Engineering Research Report 92-1*, The University of Canterbury, Christchurch New Zealand, March 1992.

Du Zhen Ping and Alan J Nicholson, *Degradable Transportation Systems: Performance, Sensitivity, and Reliability Analysis*, Civil Engineering Department, University of Canterbury, Christchurch New Zealand, August 1993.

Filiatrault, André, Stéphane Tremblay, and René Tinawi, "A rapid seismic screening procedure for existing bridges in Canada", *Canadian Journal of Civil Engineering*, Volume 21, 1994.

Gates, J H and B H Maroney, "Prioritizing Bridges for Seismic Retrofit", *Proceedings of the First US - Japan Workshop on Seismic Retrofit of Bridges*, Public Works Research Institute, Ministry of Construction, Tsukuba Science City Japan, December 1990.

Gilbert, Ann D, "Developments in Seismic Prioritization of Bridges in California", California Department of Transportation Division of Structures, 1993.

Haroun, Medhat A, Gerard C Pardoen, and Robin Shepherd, "Retrofit of Bridge Pier Walls", *Proceedings of the Second Annual Seismic Research Workshop*, California Department of Transportation Division of Structures, Sacramento California, March 1993.

Hwang, Howard H M, "Discussion of Seismic Vulnerability Evaluation of Bridges in Shelby County, Tennessee' by S Pezeshk, T S Chang, K C Yiak, and H T Kung", *Earthquake Spectra*, Volume 10, Number 4, pages 791-792 November 1994.

ICBO, International Conference of Building Officials, *The Uniform Building Code*, 1994 Edition, Whitier, California.

Ingham, Jason, Nigel Priestley, and Frieder Sieble, "Shear Strength of Knee Joints", *Proceedings of the Second Annual Seismic Research Workshop*, California Department of Transportation Division of Structures, Sacramento California, March 1993.

Kasai, K, B F Maison, and D Patel, "An Earthquake Analysis for Buildings Subjected to a Type of Pounding", *Proceedings, Fourth National Conference on Earthquake Engineering*, EERI, Palm Springs, May 1990.

Kawashima, Kazuhiko, "Seismic Design, Seismic Strengthening, and Repair of Highway Bridges in Japan", *Proceedings of the First US-Japan Workshop on Seismic Retrofit of Bridges*, Tsukuba Science City Japan, December 1990.

Kawashima K, Public Works Research Institute, Ministry of Construction, Tsukuba Japan, personal communication, 1994.

Kennedy, Don, Beca Carter Hollings and Ferner Consulting Engineers, Auckland New Zealand, personal communication, 1995.

Kordina, K, J Hegger, and M Teutsch, "Shear Strength of Prestressed Concrete Beams with Unbonded Tendons," *ACI Structural Journal* Volume 86, Number 2, pages 143-149, American Concrete Institute, Detroit Michigan, March-April 1989.

Lizundia, Bret, Rutherford and Chekene Consulting Engineers, San Francisco California, personal communication, August 1993.

Maffei, Joe, *Bridge Seismic Assessment, Inventory, and Upgrade-Management Study for the Tasman District Council*, Department of Civil Engineering, University of Canterbury, Christchurch New Zealand, May 1994.

Maragakis, E "Manos", M "Saiid" Saiidi, Shipping Feng, Daniel O'Connor, and Sabel Abdel-Ghaffar. "Effects of Hinge Restrainers on the Seismic Response of Bridges", *Proceedings of the Second Annual Seismic Research Workshop*, California Department of Transportation Division of Structures, Sacramento California, March 1993.

Maroney, Brian H and Y H Chai, "Bridge Abatement Stiffness and Strength under Earthquake Loadings", *Seismic Design and Retrofitting of Reinforced Concrete Bridges Proceedings of the Second International Workshop*, Queenstown New Zealand, August 1994.

Moehle, J P, "Displacement-Based Design of RC Structures Subjected to Earthquakes", *Earthquake Spectra*, Volume 8, Number 3, pages 403-428, Earthquake Engineering Research Institute (EERI), Oakland California, August 1992.

Moehle, J P and Mark Aschheim, "Evaluation Procedures for Bridge Structures", *Proceedings of the Second Annual Seismic Research Workshop*, California Department of Transportation Division of Structures, Sacramento California, March 1993.

Moehle, Jack P and Claudia Sawyer, "Behaviour and Retrofit of Exterior RC Connections", *Proceedings of the Second Annual Seismic Research Workshop*, California Department of Transportation Division of Structures, Sacramento California, March 1993.

Naeim, Farzad, "On Seismic Design Implications of the 1994 Northridge Earthquake Records", *Earthquake Spectra*, Volume 11, Number 1, Earthquake Engineering Research Institute, Oakland California, February 1995.

Naeim, Farzad and James C Andersen, *Classification and Evaluation of Earthquake Records for Design*, Report Number CE 93-08, Department of Civil Engineering, University of Southern California, Los Angeles California, July 1993.

NZBRC, New Zealand Building Regulations Committee, *Draft General Earthquake Building By-law*, Appendices 1 and 2 of a report to parliment following the Hawkes Bay earthquake, June 1931.

NZPW, New Zealand Public Works Engineer's Department, Structural Drawings for ["Bridge A"], 1936.

Park, R and T Paulay, *Reinforced Concrete Structures*, A Wiley-Interscience Publication, New York, 1975.

Park, R and M Rodriguez, "Retrofitting of Reinforced Concrete Bridge Piers for Seismic Performance", *Proceedings of the Technical Conference of the New Zealand Concrete Society*, Wairakei New Zealand, pages 43-58, September 1991.

Park, R, M Rodriguez, and D R Dekker, "Assessment and Retrofit of a Reinforced Concrete Bridge Pier for Seismic Resistance", *Earthquake Engineering Research Institute*, Vol. 9, No. 4, November 1993.

Paulay, T, University of Canterbury, Christchurch New Zealand, personal communication, 1993 and 1994.

Paulay, T and M J Nigel Priestley, *Reinforced Concrete and Masonry Buildings Design for Seismic Resistance*, A John Wiley & Sons Inc, New York, 1992.

Pezeshk S, T S Chang, K C Yiak and H T Kung, "Seismic Vulnerability Evaluation of Bridges in Shelby County, Tennessee", *Earthquake Spectra*, Volume 9, Number 4, pages 803-816, November 1993.

Priestley, M J Nigel, *Assessment and Design of Joints for Single-Level Bridges with Circular Columns*, Report Number SSRP-93/02, Department of Applied Mechanics and Engineering Sciences, University of California San Diego, February 1993 [1993a].

Priestley, M J Nigel, "Myths and Fallacies in Earthquake Engineering—Conflicts between Design and Reality", Paper presented at the University of Canterbury, Christchurch, New Zealand, 13 July 1993 [1993b].

Priestley, M J Nigel, University of California San Diego, personal communication, 1993 [1993c].

Priestley, M J Nigel, Frieder Seible, and Yuk Hon Chai, *Design Guidelines for Assessment Retrofit and Repair of Bridges for Seismic Performance*, University of California San Diego, Report Number SSRP 92/01, Department of Applied Mechanics and Engineering Science, August 1992 [1992a].

Priestley, M J Nigel, Frieder Seible, and Donald L Anderson, *Proof Test of a Retrofit Concept for the San Francisco Double Deck Viaducts*, Report Number SSRP-92/03, Department of Applied Mechanics and Engineering Sciences, University of California San Diego, July 1992 [1992b].

Priestley, M J Nigel, Ravindra Verma, and Yan Xiao, "Seismic Shear Strength of Reinforced Concrete Columns", to be published in the *ASCE Structural Journal*, 1994.

Restrepo, Jose I, Department of Civil Engineering, University of Canterbury, Christchurch New Zealand, personal communication, 1993-1995.

Rodriguez, M and R Park, "Seismic Load Tests of Reinforced Concrete Columns Strengthened by Jacketing", *Structural Journal of American Concrete Institute*, Vol. 91, No. 2, March/April 1994.

Rutherford and Chekene Consulting Engineers, *Seismic Retrofitting Alternatives for San Francisco's Unreinforced Masonry Buildings: Estimates of Construction Cost and Seismic Damage*, San Francisco California, May 1990.

SANZ, Standards Association of New Zealand, *Code of Practice for the Design of Concrete Structures*, NZS3101, 1982.

SANZ, Standards Association of New Zealand, *Code of Practice for General Structural Design and Design Loads for Buildings* NZS4203, 1992.

SANZ, Standards Association of New Zealand, *Code of Practice for the Design of Concrete Structures*, NZS3101, Draft copy 1995.

SEAONC, Structural Engineers Association of Northern California, *Research Bulletin Board*, BB91-1, 50 First Street, San Francisco California, January 1991.

SEAONC, Structural Engineers Association of Northern California, *Minutes of the Seismology Committee*, San Francisco California, 1995.

Seible, Frieder, M J Nigel Priestley, Christopher T Latham, and Toru Terayama, "Flexural Integrity of #18 Cap-Column Connections", *Proceedings of the Second Annual Seismic Research Workshop*, California Department of Transportation Division of Structures, Sacramento California, March 1993.

Shinozuka, Masanobu, Michael P Gaus, Seong H Kim, and George C Lee, "Regional Evaluation of Transportation Lifelines in New York State with the Aid of GIS Technology", *Proceedings of the ASCE National Convention*, New York, 1992.

Singh, S P and G L Fenves. "Earthquake Response of Multi-span Freeway Structures", *Proceedings of the Second Annual Seismic Research Workshop*, California Department of Transportation Division of Structures, Sacramento California, March 1993.

Skinner, R I, W H Robinson, and G H McVerry, *An Introduction to Seismic Isolation*, John Wiley & Sons, Chichester England, 1993

Sundstrom, Janise and Brian Maroney, "Sensitivity Study of Bridge Seismic Risk Algorithms Used in the USA", *Structure Notes 27*, California Department of Transportation Office of Structures Design, pages 3-10, July 1992.

Tanaka, Jin, Department of Civil Engineering, University of Canterbury, Christchurch New Zealand, personal communication, 1993.

Thewalt, C R and B Stojadinovic, "Behaviour of Bridge Outriggers, Summary of Test Results", *Proceedings of the Second Annual Seismic Research Workshop*, California Department of Transportation Division of Structures, Sacramento California, March 1993.

TNZ, Transit New Zealand, *Bridge Inspection and Maintenance Manual*, Wellington New Zealand, 1991, [1991a].

TNZ, Transit New Zealand, *Bridge Manual: Design and Evaluation,* Draft for comment, Wellington New Zealand, 1991, [1991b].

TNZ, Transit New Zealand, "Transearch", No. 5, Wellington, New Zealand, July 1992.

Watson S, F A Zahn and R Park, "Confining Reinforcement for Concrete Columns", *Journal of Structural Engineering, ASCE,* Vol. 20, No. 6, June 1994.

Wood, J H, *Bridge Maintenance Management,* Report prepared for Transit New Zealand, Research Project KR3-0061, Draft Revision D3, 28 April 1993.

Yan Xiao, M J Nigel Priestley, Frieder Seible, and Nobuhiko Hamada, "Assessment and Retrofit of Column Footings", *Proceedings of the Second Annual Seismic Research Workshop,* California Department of Transportation Division of Structures, Sacramento California, March 1993.

Yang, Yueh-shiu, M J Nigel Preistley and Frieder Seible, "Dynamic response of bridge frames connnected by restrainers", Report No. SSRP 94/01 University of California San Diego [in press].

Yu Ouyang, David L Allen, Vince P Drnevich, and John L Fleckenstein, *Seismic Analysis and Retrofitting Priorities for Highway Bridges in an Earthquake Priority Route System for Western Kentucky,* Kentucky Transportation Center, University of Kentucky Lexington, 1990.

Yuk Hon Chai, M J Nigel Priestley, and Frieder Seible, "Seismic Retrofit of Circular Bridge Columns for Enhanced Flexural Performance", *ACI Structural Journal,* Pages 572-584, September/October 1991.

Zelinski, Ray, Seismic Technology Section, Caltrans, Sacramento California, personal communication, July 1993.